



Durham E-Theses

Characterisation of widespread Pumice Fall Deposits within the Guajara Eruption Cluster (0.88 – 0.6 Ma), Tenerife, Canary Islands

BAILEY, RYAN

How to cite:

BAILEY, RYAN (2025) *Characterisation of widespread Pumice Fall Deposits within the Guajara Eruption Cluster (0.88 – 0.6 Ma), Tenerife, Canary Islands*, Durham theses, Durham University. Available at Durham E-Theses Online: <http://etheses.dur.ac.uk/16137/>

Use policy

The full-text may be used and/or reproduced, and given to third parties in any format or medium, without prior permission or charge, for personal research or study, educational, or not-for-profit purposes provided that:

- a full bibliographic reference is made to the original source
- a [link](#) is made to the metadata record in Durham E-Theses
- the full-text is not changed in any way

The full-text must not be sold in any format or medium without the formal permission of the copyright holders.

Please consult the [full Durham E-Theses policy](#) for further details.

Characterisation of widespread Pumice Fall Deposits within the Guajara Eruption Cluster (~0.88 – 0.6 Ma), Tenerife, Canary Islands

Ryan Bailey

Abstract

This study characterises 14 previously undescribed pumice fall deposits within the Guajara Eruption Cluster (0.88-0.6 Ma) on Tenerife, Canary Islands. Detailed fieldwork and laboratory analysis were conducted on deposits in the Fasnía region surrounding the 0.738 Ma Eras Formation. Ten of the deposits represent thin, massive, pumice-rich lapilli beds from small-volume Plinian eruptions with limited dispersal (La Linde, Honduras, Aguerche, Jurado, El Escobonal, Arco, Carretas, El Rincon, Vigas, and Gambuesa). The remaining deposits (Mena, Zarza, Icor, and Sombrera) show more complex eruptive sequences with variations in eruption intensity and column height. The Zarza Formation is the most widespread deposit identified, with a volume comparable to the ignimbrite-forming La Caleta eruption. The Eras Formation has been correlated to the previously distinct Moradas Formation, representing a larger eruption than previously recognised. Grain size, componentry, and dispersal data are presented for several key deposits. The identification of these numerous pumice fall deposits increases our understanding of eruption frequencies on Tenerife. This study suggests the likelihood of additional unidentified Plinian deposits on Tenerife and highlights the complex eruptive history of the Las Cañadas caldera.

**Characterisation of widespread Pumice Fall Deposits in Tenerife within
the Guajara Eruption Cluster (~0.88 – 0.6 Ma)**

Ryan Bailey

MScR Volcanology

Department of Earth Sciences

University of Durham

2025

Table of Contents

CHAPTER 1: INTRODUCTION	11
1.1 Introduction	11
1.2 Area of Study	12
1.3 Geological Background	13
1.3.1 Tenerife	13
1.3.1.1 Volcanic History.....	15
1.3.1.2 Explosive Eruptions from the Las Cañadas Caldera	19
1.3.1.3 Guajara Eruption Cluster	21
1.3.2 Plinian Eruptions	24
1.3.3 Pyroclastic Fall Deposits.....	30
1.3.3.1 Bedding	31
1.3.3.3 Grain Size	32
1.3.3.3.1 Componentry	33
1.3.3.4 Thickness	34
1.3.3.4.1 Volume.....	35
CHAPTER 2: METHODOLOGY	37
2.1 Fieldwork	37
2.1.1 Field Data Acquisition	37
2.1.2 Sampling.....	38
2.2 Laboratory Methods	38
2.2.1 Sieving	38
2.2.1.1 Componentry	39
2.2.1.2 Limitations	39
2.3 Lithostratigraphy and lithofacies	40
2.3.1 Stratigraphy Nomenclature	41
2.4 Data Analysis	42
2.4.1 Isopach and Isopleth Maps	42
2.4.2 Estimating Eruptive Parameters.....	42
2.4.3 Limitations	43
CHAPTER 3: RESULTS	46
3.1 Stratigraphic Succession of NE Bandas Del Sur	46
3.1.1 La Linde Formation	48
3.1.2 Honduras Formation	49
3.1.3 Aguerche Formation	54
3.1.4 Jurado Formation.....	59
3.1.5 Mena Formation	62
3.1.5.3 Mena Member A.....	65
3.1.5.2 Mena Member B.....	67
3.1.5.1 Mena Member C	69
3.1.6 El Escobonal Formation	73
3.1.7 Zarza Formation.....	76
3.1.7.3 Zarza Member A	80

3.1.7.2 Zarza Member B	82
3.1.7.1 Zarza Member C	82
3.1.8 Icor Formation	87
3.1.8.6 Icor Member A	89
3.1.8.5 Icor Member B	91
3.1.8.4 Icor Member C	93
3.1.8.3 Icor Member D	95
3.1.8.2 Icor Member E	97
3.1.8.1 Icor Member F	99
3.1.9 Arco Formation	102
3.1.10 Carretas Formation	105
3.1.11 El Rincon Formation	106
3.1.12 Eras Formation	108
3.1.13 Sombrera Formation	118
3.1.13.4 Sombrera Member A	119
3.1.13.3 Sombrera Member B	121
3.1.13.2 Sombrera Member C	123
3.1.13.1 Sombrera Member D	125
3.1.14 Vigas Formation	128
3.1.15 Gambuesa Formation	132
3.1.16 Other Volcanic Units	135
3.1.16.1 Pre-Mena Pumice Fall Deposits	135
3.1.16.2 Pre-Eras Pumice Fall Deposits	138
3.1.16.3 Scoria Fall Deposits	140
3.1.16.4 Effusive Lavas	141
 CHAPTER 4: DISCUSSION	 142
4.1 The Guajara Stratigraphic Succession	142
4.1.1 Stratigraphic Trends	142
4.1.2 Correlations from SE to NE	143
4.1.3 Unknown deposits	144
4.1.4 Eruption Frequency	145
4.1.5 Volume	146
4.1.6 Dispersal	151
4.2 Eruption Dynamics	151
4.2.1 Grain Size	153
4.2.2 Grading	153
4.2.3 Lithic Clasts	155
4.2.4 Magma Heterogeneity	156
4.3 Volcanic Hazards	157
4.4 Limitations	157
4.5 Future Studies	158
 CHAPTER 5: CONCLUSION	 160
 CHAPTER 6: BIBLIOGRAPHY	 161
 CHAPTER 7: APPENDICES	 172

Table of Figures

Figure 1.1 – Map of Tenerife, the main study area is within the black box	14
Figure 1.2 - Generalised geological map of Tenerife from Cas et al., (2022).	17
Figure 1.4 – Dispersal maps of Guajara age deposits from Middleton (2006)	23
Figure 1.5 - Cartoon explaining the differences in explosiveness and column height for various eruption styles (Cas et al., 2024).....	26
Figure 1.7 - The downwind vs crosswind for 4 different clast sizes from eruption columns between 7 and 43km with windspeeds of 10,20 and 30 m/s (Carey and Sparks, 1986)	28
Figure 1.8 - Isopleth maps (Maximum Pumice, MP; Maximum Lithic, ML) constructed from the Fasnía Formation, Tenerife (Edgar et al., 2017)	29
Figure 1.9 - Diagram of a weak and strong plume (Bonadonna et al., 2015; Cas et al., 2024).....	30
Figure 1.9 - Unit F of the Mangaone Subgroup from the Okataine Volcanic Centre, New Zealand. (D) is the Rotoehu lake shore, followed by a series of bimodal beds (B) that are inversely graded towards the top (C) (Jurado-Chichay and Walker, 2001)	32
Figure 1.10 - Thickness vs square root area plots for the Ruapehu deposit using the segment method (a) and power-law method (b) (Bonadonna and Houghton, 2005)	36
Figure 3.1 – Generalised vertical stratigraphy of pyroclastic units in the Fasnía region described in this study. The pyroclastic succession is found within the Guajara Eruption Cluster and older than the 0.668 Ma Arico Formation, consisting of at least 19 new pumice fall deposits surrounding the 0.738 Ma Eras Formation. The deposit thickness and grain size are schematic and not all units are exposed at one singular area. The inset map shows the approximate area each of these pyroclastic deposits can be found.	47
Figure 3.2 - Stratigraphic log of the La Linde Formation. UTM coordinates and inset map of locations are provided. The log represents stratigraphic relationships with under- and overlying units.	48
Figure 3.3 - Images of the La Linde Formation. A) Close up of the fine-grained lapilli above the blocky lava. B) Stratigraphic position of the La Linde Formation beneath the Honduras Formation	49
Figure 3.4 - The Honduras Formation at various localities A) Stratigraphic sequence at Icor Vineyard. B) Honduras Formation at the type locality C) Honduras Formation at North Icor	50
Figure 3.5 - Stratigraphic logs of the Honduras Formation across the Fasnía Region. UTM coordinates and inset map of locations are provided. The logs represent stratigraphic relationships with under- and overlying units.	51
Figure 3.6 – Honduras Formation. A) Proportion of components as a weight percentage of the total sample weight. B) Proportion of components within each grain size. C) Total weight percentage of components..	53
Figure 3.7 - A) Aguerche Formation found beneath a large paleosol with a distinct pink colour below the Mena Formation. B) Close up of the Aguerche Formation. C) Lens of the Aguerche Formation above the Honduras Formation at Mirador de Las Eras.	55
Figure 3.8 - Stratigraphic logs of the Aguerche Formation across the Fasnía Region. UTM coordinates and inset map of locations are provided. The logs represent stratigraphic relationships with under- and overlying units.	56
Figure 3.9 – Aguerche Formation. A) Proportion of components as a weight percentage of the total sample weight. B) Proportion of components within each grain size. C) Total weight percentage of components..	58
Figure 3.10 – A) The Jurado Formation at Icor Vineyard beneath the pink paleosol of the Mena Formation. B) The fine grained, massive pumice lapilli of the Jurado Formation.....	60
Figure 3.11 - Stratigraphic logs of the Jurado Formation across the Fasnía Region. UTM coordinates and inset map of locations are provided. The logs represent stratigraphic relationships with under- and overlying units.	61
Figure 3.12 – A) The Mena Formation at Los Roques B) Mena Formation at Aguerche	62
Figure 3.13 - Stratigraphic logs of the Mena Formation across the Fasnía Region. UTM coordinates and inset map of locations are provided. The logs represent stratigraphic relationships with under- and overlying units.	64
Figure 3.14 – Mena Formation Member A. A) Proportion of components as a weight percentage of the total sample weight. B) Proportion of components within each grain size. C) Total weight percentage of components.....	67
Figure 3.15 – Mena Formation Member B. A) Proportion of components as a weight percentage of the total sample weight. B) Proportion of components within each grain size. C) Total weight percentage of components.....	69

Figure 3.16 – Mena Formation Member C. A) Proportion of components as a weight percentage of the total sample weight. B) Proportion of components within each grain size. C) Total weight percentage of components.....	72
Figure 3.17 - Stratigraphic log of the El Escobonal Formation across the Fasnía Region. UTM coordinates and inset map of locations are provided. The logs represent stratigraphic relationships with under- and overlying units.	74
Figure 3.18 – El Escobonal Formation. A) Proportion of components as a weight percentage of the total sample weight. B) Proportion of components within each grain size. C) Total weight percentage of components.....	76
Figure 3.19 – A) The Zarza Formation at North Icor, with a coarse-grained pumice lapilli base, fine ash layer, and medium grained pumice lapilli upper. Note the coarse-grained pumice bed in the upper layer. B) Zarza Formation at Lomo de Mena, the thickest locality. C) The Zarza Formation in stratigraphic sequence, beneath the Icor, Arco, Carretas, El Rincon, Eras, Sombrera, Vigas, and Fasnía Formations.	77
Figure 3.20 - Stratigraphic logs of the Zarza Formation across the Fasnía Region. UTM coordinates and inset map of locations are provided. The logs represent stratigraphic relationships with under- and overlying units.	79
Figure 3.21 – Zarza Formation Member A. A) Proportion of components as a weight percentage of the total sample weight B) Proportion of components within each grain size C) Total weight percentage of components.....	82
Figure 3.22 – Zarza Formation Member C. A) Proportion of components as a weight percentage of the total sample weight at 50cm. B) Proportion of components within each grain size at 50cm. C) Total weight percentage of components at 50cm. D) Proportion of components as a weight percentage of the total sample weight at 120cm. E) Proportion of components within each grain size at 120cm. E) Total weight percentage of components at 120cm.....	86
Figure 3.23 – A) The Icor Formation at North Icor, beneath the Arco, Carretas, El Rincon and Eras Formations. B) Each member of the Icor Formation at North Icor.....	88
Figure 3.24 - Stratigraphic log of the Icor Formation across the Fasnía Region. UTM coordinates and inset map of locations are provided. The logs represent stratigraphic relationships with under- and overlying units.	89
Figure 3.25 – Icor Formation Member A. A) Proportion of components as a weight percentage of the total sample weight B) Proportion of components within each grain size C) Total weight percentage of components.....	91
Figure 3.26 – Icor Formation Member B. A) Proportion of components as a weight percentage of the total sample weight B) Proportion of components within each grain size C) Total weight percentage of components.....	93
Figure 3.27 – Icor Formation Member C. A) Proportion of components as a weight percentage of the total sample weight B) Proportion of components within each grain size C) Total weight percentage of components.....	95
Figure 3.28 – Icor Formation Member D. A) Proportion of components as a weight percentage of the total sample weight B) Proportion of components within each grain size C) Total weight percentage of components.....	97
Figure 3.29 – Icor Formation Member E. A) Proportion of components as a weight percentage of the total sample weight B) Proportion of components within each grain size C) Total weight percentage of components.....	99
Figure 3.30 – Icor Formation Member F. A) Proportion of components as a weight percentage of the total sample weight B) Proportion of components within each grain size C) Total weight percentage of components.....	101
Figure 3.31 – A) The Arco, Carretas, and El Rincon Formations, below the Eras Formation in North Icor. Note the distinct dark brown paleosol between the Eras and El Rincon Formations. B) The Arco, Carretas, and El Rincon Formations beneath the Eras Formation and above the Icor Formation in La Zarza.	103
Figure 3.32 - Stratigraphic log of the Arco Formation across the Fasnía Region. UTM coordinates and inset map of locations are provided. The logs represent stratigraphic relationships with under- and overlying units.	104
Figure 3.33 - Stratigraphic log of the Carretas Formation across the Fasnía Region. UTM coordinates and inset map of locations are provided. The logs represent stratigraphic relationships with under- and overlying units.	105
Figure 3.34 - Stratigraphic log of the El Rincon Formation across the Fasnía Region. UTM coordinates and inset map of locations are provided. The logs represent stratigraphic relationships with under- and overlying units.	107

Figure 3.35 - Stratigraphic logs of the Eras and Moradas Formations, showing the similarities between them. UTM coordinates and inset map of locations and thicknesses are provided. The logs represent stratigraphic relationships with under- and overlying units.	109
Figure 3.36 – A) The Eras Formation at Barranco del Rio (locality 9) beneath a phonolite lava and above at least three UPFDs, before an unconformity and the Barco Formation at the base. B) The Eras Formation, including the Eras Ignimbrite, beneath the Arico Formation at Poris de Abona (locality 11). C) The Eras Formation beneath the Arico Formation at the previous type locality of the Moradas Formation at Barranco de las Moradas (locality 6). D) The Eras Formation, above at least 4 UPFDs at the current thickest locality at Barranco de las Vegas (locality 7).	110
Figure 3.37 – A) The Eras Formation at Las Eras above the Icor and Zarza Formations (locality 16). B) The Eras Formation at Mirador de las Eras above the El Rincon Formation (locality 13). C) The black, mingled pumice that can be found in the Eras Formation. D) The Eras Formation above the El Rincon Formation at North Icor (locality 15).	111
Figure 3.38 – Eras Formation A) Proportion of components as a weight percentage of the total sample weight at 50cm. B) Proportion of components within each grain size at 50cm. C) Total weight percentage of components at 50cm. D) Proportion of components as a weight percentage of the total sample weight at 100cm. E) Proportion of components within each grain size at 100cm. F) Total weight percentage of components at 100cm. G) Proportion of components as a weight percentage of the total sample weight at 150cm. H) Proportion of components within each grain size at 150cm. I) Total weight percentage of components at 150cm.	117
Figure 3.39 – A) The Sombrera Formation at Icor Vineyard (locality 2). B) The Sombrera Formation beneath the Vigas and Gambuesa Formations at Fasnía Cone (locality 3).	118
Figure 3.40 - Stratigraphic log of the Sombrera Formation. UTM coordinates and inset map of locations and thicknesses are provided. The logs represent stratigraphic relationships with under- and overlying units.	119
Figure 3.41 – Sombrera Formation Member A A) Proportion of components as a weight percentage of the total sample weight B) Proportion of components within each grain size C) Total weight percentage of components.	121
Figure 3.42 – Sombrera Formation Member B A) Proportion of components as a weight percentage of the total sample weight B) Proportion of components within each grain size C) Total weight percentage of components.	123
Figure 3.43 – Sombrera Formation Member C A) Proportion of components as a weight percentage of the total sample weight B) Proportion of components within each grain size C) Total weight percentage of components.	125
Figure 3.44 – Sombrera Formation Member D A) Proportion of components as a weight percentage of the total sample weight B) Proportion of components within each grain size C) Total weight percentage of components.	128
Figure 3.45 – A) The Vigas Formation above the Sombrera Formation at Icor Vineyard (locality 1). B) The Vigas Formation above the Sombrera Formation and below the Gambuesa Formation at Fasnía Cone (locality 3).	129
Figure 3.46 - Stratigraphic log of the Vigas Formation. UTM coordinates and inset map of locations and thicknesses are provided. The logs represent stratigraphic relationships with under- and overlying units.	130
Figure 3.47 – Vigas Formation A) Proportion of components as a weight percentage of the total sample weight B) Proportion of components within each grain size C) Total weight percentage of components.	132
Figure 3.48 - Stratigraphic log of the Gambuesa Formation. UTM coordinates and inset map of locations and thicknesses are provided. The logs represent stratigraphic relationships with under- and overlying units.	133
Figure 3.49 – Gambuesa Formation A) Proportion of components as a weight percentage of the total sample weight B) Proportion of components within each grain size C) Total weight percentage of components.	135
Figure 3.50 – The pre-Mena pumice fall deposits in La Medida (UTM: 361611; 3128810).	138
Figure 3.51 – Pre-Eras fall deposits nearby Mirador de las Eras (UTM: 356768; 3120066).	140
Figure 4.1 - An example of a concave curve produced by the Weibull method when calculating the estimated volume of the Zarza Formation.	147
Figure 4.2 – Minimum volume of all pyroclastic deposits where calculated, separated into the three eruption clusters. The dashed line is a moving average.	148
Figure 4.3 – Thickness vs Area ^{1/2} plot comparing eruptions in this study with known Plinian eruptions: Askja D 1875 (Sparks et al., 1981); Novarupta 1912 (Fierstein and Hildreth, 1992); Quizapu 1932 (Hildreth and Drake, 1992); Tuapo AD186 (Walker, 1980); Hudson 1991 (Scasso et al., 1994). Data extrapolated from similar pots produced by Alfano et al., (2011) and Miyabuchi et al., (2013).	152

Figure 4.4 – Median diameter ($Md\phi$) versus sorting coefficient ($\sigma\phi$) for single locality grain-size data for each eruption. The dashed lines represent 8%, 4%, 2%, 1% contours of Plinian fall deposits from Walker (1971; 1983).153

Table of Tables

Table 1.1 - The volcanic history of Tenerife, modified from Edgar (2003) and Cas et al., (2022) to include data from Davila-Harris et al., (2023)	18
Table 1.2 – All known eruptions from the Las Cañadas Caldera	20
Table 1.3 – All caldera wall deposits uncorrelated to distal deposits	21
Table 2.1 – summarised codes for the lithofacies used in the study, modified from Branney and Kokelaar (2002)	41
Table 2.2 – Nomenclature of eruption deposits in this study	42
Table 2.3 – Error associated with calculating isopach and isopleth maps	44
Table 3.1 – Eruption parameters for the Honduras Formation	54
Table 3.2 - Eruption parameters for the Aguerche Formation	59
Table 3.3 - Eruption parameters for the Mena Formation	72
Table 3.4 - Eruption parameters for the Zarza Formation	87
Table 3.5 - Eruption parameters for the Icor Formation	102
Table 3.6 - Eruption parameters for the El Rincon Formation	107
Table 3.7 - Eruption parameters for the Eras Formation pumice fall	117
Table 4.1 – Eruptions within the Guajara Eruption Cluster and the region they are found, correlations across regions are highlighted in dark grey. Ages are from Davila-Harris et al., (2023)	146
Table 4.2 – Minimum volumes for all pyroclastic deposits on Tenerife where calculated from: ^a Bryan et al., (2000), ^b Edgar et al., (2003;2007), ^c Middleton (2006), ^d Davila-Harris et al., (2009;2023). Ages from: ^e Bryan et al., (1998), ^f Brown et al., (2003), ^g Brown and Branney, (2013)	150

Statement of Copyright

The copyright of this thesis (including any appendices or supplementary materials to this thesis) rests with the author, unless otherwise stated.

© Ryan Bailey, 2025

This copy has been provided under licence to the University to share in accordance with the University's Open Access Policy, and is done so under the following terms:

- This copy can be downloaded for personal non-commercial research or study, without prior permission or charge.
- Any quotation from the work (e.g. for the purpose of citation, criticism or review) should be insubstantial, should not harm the rights owner's interests, and must be accompanied with an acknowledgement of the author, the work and the awarding institution.
- The content must not be changed in any way or sold commercially in any format or medium without the formal permission of the author.

Acknowledgements

I would like to thank Dr Richard Brown for his unwavering support throughout this thesis, both as a supervisor and a friend. From teaching me the basics at GeoTenerife back in 2021, to sharing laughs and stories during weeks of fieldwork on Tenerife, and hopefully to many more research collaborations in the future. I would also like to thank Alexis Schwartz, Sharon Backhouse, and Ignacio Garcia for their support during fieldwork and throughout the completion of this project, without them, this project would not have been possible. Alongside the GeoTenerife Team is all the students over the last 3 years that have contributed to fieldwork on Tenerife. A big thanks to my partner in crime Sparky (Louis), for joining me on this adventure for the whole journey, collecting stories and making it out of Tenerife alive – may our collaboration continue. Then to all those at Durham who have been incredibly supportive and made this master's incredibly enjoyable, particularly Gem, Bex, Katie, David and all those in the Durham Volcanology Group that answered my never-ending list of questions. Finally, thanks to my parents for letting me stay back home to finish this thesis, and to Shes for all the support and love.

Chapter 1: Introduction

1.1 Introduction

Tenerife, located ~350km off the northwest coast of Africa, is the largest intraplate shield volcano of the Canarian Archipelago. A complex volcanic island, starting with a basaltic shield building phase ~12 million years ago (Ma), that over the last ~3 Ma has erupted effusively and explosively, from basaltic to phonolitic in composition, forming scoria cones, composite volcanoes, and the Las Cañadas caldera complex (Marti et al., 1994; Cas et al., 2022). The Las Cañadas volcanic deposits have been separated into a Lower Group, 3.05 Ma to 1.8Ma, and an Upper Group (also known as the Bandes del Sur Group), 1.66 Ma to 0.16 Ma (Middleton et al., 2006; Cas et al., 2022; Dávila-Harris et al., 2023). The Lower Group consists of felsic and mafic lavas and pyroclastic deposits, representing a construction phase within the Las Cañadas edifice (Middleton et al., 2006; Cas et al., 2022). The Upper Group contains three cycles of eruption clusters: The Ucanca cluster (1.84 to 1.31 Ma), the Guajara cluster (0.88 to 0.6 Ma), and the Diego Hernández cluster (0.34 to 0.16 Ma) (Dávila-Harris et al., 2023). They each contain large explosive eruptions and caldera collapse leading to various ignimbrites and pumice fall deposits, typically exposed in the South of Tenerife known as the Bandes Del Sur.

The Guajara eruption cluster is currently understood to record seven ignimbrite-forming eruptions in the southeast Bandas Del Sur, from oldest to youngest: Rio (Dávila-Harris et al., 2023), Morades (Dávila-Harris et al., 2009), Eras (Brown et al., 2003; Middleton et al., 2006), Helecho (Dávila-Harris et al., 2011), Arico (Middleton et al., 2006), Abades (Brown et al., 2003), and Granadilla (Booth, 1973; Bryan et al., 1998; Bryan et al., 2000; Middleton et al., 2006). Studies have focussed on the deposits of the large ignimbrite-forming eruptions (e.g. Bryan et al 1998; Brown et al 2003; Dávila-Harris et al., 2023). However, there are often smaller Plinian and subplinian fall deposits that occur between the formations, such as the Zarza Member, with at least 14 unnamed pumice fall units (UPFU) (Middleton et al., 2006; Dávila-Harris et al., 2009). These unknown fall deposits are yet to be fully constrained despite representing many eruptive episodes not yet factored into eruption frequency estimations and our understanding of eruptive activity on Tenerife.

This project aims to characterise several of these unnamed pumice fall units to attempt to further reconstruct the eruption history of the Las Cañadas edifice. The specific objectives include:

- To identify new pyroclastic deposits in the Bandas Del Sur.
- To constrain the dispersal of several unnamed pumice fall units.
- To provide a more complete stratigraphy of the Guajara Eruption Cluster.
- To correlate the southwest stratigraphy (Davila-Harris et al., 2023) and southeast stratigraphy (Middleton et al., 2006) of the Bandas Del Sur.
- To reconstruct the eruption histories of widespread fall deposits.

This study presents detailed descriptions and interpretations of at least 10 newly described pumice fall deposits in southeast Tenerife, including thicknesses, grain size analysis, componentry and dispersal maps. It documents the correlation of two previously unique ignimbrite-forming eruptions as a singular, large-scale eruption.

1.2 Area of Study

Tenerife is an ideal location for studying pumice fall deposits, with ~2 Ma of explosive volcanic activity recorded across the entire island (Cas et al., 2022). Pyroclastic deposits on the southern flanks of the island are well exposed due to a variety of reasons. Many eruptions were dispersed to the south, with a persistent semi-arid climate reducing erosion from rainfall and consistent soil formation, thereby preserving the deposits (Bechtel, 2016). Intermittent effusive activity resulted in lava flows capping and protecting the underlying pyroclastic deposits, with deep valleys, known locally as barrancos, cutting through the deposits and providing cross-sectional exposure. The southern flanks are partly urbanised, which has generated numerous accessible roadcuts without the destruction of exposures from the development of a large city or town. The southern flanks are also free of large destructive landslide events younger than 0.6 Ma, such as the ~0.54-0.84 Ma Guimar landslide towards Santa Cruz de Tenerife in the north, allowing older deposits to remain intact (Ancochea et al., 1990; Marti et al., 1997). This combination of deposition patterns, climate, topography, volcanic processes, and partial urbanisation has created an ideal setting for studying the island's eruptive history.

1.3 Geological Background

Tenerife has been the subject of volcanological studies since the 1970s, with work on pyroclastic deposits completed by Booth and Walker (unpublished data) and Booth (1973) forming the basis of volcanological studies on Tenerife. Since then, detailed studies have attempted to understand: the chemistry and petrology of magmas (Wolff, 1985; Bryan et al., 2002; Davila-Harris et al., 2013; Horn et al., 2022), the evolution of the Canary Islands (Ancochea et al., 1990; Ancochea et al., 1999; Carracedo et al., 2011; Cas et al., 2022), the eruption dynamics of large ignimbrite-forming eruptions (Bryan et al., 2000; Brown and Branney, 2004; Smith and Kokelaar, 2013; Edgar et al., 2017), and the overall stratigraphy of pyroclastic units (Bryan et al., 1998; Huertas et al., 2002; Brown et al., 2003; Middleton et al., 2006; Davila-Harris et al., 2023). However, previous studies on Tenerife have focussed on the larger-scale eruptive episodes, with little work on the smaller pyroclastic units. The Quaternary succession by Brown et al., (2003) and the new stratigraphic framework of pyroclastic units in the Bandas Del Sur by Davila-Harris et al., (2009;2023) have provided evidence of many smaller-scale pumice fall deposits but lacks detailed descriptions, as they were not the focus of the study. This chapter will review our current understanding of the eruptive history of Tenerife, as well as the nature of pyroclastic deposits and the Plinian eruptions that form them.

1.3.1 Tenerife

Tenerife represents the largest island of the Canary Islands, with an area of 2058 km² and a peak of 3718 m a.s.l (figure 1.1). Each Canary Island, which includes: La Palma, Gran Canaria, Lanzarote, Fuerteventura, La Gomera, and El Hierro, is at a different stage of volcanism (Carracedo, 1999; Guillou et al., 2004). La Palma and El Hierro are within a shield-building stage, and Lanzarote, Fuerteventura, and Gran Canaria in a post-erosional stage (Carracedo, 1999; Carracedo et al., 2007). Typically, intraplate ocean islands, such as Hawaii, are located over fast-moving lithospheric plates and compositionally uniform magmas, as they become submerged from subsidence before magma can evolve (Carracedo et al., 2007; Troll and Carracedo, 2016). However, the Canary Islands are located on the old oceanic crust and subsidence is minimal, therefore Tenerife has experienced a long history of subaerial volcanism allowing for significant magma

differentiation and the growth of large central volcanoes, therefore suggested to be at its peak of development (Guillou et al., 2004; Nelson et al., 2005; Carracedo et al., 2007; Troll and Carracedo et al., 2016). Over the ~12 Ma of volcanic history, Tenerife has produced a wide range of volcanic landforms, e.g. calderas, scoria cones, composite volcanoes, and volcanic domes, and volcanic products, e.g. ignimbrites, lava flows, pumice fall deposits, and debris avalanches. Tenerife has experienced 4 stages of activity:

- Stage I (~12 Ma – 3.9 Ma), a shield-building phase producing basaltic lavas, dykes, and scoria cones, known as the Old Basaltic Series (OBS)
- Stage II (3.05 Ma – 1.8 Ma), the construction of a central volcanic complex known as the Lower Group of the Las Cañadas edifice
- Stage III (1.66 Ma – 0.16 Ma), a period of explosive phonolitic activity, caldera formation, and basaltic flank eruptions, known as the Upper Group
- Stage IV (0.16 – Present), the formation of the bimodal Teide-Pico Viejo composite volcano and basaltic rift volcanism

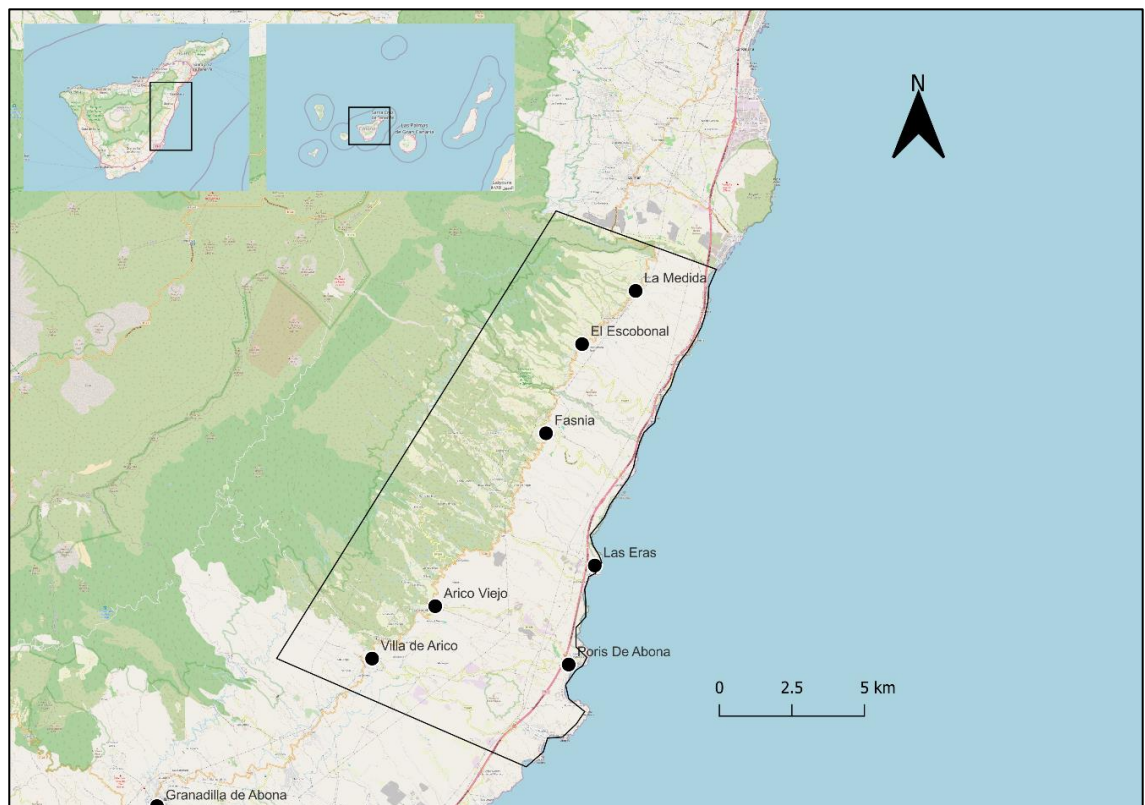


Figure 1.1 – Map of Tenerife, the main study area is within the black box

1.3.1.1 Volcanic History

The oldest deposits on Tenerife, the OBS, represent the initial shield-building volcanism from 11.9 Ma to ~3.9 Ma (Thirlwall et al., 2000; Guillou et al., 2004; Cas et al., 2022). The OBS includes three basaltic massifs - Roque del Conde in the SW, Teno in the NW, and Anaga in the NE (figure 1.2) (Ancochea et al., 1990; Carracedo et al., 2007; Cas et al., 2022). It is assumed that, given the massifs are mostly basaltic, eruptions would have been similar to Hawaii, producing large-scale effusive lava flows (Cas et al., 2022). The end of the OBS is thought to be the 3.0 Ma Boca de Tauce member and therefore there is suspected to be no hiatus before the building of the Las Cañadas edifice at ~3.05 Ma and the beginning of the post-shield volcanic activity (Ablay and Kearey, 2000; Gottsmann et al., 2008; Geyer and Marti, 2010; Cas et al., 2022).

Directly after the OBS saw the construction of a central volcanic complex known as the Las Cañadas edifice, which can be split into two phases, a constructive Lower Group and an explosive Upper Group (table 1). The Lower Group of the Las Cañadas edifice is comprised of mafic and phonolite lavas with minor pyroclastic deposits (Martí et al., 1994; Bryan et al., 1998; Cas et al., 2022). This constructive phase was thought to be from 3.05 Ma to 1.8 Ma, ending with the large explosive eruption recorded by the Gaviotas Formation, and marking the beginning of the recently defined ‘Ucanca Eruption Cluster’ from 1.84 Ma to 1.31 Ma, one of three eruption clusters in the Las Cañadas edifice Upper Group (Davilla-Harris et al., 2023).

The Ucanca Eruption Cluster (1.84 to 1.31 Ma) is one of three eruption clusters within the Upper Group of the Las Cañadas edifice, alongside the Guajara Eruption Cluster (0.88 to 0.6 Ma) and Diego Hernandez Eruption Cluster (0.34 to 0.16 Ma) (Cas et al., 2022; Davilla-Harris et al., 2023). Each eruption cluster composed of a series of phonolite ignimbrites and proximal fall deposits from successive explosive eruptions, separated by a hiatus (Cas et al., 2022; Davilla-Harris et al., 2023). It is likely that explosive eruptions occurred during each hiatus, however, are yet to be identified, dated, or removed from the stratigraphic succession from erosion or major landslide events. Initial evidence of explosive eruptions during the hiatuses was found in dated offshore tephra layers, such as sample 157-953A-5H-1, 56–57 cm dated from 0.5 ± 0.01 Ma to 0.72 ± 0.07 Ma (Bogaard, 1998; Rodehorst et al., 1998).

During the Las Cañadas edifice, three major landslide events occurred on the flanks of Tenerife, most notably the Güímar, La Orotava and Icod landslide valleys. It is

suggested that the lateral collapses of the Icod (<0.16 Ma) and La Orotava (0.54 Ma) landslides, located north of the Las Cañadas caldera, were triggered by vertical collapses of the Abrigo (0.16 Ma) and Granadilla (0.6 Ma) caldera forming eruptions. The Güímar valley may be related to rapid growth of the Dorsal Ridge (0.9 to 0.78 Ma) causing instability (Ancochea et al., 1990; Marti et al., 1997; Cas et al., 2022).

Simultaneously, the Las Cañadas edifice has continued to erupt flank basalts, producing ~297 monogenetic cones and numerous basalt lava flows across Tenerife (Doniz-Paez et al., 2012; Cas et al., 2022). The basaltic volcanism has continued to the present day, burying, subsequently preserving, the pyroclastic deposits from explosive Upper Group volcanism. The basalt volcanism is typically concentrated across three rift zones: the northwest Santiago Rift Zone, the northeast Dorsal Rift Zone, and Southern Volcanic Zone. Recent volcanic activity has most occurred on the Santiago Rift Zone, including the most recent 1909 AD Chinyero scoria cone eruption, and a potential location for a future scoria cone forming eruption.

The end of the Las Cañadas edifice saw the formation of twin stratovolcanoes, Teide and Pico Viejo, that infill the caldera with progressively basalt to phonolite lavas (Ablay and Marti, 2000). Teide and Pico Viejo have produced multiple sub-Plinian eruptions during the Holocene, such as the Boqueron eruption in 5660 BP and Montaña Blanca eruption 2000 years ago, with future eruptions of this magnitude being a significant hazard (Garcia et al., 2011, 2012, 2014).

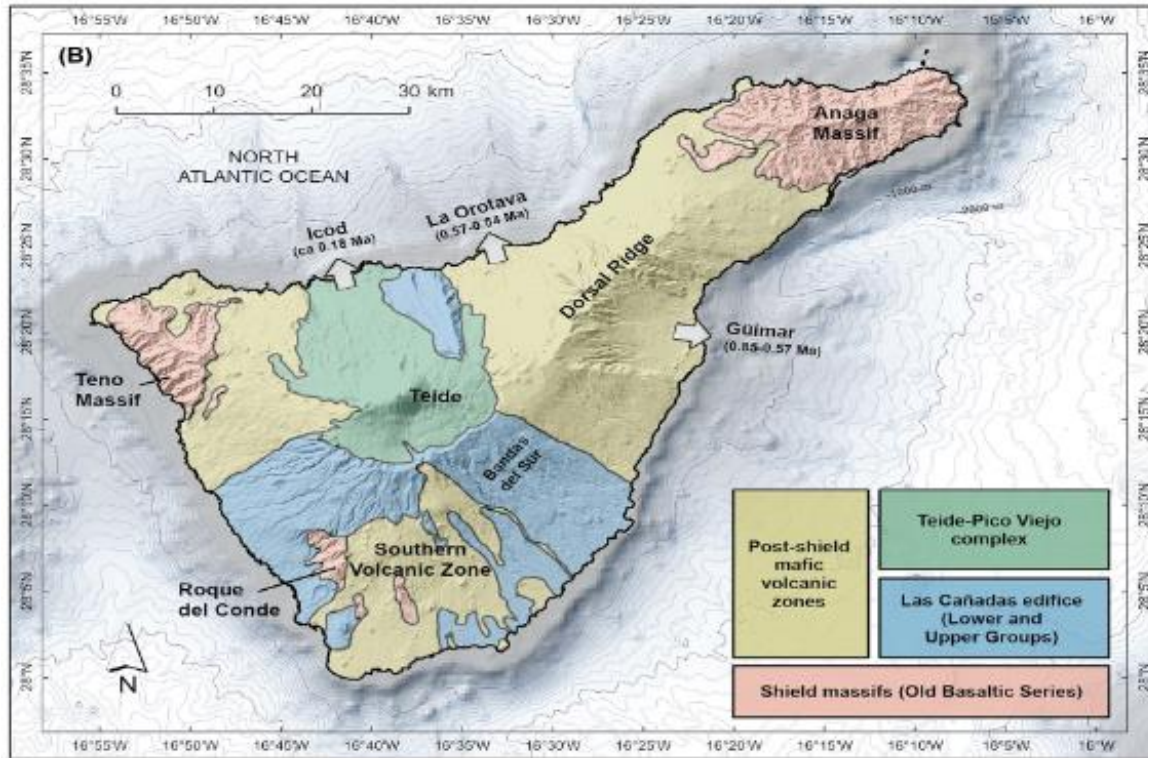


Figure 1.2 - Generalised geological map of Tenerife from Cas et al., (2022).

Table 1.1 - The volcanic history of Tenerife, modified from Edgar (2003) and Cas et al., (2022) to include data from Davila-Harris et al., (2023)

POST SHIELD VOLCANISM	MOST HISTORIC ERUPTIONS				
	Chinyero (1909 AD; Santiago Ridge)				
	Garachico (M. Negra, 1706 AD; Santiago Ridge)				
	Chahorra (1798 AD; Pico Viejo)				
	Boca Cangrejo (1492 AD; Santiago Ridge)				
	Siete Fuentes, Volcan de Fasnía, Las Arenas (1704-1705 AD; Dorsal Ridg Teide (1150 BP)				
	FLANK ERUPTIONS		CENTRAL VOLCANIC COMPLEX		
	DORSAL SERIES (1.8 Ma-)	SANTIAGO SERIES (0.3 Ma-)	TEIDE-PV FMN - Stage IV	Pico Viejo Series 2	Composition: Phonolite (Montana Blanca, ~2 ka; Pico Viejo, 1798)
				Pico Teide Series 2	Composition: Tephriphonolite
				Pico Viejo Series 1	Composition: Plagioclase basanite, phonotephrite, tephriphonolite, phonolite
Pico Teide Series 1				Composition: Plagioclase basanite, phonotephrite, tephriphonolite, phonolite	
Early Episode				Composition: Primitive basanite, alkali basalt (Teide, 0.19-0.16 Ma)	
SERIES III FLANK BASALTS		Las Canadas Edifice	Upper Group - Stage III	↴ Climatic Caldera Collapse (0.16 Ma)	↴ Icod Landslide (0.175-0.19 Ma)
				Diego Hernandez Eruption Cluster (0.34-0.16 Ma)	
				Proximal facies: Non-welded ignimbrites, co-ignimbrite lag breccias, non-welded plinian fall deposits, surge & ash deposits, welded fall and clastogenic lava (La Fortezela only)	
				Distal facies: Non-welded ignimbrites, plinian fall deposits, base surge deposits	
				Caldera Collapses: 4	
SERIES II FLANK BASALTS	SERIES II FLANK BASALTS		Upper Group - Stage III	Composition: Highly evolved phonolite	↴ East Dorsal landslide (<0.56 Ma)
				↴ Climatic Caldera Collapse (0.6 Ma)	↴ La Orotava landslide (0.57-0.54 Ma)
				Guajara Eruption Cluster (0.88-0.6 Ma)	
				Proximal facies: Variably welded ignimbrite & proximal fall deposits, clastogenic lavas, surge deposits.	
				Distal facies: Non-welded ignimbrites, plinian fall deposits, base surge deposits	
SERIES II FLANK BASALTS	SERIES II FLANK BASALTS	Upper Group - Stage III	Maximum Thickness: 250 m (eastern sector)		
			Caldera Collapses: 2		
			Composition: Highly evolved phonolite, interbedded alkali basalt.		
			↴ Guimar landslide (0.85-0.6 Ma)		
			↴ Climatic Caldera Collapse (1.31 Ma)		
SERIES II FLANK BASALTS	SERIES II FLANK BASALTS	Upper Group - Stage III	Ucanca Eruption Cluster (>1.84 Ma - 1.31 Ma)		
			Proximal facies: Variably welded ignimbrite & proximal fall deposits, clastogenic lavas, surge deposits.		
			Distal facies: Welded and non-welded ignimbrites, plinian fall deposits, base surge deposits		
			Maximum Thickness: 375 m?		
			Caldera Collapses: 5		
SERIES II FLANK BASALTS	SERIES II FLANK BASALTS	Upper Group - Stage III	Composition: Phonolite, phonotephrite, interbedded alkali basalt.		
			↴ Climatic Caldera Collapse (1.31 Ma)		
			Ucanca Eruption Cluster (>1.84 Ma - 1.31 Ma)		
			Proximal facies: Variably welded ignimbrite & proximal fall deposits, clastogenic lavas, surge deposits.		
			Distal facies: Welded and non-welded ignimbrites, plinian fall deposits, base surge deposits		
SERIES II FLANK BASALTS	SERIES II FLANK BASALTS	Upper Group - Stage III	Maximum Thickness: 375 m?		
			Caldera Collapses: 5		
			Composition: Phonolite, phonotephrite, interbedded alkali basalt.		
			↴ Climatic Caldera Collapse (1.31 Ma)		
			Ucanca Eruption Cluster (>1.84 Ma - 1.31 Ma)		
SERIES II FLANK BASALTS	SERIES II FLANK BASALTS	Upper Group - Stage III	Proximal facies: Variably welded ignimbrite & proximal fall deposits, clastogenic lavas, surge deposits.		
			Distal facies: Welded and non-welded ignimbrites, plinian fall deposits, base surge deposits		
			Maximum Thickness: 375 m?		
			Caldera Collapses: 5		
			Composition: Phonolite, phonotephrite, interbedded alkali basalt.		
SERIES II FLANK BASALTS	SERIES II FLANK BASALTS	Upper Group - Stage III	↴ Climatic Caldera Collapse (1.31 Ma)		
			Ucanca Eruption Cluster (>1.84 Ma - 1.31 Ma)		
			Proximal facies: Variably welded ignimbrite & proximal fall deposits, clastogenic lavas, surge deposits.		
			Distal facies: Welded and non-welded ignimbrites, plinian fall deposits, base surge deposits		
			Maximum Thickness: 375 m?		
SERIES II FLANK BASALTS	SERIES II FLANK BASALTS	Upper Group - Stage III	Caldera Collapses: 5		
			Composition: Phonolite, phonotephrite, interbedded alkali basalt.		
			↴ Climatic Caldera Collapse (1.31 Ma)		
			Ucanca Eruption Cluster (>1.84 Ma - 1.31 Ma)		
			Proximal facies: Variably welded ignimbrite & proximal fall deposits, clastogenic lavas, surge deposits.		
SERIES II FLANK BASALTS	SERIES II FLANK BASALTS	Upper Group - Stage III	Distal facies: Welded and non-welded ignimbrites, plinian fall deposits, base surge deposits		
			Maximum Thickness: 375 m?		
			Caldera Collapses: 5		
			Composition: Phonolite, phonotephrite, interbedded alkali basalt.		
			↴ Climatic Caldera Collapse (1.31 Ma)		
SERIES II FLANK BASALTS	SERIES II FLANK BASALTS	Upper Group - Stage III	Ucanca Eruption Cluster (>1.84 Ma - 1.31 Ma)		
			Proximal facies: Variably welded ignimbrite & proximal fall deposits, clastogenic lavas, surge deposits.		
			Distal facies: Welded and non-welded ignimbrites, plinian fall deposits, base surge deposits		
			Maximum Thickness: 375 m?		
			Caldera Collapses: 5		
SERIES II FLANK BASALTS	SERIES II FLANK BASALTS	Upper Group - Stage III	Composition: Phonolite, phonotephrite, interbedded alkali basalt.		
			↴ Climatic Caldera Collapse (1.31 Ma)		
			Ucanca Eruption Cluster (>1.84 Ma - 1.31 Ma)		
			Proximal facies: Variably welded ignimbrite & proximal fall deposits, clastogenic lavas, surge deposits.		
			Distal facies: Welded and non-welded ignimbrites, plinian fall deposits, base surge deposits		
SERIES II FLANK BASALTS	SERIES II FLANK BASALTS	Upper Group - Stage III	Maximum Thickness: 375 m?		
			Caldera Collapses: 5		
			Composition: Phonolite, phonotephrite, interbedded alkali basalt.		
			↴ Climatic Caldera Collapse (1.31 Ma)		
			Ucanca Eruption Cluster (>1.84 Ma - 1.31 Ma)		
SERIES II FLANK BASALTS	SERIES II FLANK BASALTS	Upper Group - Stage III	Proximal facies: Variably welded ignimbrite & proximal fall deposits, clastogenic lavas, surge deposits.		
			Distal facies: Welded and non-welded ignimbrites, plinian fall deposits, base surge deposits		
			Maximum Thickness: 375 m?		
			Caldera Collapses: 5		
			Composition: Phonolite, phonotephrite, interbedded alkali basalt.		
SERIES II FLANK BASALTS	SERIES II FLANK BASALTS	Upper Group - Stage III	↴ Climatic Caldera Collapse (1.31 Ma)		
			Ucanca Eruption Cluster (>1.84 Ma - 1.31 Ma)		
			Proximal facies: Variably welded ignimbrite & proximal fall deposits, clastogenic lavas, surge deposits.		
			Distal facies: Welded and non-welded ignimbrites, plinian fall deposits, base surge deposits		
			Maximum Thickness: 375 m?		
SERIES II FLANK BASALTS	SERIES II FLANK BASALTS	Upper Group - Stage III	Caldera Collapses: 5		
			Composition: Phonolite, phonotephrite, interbedded alkali basalt.		
			↴ Climatic Caldera Collapse (1.31 Ma)		
			Ucanca Eruption Cluster (>1.84 Ma - 1.31 Ma)		
			Proximal facies: Variably welded ignimbrite & proximal fall deposits, clastogenic lavas, surge deposits.		
SERIES II FLANK BASALTS	SERIES II FLANK BASALTS	Upper Group - Stage III	Distal facies: Welded and non-welded ignimbrites, plinian fall deposits, base surge deposits		
			Maximum Thickness: 375 m?		
			Caldera Collapses: 5		
			Composition: Phonolite, phonotephrite, interbedded alkali basalt.		
			↴ Climatic Caldera Collapse (1.31 Ma)		
SERIES II FLANK BASALTS	SERIES II FLANK BASALTS	Upper Group - Stage III	Ucanca Eruption Cluster (>1.84 Ma - 1.31 Ma)		
			Proximal facies: Variably welded ignimbrite & proximal fall deposits, clastogenic lavas, surge deposits.		
			Distal facies: Welded and non-welded ignimbrites, plinian fall deposits, base surge deposits		
			Maximum Thickness: 375 m?		
			Caldera Collapses: 5		
SERIES II FLANK BASALTS	SERIES II FLANK BASALTS	Upper Group - Stage III	Composition: Phonolite, phonotephrite, interbedded alkali basalt.		
			↴ Climatic Caldera Collapse (1.31 Ma)		
			Ucanca Eruption Cluster (>1.84 Ma - 1.31 Ma)		
			Proximal facies: Variably welded ignimbrite & proximal fall deposits, clastogenic lavas, surge deposits.		
			Distal facies: Welded and non-welded ignimbrites, plinian fall deposits, base surge deposits		
SERIES II FLANK BASALTS	SERIES II FLANK BASALTS	Upper Group - Stage III	Maximum Thickness: 375 m?		
			Caldera Collapses: 5		
			Composition: Phonolite, phonotephrite, interbedded alkali basalt.		
			↴ Climatic Caldera Collapse (1.31 Ma)		
			Ucanca Eruption Cluster (>1.84 Ma - 1.31 Ma)		
SERIES II FLANK BASALTS	SERIES II FLANK BASALTS	Upper Group - Stage III	Proximal facies: Variably welded ignimbrite & proximal fall deposits, clastogenic lavas, surge deposits.		
			Distal facies: Welded and non-welded ignimbrites, plinian fall deposits, base surge deposits		
			Maximum Thickness: 375 m?		
			Caldera Collapses: 5		
			Composition: Phonolite, phonotephrite, interbedded alkali basalt.		
SERIES II FLANK BASALTS	SERIES II FLANK BASALTS	Upper Group - Stage III	↴ Climatic Caldera Collapse (1.31 Ma)		
			Ucanca Eruption Cluster (>1.84 Ma - 1.31 Ma)		
			Proximal facies: Variably welded ignimbrite & proximal fall deposits, clastogenic lavas, surge deposits.		
			Distal facies: Welded and non-welded ignimbrites, plinian fall deposits, base surge deposits		
			Maximum Thickness: 375 m?		
SERIES II FLANK BASALTS	SERIES II FLANK BASALTS	Upper Group - Stage III	Caldera Collapses: 5		
			Composition: Phonolite, phonotephrite, interbedded alkali basalt.		
			↴ Climatic Caldera Collapse (1.31 Ma)		
			Ucanca Eruption Cluster (>1.84 Ma - 1.31 Ma)		
			Proximal facies: Variably welded ignimbrite & proximal fall deposits, clastogenic lavas, surge deposits.		
SERIES II FLANK BASALTS	SERIES II FLANK BASALTS	Upper Group - Stage III	Distal facies: Welded and non-welded ignimbrites, plinian fall deposits, base surge deposits		
			Maximum Thickness: 375 m?		
			Caldera Collapses: 5		
			Composition: Phonolite, phonotephrite, interbedded alkali basalt.		
			↴ Climatic Caldera Collapse (1.31 Ma)		
SERIES II FLANK BASALTS	SERIES II FLANK BASALTS	Upper Group - Stage III	Ucanca Eruption Cluster (>1.84 Ma - 1.31 Ma)		
			Proximal facies: Variably welded ignimbrite & proximal fall deposits, clastogenic lavas, surge deposits.		
			Distal facies: Welded and non-welded ignimbrites, plinian fall deposits, base surge deposits		
			Maximum Thickness: 375 m?		
			Caldera Collapses: 5		
SERIES II FLANK BASALTS	SERIES II FLANK BASALTS	Upper Group - Stage III	Composition: Phonolite, phonotephrite, interbedded alkali basalt.		
			↴ Climatic Caldera Collapse (1.31 Ma)		
			Ucanca Eruption Cluster (>1.84 Ma - 1.31 Ma)		
			Proximal facies: Variably welded ignimbrite & proximal fall deposits, clastogenic lavas, surge deposits.		
			Distal facies: Welded and non-welded ignimbrites, plinian fall deposits, base surge deposits		
SERIES II FLANK BASALTS	SERIES II FLANK BASALTS	Upper Group - Stage III	Maximum Thickness: 375 m?		
			Caldera Collapses: 5		
			Composition: Phonolite, phonotephrite, interbedded alkali basalt.		
			↴ Climatic Caldera Collapse (1.31 Ma)		
			Ucanca Eruption Cluster (>1.84 Ma - 1.31 Ma)		
SERIES II FLANK BASALTS	SERIES II FLANK BASALTS	Upper Group - Stage III	Proximal facies: Variably welded ignimbrite & proximal fall deposits, clastogenic lavas, surge deposits.		
			Distal facies: Welded and non-welded ignimbrites, plinian fall deposits, base surge deposits		
			Maximum Thickness: 375 m?		
			Caldera Collapses: 5		
			Composition: Phonolite, phonotephrite, interbedded alkali basalt.		
SERIES II FLANK BASALTS	SERIES II FLANK BASALTS	Upper Group - Stage III	↴ Climatic Caldera Collapse (1.31 Ma)		
			Ucanca Eruption Cluster (>1.84 Ma - 1.31 Ma)		
			Proximal facies: Variably welded ignimbrite & proximal fall deposits, clastogenic lavas, surge deposits.		
			Distal facies: Welded and non-welded ignimbrites, plinian fall deposits, base surge deposits		
			Maximum Thickness: 375 m?		
SERIES II FLANK BASALTS	SERIES II FLANK BASALTS	Upper Group - Stage III	Caldera Collapses: 5		
			Composition: Phonolite, phonotephrite, interbedded alkali basalt.		
			↴ Climatic Caldera Collapse (1.31 Ma)		
			Ucanca Eruption Cluster (>1.84 Ma - 1.31 Ma)		
			Proximal facies: Variably welded ignimbrite & proximal fall deposits, clastogenic lavas, surge deposits.		
SERIES II FLANK BASALTS	SERIES II FLANK BASALTS	Upper Group - Stage III	Distal facies: Welded and non-welded ignimbrites, plinian fall deposits, base surge deposits		
			Maximum Thickness: 375 m?		
			Caldera Collapses: 5		
			Composition: Phonolite, phonotephrite, interbedded alkali basalt.		
			↴ Climatic Caldera Collapse (1.31 Ma)		
SERIES II FLANK BASALTS	SERIES II FLANK BASALTS	Upper Group - Stage III	Ucanca Eruption Cluster (>1.84 Ma - 1.31 Ma)		
			Proximal facies: Variably welded ignimbrite & proximal fall deposits, clastogenic lavas, surge deposits.		
			Distal facies: Welded and non-welded ignimbrites, plinian fall deposits, base surge deposits		
			Maximum Thickness: 375 m?		
			Caldera Collapses: 5		
SERIES II FLANK BASALTS	SERIES II FLANK BASALTS	Upper Group - Stage III	Composition: Phonolite, phonotephrite, interbedded alkali basalt.		
			↴ Climatic Caldera Collapse (1.31 Ma)		
			Ucanca Eruption Cluster (>1.84 Ma - 1.31 Ma)		
			Proximal facies: Variably welded ignimbrite & proximal fall deposits, clastogenic lavas, surge deposits.		
			Distal facies: Welded and non-welded ignimbrites, plinian fall deposits, base surge deposits		
SERIES II FLANK BASALTS	SERIES II FLANK BASALTS	Upper Group - Stage III	Maximum Thickness: 375 m?		
			Caldera Collapses: 5		
			Composition: Phonolite, phonotephrite, interbedded alkali basalt.		
			↴ Climatic Caldera Collapse (1.31 Ma)		
			Ucanca Eruption Cluster (>1.84 Ma - 1.31 Ma)		
SERIES II FLANK BASALTS	SERIES II FLANK BASALTS	Upper Group - Stage III	Proximal facies: Variably welded ignimbrite & proximal fall deposits, clastogenic lavas, surge deposits.		
			Distal facies: Welded and non-welded ignimbrites, plinian fall deposits, base surge deposits		
			Maximum Thickness: 375 m?		
			Caldera Collapses: 5		
			Composition: Phonolite, phonotephrite, interbedded alkali basalt.		
SERIES II FLANK BASALTS	SERIES II FLANK BASALTS	Upper Group - Stage III	↴ Climatic Caldera Collapse (1.31 Ma)		
			Ucanca Eruption Cluster (>1.84 Ma - 1.31 Ma)		
			Proximal facies: Variably welded ignimbrite & proximal fall deposits, clastogenic lavas, surge deposits.		
			Distal facies: Welded and non-welded ignimbrites, plinian fall deposits, base surge deposits		
			Maximum Thickness: 375 m?		
SERIES II FLANK BASALTS	SERIES II FLANK BASALTS	Upper Group - Stage III	Caldera Collapses: 5		
			Composition: Phonolite, phonotephrite, interbedded alkali basalt.		
			↴ Climatic Caldera Collapse (1.31 Ma)		
			Ucanca Eruption Cluster (>1.84 Ma - 1.31 Ma)		
			Proximal facies: Variably welded ignimbrite & proximal fall deposits, clastogenic lavas, surge deposits.		
SERIES II FLANK BASALTS	SERIES II FLANK BASALTS	Upper Group - Stage III	Distal facies: Welded and non-welded ignimbrites, plinian fall deposits, base surge deposits		
			Maximum Thickness: 375 m?		
			Caldera Collapses: 5		
			Composition: Phonolite, phonotephrite, interbedded alkali basalt.		
			↴ Climatic Caldera Collapse (1.31 Ma)		
SERIES II FLANK BASALTS	SERIES II FLANK BASALTS	Upper Group - Stage III	Ucanca Eruption Cluster (>1.84 Ma - 1.31 Ma)		
			Proximal facies: Variably welded ignimbrite & proximal fall deposits, clastogenic lavas, surge deposits.		
			Distal facies: Welded and non-welded ignimbrites, plinian fall deposits, base surge deposits		
			Maximum Thickness: 375 m?		
			Caldera Collapses: 5		
SERIES II FLANK BASALTS	SERIES II FLANK BASALTS	Upper Group - Stage III	Composition: Phonolite, phonotephrite, interbedded alkali basalt.		
			↴ Climatic Caldera Collapse (1.31 Ma)		
			Ucanca Eruption Cluster (>1.84 Ma - 1.31 Ma)		
			Proximal facies: Variably welded ignimbrite & proximal fall deposits, clastogenic lavas, surge deposits.		
			Distal facies: Welded and non-welded ignimbrites, plinian fall deposits, base surge deposits		
SERIES II FLANK BASALTS	SERIES II FLANK BASALTS	Upper Group - Stage III	Maximum Thickness: 375 m?		
			Caldera Collapses: 5		
			Composition: Phonolite, phonotephrite, interbedded alkali basalt.		
			↴ Climatic Caldera Collapse (1.31 Ma)		
			Ucanca Eruption Cluster (>1.84 Ma - 1.31 Ma)		
SERIES II FLANK BASALTS	SERIES II FLANK BASALTS	Upper Group - Stage III	Proximal facies: Variably welded ignimbrite & proximal fall deposits, clastogenic lavas, surge deposits.		
			Distal facies: Welded and non-welded ignimbrites, plinian fall deposits, base surge deposits		
			Maximum Thickness: 375 m?		
			Caldera Collapses: 5		
			Composition: Phonolite, phonotephrite, interbedded alkali basalt.		
SERIES II FLANK BASALTS	SERIES II FLANK BASALTS	Upper Group - Stage III	↴ Climatic Caldera Collapse (1.31 Ma)		
			Ucanca Eruption Cluster (>1.84 Ma - 1.31 Ma)		
			Proximal facies: Variably welded ignimbrite & proximal fall deposits, clastogenic lavas, surge deposits.		
			Distal facies: Welded and non-welded ignimbrites, plinian fall deposits, base surge deposits		
			Maximum Thickness: 375 m?		
SERIES II FLANK BASALTS	SERIES II FLANK BASALTS	Upper Group - Stage III	Caldera Collapses: 5		
			Composition: Phonolite, phonotephrite, interbedded alkali basalt.		
			↴ Climatic Caldera Collapse (1.31 Ma)		
			Ucanca Eruption Cluster (>1.84 Ma - 1.31 Ma)		
			Proximal facies: Variably welded ignimbrite & proximal fall deposits, clastogenic lavas, surge deposits.		
SERIES II FLANK BASALTS	SERIES II FLANK BASALTS	Upper Group - Stage III	Distal facies: Welded and non-welded ignimbrites, plinian fall deposits, base surge deposits		
			Maximum Thickness: 375 m?		
			Caldera Collapses: 5		
			Composition: Phonolite, phonotephrite, interbedded alkali basalt.		
			↴ Climatic Caldera Collapse (1.31 Ma)		
SERIES II FLANK BASALTS	SERIES II FLANK BASALTS	Upper Group - Stage III	Ucanca Eruption Cluster (>1.84 Ma - 1.31 Ma)		
			Proximal facies: Variably welded ignimbrite & proximal fall deposits, clastogenic lavas, surge deposits.		
			Distal facies: Welded and non-welded ignimbrites, plinian fall deposits, base surge deposits		
			Maximum Thickness: 375 m?		
			Caldera Collapses: 5		
SERIES II FLANK BASALTS	SERIES II FLANK BASALTS	Upper Group - Stage III	Composition: Phonolite, phonotephrite, interbedded alkali basalt.		
			↴ Climatic Caldera Collapse (1.31 Ma)		
			Ucanca Eruption Cluster (>1.84 Ma - 1.31 Ma)		
			Proximal facies: Variably welded ignimbrite & proximal fall deposits, clastogenic lavas, surge deposits.		
			Distal facies: Welded and non-welded ignimbrites, plinian fall deposits, base surge deposits		
SERIES II FLANK BASALTS	SERIES II FLANK BASALTS	Upper Group - Stage III	Maximum Thickness: 375 m?		
			Caldera Collapses: 5		
			Composition: Phonolite, phonotephrite, interbedded alkali basalt.		
			↴ Climatic Caldera Collapse (1.31 Ma)		
			Ucanca Eruption Cluster (>1.84 Ma - 1.31 Ma)		
SERIES II FLANK BASALTS	SERIES II FLANK BASALTS	Upper Group - Stage III	Proximal facies: Variably welded ignimbrite & proximal fall deposits, clastogenic lavas, surge deposits.		
			Distal facies: Welded and non-welded ignimbrites, plinian fall deposits, base surge deposits		
			Maximum Thickness: 375 m?		
			Caldera Collapses: 5		
			Composition: Phonolite, phonotephrite, interbedded alkali basalt.		
SERIES II FLANK BASALTS	SERIES II FLANK BASALTS	Upper Group - Stage III	↴ Climatic Caldera Collapse (1.31 Ma)		
			Ucanca Eruption Cluster (>1.84 Ma - 1.31 Ma)		
			Proximal facies: Variably welded ignimbrite & proximal fall deposits, clastogenic lavas, surge deposits.		
			Distal facies: Welded and non-welded ignimbrites, plinian fall deposits, base surge deposits		
			Maximum Thickness: 375 m?		
SERIES II FLANK BASALTS	SERIES II FLANK BASALTS	Upper Group - Stage III	Caldera Collapses: 5		
			Composition: Phonolite, phonotephrite, interbedded alkali basalt.		
			↴ Climatic Caldera Collapse (1.31 Ma)		
			Ucanca Eruption Cluster (>1.84 Ma - 1.31 Ma)		
			Proximal facies: Variably welded ignimbrite & proximal fall deposits, clastogenic lavas, surge deposits.		
SERIES II FLANK BASALTS	SERIES II FLANK BASALTS	Upper Group - Stage III	Distal facies: Welded and non-welded ignimbrites, plinian fall deposits, base surge deposits		
			Maximum Thickness: 375 m?		
			Caldera Collapses: 5		
			Composition: Phonolite, phonotephrite, interbedded alkali basalt.		
			↴ Climatic Caldera Collapse (1.31 Ma)		
SERIES II FLANK BASALTS	SERIES II FLANK BASALTS	Upper Group - Stage III	Ucanca Eruption Cluster (>1.84 Ma - 1.31 Ma)		
			Proximal facies: Variably welded ignimbrite & proximal fall deposits, clastogenic lavas, surge deposits.		
			Distal facies: Welded and non-welded ignimbrites, plinian fall deposits, base surge deposits		
			Maximum Thickness: 375 m?		
			Caldera Collapses: 5		
SERIES II FLANK BASALTS	SERIES II FLANK BASALTS	Upper Group - Stage III	Composition: Phonolite, phonotephrite, interbedded alkali basalt.		
			↴ Climatic Caldera Collapse (1.31 Ma)		
			Ucanca Eruption Cluster (>1.84 Ma - 1.31 Ma)		
			Proximal facies: Variably welded ignimbrite & proximal fall deposits, clastogenic lavas, surge deposits.		
			Distal facies: Welded and non-welded ignimbrites, plinian fall deposits, base surge deposits		
SERIES II FLANK BASALTS	SERIES II FLANK BASALTS	Upper Group - Stage III	Maximum Thickness: 375 m?		
			Caldera Collapses: 5		
			Composition: Phonolite, phonotephrite, interbedded alkali basalt.		
			↴ Climatic Caldera Collapse (1.31 Ma)		
			Ucanca Eruption Cluster (>1.84 Ma - 1.31 Ma)		
SERIES II FLANK BASALTS	SERIES II FLANK BASALTS	Upper Group - Stage III	Proximal facies: Variably welded ignimbrite & proximal fall deposits, clastogenic lavas, surge deposits.		
			Distal facies: Welded and non-welded ignimbrites, plinian fall deposits, base surge deposits		
			Maximum Thickness: 375 m?		
			Caldera Collapses: 5		
			Composition: Phonolite, phonotephrite, interbedded alkali basalt.		
SERIES II FLANK BASALTS	SERIES II FLANK BASALTS	Upper Group - Stage III	↴ Climatic Caldera Collapse (1.31 Ma)		
			Ucanca Eruption Cluster (>1.84 Ma - 1.31 Ma)		
			Proximal facies: Variably welded ignimbrite & proximal fall deposits, clastogenic lavas, surge deposits.		
			Distal facies: Welded and non-welded ignimbrites, plinian fall deposits, base surge deposits		
			Maximum Thickness: 375 m?		
SERIES II FLANK BASALTS	SERIES II FLANK BASALTS	Upper Group - Stage III	Caldera Collapses: 5		
			Composition: Phonolite, phonotephrite, interbedded alkali basalt.		
			↴ Climatic Caldera Collapse (1.31 Ma)		
			Ucanca Eruption Cluster (>1.84 Ma - 1.31 Ma)		
			Proximal facies: Variably welded ignimbrite & proximal fall deposits, clastogenic lavas, surge deposits.		
SERIES II FLANK BASALTS	SERIES II FLANK BASALTS	Upper Group - Stage III	Distal facies: Welded and non-welded ignimbrites, plinian fall deposits, base surge deposits		
			Maximum Thickness: 375 m?		
			Caldera Collapses: 5		
			Composition: Phonolite, phonotephrite, interbedded alkali basalt.		
			↴ Climatic Caldera Collapse (1.31 Ma)		
SERIES II FLANK BASALTS	SERIES II FLANK BASALTS	Upper Group - Stage III	Ucanca Eruption Cluster (>1.84 Ma - 1.31 Ma)		
			Proximal facies: Variably welded ignimbrite & proximal fall deposits, clastogenic lavas, surge deposits.		
			Distal facies: Welded and non-welded ignimbrites, plinian fall deposits, base surge deposits		
			Maximum Thickness: 375 m?		
			Caldera Collapses: 5		
SERIES II FLANK BASALTS	SERIES II FLANK BASALTS	Upper Group - Stage III	Composition: Phonolite, phonotephrite, interbedded alkali basalt.		
			↴ Climatic Caldera Collapse (1.31 Ma)		
			Ucanca Eruption Cluster (>1.84 Ma - 1.31 Ma)		
			Proximal facies: Variably welded ignimbrite & proximal fall deposits, clastogenic lavas, surge deposits.		
			Distal facies: Welded and non-welded ignimbrites, plinian fall deposits, base surge deposits		
SERIES II FLANK BASALTS	SERIES II FLANK BASALTS	Upper Group - Stage III	Maximum Thickness: 375 m?		
			Caldera Collapses: 5		
			Composition: Phonolite, phonotephrite, interbedded alkali basalt.		
			↴ Climatic Caldera Collapse (1.31 Ma)		
			Ucanca Eruption Cluster (>1.84 Ma - 1.31 Ma)		
SERIES II FLANK BASALTS	SERIES II FLANK BASALTS	Upper Group - Stage III	Proximal facies: Vari		

1.3.1.2 Explosive Eruptions from the Las Cañadas Caldera

The Las Cañadas caldera has produced numerous pyroclastic deposits within three eruption clusters, typically deposited in a region in SE Tenerife called the Bandas Del Sur. The Ucanca Eruption Cluster contains at least 14 pyroclastic deposits from explosive eruptions, representing the earliest deposits of explosive activity with on average 1 major eruption every 40.8 kyrs, however, there is no evidence for the onset of this activity as the base is not exposed (Davilla-Harris et al., 2009; 2023). There was a ~0.43 Ma hiatus before the beginning of the Guajara Eruption Cluster which will be discussed in further detail in Chapter 1.3.1.3. The Diego Hernandez Eruption Cluster contains at least 16 pyroclastic deposits from explosive eruptions, with 1 major eruption every 25.7 kyrs (table 1.2) (Brown et al., 2003; Brown and Branney, 2004; Edgar et al., 2007; Brown and Branney, 2013; Edgar et al., 2017; Davilla-Harris et al., 2023). The Abrigo formation concluded the large-scale ignimbrite forming eruptions from the Las Cañadas caldera, however explosive, silicic activity has occurred since the Abrigo eruption, such as the 2 ka Montaña Blanca eruption (Ablay et al., 1995; 2000). The Montaña Blanca eruption produced a single, well-sorted, angular phonolite pumice lapilli fall deposit typical of a Plinian eruption across a ~40 km² area. Such eruptions may have occurred throughout the Las Cañadas eruptive history however have yet to be identified or eroded (Ablay et al., 1995).

Table 1.2 – All known eruptions from the Las Cañadas Caldera

*Eruptions found in the caldera wall		
Cluster	Formation	Age (Ma)
Diego Hernandez	Abrigo*	0.169
	Cruz Sequence	-
	La Caleta*	0.221
	Arafo*	-
	Poris*	0.273
	Maja	-
	Fasnía*	0.312
	Taco	-
	Tarta	-
	Guirres	-
	Tarasca	-
	Cabazon	-
	Aldea Blanca*	0.319
	Roque	0.347
	Espigon	-
	Fortaleza*	0.370
Guajara	Granadilla*	0.6
	Abades	-
	Incendio	-
	Arico*	0.668
	Helecho	0.734
	Eras	-
	Moradas	0.738
	Pre-Moradas	-
	Rio	0.747
	Zarza	-
	Blanquitos	-
	Mena	-
	Vegas	-
	Tosca	0.88
Ucanca	Monjas	1.31
	Mocan	1.494
	San Juan	1.5
	Vallito	-
	Adeje	1.577
	Fañabe	1.58
	Barco	1.601
	Pre-Barco	-
	Nicolas	-
	Agua	-
	Morro	-
	Enramada	1.66
	Morteros	-
	Gaviotas	1.84

Identification of caldera wall deposits is complex, with pyroclastic deposits typically forming a continuous succession, without the formation of paleosols in between eruptions, and deposits sharing similar characteristics. Currently, 9 pyroclastic deposits in the caldera wall have been correlated with deposits in the Bandas Del Sur, with 11 pyroclastic deposits identified in the caldera wall without correlation to known deposits (table 1.2 and 1.3) (Marti et al., 1994; Byran et al., 1998; Soriano et al., 2002; Edgar et al., 2003; Middleton, 2006; Soriano et al., 2006). Further deposits have been dated in the Guajara caldera, however, have yet to be constrained to an individual pyroclastic deposit (Marti et al., 1994). It has been suggested that the El Palomar Formation can be correlated with the Eras Formation due to geochemical similarities (Middleton, 2006).

Table 1.3 – All caldera wall deposits uncorrelated to distal deposits

Caldera	Formation/(Sample)	Age (Ma)
Guajara	El Palomar (PA3)	0.71
	Valle Blanco	-
	(G3)	0.754
	La Grieta	-
	Pasajirón (9377)	0.8
	La Camellita	-
Ucanca	(AD32)	0.85
	Los Almendros	-
	Chasna	1.07
	Los Retamares	-
	El Sombrero	-
	Pedro Méndez	-
Lower Group	Boca de Tauce	3.0

1.3.1.3 Guajara Eruption Cluster

The Guajara Eruption Cluster contains at least 14 pyroclastic deposits, including at least 19 unnamed pumice fall units (UPFUs) that are yet to be characterised and understood (Brown et al 2003; Middleton, 2006; Davilla-Harris et al., 2009; Harris et al., 2011; Davilla-Harris et al., 2023). The Guajara Eruption Cluster is thought to include two caldera collapses, the Arico and Granadilla eruptions, due to the presence of extensive lithic breccias and ignimbrite sheets (Davilla-Harris et al., 2023). Although the UPFUs have been identified, not all the units have been correlated from the NE Bandas Del Sur (Middleton, 2006) to the SW Bandas Del Sur (Davilla-Harris, 2009; 2023), and two, or more, different units identified between authors may be the same. The large number of

UPFUs identified poses a challenge towards the understanding of eruptive activity on Tenerife such as eruption frequencies and cyclicity.

There is uncertainty surrounding the stratigraphic position for all UPFUs and the ‘Vegas’ to ‘Zarza’ formations due to the lack of correlation between formations in the differing SE and SW Bandas del Sur stratigraphy. They are mostly known to be below the Eras Formation; however, it is uncertain whether they are found beneath the Rio Formation. Furthermore, the UPFUs mentioned often lack spatial references or descriptions to aid future identification. Unpublished data from Middleton (2006) suggests the Mena, Blanquitos, and Zarza members are exposed in the NE and SE Bandas Del Sur, which could aid correlation to the stratigraphy of Davila-Harris et al., (2023). Middleton (2006) also suggested the deposits are in Las Eras, where Brown et al., (2003) identified 8 unnamed pumice fall deposits (figure 1.3), increasing the likelihood both authors were identifying the same deposits. However, a lack of spatial references and images from Middleton (2006) makes tracing Mena, Blanquitos, and Zarza across Tenerife challenging (figure 1.4). Given the UPFUs are typically described to be thin and uncharacteristic pumice fall deposits, identifying these relatively known deposits will be key in determining the stratigraphic position of the UPFUs-, as well as the ignimbrite bearing Eras and Arico Formations.

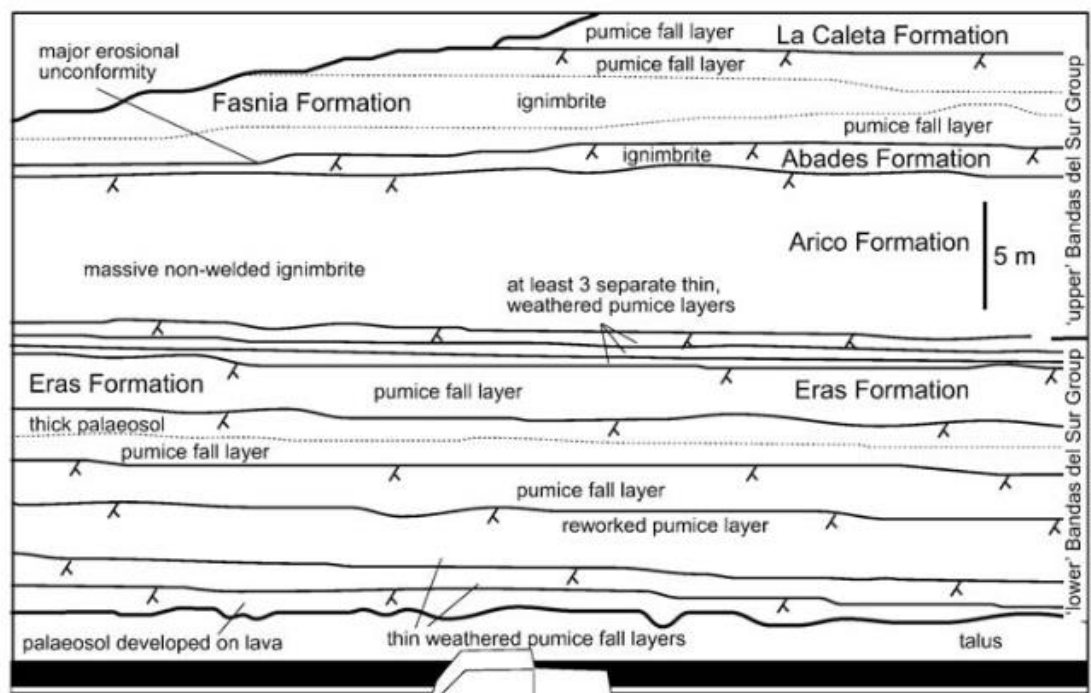


Figure 1.3 - A roadcut near Las Eras comprising of at least 8 UPFUs, by Brown et al., (2003)

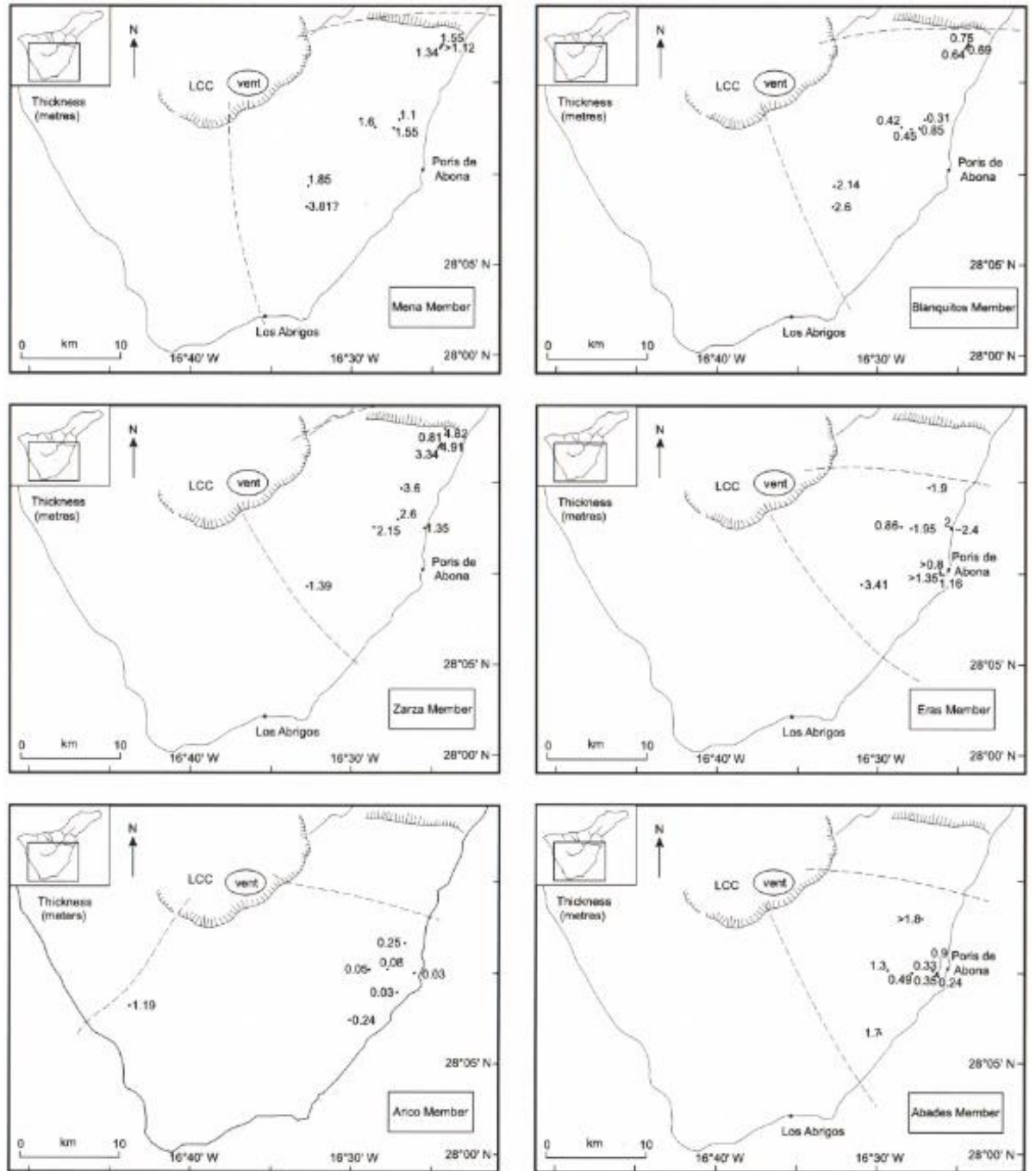


Figure 1.4 – Dispersal maps of Guajara age deposits from Middleton (2006)

1.3.2 Plinian Eruptions

Plinian eruptions are highly explosive eruptions characterised by their high, steady eruption columns containing a mixture of pyroclasts, magmatic gas, and liquid particles, reaching tens of kilometres high (Sparks, 1986; Wilson and Walker, 1987; Carey and Bursik, 2015). Volatiles are a major component in the physical characteristics of magma and a controlling factor in the eruption style of Plinian eruptions. As magma ascends and pressure decreases, dissolved gases like water, carbon dioxide, and sulfur dioxide exsolve, forming bubbly, buoyant foam (Sparks and Whitham, 1986; Sparks et al., 1994). Fragmentation occurs as magma reaches the surface, either through rapid acceleration or decompression, generating a mixture of gas and vesiculated pyroclasts. In highly viscous felsic magmas, gas retention due to inefficient outgassing can lead to explosive eruptions (Gardner et al., 1996; De Vivo et al., 2005; Ruzié and Moreira, 2010; Cashman and Scheu, 2015; Bernard et al., 2022).

Plinian eruptions are classified within the Volcanic Explosivity Index (VEI) of values 4-6, or 7-9 on the modified VEI scale (VEI*) (Wilson, 1976; Walker, 1981; Carey and Sigurdsson, 1989; Valentine and Wohletz, 1989; Pyle, 1998; Cioni et al., 2015; Cas et al., 2024). They deposit well-sorted and coarse pyroclasts, often with a high percentage of juvenile clasts across a wide dispersal, typically alongside welded and nonwelded ignimbrites (Walker, 1981; Cioni et al., 2015). Plinian eruptions are often associated with calderas, and their subsequent collapse, and typically erupt from highly silicic magma ($\text{SiO}_2 > 60 \text{ wt}\%$) tapped from either large magma chambers or compositionally stratified magma chambers (Wilson et al., 1980; Blake, 1981; Carey and Sigurdsson, 1989; Civetta et al., 1991; Cioni et al., 2015; Suhendro et al., 2021). Plinian eruptions have high discharge rates ($>10^6 \text{ kg s}^{-1}$) and exit velocities ($>400 \text{ m s}^{-1}$) sustained for hours to days and can exhibit pulsing, which can be separated by a few hours, ultimately producing volumes of material between 0.1 and 10 km^3 (Carey and Sigurdsson, 1989; Sparks et al., 1994; Cioni et al., 2015; Cas et al., 2024). If the velocity of the plume rising is greater than the wind velocity, a strong vertical plume forms until the density and buoyancy are equal to the surrounding atmosphere, where it spreads laterally (known as the zone of neutral buoyancy H_b), typically at heights $>20 \text{ km}$ (figure 1.5 and 1.6) (Bursik et al., 1992; Woods, 1995; Bonadonna et al., 2015b). The maximum height of an eruption column (H_T) is determined by the eruption rate and volume of erupted magma. The column carries pyroclastic material upward and laterally, with

particles remaining airborne if their terminal fall velocity is lower than the plume's ascent velocity. This process leads to hydraulic sorting of particles, resulting in unimodal grain size distributions. Smaller dense clasts and larger light clasts travel further downwind (Sparks et al., 1992; Pyle, 2016). High-altitude eruption columns can distribute pumice and lithic clasts over large areas (500-5000 km²) as fall deposits, with gradual thinning and fining of deposits away from the vent (Pyle, 1989; Eychenne and Engwell, 2022). Column collapse can occur if its density exceeds that of the surrounding atmosphere, due to insufficient air entrainment, lack of thermal energy, or higher particle density (often related to low water content <0.55%). Variations in grain size may indicate fluctuations in column height. The eruption's duration is controlled by the sustained supply of buoyant magmatic foam within the conduit. Decreasing magma supply and pressure can cause volatiles to migrate downward, potentially leading to caldera collapse and eruption cessation (Sparks and Wilson, 1976; Cioni et al., 2015).

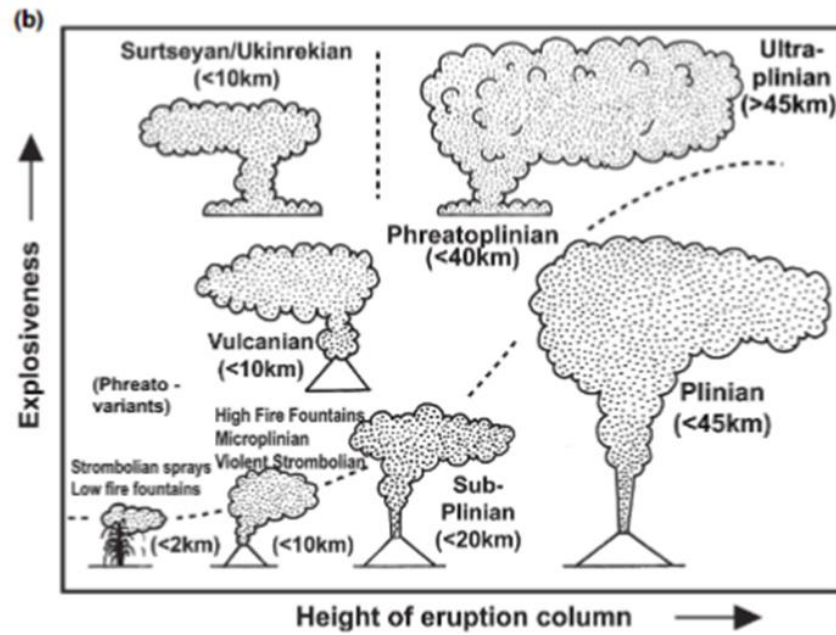


Figure 1.5 - Cartoon explaining the differences in explosiveness and column height for various eruption styles (Cas et al., 2024).

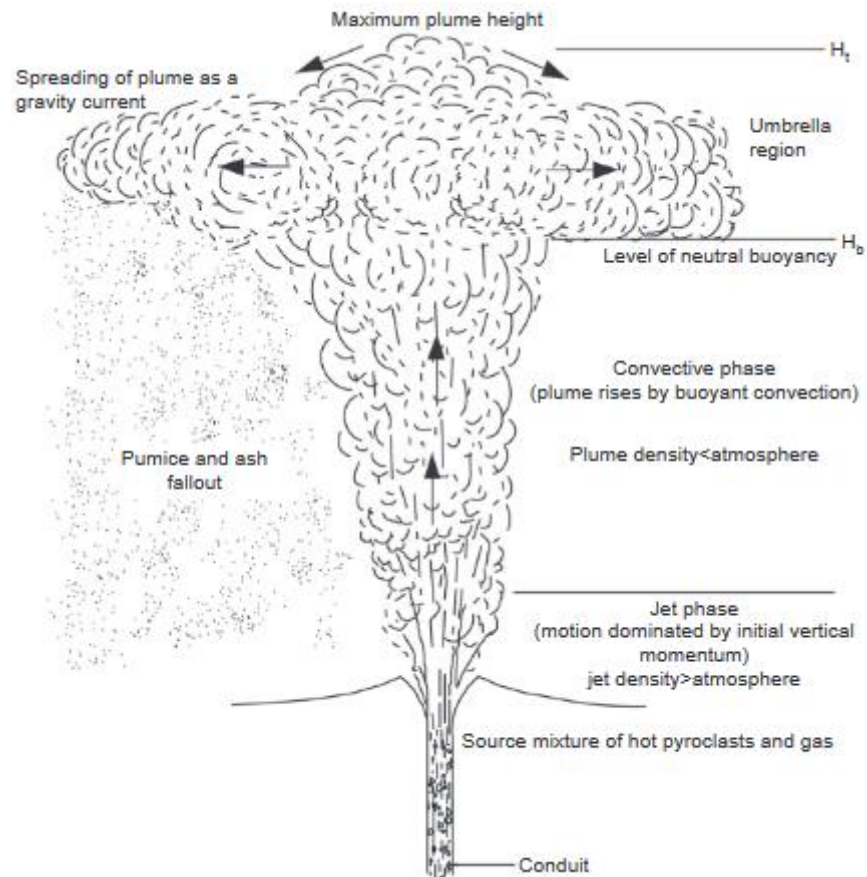


Figure 1.6 - The structure of a volcanic plume from a Plinian eruption (Carey and Bursik, 2015)

The atmosphere significantly influences eruption column physics and pyroclastic material distribution. Wind speed and direction strongly affect plume behaviour and tephra dispersal patterns. Carey and Sparks (1986) demonstrated that higher wind speeds lead to more elongated and narrower dispersal of pyroclasts, with a 30 m/s wind potentially extending the maximum dispersal length of clasts by ~10 km compared to a 10 m/s wind in a 28 km high plume (figure 1.7). Various models for calculating column height have been developed:

1. Wilson et al. (1976): $H_T = 8.2Q^{1/4}$, where Q is energy release in watts.
2. Sparks (1986), simplified by Sparks et al. (1997): $H_T = 1.67\phi^{0.259}$, where ϕ is magma volume discharge rate.
3. Bonadonna and Costa (2013): $H_T = 5.01\lambda_{ML}^{0.55}$, where λ_{ML} is the decay length scale of average maximum clast fining.
4. Aubry et al. (2023): $H_T = 0.345MER^{0.226}$, based on 130 eruptions' average results, where MER is the mass eruption rate.

Each of these formulas, along with numerical models such as Tephra3D and Fall3D, may require sufficient data or observations that ancient eruptions do not preserve. For ancient eruptions with limited data, isopleth contours from maximum clast sizes can be used to estimate column height, as the maximum clast sizes relative to the distance travelled to represent the ability of the eruption plume to transport clasts of a certain size, which is largely dependent on the height and gas thrust velocity of the eruption plume (figure 1.8) (Walker, 1981; Carey and Sparks., 1986; Pyle, 1989; Biass and Bonadonna, 2011; Burden et al., 2011; Houghton and Carey, 2015; Cas et al., 2024). Applications such as TephraFits have been made to use isopleths, as well as isopach and isomass maps, to determine eruption parameters (Biass et al., 2019). Comparing column heights between eruptions can be challenging due to different calculation methods and data availability, potentially leading to misinterpretations.

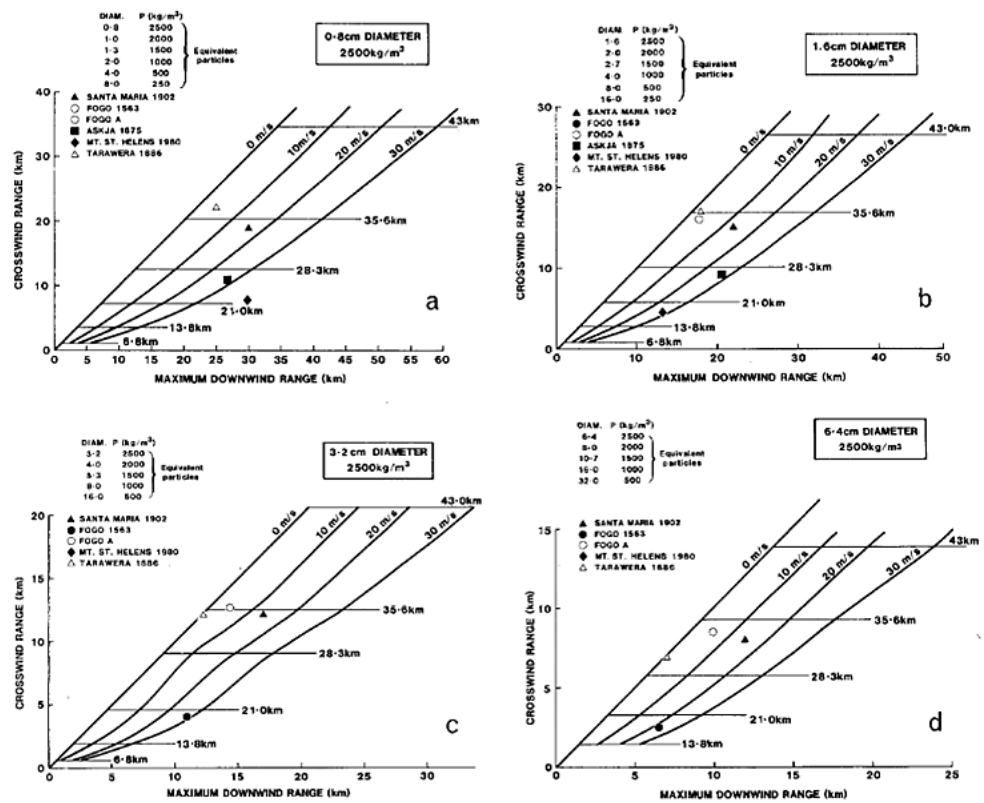


Figure 1.7 - The downwind vs crosswind for 4 different clast sizes from eruption columns between 7 and 43km with windspeeds of 10,20 and 30 m/s (Carey and Sparks, 1986)

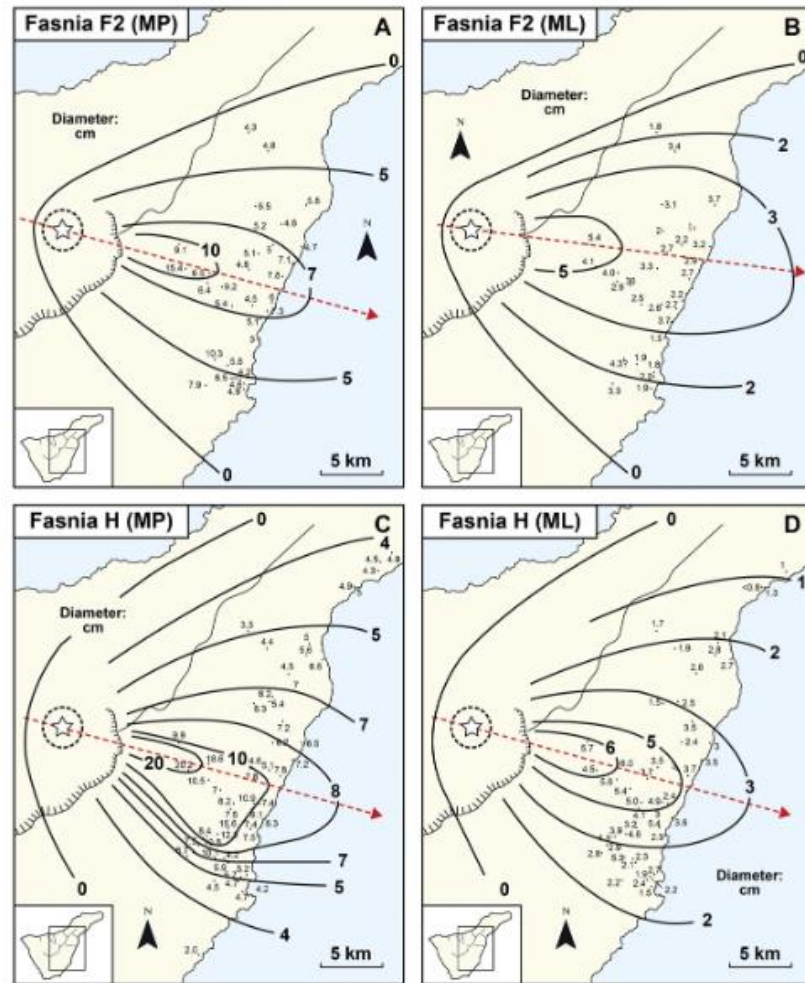


Figure 1.8 - Isopleth maps (Maximum Pumice, MP; Maximum Lithic, ML) constructed from the Fasnía Formation, Tenerife (Edgar et al., 2017)

Subplinian eruptions are smaller scale (VEI 4), with shorter column heights (<20km), narrower dispersal, and lower intensity (10^5 to 10^7 kg s⁻¹) compared to Plinian events (figure 1.9) (Bursik, 1993; Cioni et al., 2003; Cioni et al., 2015). These smaller, weaker plumes can be highly influenced by strong winds and small-scale partial column collapses can occur frequently, which may generate narrow depositional regions and small-scale, proximal pyroclastic density current deposits. Subplinian eruptions often produce bedded deposits, suggesting pulsatory behaviour, such as the 512AD subplinian eruption of Vesuvius (Bursik, 1993; Cioni et al., 2011).

Plinian and Subplinian eruptions can produced compositionally heterogenous deposits, preserving evidence of the magmatic evolution prior or during an eruption, such as magma fractionation, mixing, and recharge (Sparks et al., 1977; Walker, 1981;

Blake, 1981; Wolff, 1985; Cioni et al., 2015; Chamberlain et al., 2016; Melluso et al., 2022; Gonzalez-Garcia et al., 2022). This process can result in deposits characterised by an increasing mafic component from bottom to top or mingled, banded, or streaky pumice of varying compositions throughout the deposit.

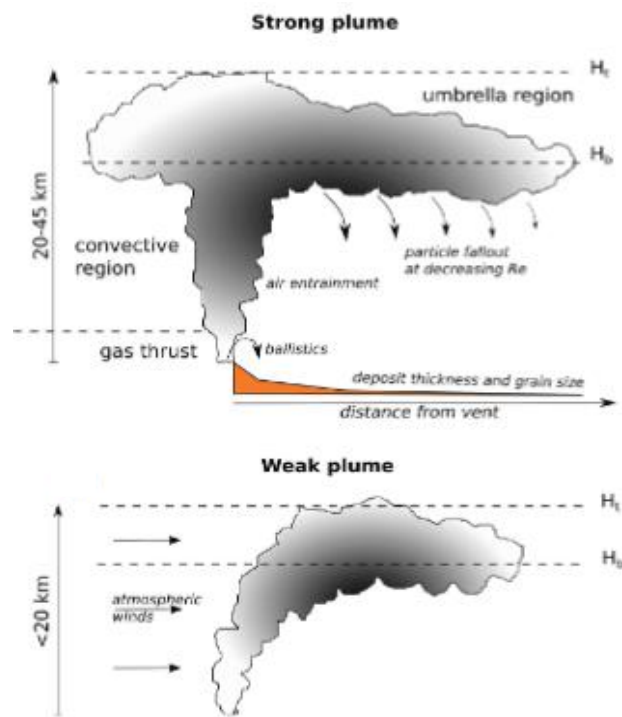


Figure 1.9 - Diagram of a weak and strong plume (Bonadonna et al., 2015b; Cas et al., 2024)

1.3.3 Pyroclastic Fall Deposits

Pyroclastic fall deposits represent the emplacement of volcanic material held within the eruption column until it falls under gravity, with the nature of pyroclastic deposits influenced by plume dynamics, particle characteristics, sedimentation, and atmospheric conditions (Bonadonna et al., 2015b). Therefore, measuring the thickness of deposits, sorting of pyroclasts, grain size distribution, lithic content, vesicularity, and free crystal content are important variables in understanding the nature and reconstruction of Plinian eruptions. Depending on the data availability, the eruption magnitude, exit velocities, column height, mass eruption rate, dispersal areas, and fragmentation rates can be

calculated. However, for ancient deposits that lack the appropriate data, qualitative assessments are useful for interpretations of eruption dynamics.

1.3.3.1 Bedding

Bedding is defined by distinct lateral layers of pyroclastic material through a vertical strata. The bedding of pyroclastic deposits can vary depending on eruption style, intensity, wind conditions, and distance to the vent, seen in varying grain sizes or composition (figure 1.9). A sustained eruption results in a massive, non-graded, with thin ash layers representing pauses in an eruption or changes in eruption intensity. However, brief changes in grain size can also represent wind gusts or changes in wind direction. A challenging aspect of deposits is separating deposits with multiple beds from that of a stratified deposit. Multiple beds should be treated independently when collecting data, calculating unique volumes and eruptive parameters; distinguished by careful mapping of distinct changes in the beds across the dispersal axis. Stratified deposits result from rapid changes in eruption intensity (Cioni et al., 2015; Cas et al., 2024).

Pumice fall deposits often exhibit grading patterns that provide insights into eruption dynamics (Keating and Valentine, 1998; Jurado-Chichay and Walker, 2001; Houghton and Carey, 2015):

1. Normal grading: Grain size decreases upwards, indicating:
 - Waning eruption intensity
 - Possible shift in wind direction
2. Inverse grading: Grain size increases upwards, suggesting:
 - Waxing eruption intensity
 - Potential vent widening
3. Symmetrical grading: Combines normal and inverse patterns, representing:
 - Rapid waxing and waning of the eruption

It is possible that deposits on steep topography can show frequent beds of finer material that have rolled, often exaggerating the thickness of deposits and roundness of clasts within each bed. High lithic contents at the bottom of a deposit could represent the initial opening of a new vent, with lithic-rich horizons throughout the deposit representing potential wall rock instability, erosion, or phreatomagmatic pulses (Pittari et al., 2008; Houghton and Carey, 2015).

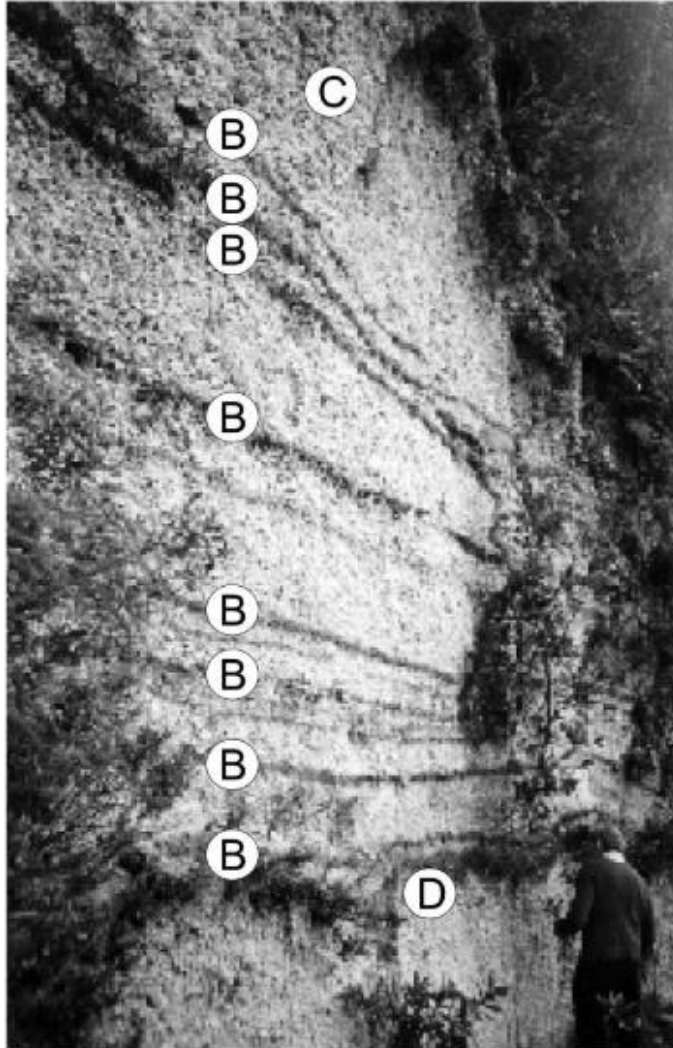


Figure 1.9 - Unit F of the Mangaone Subgroup from the Okataine Volcanic Centre, New Zealand. (D) is the Rotoehu lake shore, followed by a series of bimodal beds (B) that are inversely graded towards the top (C) (Jurado-Chichay and Walker, 2001)

1.3.3.3 Grain Size

Grain size characteristics are a key parameter in understanding pyroclastic fall deposits. The grain size of a deposit represents the fragmentation process, and the height particles of a given size are carried (Houghton and Carey, 2015). In theory, the coarsest clasts are deposited closer to the vent, with finer clasts reaching the distal locations, however, this is dependent on the column height, wind speed and direction, componentry (lithic, pumice and crystal content), and clast densities, which impact the rate of grain size decay (Pyle, 1989; Sparks et al., 1992; Eychenne and Engwell, 2022). There are multiple approaches involving grain size distribution, each dependent on the purpose of the study. Grain size can be measured using $Md\phi$ ($=\phi_{50}$) and Mz ($=[\phi_{16} + \phi_{50} + \phi_{84}]/3$), where the

numbers refer to percentiles coarser than the phi size stated and ϕ is the negative log to the base 2 of the grain size (Houghton and Carey, 2015)

Total Grain Size Distribution (TGSD) requires sample grain size distributions from the whole deposit, including proximal and distal deposits. Such a technique is required to have a complete understanding of the rate of decay of grain size relative to distance from the vent, fractionation of particles in the eruption plume, and bimodality of grain size distributions, however, it is time-consuming, requires a significant number of data points, and is typically for studies focussing on grain size alone with large data points available (Bonadonna and Houghton, 2005). For ancient deposits with few exposures, TGSD may not be appropriate.

Single point grain size analysis can be used for deposits to gain an understanding of the componentry of the deposit, i.e. the fraction of lithic, juvenile, and crystal components that make up the deposit, and quantifying the variations in grain size across varying beds within the deposit. Such a technique is used for studies dealing with multiple eruptions to quantify the differences between them and attempt to reconstruct each eruption (e.g. Juarno-Chichay and Walker, 2000).

Another application of grain size is the maximum pumice (MP) and lithic (ML) clast sizes relative to their distance from the vent source, plotted on isopleth maps (see Chapter 1.3.2).

1.3.3.3.1 Componentry

A typical pyroclastic fall deposit consists of various particle types:

1. Juvenile clasts: Vesiculated magma (pumice or scoria)
2. Lithic fragments:
 - Foreign lithics: Preexisting rock from the vent wall
 - Juvenile lithics: From the erupting magma
3. Crystals: Separated from the melt during eruption
4. Dense glassy non-vesiculated juvenile material (occasional)

These components provide valuable information about the eruption dynamics and the materials involved in the volcanic event (Walker, 1971; 1981; Juarno-Chichay and Walker, 2000; Houghton and Carey, 2015).

Felsic eruptions are dominated by a highly vesicular pyroclastic rock called pumice, typically pale in colour and ranging between ash and block sizes, although

typically found between the ash and lapilli range. Pumice can be found as darker colours, black or brown, that can be related to the composition of erupted magma, although it is possible for colour to bear no significance to magma chemistry or petrology (Paulick and Franz, 1997; Cas et al., 2024). Pumice is often angular or sub-angular, with rounding occurring during transportation. Pumice has typically between 70-80% vesicles that range in morphology, from spherical to tube-shaped. Spherical vesicles could indicate a closed system with little degassing, coalesced vesicles could indicate early vesiculation in the conduit, and tube vesicles can indicate high shear in the magma.

Lithics can include volcanic, metamorphic, plutonic, sedimentary, and hydrothermally altered rock. Lithic clasts can provide information about the subsurface geology and can be used to identify the fragmentation depth if the lithic can be identified to a known stratigraphic unit. Changes in the lithic population can help to identify changes in eruption phases.

Free crystals are incorporated into the eruption plume through the fragmentation process and typically increase in abundance away from the vent, due to having low terminal fall velocities. Free crystals can reflect the magma crystallinity and have been used to obtain deposit volumes (Walker, 1971; Fierstein and Nethenson, 1992). Free crystals can range in morphologies, either as whole euhedral/subhedral crystals, or as crystal fragments.

1.3.3.4 Thickness

The thickness of fall deposits typically decreases with distance from the vent, exhibiting a pattern similar to grain size distribution. Isopach maps and semilog plots of thickness versus the square root of isopach area to determine eruption magnitude and intensity. Pyle (1995;1989) introduced the concept of "thickness half-distance," which calculates the distance required for deposit thickness to halve, assuming a linear or exponential relationship. However, thickness/area plots may deviate from linear or exponential relationships due to several factors. These include steeper thinning rates in proximal deposits, varying settling behaviours of clasts with different sizes and densities, ash aggregation increasing thicknesses in medial areas, and the occurrence of multi-vent eruptions. Field measurements of deposit thickness face additional challenges that must be considered. Paleotopography can affect thickness measurements, with steep slopes potentially leading to downslope creep of pyroclastic material. Soil formation may

introduce inaccuracies in thickness measurements. Furthermore, overlying lava flows can thin deposits by crushing or bulldozing the underlying material.

1.3.3.4.1 Volume

Thickness measurements and isopach maps are valuable tools for calculating deposit volumes, but they come with significant challenges and uncertainties. The main issue is often the lack of accessible distal or extremely proximal deposits and small datasets (Bonadonna and Houghton, 2005). Several models have been developed to estimate deposit volumes (figure 1.10):

1. Pyle (1989) model: Assumes exponential decay of thickness with distance from the vent.

$$V = \frac{13.08T_0b_t^2}{\alpha} \text{ or } V = 13.08T_0b_t^2 + \delta$$
2. Power law method (Bonadonna and Houghton, 2005): Provides better estimates when distal data is missing.
3. Weibull method (Bonadonna and Costa, 2012): Doesn't require segmentation or integration limits.

Each method has limitations and depends on available data. The exponential method tends to underestimate volumes for eruptions with significant distal ash, with large discrepancies possible between the choice of 1, 2, or 3 segments, such as 2 segments resulting in a 29% larger volume than using 1 segment for Layer 5 of the Cotopaxi eruption (Biass and Bonadonna, 2011). The power law and Weibull methods may overestimate volumes with limited data. Software tools like Ashcalc, TephraFits, and TError facilitate calculations and uncertainty analysis (Biass et al., 2014; Daggitt et al., 2014; Biass et al., 2019). For poorly preserved deposits, alternative approaches include:

1. Legros (2000) method: $V = 3.69 T A$
2. Sulpizio et al. (2024) method: Uses two thickness measurements but requires specific distance ratios.

These methods provide options for volume estimation in challenging settings, such as ocean islands, where deposit areas may be limited.

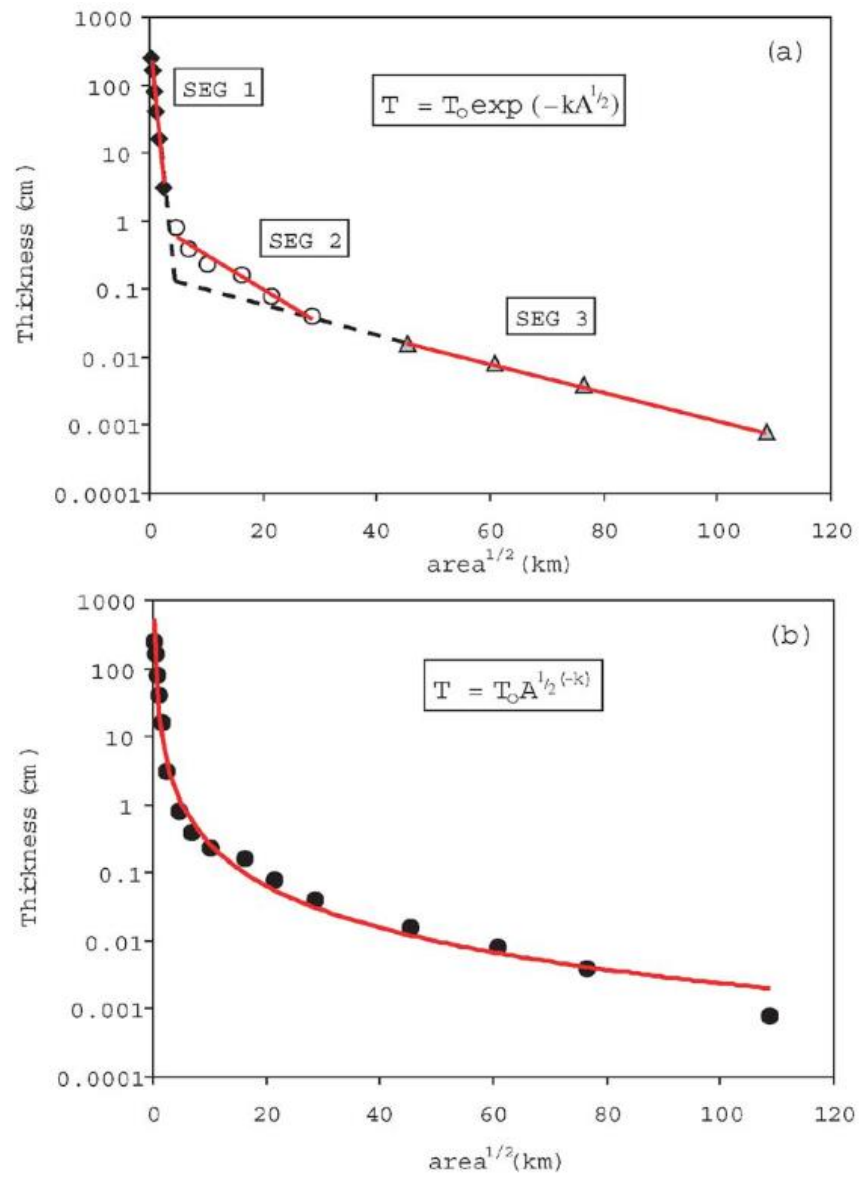


Figure 1.10 - Thickness vs square root area plots for the Ruapehu deposit using the segment method (a) and power-law method (b) (Bonadonna and Houghton, 2005)

Chapter 2: Methodology

2.1 Fieldwork

The project aims to generate a more complete stratigraphy of the Guajara Eruption Cluster in the Bandas Del Sur from southwest to northeast Tenerife and understand the eruptive processes and emplacement of widespread pumice fall deposits. This was achieved through detailed fieldwork identifying and characterising lithofacies. Exposure is generally excellent for the larger, widespread deposits; however, the smaller deposits have limited exposure due to burial from younger deposits and erosional surfaces. This restricted the ability to obtain data for in-depth analysis of all deposits identified.

Fieldwork was divided into two different visits to Tenerife, with 3 weeks in November 2023 and 2 weeks in March 2024, with primary conclusions in this project derived from field observations. Detailed logging of lithofacies was carried out on sections within barrancos, by roadcuts, or abandoned farms and vineyards, identifying, characterising, and interpreting each deposit. Fieldwork was supervised by Dr Richard Brown for 2 of the 5 total weeks, with support given by local geologist Alexis Schwartz of GeoTenerife on occasion.

2.1.1 Field Data Acquisition

The pyroclastic deposits studied were identified and measured at a total of 13 localities, over a $\sim 100 \text{ km}^2$ area, recorded in UTM coordinates, grid zone 28N, provided in Appendix II. At each locality sections were logged, thickness measured where possible, and photographs taken, irrespective of the pyroclastic units identified. Each formation is defined as a single eruptive unit separated by a paleosol.

Thicknesses are likely to be a minimum estimate due to erosion or part of the deposit unexposed to the surface. The thickness was measured from soil top to soil bottom and measured to counteract the deposits angle of emplacement (perpendicular to the dip). Deposits with extreme dip were not measured as they can exhibit exaggerated thicknesses due to the rolling of pyroclasts during emplacement or post-emplacement slumping.

For the units chosen for more detailed analysis, at each locality, the 20-maximum pumice (MP) and lithic (ML) sizes were taken within an unspecified-area section based on the method by Bonadonna et al (2013). The measurements were not taken in situ, with the largest clasts extracted from the deposit and often taken away from the deposit area to measure in the safer, more accessible location.

Sampling was performed when appropriate and 706 photos were taken, some are included as figures within the study.

2.1.2 Sampling

A total of 95 samples were collected from various deposits and localities within the Guajara Eruption Cluster. Samples from each deposit were taken with the purpose of future glass chemistry data that can be used to correlate unknown deposits, a full list is in Appendix I.

2.2 Laboratory Methods

2.2.1 Sieving

Field sieving was performed on 10 unique deposits at the best-exposed locality, with deposits >1m sieved at multiple points in the vertical section or at a change in lithofacies. Pyroclastic deposits were sieved in the field at 0.5 ϕ intervals from 45mm to 4mm, weighed at each interval using field scales, with material <4mm taken as a sample to sieve in the laboratory. The fine fractions were dried in foil containers at 70 °C in an oven for at least 24 hours. The samples were sieved at half ϕ intervals down to 250 micrometres or 355 micrometres depending on the nature of the deposit, as finer material for coarse deposits is likely to be either crushed pumice during transportation or unrepresentative material from other sources.

The size fractions of material were represented as a percentage of the entire sample (course + fine), which can be used to obtain a sorting parameter ($\sigma\phi$) and median grain size ($Md\phi_{50}$). In this study, well-sorted deposits have a $\sigma\phi$ value of 0 to 1, moderately sorted from 1 to 2, poorly sorted from 2 to 4, and very poorly sorted have values of >4, calculated using Gradistatv9.1 (Blott and Pye, 2001).

2.2.1.1 Componentry

Sieved samples for each interval from 2.8mm were analysed until at least 95% of the weight fraction was analysed. Following Houghton and Carey's (2015) recommendation of analysing 200 clasts, a comparative study of 200, 300, 400, and 500 clasts revealed a <2% difference in total lithic clast populations between 200 and 500 clasts, validating the representativeness of the 200-clast sample. Componentry categories included juvenile pumice, scoria, lithic clasts, free crystals, dense juvenile glass, hydrothermally altered clasts, and subvolcanic rocks. Using a binocular microscope, components were separated and counted to determine their percentage fractions. The total number of counted clasts exceeded 22,000, with each clast collected from Icor (UTM: 356554, 3121207), except for the Vigas and Gambuesa Formations collected at Icor Vineyard (UTM: 357813, 3121561).

To calculate a weight percent, as the mass of particles is too light to be accurately measured using scales, an average density for each component was used to calculate the mass of a singular clast at any given fraction. Lithic clasts, free crystals, and hydrothermally altered clasts were average to 0.0026 g/cm³, scoria at 0.0024 g/cm³, subvolcanic rock at 0.0027 g/cm³, and juvenile glass at 0.00242 g/cm³ (the density of phonolite magma (Seifert et al., 2013)). As the density of pumice varies with grain size significantly from -1.5 ϕ to 1.5 ϕ , and between unique deposits, an average density would lead to significant errors. Therefore, density was calculated for individual grain size fractions using the weighed mass of the pumice components of a given grain size. As the proportions of components change between grain sizes, with pumice dominating coarser fractions, the total proportions of components were estimated by combining the componentry data in each fraction with grain size data (total wt% for each fraction) and normalised to 100%.

2.2.1.2 Limitations

Wind was a large limitation when sieving in the field as it caused large fluctuations in weight measurements, leading to deviations as large as 5% when comparing the initial weight to the total sieved weight. Furthermore, there was typically ~5% of material <1 ϕ that was crushed material from transportation, wind-blown dust, or soil particles, and not representative of the analysed unit, although in a few of the finer-grained deposits, this value rose to as much as 9%. It is important to note that in such a scenario, >90wt% of

the deposit is analysed and therefore representative. During componentry analysis, it is challenging to identify the source and composition of rock components and identification is likely to have errors.

Due to the inaccessibility of high precision scales, the mass of individual components could not be easily measured. Therefore, using an average density of components to calculate mass is likely to incur errors that cannot be quantified.

2.3 Lithostratigraphy and lithofacies

Although various lithostratigraphic terminology has been used on Tenerife, the mappable units are described as a formation following the scheme used for the Bandas Del Sur deposits used previously (e.g. Brown et al., 2003; Davila-Harris et al., 2011; Davila-Harris et al., 2023). Formations are described as singular eruptions, which can be subdivided into members that correspond to phases within the eruption. Members can be further divided into units, described as lithofacies using lithofacies codes (table 2.1). Where present, palaeosols and sediments are recorded as they represent periods of repose between volcanic eruptions. Existing formation and member names have been used following Davila-Harris et al (2023) to remain consistent with the literature, with new names and definitions for eruptive deposits not previously described.

Each pyroclastic deposit was described using a lithofacies approach, previously discussed for volcanic rocks by Cas and Wright (1987), that can characterise a body of rock, a facies, by its colour, grain size, geometry, texture, and internal structure. The lithofacies used in this study are modified from Branney and Kokelaar (2002) to suit the needs of this study and represent the structure, grain size, and internal architecture of the unit.

Table 2.1 – summarised codes for the lithofacies used in the study, modified from Branney and Kokelaar (2002)

Code	Lithofacies
mpL	Massive pumice lapilli
spL	Stratified pumice lapilli
dspL	Diffuse stratified pumice lapilli.
mLT	Massive lapilli-tuff
plens	Lens of pumice lapilli

Code	Meaning
T	Tuff
LT	Lapilli-Tuff
L	Lapilli
l	Lithics
m	Massive
s	Stratified
p	Pumice-rich
o	Obsidian-rich
sc	Scoria-rich
lens	Lens
cr	Crystal-rich
l	Lithic-rich

2.3.1 Stratigraphy Nomenclature

Following the classification of Brown et al (2003) and Davila-Harris et al (2023), pyroclastic units are separated by bounding paleosols, where a singular eruptive episode is considered a formation and given a name (typically related to nearby towns). Further subdivisions are based on clear changes in deposit structure and architecture, within a singular formation, that is consistent across the study area. These subdivisions are lettered from A at the bottom and sequentially go through the alphabet to the top of the formation. Where formations or members have been previously identified, the nomenclature remains consistent, however, the nomenclature for existing deposits has been changed where sufficient new data is available (table 2.2).

Table 2.2 – *Nomenclature of eruption deposits in this study*

This Work	Previous Studies
Gambuesa	New
Vigas	New
Sombrera	New
Eras (Moradas)	Brown et al (2003) and Davila-Harris et al (2023)
El Rincon	New
Carretas	New
Arco	New
Icor	New
Zarza	Zarza Member from Middleton (2006)
El Escobonal	New
Mena	Mena Member from Middleton (2006)
Jurado	New
Aguerche	New
Honduras	New
La Linde	New

2.4 Data Analysis

2.4.1 Isopach and Isopleth Maps

The isopach and isopleth maps were hand drawn due to several uncertainties: lack of data points, lack of proximal and distal data, incomplete contours (e.g. only one-half of the thinning data is available), and uncertainty of the vent location. Hand-drawn isopach and isopleth maps are common but include an essence of bias which can lead to uncertainty and therefore extrapolation of data is not possible (Engwell et al., 2015). The vent location is largely uncertain, therefore the isopach contours were drawn up to the caldera wall, with the vent location assumed to be within the Guajara caldera. The contours were limited to the coastline of Tenerife, as there is no offshore data and isopach contours are often not regular shapes.

2.4.2 Estimating Eruptive Parameters

To calculate eruptive parameters the *tephraFits* program was used, as it incorporates multiple methods to obtain estimates for volume, VEI, column height, and eruption

classifications. Data inputs can be easily edited to suit the needs of the user to obtain the most accurate estimate possible, providing guidance when needed to streamline the calculations (Biass et al., 2019). The three methods calculated include:

- 1) The exponential method (Pyle, 1989; Fierstein and Nathenson, 1992)
 - Calculated using 1-3 segments
- 2) The power-law method (Bonadonna and Houghton, 2005)
 - Proximal limit defined from the exponential limit
 - Distal limit set to 200km
- 3) The Weibull method (Bonadonna and Costa, 2012)
 - RSE range set from 0.1 to 1000

Each of these methods can be used to calculate:

- 1) Volume: Isopach thickness and $\sqrt{\text{area}}$
- 2) Clast half-distance: Isopleth clast diameter (lithic and pumice clasts) and $\sqrt{\text{area}}$
- 3) VEI

The result from using the exponential and Weibull methods can be used to plot on the classification schemes of Pyle (1989) and Bonadonna and Costa (2013).

Column height can be calculated from isopleth data using a Matlab program implementing the Carey and Sparks (1986) model (Biass et al., 2015). The four inputs required are:

- 1) Downwind distance (km)
- 2) Crosswind distance (km)
- 3) Clast diameter (cm)
- 4) Clast density (kg m^{-3})

The downwind and crosswind distances were calculated from the same isopleth maps used for the *tephraFits* model. Pumice clast densities are significantly varied for each deposit, therefore using lithic clast isopleth maps are more reliable, stating a clast density of 2500 kg m^{-3} .

2.4.3 Limitations

Calculating eruption parameters accompanies many errors, both in the drawing of isopachs and isopleths, and in the empirical formulas used. The errors associated with isopach and isopleth maps has been quantified by various authors and summarised by Biass et al., (2019).

Table 2.3 – Error associated with calculating isopach and isopleth maps

Isopach	Natural variance	30%	Engwell et al., (2013)
		9%	
	Observational error	4% (Proximal)	Le Pennec et al., (2012)
		8% (Medial)	
		21% (Distal)	
	Data contouring	7%	Engwell et al., (2013)
		15-40% (Proximal)	Klawonn et al., (2014a, b)
		<10% (Medial)	
Isopleth		20-25% (Distal)	
	Clast characterisation	10%	Bonadonna et al., (2013)
	Averaging technique	Up to 100%	

Tephra deposits are often subject to erosion, reworking, and often have limited exposure, particularly on ocean islands where distal deposits are not exposed. Therefore, datasets are often small (<50 data points), and anomalies are impactful. Only few deposits exhibited their maximum thickness and clast sizes at the outer edge of their dispersal, therefore it was assumed one half of the dispersal is available and the isopach and isopleth contours are mirrored. Furthermore, the vent location is highly uncertain, estimated to be within the Guajara caldera. Therefore, actual isopach and isopleth contours may significantly differ from those estimated.

Each computational method is then required to interpolate an extreme amount of data, leading to errors in results. The power-law method requires a proximal and distal limit to be defined, which for small datasets, is highly subjective and can lead to dramatic overestimations of volume. The Weibull method requires a ranged input to calculate residual standard error, that is best determined using multiple iterations and interpreting the results. The Weibull method can be highly sensitive to individual data points. The computation error can be partially quantified using the probabilistic assessment within the *tephraFits* program. Final values are therefore calculated using the 5th and 95th percentile error bounds from 100 simulated runs of the program.

Given the error uncertainty in calculating column height and volume, therefore VEI and eruption classification, it is not appropriate to provide results for all deposits. Results were not calculated for eruptions where only a singular isopach could be made or

produced extreme results. Nevertheless, any estimated eruption parameter should be treated with caution.

Chapter 3: Results

3.1 Stratigraphic Succession of NE Bandas Del Sur

The region defined as NE Bandas Del Sur ranges from Arico El Nuevo and Poris de Abona to the Guimar Valley, where at least 19 eruptive units older than the 0.668 Ma Arico Formation can be found (figure 3.1). Each eruptive unit, including unidentified units, is described in detail

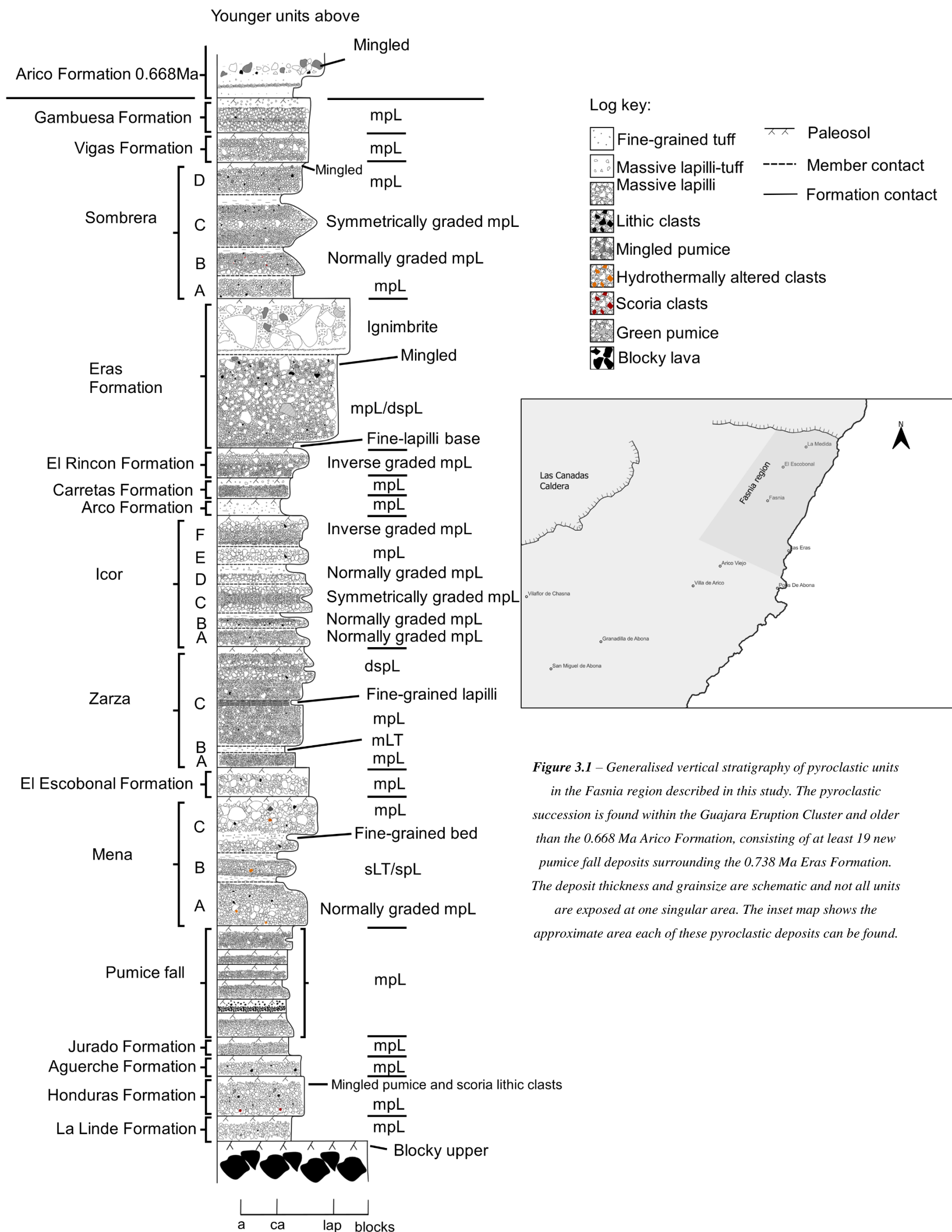


Figure 3.1 – Generalised vertical stratigraphy of pyroclastic units in the Fasnía region described in this study. The pyroclastic succession is found within the Guajara Eruption Cluster and older than the 0.668 Ma Arico Formation, consisting of at least 19 new pumice fall deposits surrounding the 0.738 Ma Eras Formation. The deposit thickness and grain size are schematic and not all units are exposed at one singular area. The inset map shows the approximate area each of these pyroclastic deposits can be found.

3.1.1 La Linde Formation

La Linde is seen at one location at Icor Vineyard (figure 3.2), near Barranco de la Linde where this formation bears its name, and is inferred to be the oldest formation in the stratigraphy. The La Linde formation is 10 cm thick, massive, moderately sorted, medium to fine-grained, sub-angular pumice lapilli (figure 3.3). The pumice is <2 cm in diameter, cream, aphyric, and typically microvesicular, although when present vesicles are elongated between 1-2 mm in length. The deposit has a low content of lithic clasts (2-3 vol%) that are <5 mm in diameter. The deposit drapes into the blocks of underlying lava and has a sharp contact with the soil above, which is 40 cm thick, orange to brown, and includes scattered pumice lapilli and large blocks of lava (>64 mm), before the Honduras Formation.

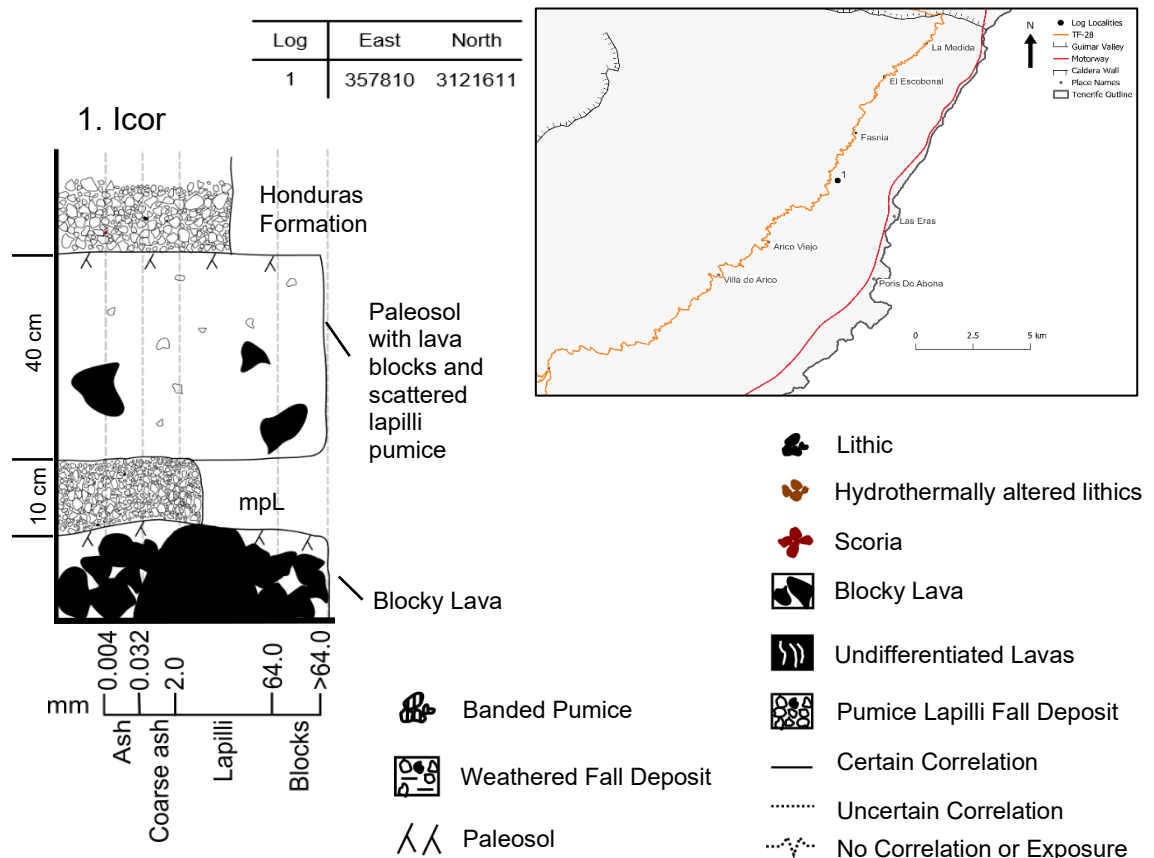


Figure 3.2 - Stratigraphic log of the La Linde Formation. UTM coordinates and inset map of locations are provided. The log represents stratigraphic relationships with under- and overlying units.

Interpretation:

The medium to fine-grained, vesiculated pumice lapilli suggests the La Linde Formation is a deposit from a Plinian eruption with an easterly directed eruption column. The thinness and lack of widespread dispersal suggest this is a small-volume eruption which has been largely buried or eroded, however further data is required to make interpretations with greater certainty. The La Linde Formation represents the bottom of this set of stratigraphy in the SE Bandes Del Sur, however, uncertainties remain whether it is the beginning of the Guajara Eruption Cluster due to the thick lava underlying the deposit. Given the lack of distribution, lateral inconsistencies, and size of the deposit, no further analysis was performed on this formation.

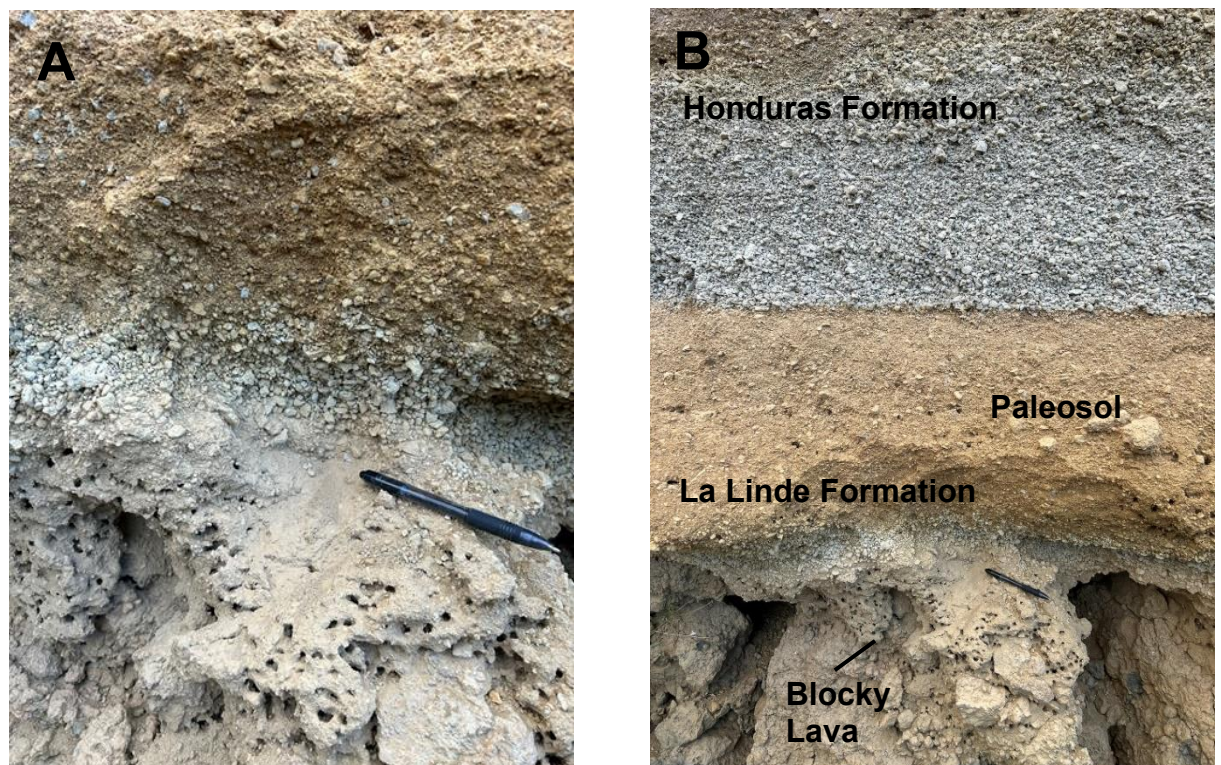


Figure 3.3 - Images of the La Linde Formation. A) Close up of the fine-grained lapilli above the blocky lava. B) Stratigraphic position of the La Linde Formation beneath the Honduras Formation

3.1.2 Honduras Formation

The Honduras Formation is often exposed at the bottom of the stratigraphy and is a newly identified pumice fall deposit, named after Punta de Honduras near its original identification in Las Eras. The type locality is located on a roadside west of Mirador de las Eras, resting at an angle of $\sim 15^\circ$ beneath a weathered, pumiceous paleosol and above

a blocky upper surface of a lava flow (Site 1, figure 3.5). The Honduras formation is exposed across $\sim 19\text{km}^2$ of SE Tenerife between Mirador de las Eras and Fasnía scoria cone. At the type locality, it is 86 cm thick, normally graded, and composed of moderately sorted, medium to fine-grained, angular pumice lapilli. As the deposit grades it becomes more poorly sorted, although as the deposit thins towards the east, it becomes entirely moderately sorted and more massive, with typical thicknesses <50 cm (figure 3.4). A distinct characteristic in the field is the lithic content (5-10 vol%), with abundant large red and black vesiculated scoria found throughout, alongside obsidian and lava. The pumice is typically <5 cm with sparse pyroxene (?) and sanidine phenocrysts. Generally, pumice is microvesicular, with few elongated vesicles at <1 mm in length. Abundant banded pumice can be found towards the top of the deposit. It is commonly found beneath the Aguerche formation and rests at the base of the stratigraphic sequence above a lava flow or the surface of present-day soil. The Honduras Formation grades upwards into a <40 cm thick, light brown paleosol, with scattered pumice clasts and abundant lithic clasts.

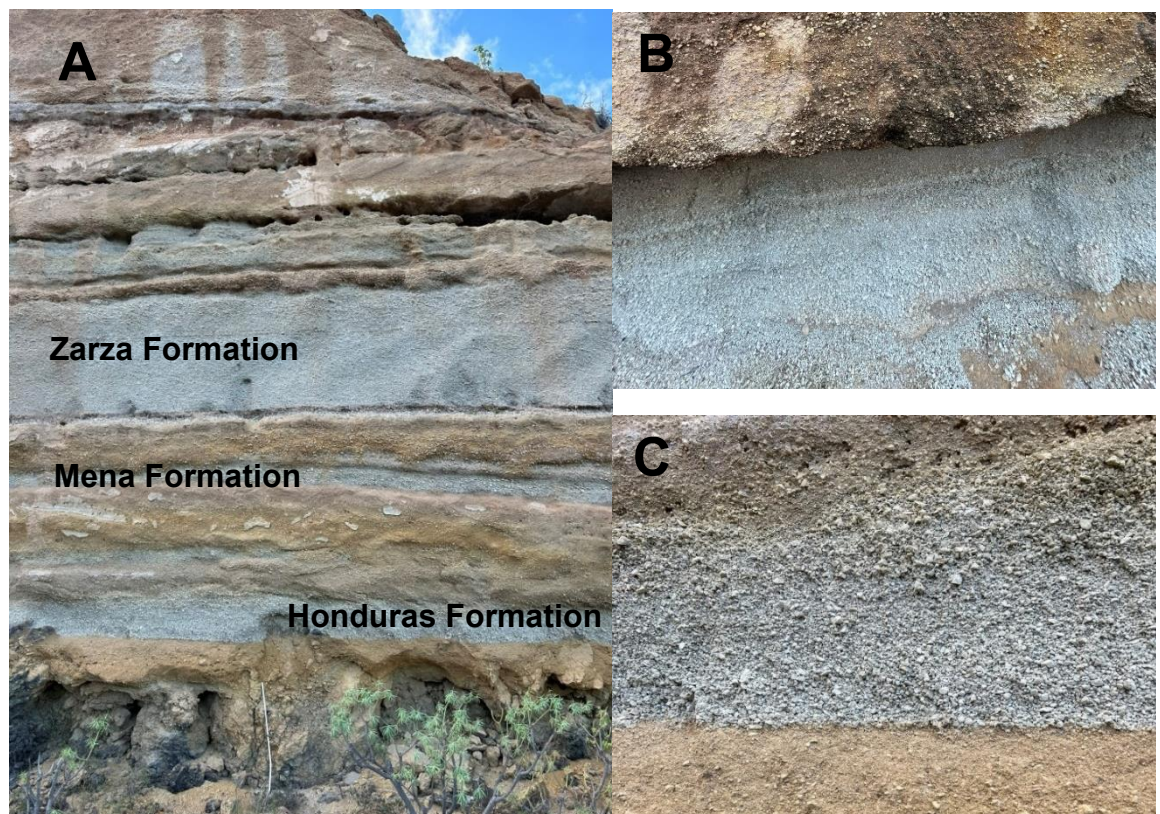


Figure 3.4 - The Honduras Formation at various localities A) Stratigraphic sequence at Icor Vineyard. B) Honduras Formation at the type locality C) Honduras Formation at North Icor

Honduras Formation

Southwest →

← Northeast

1. Mirador de las Eras
(Type Locality)

2. TF-622
Windfarm

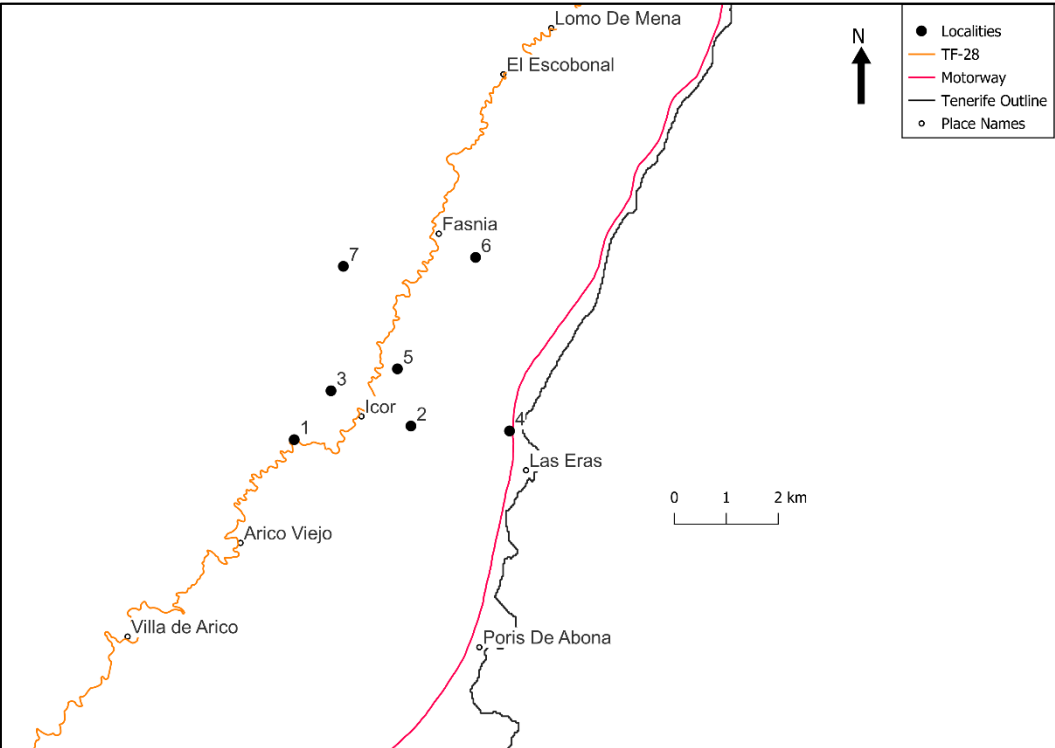
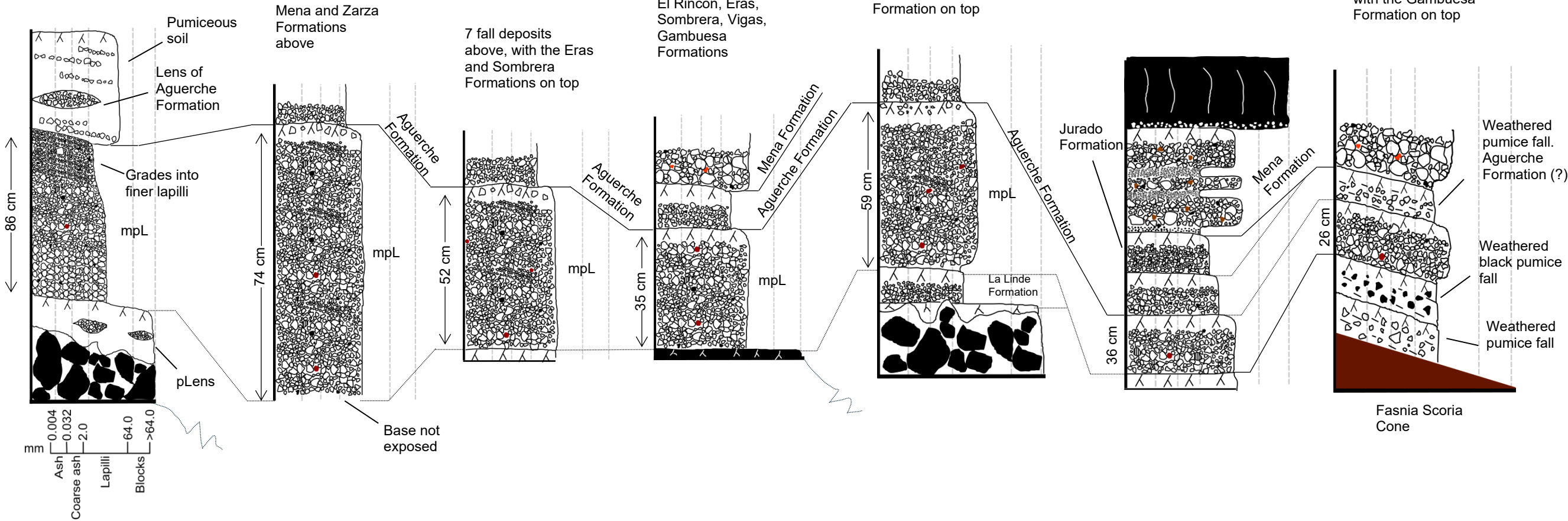
3. North Icor

4. Las Eras

5. Icor Vineyard

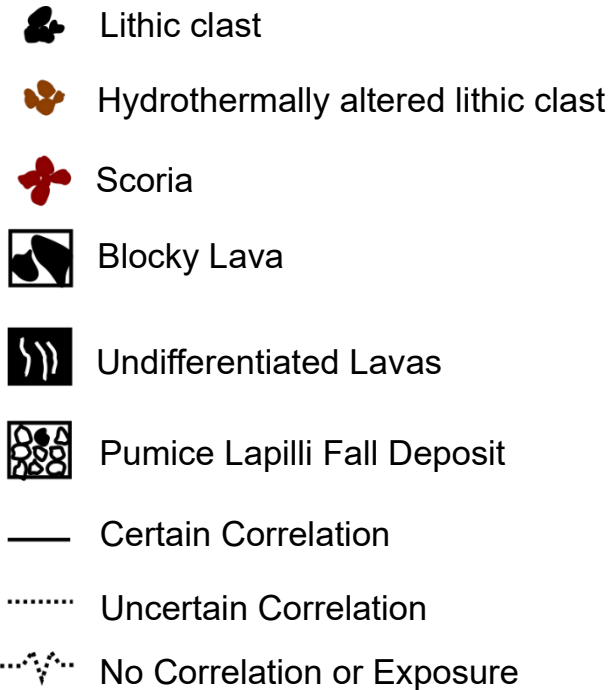
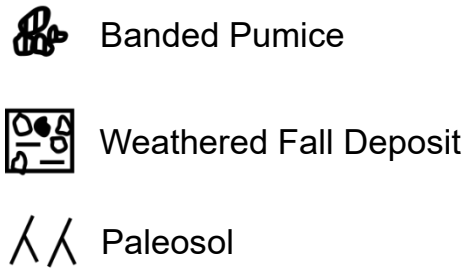
6. Sabina Alta

7. Fasnía
Cone



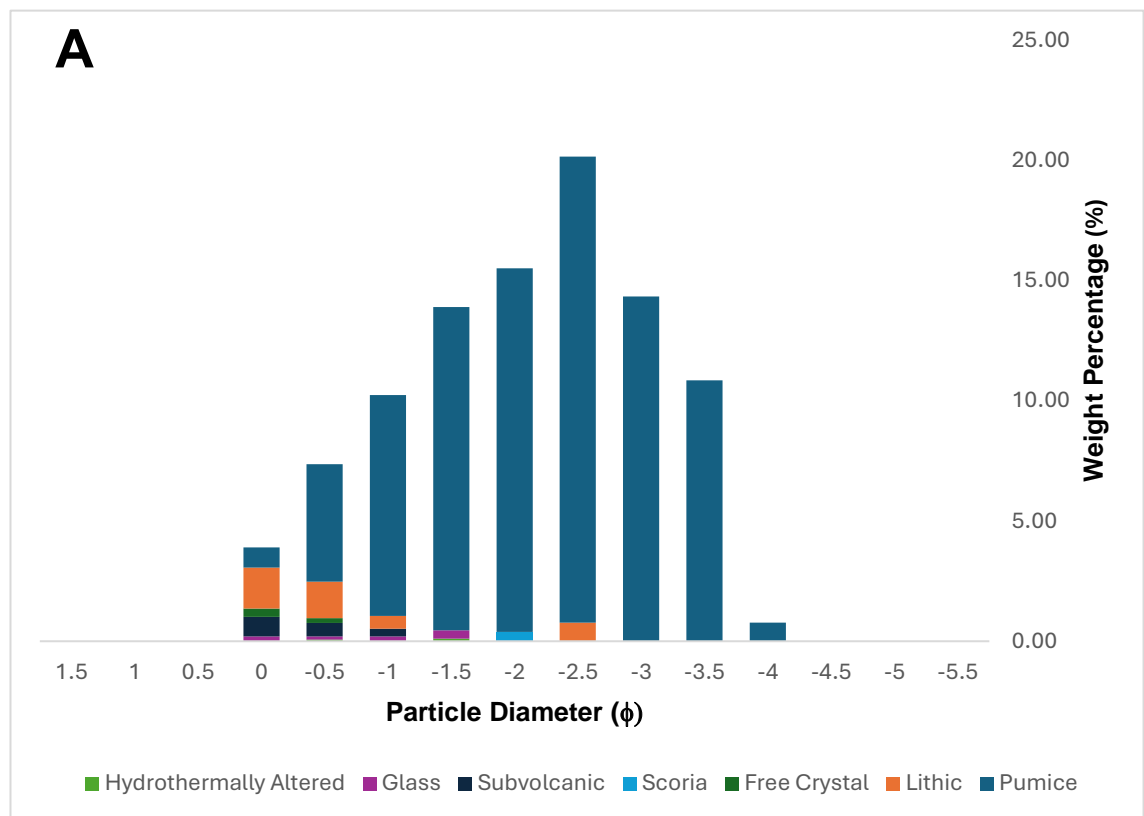
Log	East	North
1	355807	3120280
2	358057	3120514
3	356527	3121207
4	359953	3120397
5	357810	3121611
6	356793	3123587
7	359340	3123727

Figure 3.5 - Stratigraphic logs of the Honduras Formation across the Fasnía Region. UTM coordinates and inset map of locations are provided. The logs represent stratigraphic relationships with under- and overlying units.



Grain-Size and Componentry:

The Honduras Formation was sieved northwest of Icor at the top of Barranco de Icor O las Carretas, ~1.3 km NW of the type locality, in 0.5ϕ intervals from -5.5ϕ to -2ϕ and in the laboratory from -1.5ϕ to 1.5ϕ . The deposit is unimodal, well-sorted ($\sigma\phi = 1.11$), and medium-grained lapilli ($Md\phi = -2.36$). Componentry was performed on fractions coarser than 0ϕ , where 97% of material is analysed. The formation contains components of pumice, lithics, free crystals, scoria, subvolcanic, juvenile glass, and hydrothermally altered rock in fractions coarser than 0ϕ . Proportionally, pumice clasts dominate in fractions coarser than -1ϕ and lithic clasts are abundant in fractions finer than -0.5ϕ . Crystals only occur in fractions finer than -0.5ϕ and subvolcanic rocks are abundant at 0ϕ . As a weight percentage, the deposit is mostly pumice (91.5%) with minor lithic fragments (4.7%) and subvolcanic rock (1.8%) with the remaining components each $<1\%$ of the total weight (figure 3.6).



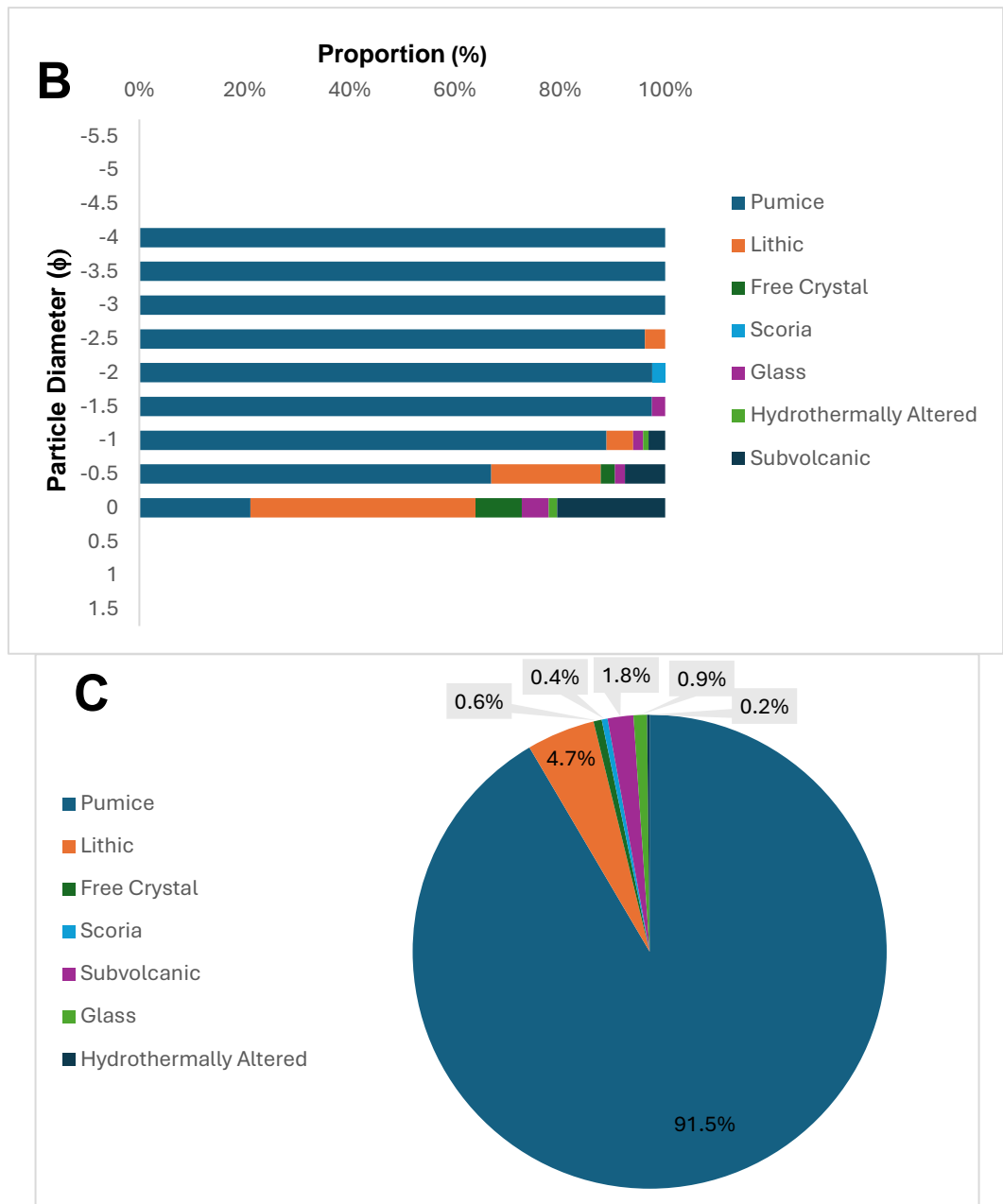


Figure 3.6 – Honduras Formation. A) Proportion of components as a weight percentage of the total sample weight. B) Proportion of components within each grain size. C) Total weight percentage of components

Dispersal, Volume, and Column Height:

The Honduras Formation is dispersed across the SE Bandas Del Sur from Icor to Fasnía. The maximum onshore thickness occurs at Mirador de Las Eras, SW of the town of Icor, at 86 cm and thins to the NE to 26 cm at Fasnía Scoria Cone. There is no recorded thickness SW of the maximum thickness, therefore only half of the dispersal is available,

therefore isopach contours were mirrored. The Honduras Formation has a minimum dispersal of $\sim 237\text{km}^2$ and a minimum onshore volume of 0.128km^3 (table 3.1).

Table 3.1 – Eruption parameters for the Honduras Formation

Volume (km^3)			VEI	Column Height (km)		
<i>Exponential</i>	<i>Power-law</i>	<i>Weibull</i>		<i>Carey and Sparks (1986)</i>	<i>Pyle (1989)</i>	<i>Bonadonna and Costa (2013)</i>
0.178 – 0.233	0.632 – 1.479	0.128 – 0.186	4	>19.55	24 - 41	29 - 45

Interpretation:

The Honduras Formation is the product of a Plinian eruption with an easterly dispersal. The deposit is pumice-rich and well sorted throughout, suggesting a steady eruption column with limited vent clearance and wall erosion. The eruption remained steady throughout, before decreasing in intensity towards termination, seen in the normal grading. The phonolitic eruption may have tapped basaltic magma due to the mafic banding seen in few pumices seen towards the top of the deposit. The eruption is small volume, however only half of the dispersal is seen, therefore interpretation of eruption size is challenging.

3.1.3 Aguerche Formation

The Aguerche Formation, named after a small village east of La Zarza on the edge of its dispersal, comprises of a phonolitic pumice fall deposit. The type section is found northwest of Icor at the top of Barranco de Icor O las Carretas (site 3, figure 3.8). At the type locality, it is 23 cm thick, massive, non-graded, with moderately to well-sorted, medium to fine-grained, sub-angular pumice lapilli (figure 3.7). The deposit is homogenous in structure across the dispersal area and has no distinct characteristics. The pumice is <3 cm in diameter, dark cream to light grey, generally aphyric with sparse biotite phenocrysts, and elongated vesicles <2 mm, with sparse tube vesicles. The formation has low lithic populations (2-3 vol%) of dark grey lava that are <2 cm in diameter. At the type locality, the Aguerche Formation has a sharp contact with the paleosol below, above the Honduras Formation. The formation grades into the overlying 99 cm thick, dark orange grading into a distinct pink paleosol, with lenses of matrix-supported, angular, pumice lapilli. This paleosol is in turn overlain by the Mena

Formation. At Sabina Alta and Icor Vinyard, the Jurado Formation can be found separating the Aguerche and Mena Formations.

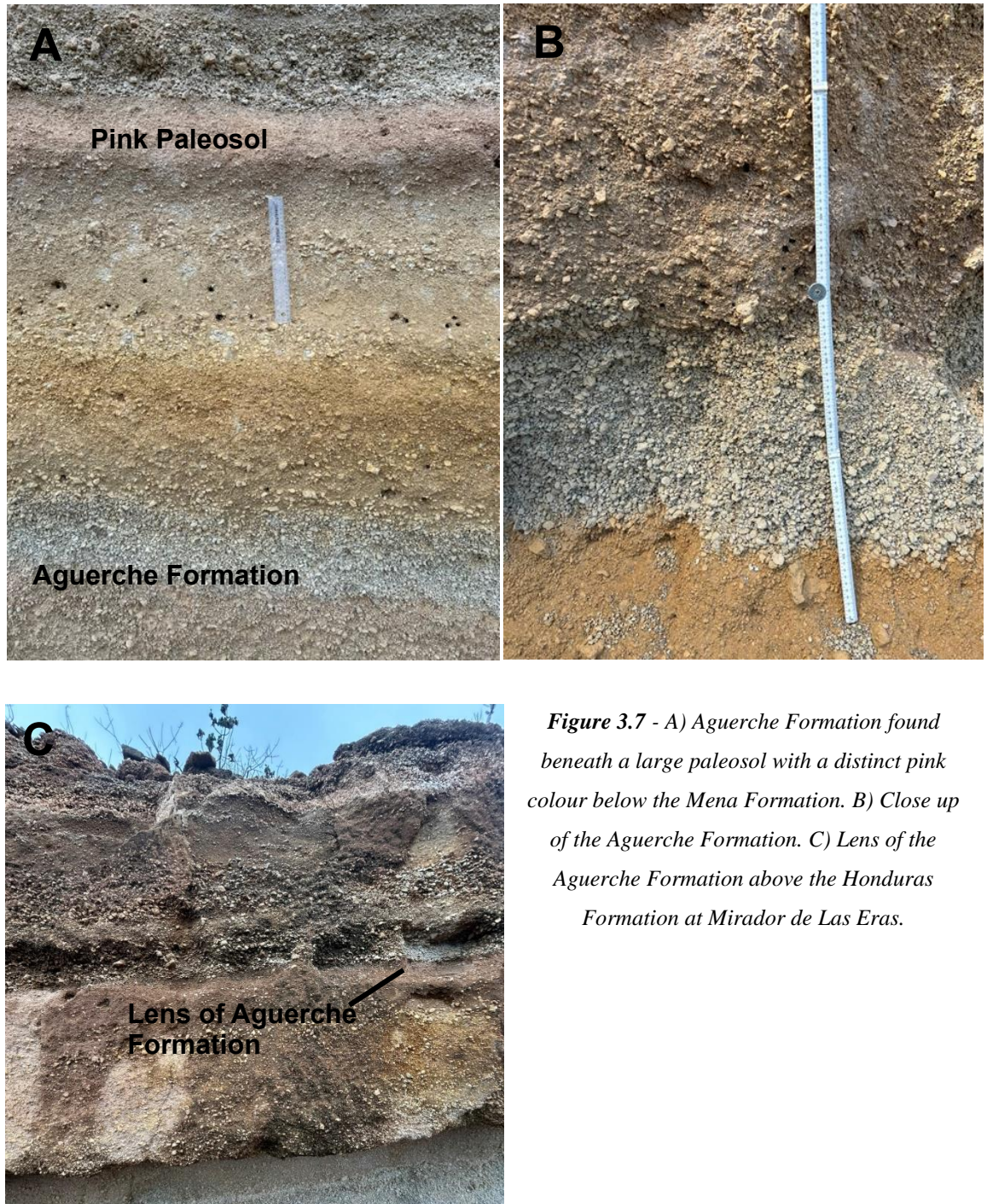
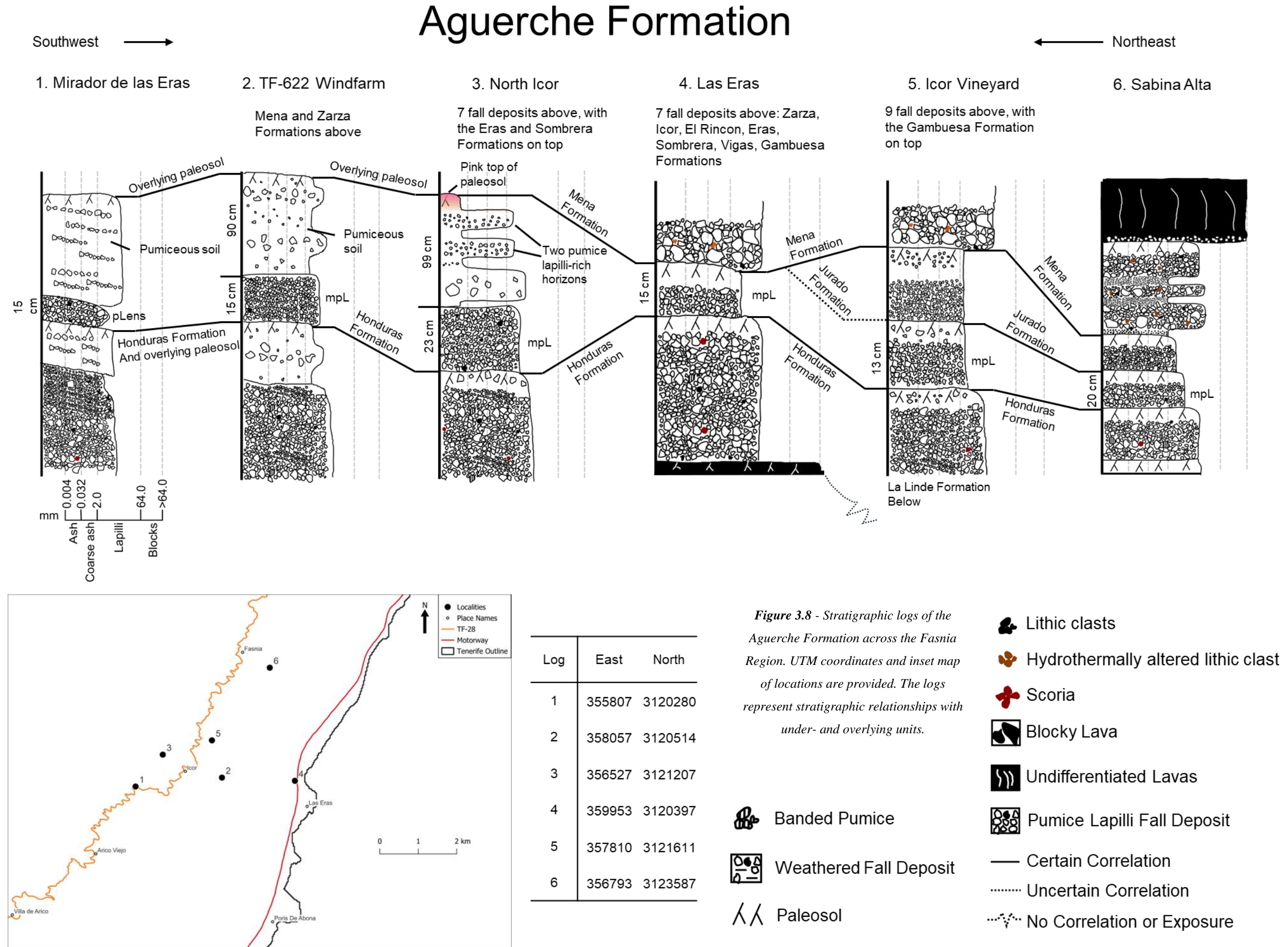
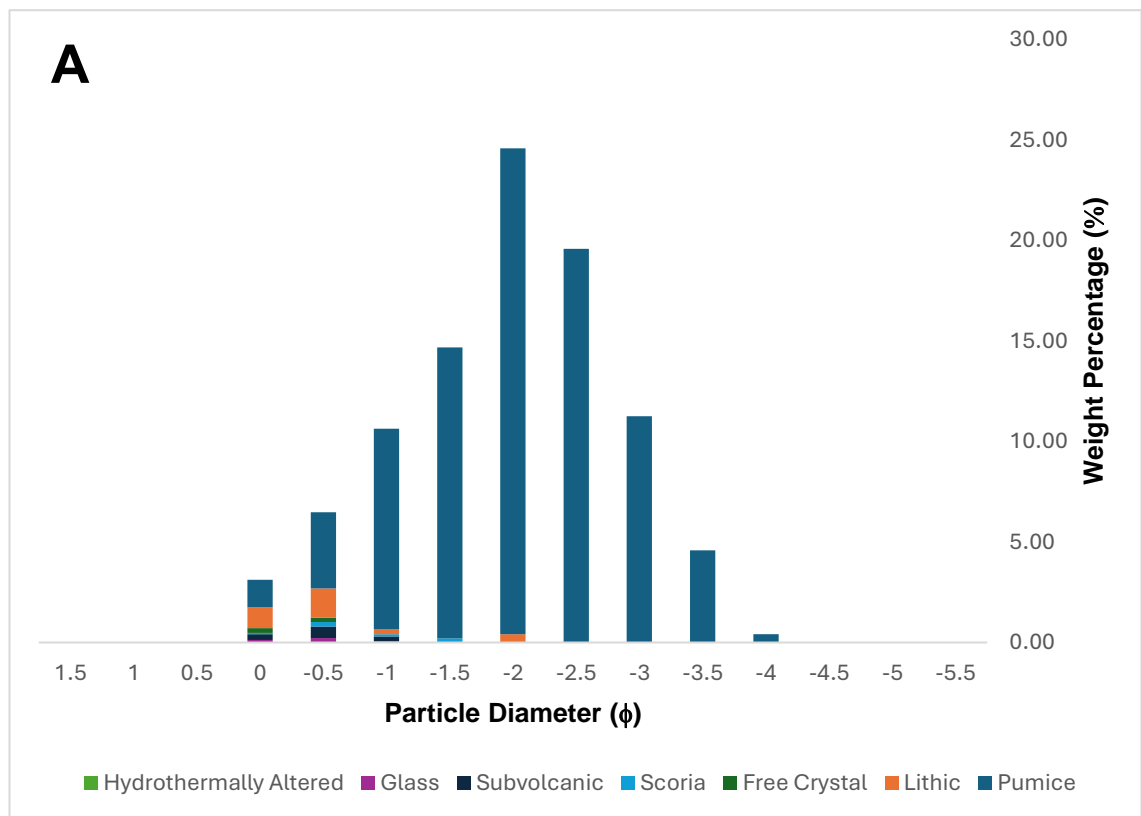


Figure 3.7 - A) Aguerche Formation found beneath a large paleosol with a distinct pink colour below the Mena Formation. B) Close up of the Aguerche Formation. C) Lens of the Aguerche Formation above the Honduras Formation at Mirador de Las Eras.



Grain-Size and Componentry:

The Aguerche Formation was sieved to 1.5ϕ . The deposit is unimodal, well-sorted ($\sigma\phi = 0.97$) and medium-grained lapilli ($Md\phi = -2.21$). Componentry was performed on fractions coarser than 0ϕ , where 95% of material is analysed. The formation contains components of pumice, lithics, free crystals, scoria, subvolcanic, juvenile glass, and hydrothermally altered rock in fractions coarser than 0ϕ . Proportionally, pumice clasts dominate in fractions coarser than -0.5ϕ and lithic clasts are abundant in fractions finer than -1ϕ . Crystals only occur in fractions -0.5ϕ and finer. As a weight percentage, the deposit is mostly pumice (94%) and minor lithic clasts (3.3%) and subvolcanic rock (1.2%), with the remaining components each $<1\%$ of the total weight (figure 3.9).



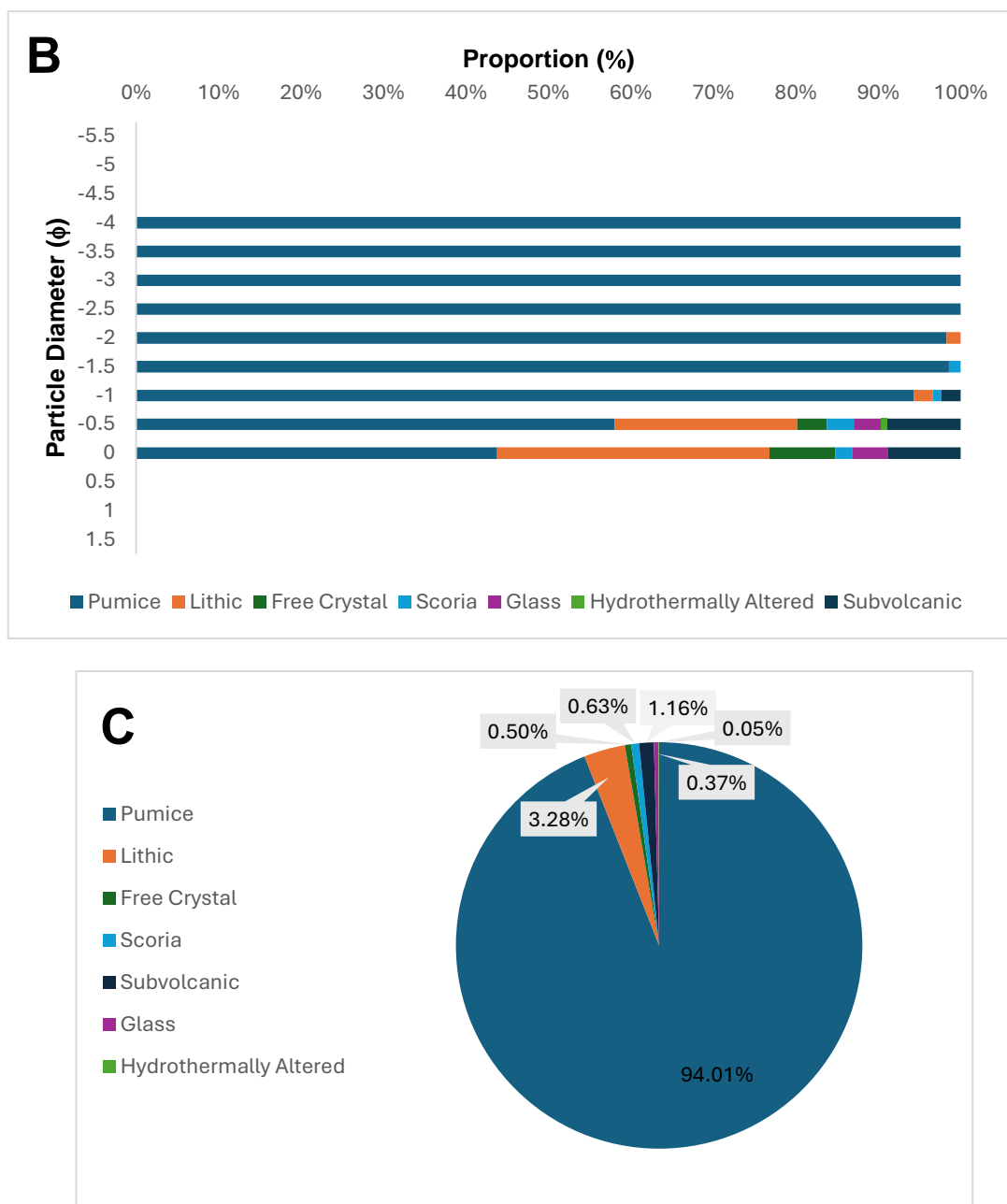


Figure 3.9 – Aguerche Formation. A) Proportion of components as a weight percentage of the total sample weight. B) Proportion of components within each grain size. C) Total weight percentage of components

Dispersal and Volume:

The Aguerche Formation has limited dispersal across the SE Bandas Del Sur from Icor to Fasnía. The maximum onshore thickness occurs at Icor at 23 cm, dictating an easterly dispersal axis. The Aguerche eruption has a minimum dispersal of $\sim 71.94 \text{ km}^2$ and has a minimum bulk volume of 0.035 km^3 (table 3.2).

Table 3.2 - Eruption parameters for the Aguerche Formation

Volume (km ³)			VEI
<i>Exponential</i>	<i>Powerlaw</i>	<i>Weibull</i>	
0.038 – 0.188	0.383 – 2.688	0.035 – 0.152	3-5

Interpretation:

The Aguerche Formation is the product of a small-volume Plinian or sub-Plinian eruption with an easterly dispersal. The eruption is pumice-rich and well sorted throughout, suggesting a steady eruption column with limited vent clearance, wall erosion or a shallow fragmentation level. Given the steady behaviour of the eruption, it is possible this eruption is a short-lived Plinian eruption with poor exposure; therefore, interpretation is challenging.

3.1.4 Jurado Formation

The Jurado Formation is named after Barranco Jurado ~1.2 km west of the type locality at the Icor Vinyard, it is only found elsewhere at Sabina Alta (figure 3.11). At the type locality, it is 14 cm thick, massive, non-graded, composed of poorly sorted, medium-grained, sub-angular pumice lapilli. The deposit has no distinct characteristics (figure 3.10). The pumice is ≤ 3 cm in diameter, cream to light grey, aphyric, with high proportions of rounded vesicles < 1 mm in length. The deposit is lithic poor (0-2 vol%) and < 3 mm in diameter. At the type locality, the Jurado Formation grades into the paleosol above and below, pinching into the paleosol at the end of the outcrop. The paleosol above is 76 cm thick, dark orange that grades into pink, with a 13 cm thick lens of matrix-supported, angular pumice lapilli 30 cm from the base. This is in turn overlain by the Mena Formation.

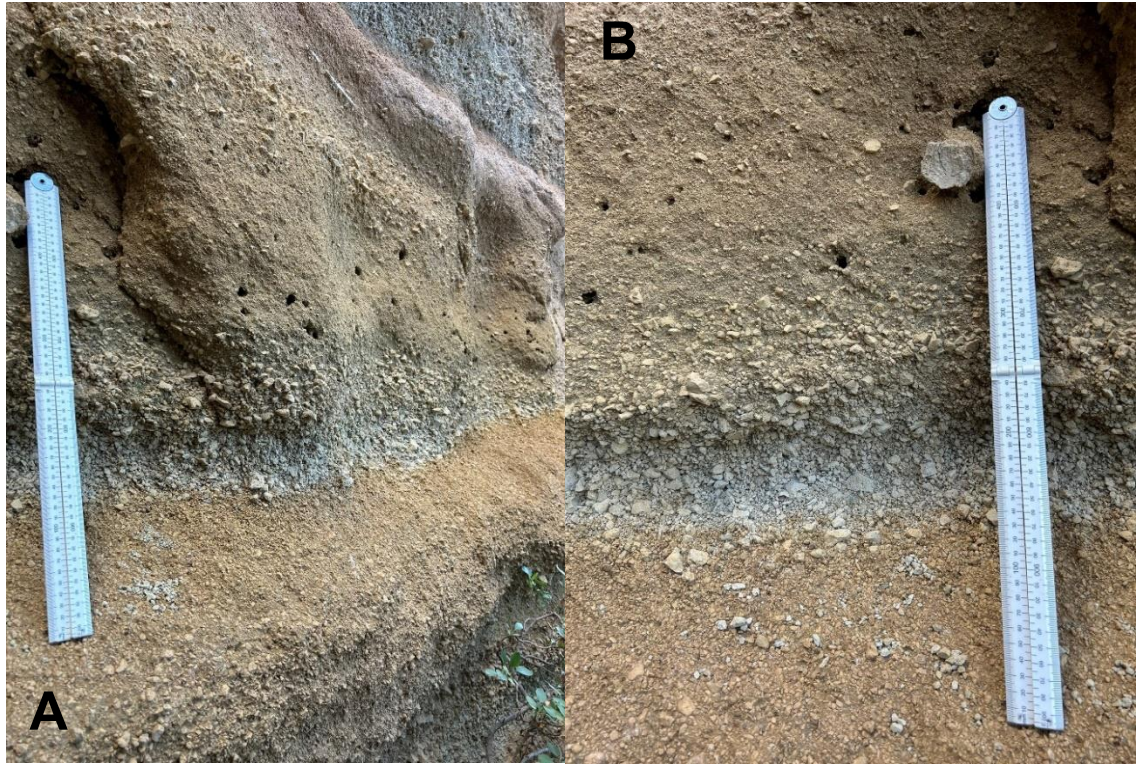


Figure 3.10 – A) The Jurado Formation at Icor Vineyard beneath the pink paleosol of the Mena Formation. B) The fine grained, massive pumice lapilli of the Jurado Formation.

Jurado Formation

1. Icor Vineyard (Type Locality)

9 fall deposits above, with the
Gambuesa Formation on top

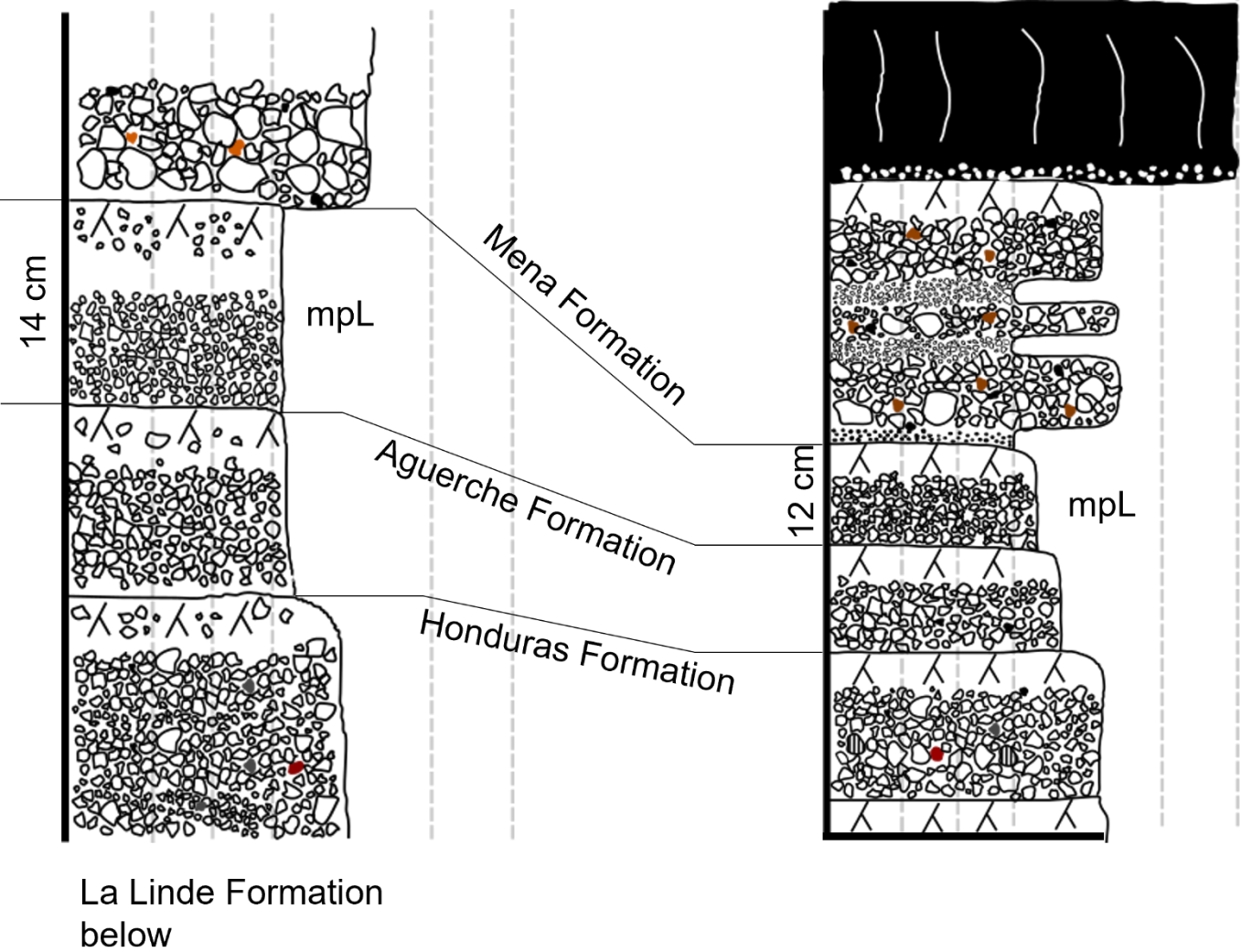
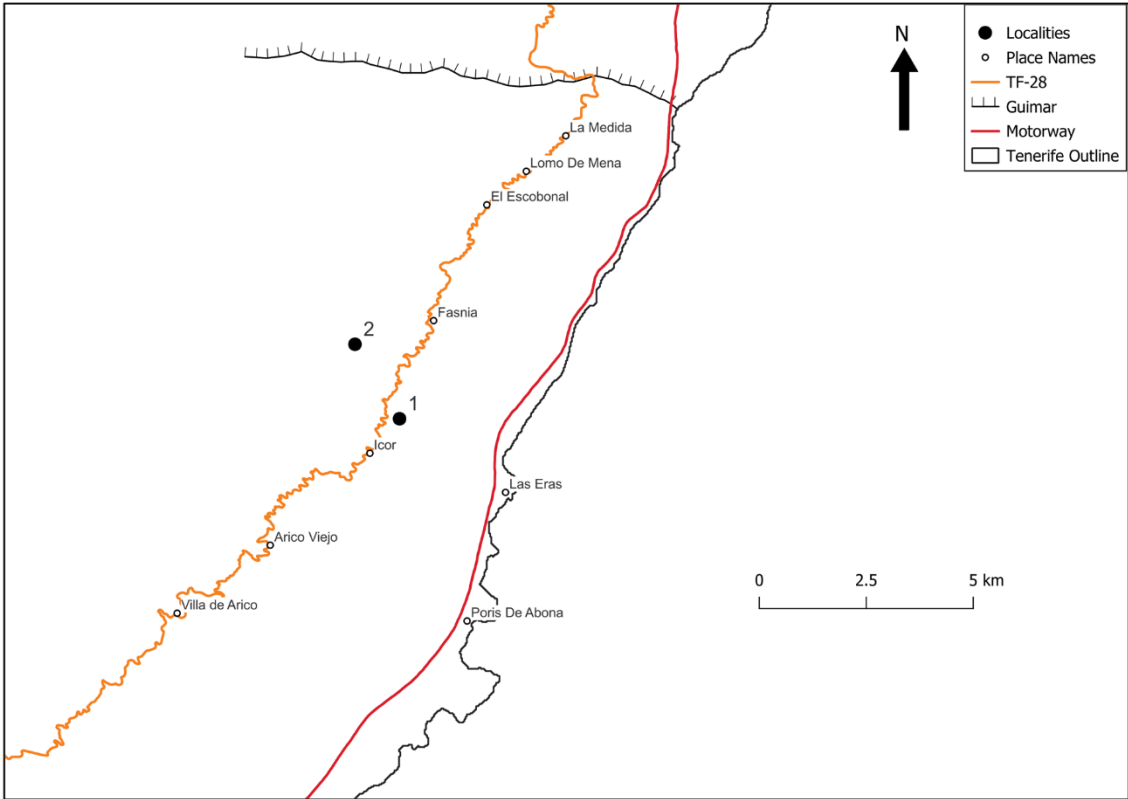
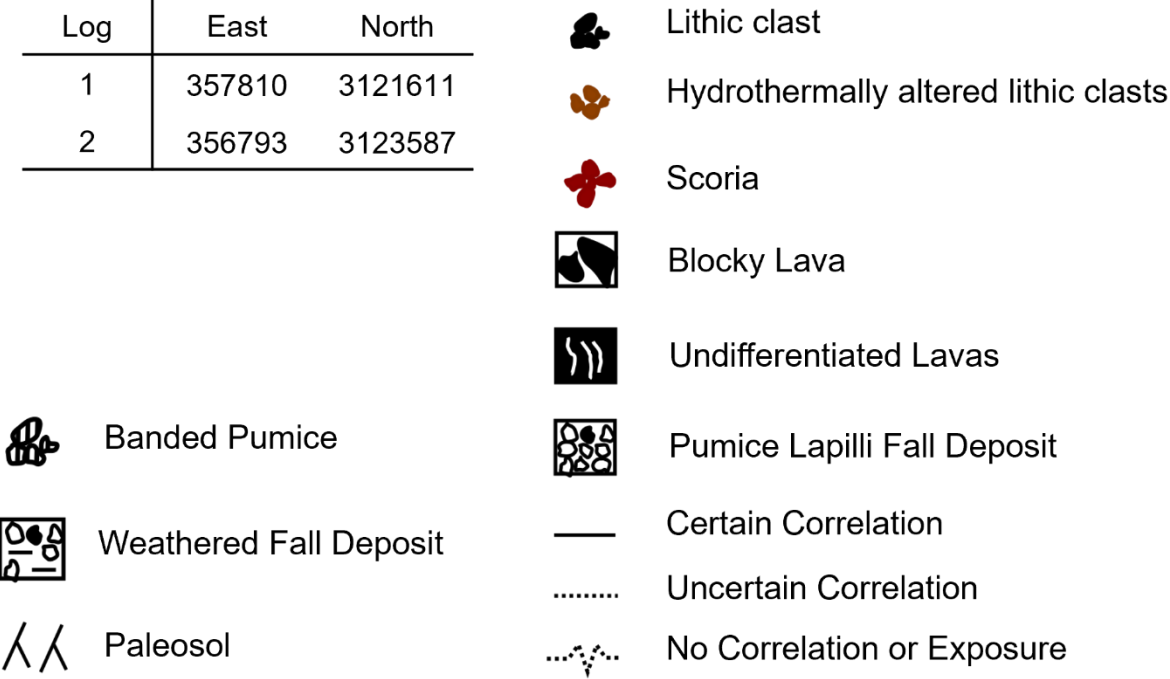


Figure 3.11 - Stratigraphic logs of the Jurado Formation across the Fasnía Region. UTM coordinates and inset map of locations are provided. The logs represent stratigraphic relationships with under- and overlying units.



Log	East	North
1	357810	3121611
2	356793	3123587



Interpretation:

The Jurado Formation is the product a small-volume Plinian or sub-Plinian eruption with an easterly dispersal. The poor sorting may be caused by an unstable eruption column, indicative of a sub-Plinian eruption, however a lack of exposure makes interpretation difficult. It is possible the Jurado Formation is related to the pumicious paleosols above the Aguerche Formation at various localities.

3.1.5 Mena Formation

The Mena Formation is one of the most widespread and complex pumice fall deposits in the eastern Bandas Del Sur and is interpreted to have three members (Mena A, Mena B, and Mena C), totalling a maximum thickness of 131 cm (site 11, figure 3.13). This formation is related to the Mena Formation from Middleton (2006) and Cas et al., (2022), and is widely exposed across a ~37 km² area from Icor to La Medida. The type locality of the Mena formation is between the towns of Lomo de Mena and La Medida at a roadcut section on TF-28 (site 10, figure 3.13).

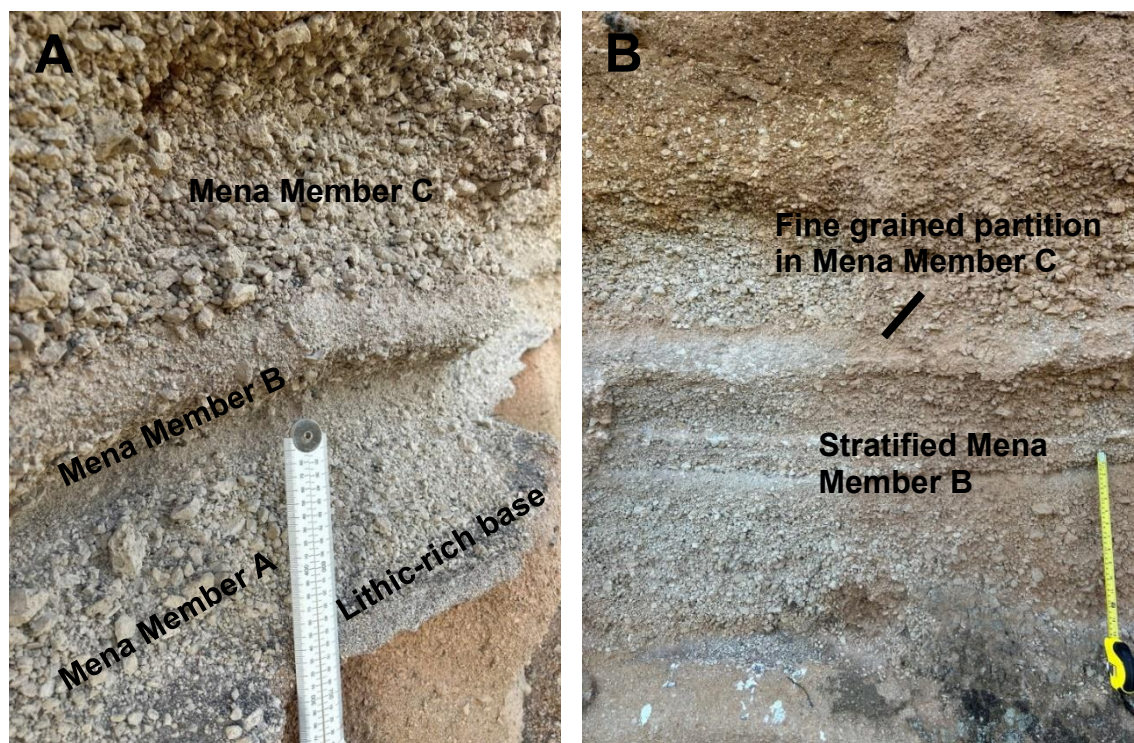


Figure 3.12 – A) The Mena Formation at Los Roques B) Mena Formation at Aguerche



Mena Formation

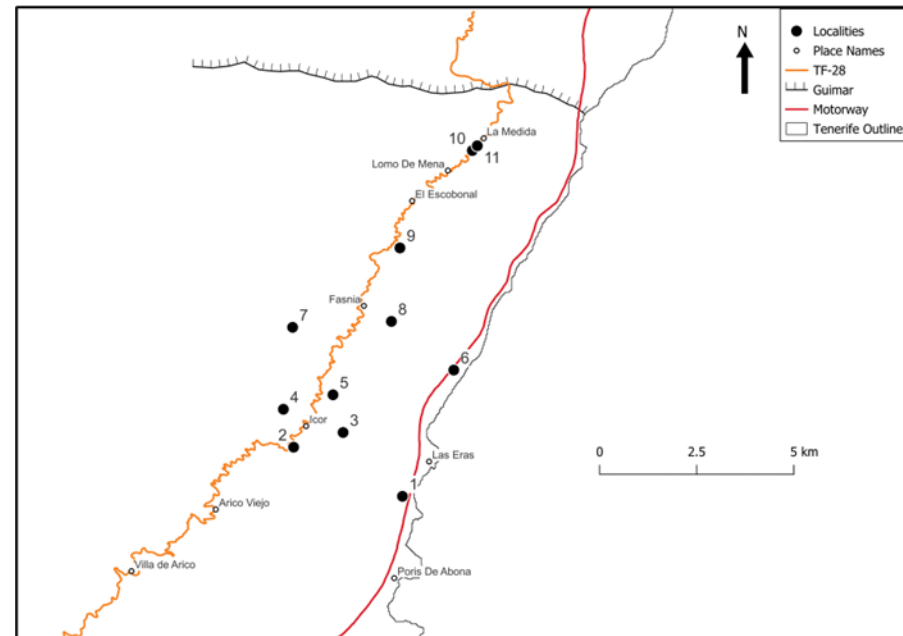
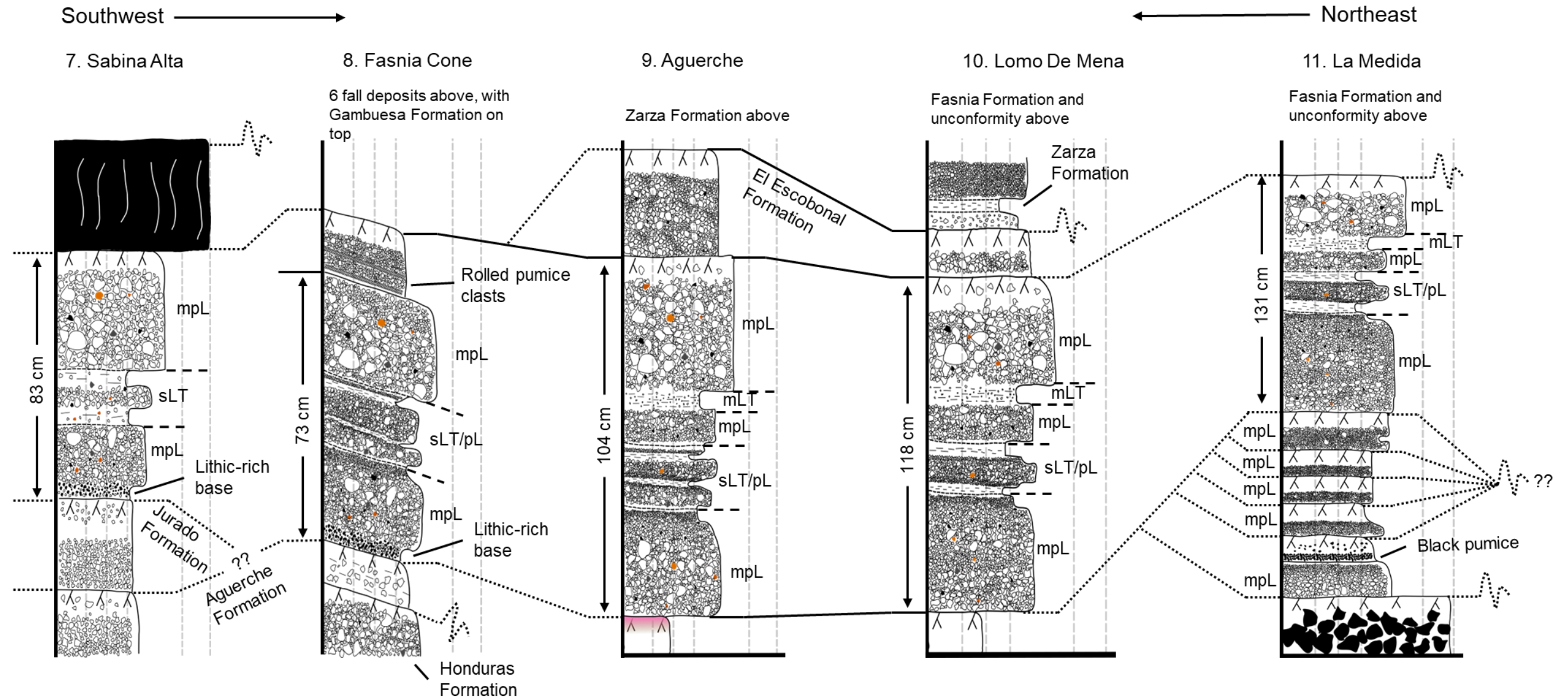


Figure 3.13 - Stratigraphic logs of the Mena Formation across the Fasnía Region. UTM coordinates and inset map of locations are provided. The logs represent stratigraphic relationships with under- and overlying units.

Log	East	North
7	356793	3123587
8	359340	3123727
9	359584	3125862
10	361482	3128672
11	361611	3128810



Banded Pumice



Weathered Fall Deposit



Paleosol



Lithic clast



Hydrothermally altered lithic clasts



Scoria



Blocky Lava



Undifferentiated Lavas



Pumice Lapilli Fall Deposit



Certain Correlation



Uncertain Correlation



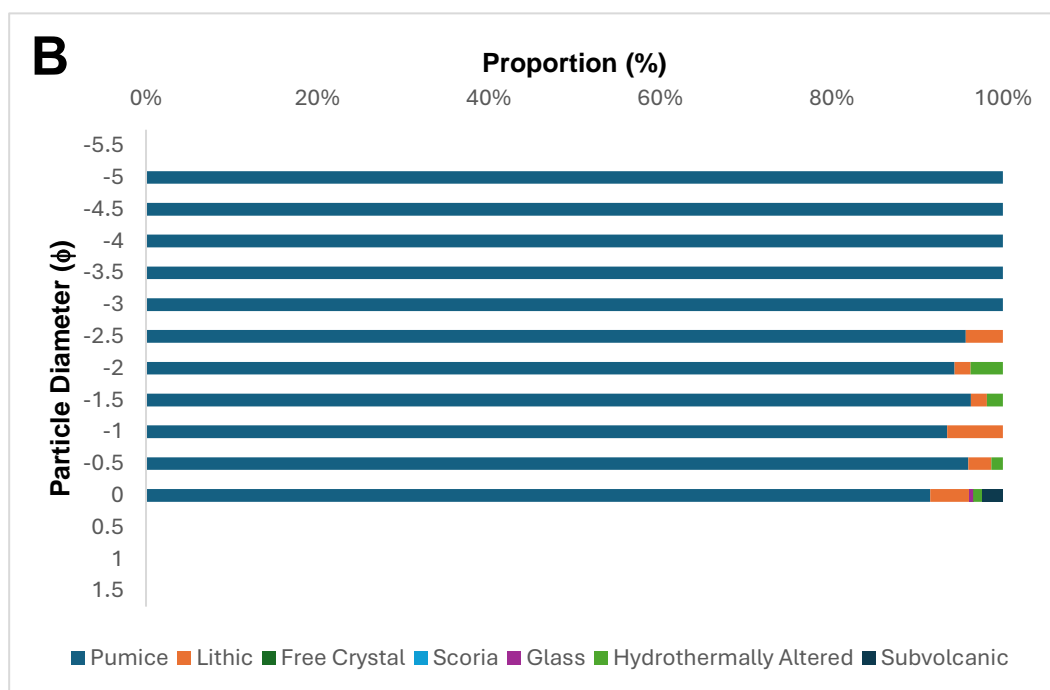
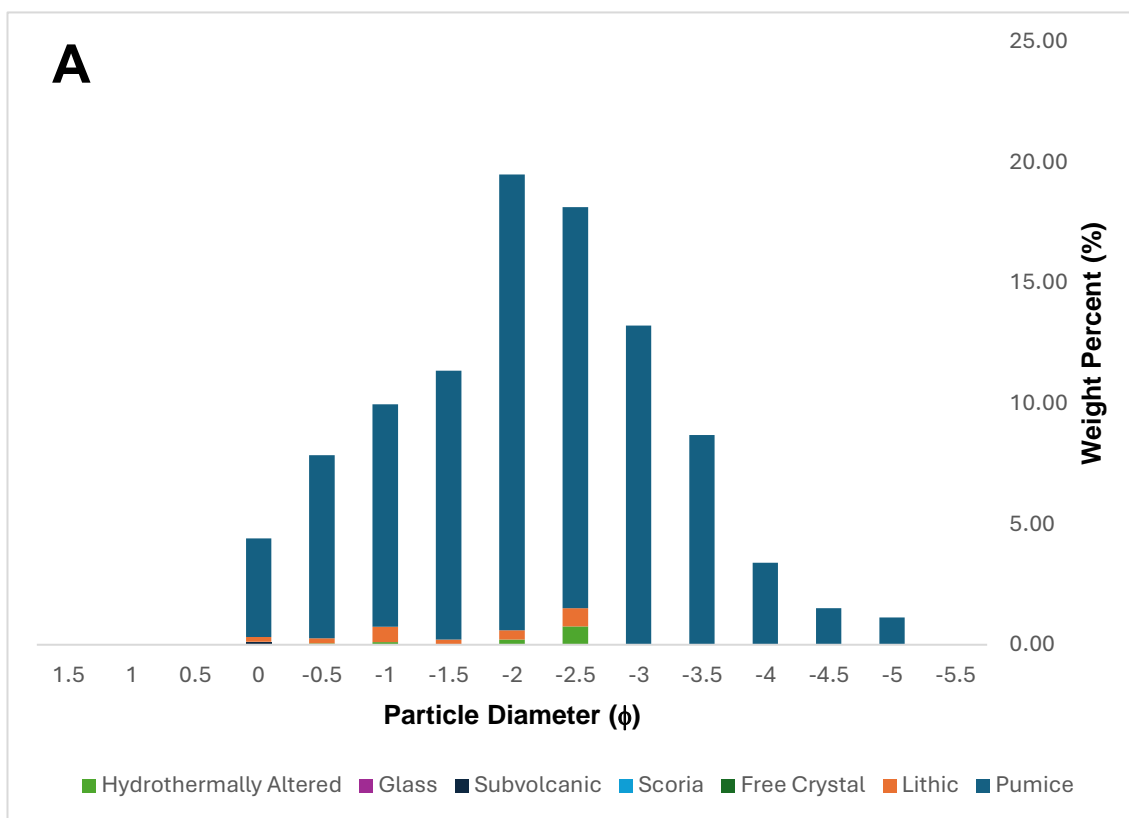
No Correlation or Exposure

3.1.5.3 Mena Member A

Mena Member A represents the bottom of the Mena Formation. At the type section, it is 40 cm thick, moderately to well-sorted, massive, non-graded, with a <3 cm, fine-grained, lithic-rich band at the base (figure 3.12). The pumice is ≤ 5 cm in diameter, generally aphyric with sparse biotite (?) phenocrysts. The pumice has variable vesicle morphologies, with rounded vesicles (<1 mm in diameter) and large tube vesicles (1-3 mm in diameter). The member has 5-7 vol% lithic clasts, that are ≤ 2 cm, with orange, hydrothermally altered lithic clasts found throughout. At the type locality, the member has sharp contact with Mena Member B above and the paleosol below, representing the base of the roadcut section. The paleosol below has a distinct pink colouration at the contact point to the Mena Formation. Elsewhere, the Mena Formation commonly rests above the Aguerche Formation. At Icor Vineyard, the Jurado formation is found beneath the Mena formation and in La Medida, the Mena formation is the only recognisable formation, as it rests above 5 unknown pumice fall deposits and a scoria fall deposit (site 11, figure 3.13).

Grain-Size and Componentry:

Mena Member A was sieved northwest of Icor at the top of Barranco de Icor O las Carretas in 0.5ϕ intervals from -5.5ϕ to -2ϕ and in the laboratory from -1.5ϕ to 1.5ϕ . The deposit is unimodal, moderately sorted ($\sigma\phi = 1.20$) lapilli pumice ($Md\phi = -2.34$). Componentry was performed on fractions coarser than 0ϕ , where 99% of material is analysed. The formation contains components of pumice, lithics, subvolcanic, juvenile glass, and hydrothermally altered rock. Proportionally, pumice clasts dominate in all fractions. As a weight percentage, the deposit is majority pumice (96.3%) with minor lithic fragments (2.42%) and hydrothermally altered rock (1.14%) with the remaining components each <1% of the total weight (figure 3.15).



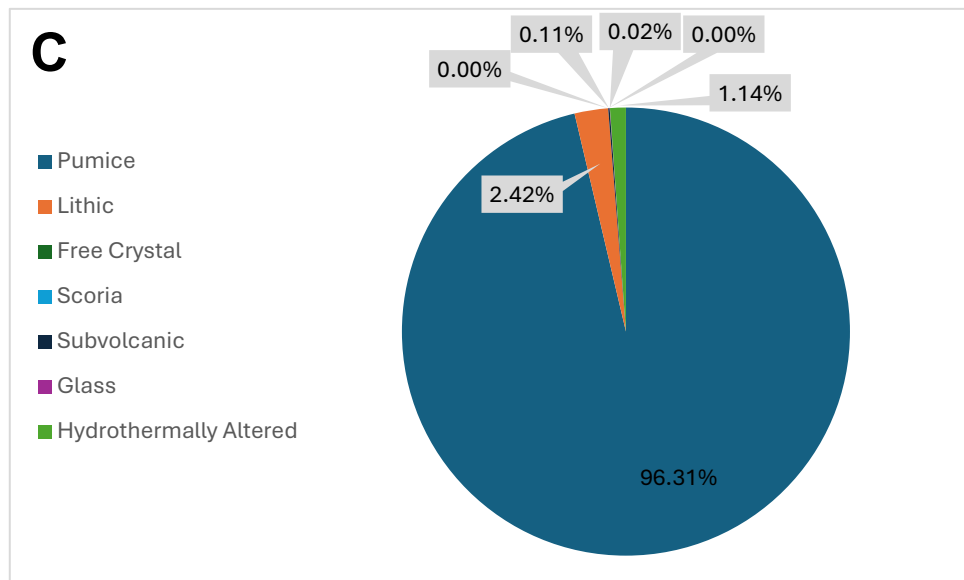


Figure 3.14 – Mena Formation Member A. A) Proportion of components as a weight percentage of the total sample weight. B) Proportion of components within each grain size. C) Total weight percentage of components

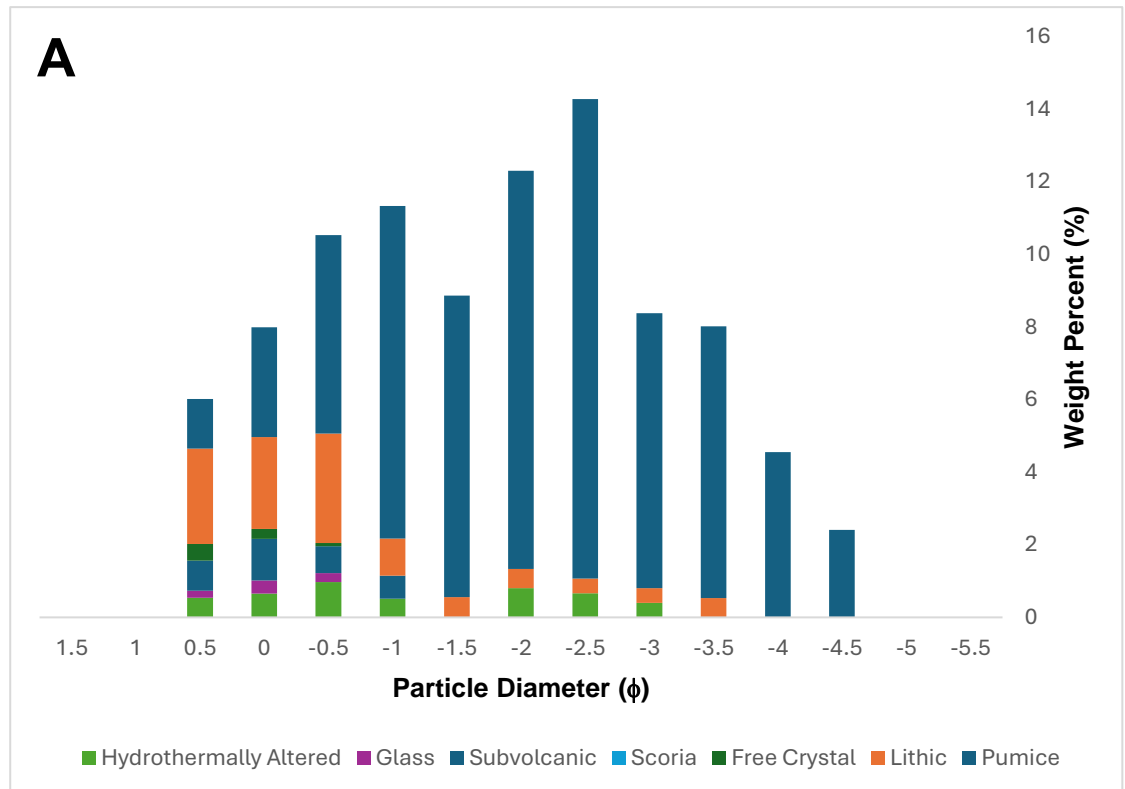
3.1.5.2 Mena Member B

Mena Member B is the middle of the Mena Formation. At the type locality, it is 19 cm thick, poorly sorted, stratified, with two bands of fine-grained lapilli and ash separated by coarse-grained, angular lapilli pumice. As the deposit thins to the west, the unit becomes massive, poorly sorted, and increasingly finer grained with coarse-grained pumice scattered throughout the unit (figure 3.12). The pumice is ≤ 5 cm in diameter, aphyric, with variably rounded and elongated vesicles, and often stained orange. The member has 10-15 vol% lithic clasts that are ≤ 3 cm in diameter, distinctly orange, and hydrothermally altered. This member has sharp contacts to both Mena Member A above and Mena Member C below.

Grain-Size and Componentry:

Mena Member B was sieved northwest of Icor at the top of Barranco de Icor O las Carretas in 0.5 ϕ intervals from -5.5 ϕ to -2 ϕ and in the laboratory from -1.5 ϕ to 2 ϕ . The deposit is bimodal, moderately to poorly sorted ($\sigma\phi = 1.52$) lapilli pumice ($Md\phi = -1.996$). Componentry was performed on fractions coarser than 0.5 ϕ , where 95% of material is analysed. The formation contains components of pumice, lithics, free crystals, subvolcanic, juvenile glass, and hydrothermally altered rock. Proportionally, pumice

clasts dominate in fractions coarser than -1ϕ and lithic clasts are abundant in fractions finer than -0.5ϕ . Crystals only occur in fractions finer than -0.5ϕ and hydrothermally altered rocks are apparent from -3ϕ to 0.5ϕ . As a weight percentage, the deposit is pumice (77.7%) with lithic fragments (12.3%) and minor hydrothermally altered rock (4.81%) and subvolcanic rock (3.52%) with the remaining components each $<1\%$ of the total weight (figure 3.15).



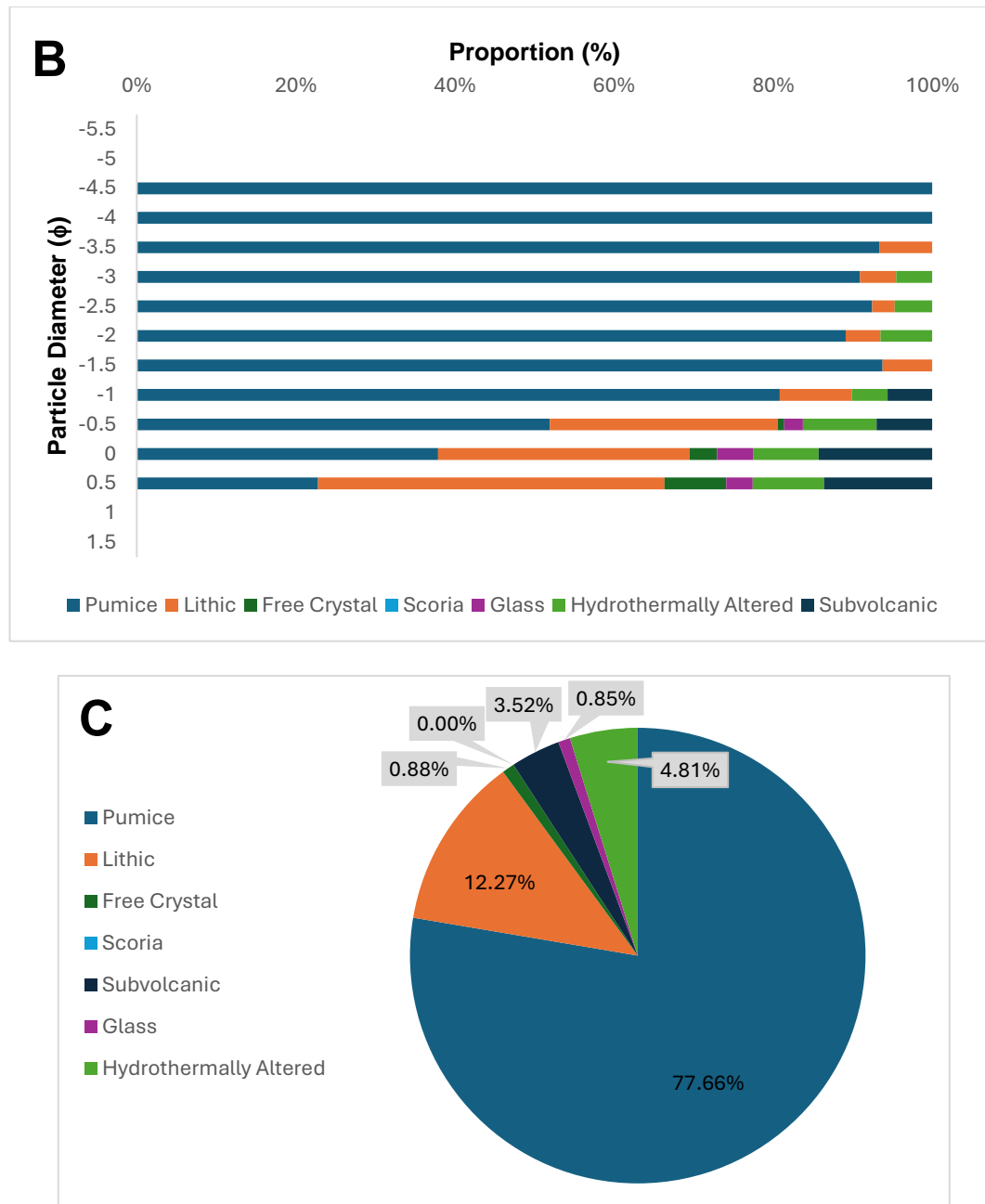


Figure 3.15 – Mena Formation Member B. A) Proportion of components as a weight percentage of the total sample weight. B) Proportion of components within each grain size. C) Total weight percentage of components

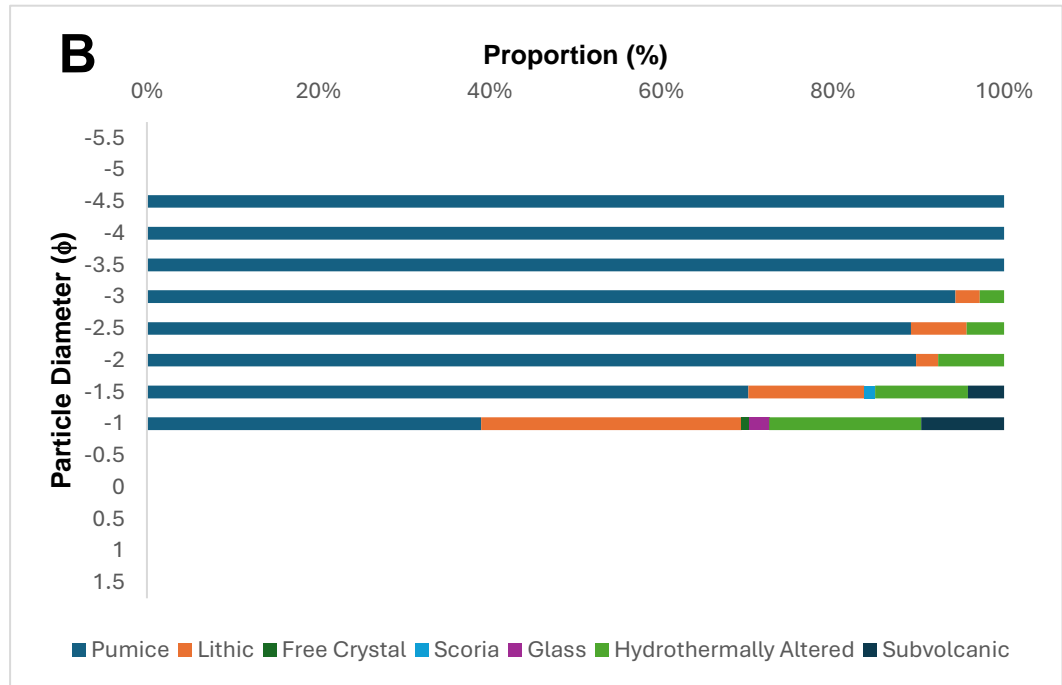
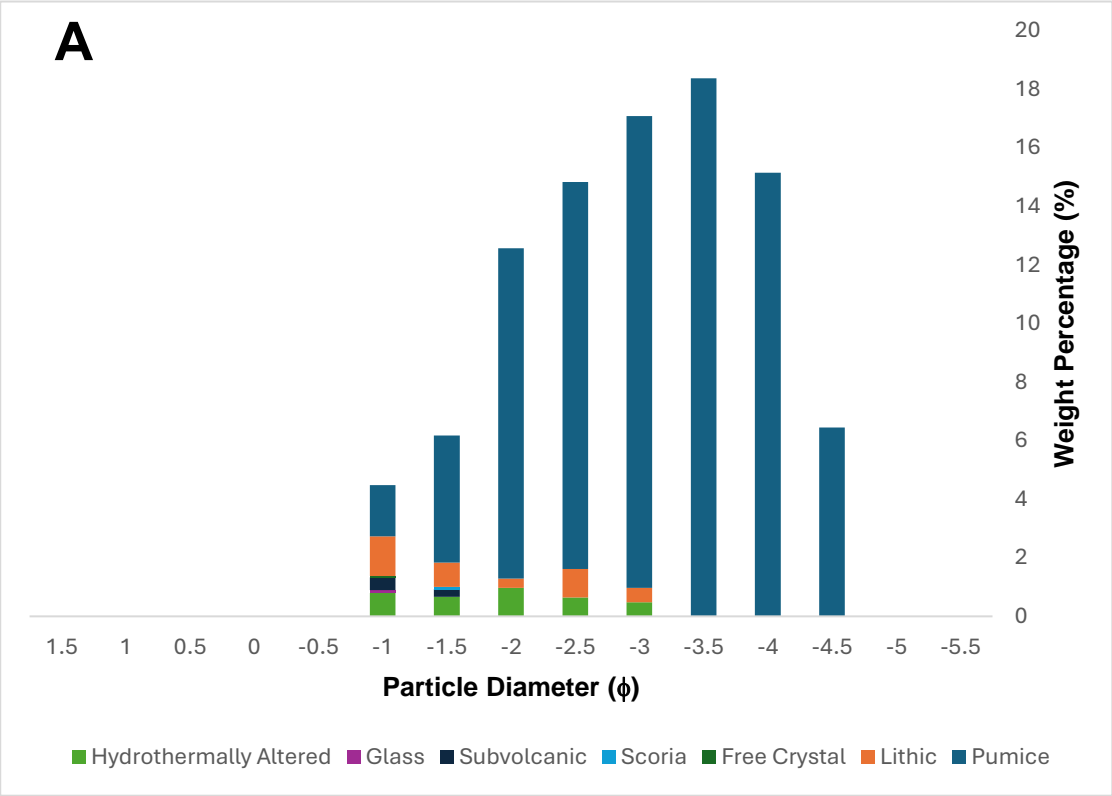
3.1.5.1 Mena Member C

Mena Member C is the top of the Mena Formation. At the type locality, it is 59 cm thick and symmetrically graded, with a ~10cm band of well-sorted fine lapilli and ash between well-sorted coarse, sub-angular lapilli pumice. As the deposit thins towards the west, the fine-grained band disappears, and unit A becomes a massive coarse-grained, well-sorted pumice lapilli deposit (figure 3.12). The pumice is ≤ 6 cm in diameter, aphyric, with densely packed small vesicles and occasional elongation. The member has 6-7 vol%

lithic clasts, with abundant large (10-20 mm), distinctly orange, hydrothermally altered lithics; pumices are often stained orange surrounding such lithic. This member has sharp contact with the paleosol above, which is overlain by the El Escobonal Formation, and a sharp contact with Mena Member B below. The paleosol above is light orange, grading into a dark cream, and is <86 cm thick. At Los Roques, an 8 cm thick, black scoria fall deposit is found resting directly above the Mena Formation (site 6, figure 3.13).

Grain-Size and Componentry:

Mena Member C was sieved northwest of Icor at the top of Barranco de Icor O las Carretas in 0.5 ϕ intervals from -5.5 ϕ to -2 ϕ and in the laboratory from -1.5 ϕ to 1.5 ϕ . The deposit is unimodal, moderately sorted ($\sigma\phi = 1.25$) lapilli pumice ($Md\phi = -3.15$). Componentry was performed on fractions coarser than 1 ϕ , where 95% of material is analysed. The formation contains components of pumice, lithics, free crystals, scoria, subvolcanic, juvenile glass, and hydrothermally altered rock. Proportionally, pumice clasts dominate in fractions coarser than -1.5 ϕ and lithic clasts are abundant in fractions finer than -1 ϕ . Crystals only occur in fractions finer than -1 ϕ and hydrothermally altered rocks are abundant at -1 ϕ . As a weight percentage, the deposit is mostly pumice (91.1%) with minor lithic fragments (4.18%) and hydrothermally altered rock (3.74%) with the remaining components each <1% of the total weight (figure 3.14).



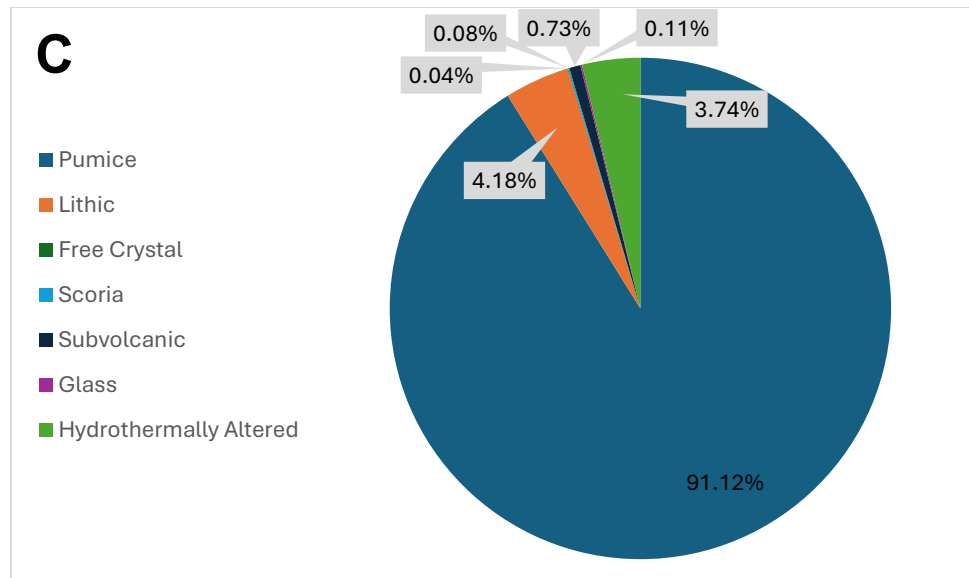


Figure 3.16 – Mena Formation Member C. A) Proportion of components as a weight percentage of the total sample weight. B) Proportion of components within each grain size. C) Total weight percentage of components

Dispersal, Volume, and Column Height:

The Mena Formation is dispersed across SE Bandas Del Sur from Icor to La Medida. Each member of the formation has a northeasterly dispersal, thinning to the southwest, with only one half of the dispersal available. The formation has a dispersal of $\sim 354 \text{ km}^2$ with a minimum onshore volume of 0.447 km^3 (table 3.3).

Table 3.3 - Eruption parameters for the Mena Formation

Volume (km^3)			VEI	Column Height		
<i>Exponential</i>	<i>Powerlaw</i>	<i>Weibull</i>		Carey and Spark (1986)	Pyle (1989)	Bonadonna and Costa (2013)
				Mena C	Mena B	Mena A
0.591 – 1.392	3.988 – 8.122	0.447 – 3.142	4-5	>17.2	>16.3	>19.2
					24-41	29-45

Interpretation:

The Mena Formation is the product of a Plinian eruption that underwent three main phases of activity through the duration of the eruption. The presence of hydrothermally altered clasts throughout suggests a shallow hydrothermal reservoir beneath the vent. A similar dispersal axis throughout each phase of the eruption suggests the wind direction remained stable, suggesting changes in deposit characteristics are likely caused by eruption intensity and plume heights. The eruption began with an initial vent opening, seen in the thin lithic layer at the base, producing a steady plume up. The eruption

waned, before heading into stop-start or fluctuating behaviour, seen in the stratifications of fine and coarse material at the dispersal axis, and massive fine-grained lapilli and ash at the edge of the dispersal. The eruption then produced a steady plume for the remaining duration of the eruption.

3.1.6 El Escobonal Formation

The El Escobonal Formation is a phonolite pumice fall deposit named after a town located 900 m east of the type locality at Calle Madriguera vineyard (locality 1, figure 3.17). The formation is exposed across a $\sim 4 \text{ km}^2$ area from Barranco de Fasnía to Lomo De Mena. At the type locality, it is 52 cm thick, moderately sorted, medium-grained, sub-angular to angular pumice lapilli (figure 3.16). The pumice is $\leq 3 \text{ cm}$, light cream, highly vesiculated with common tube vesicles, with sparse pyroxene (?) phenocrysts. The formation has $< 2 \text{ vol\%}$ lithic clasts of lava. At the type locality, the El Escobonal Formation has a sharp contact with a 45 cm thick, light brown paleosol below, which overlies the Mena Formation, and grades into 40 cm thick, cream to light brown paleosol above, which in turn rests below the Zarza Formation (figure 3.16).

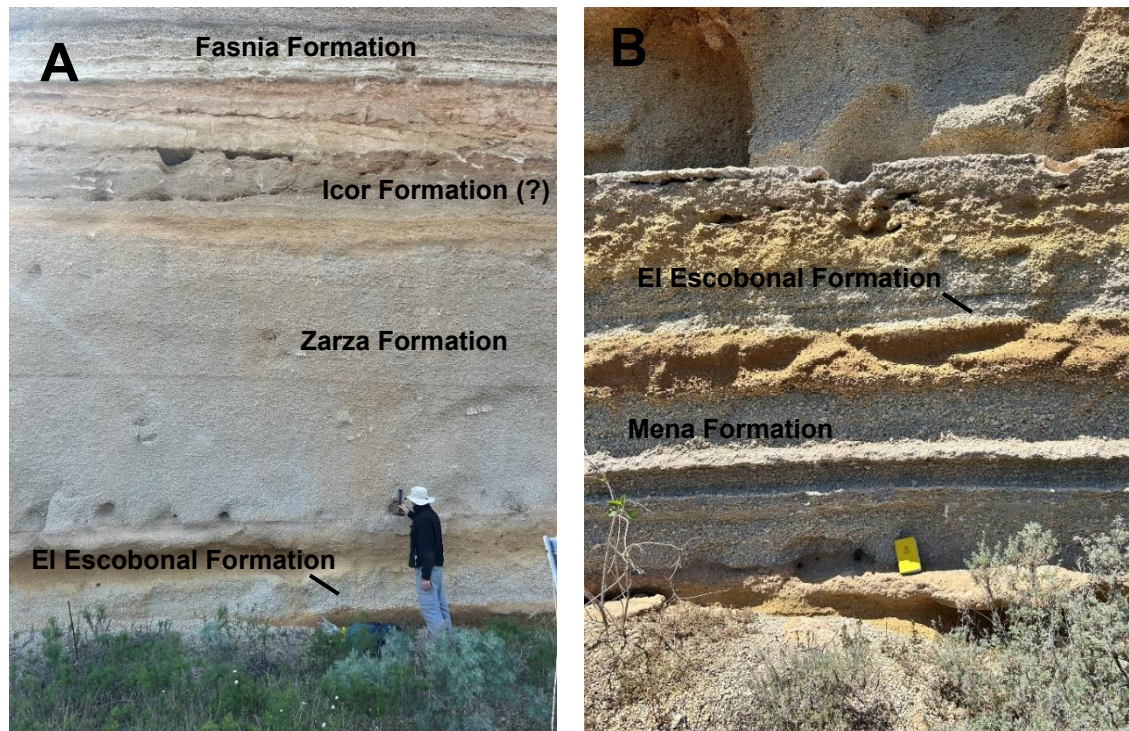


Figure 3.16 – *A) The El Escobonal Formation beneath the Zarza Formation at Aguerche (locality 1). B) The El Escobonal Formation above the Mena Formation at Aguerche (locality 1).*

El Escobonal Formation

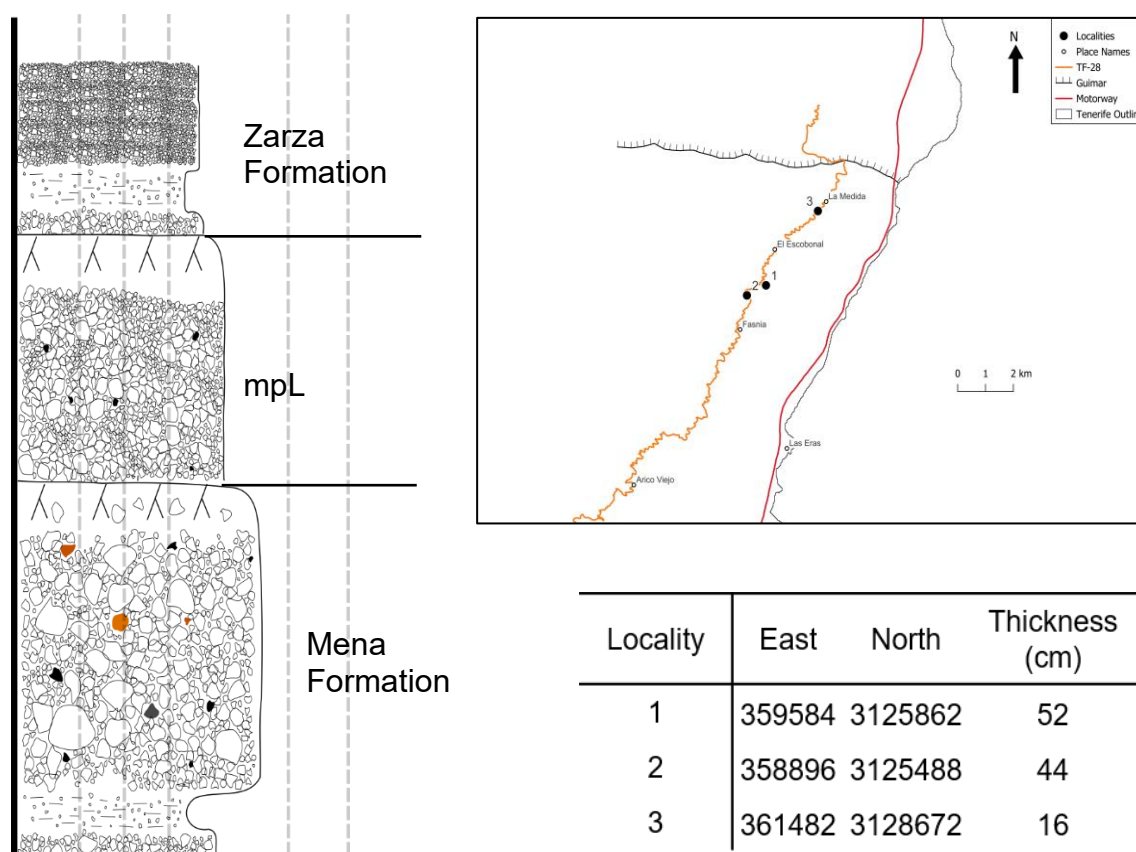
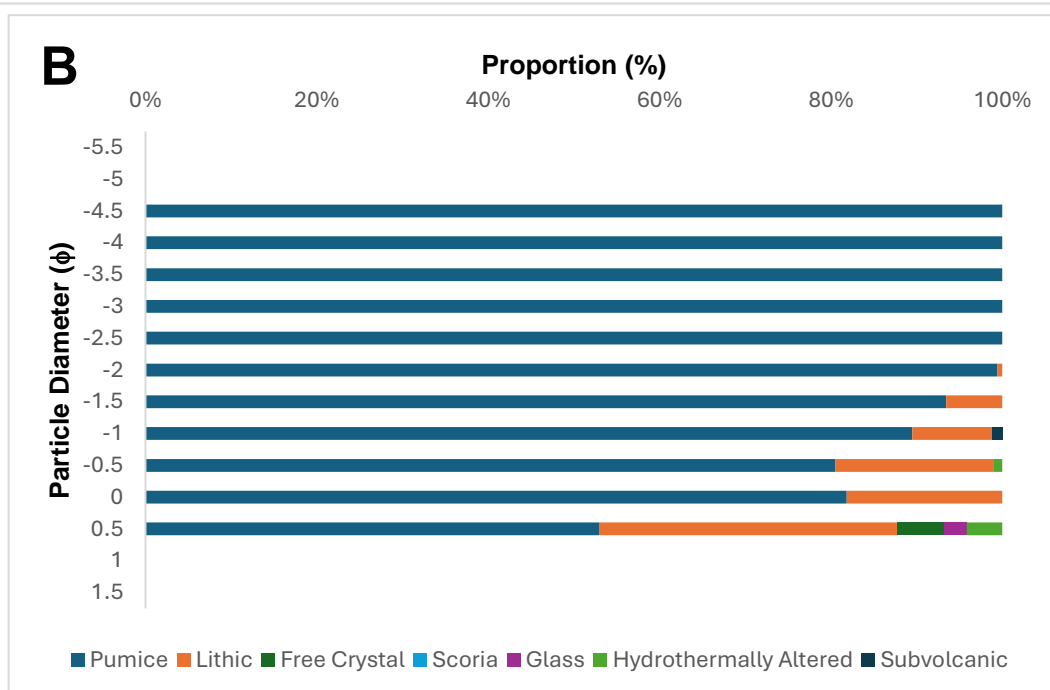
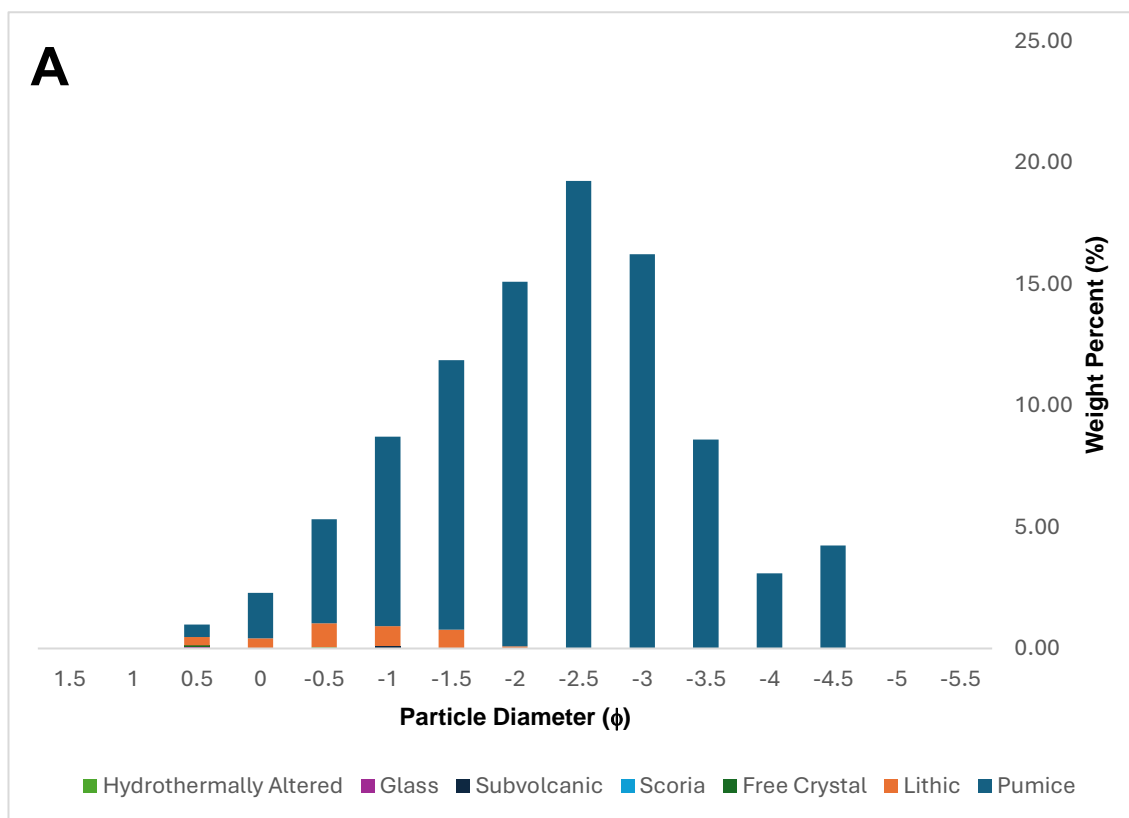


Figure 3.17 - Stratigraphic log of the El Escobonal Formation across the Fasnia Region. UTM coordinates and inset map of locations are provided. The logs represent stratigraphic relationships with under- and overlying units.

Grain Size and Componentry:

The El Escobonal Formation was sieved at the type locality in 0.5ϕ intervals from -5.5ϕ to -3ϕ and in the laboratory from -2.5ϕ to 1.5ϕ . The deposit is unimodal, well-sorted ($\sigma\phi = 1.13$) and medium-grained lapilli ($Md\phi = -2.47$). Componentry was performed on fractions coarser than 0.5ϕ , where 95% of material is analysed. The formation contains components of pumice, lithic clasts, free crystals, subvolcanic rock, juvenile glass, and hydrothermally altered rock in fractions coarser than 0.5ϕ . Proportionally, pumice clasts dominate in fractions coarser than 0ϕ and lithic clasts are abundant in fractions finer than 0.5ϕ . Crystals and juvenile glass only occur in the 0.5ϕ fraction. As a weight percentage, the deposit is mostly pumice (96.1%) and minor lithic clasts (3.6%), with the remaining components each $<1\%$ of the total weight (figure 3.18).



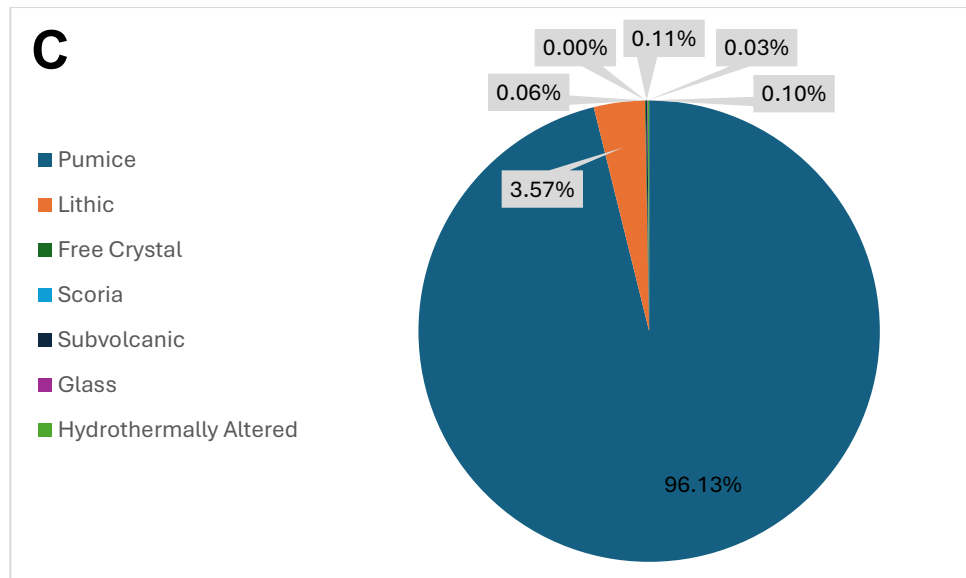


Figure 3.18 – El Escobonal Formation. A) Proportion of components as a weight percentage of the total sample weight. B) Proportion of components within each grain size. C) Total weight percentage of components

Interpretation:

The El Escobonal Formation is the product of a Plinian eruption with a steady eruption column heading northeast. The eruption remained stable throughout its duration, with limited vent wall erosion and no evidence of an initial vent opening.

3.1.7 Zarza Formation

The Zarza Formation, related to the Zarza Formation of Middleton (2006) and Cas et al., (2022), comprises of two phonolitic pumice fall deposits and one ash layer (Zarza Member A, B, and C). The formation is exposed across ~37 km² from Mirador de las Eras to La Medida, with a total thickness of 512 cm in Lomo De Mena. The type section is found northwest of Icor at the top of Barranco de Icor O las Carretas (site 4, figure 3.20). The Zarza Formation can be found in La Zarza, however, was not measured due to the presence of reworked pumice clasts exaggerating the thickness and altering the deposit structure.

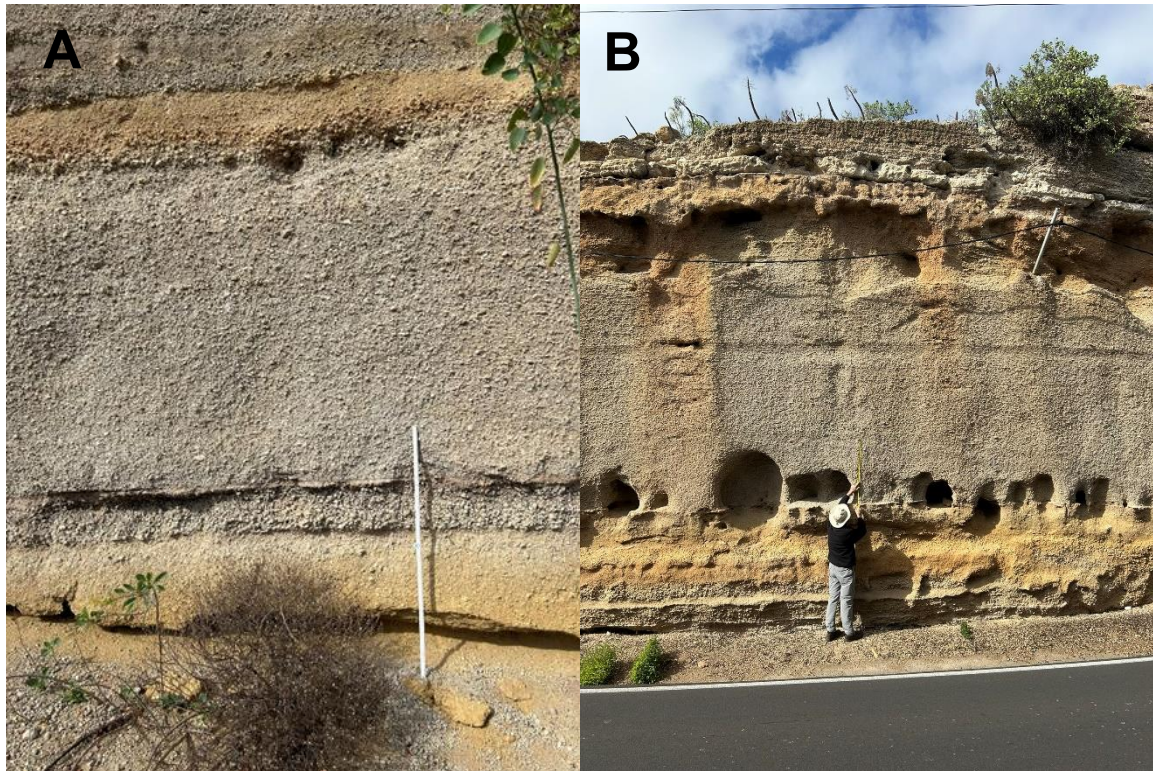
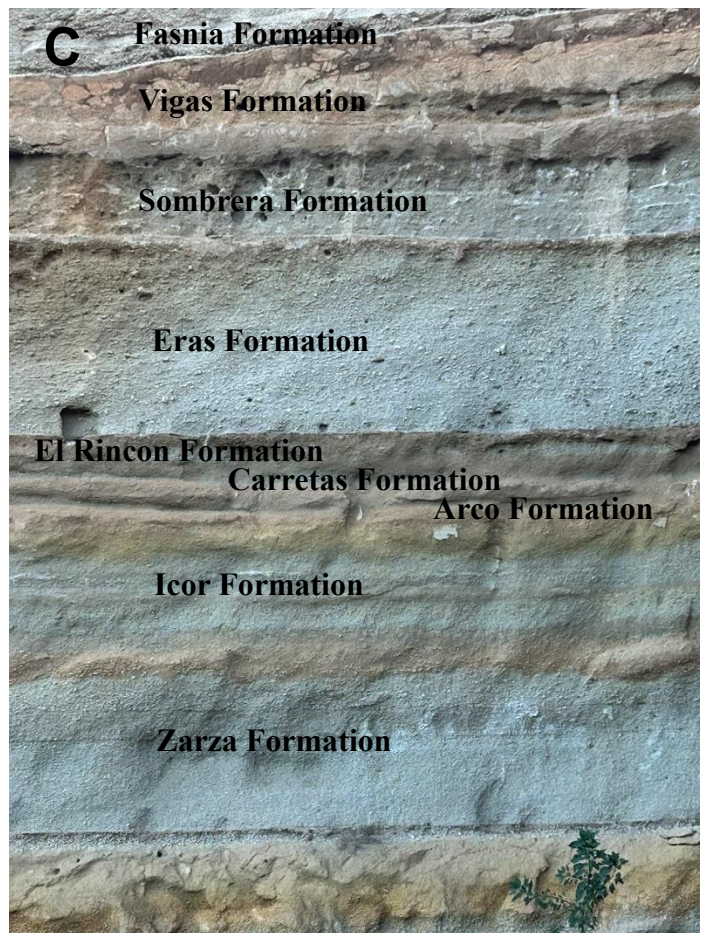
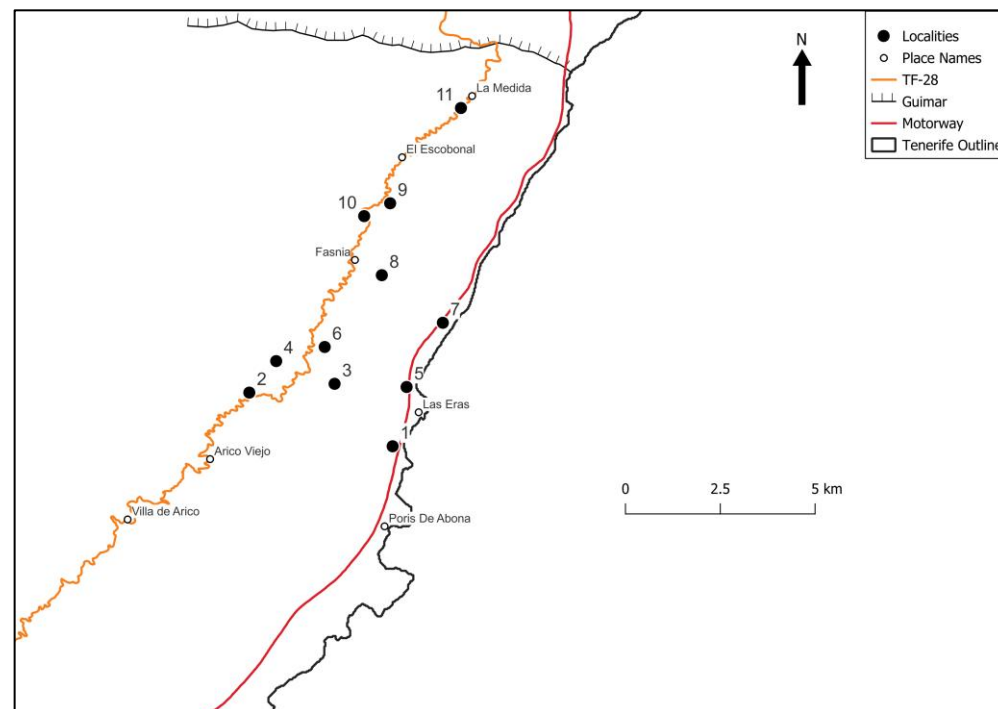
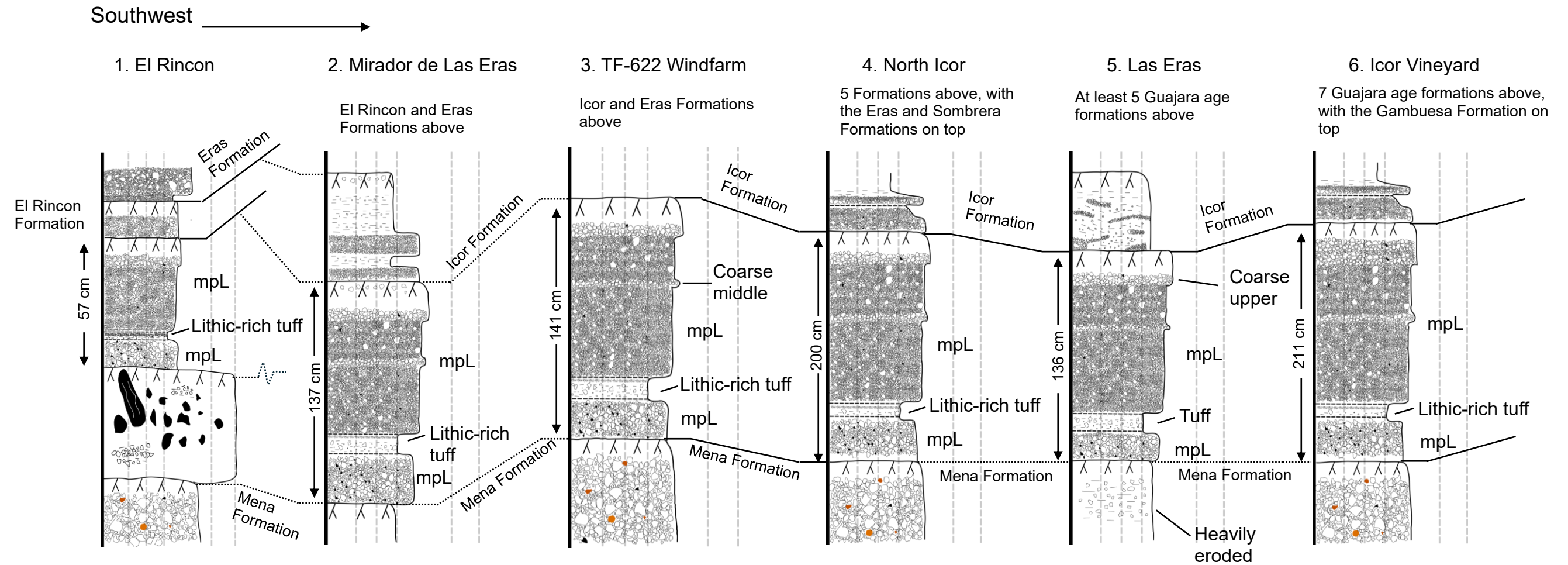


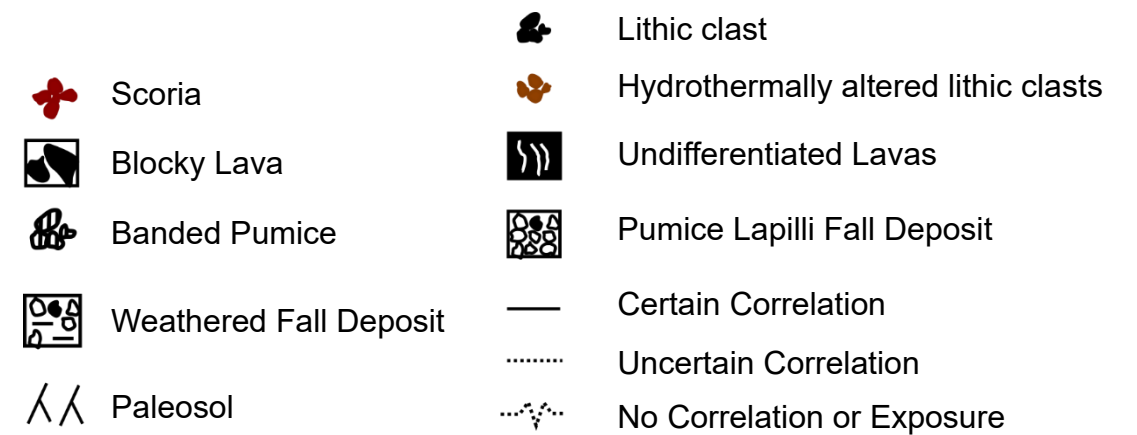
Figure 3.19 – A) The Zarza Formation at North Icor, with a coarse-grained pumice lapilli base, fine ash layer, and medium grained pumice lapilli upper. Note the coarse-grained pumice bed in the upper layer. B) Zarza Formation at Lomo de Mena, the thickest locality. C) The Zarza Formation in stratigraphic sequence, beneath the Icor, Arco, Carretas, El Rincon, Eras, Sombrera, Vigas, and Fasnía Formations.



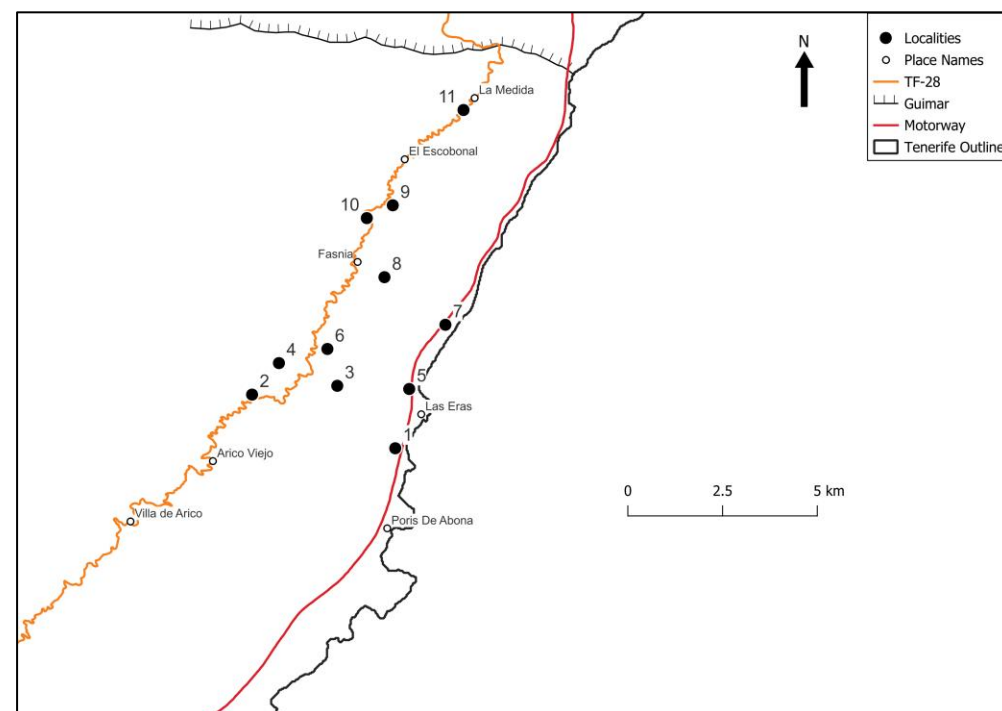
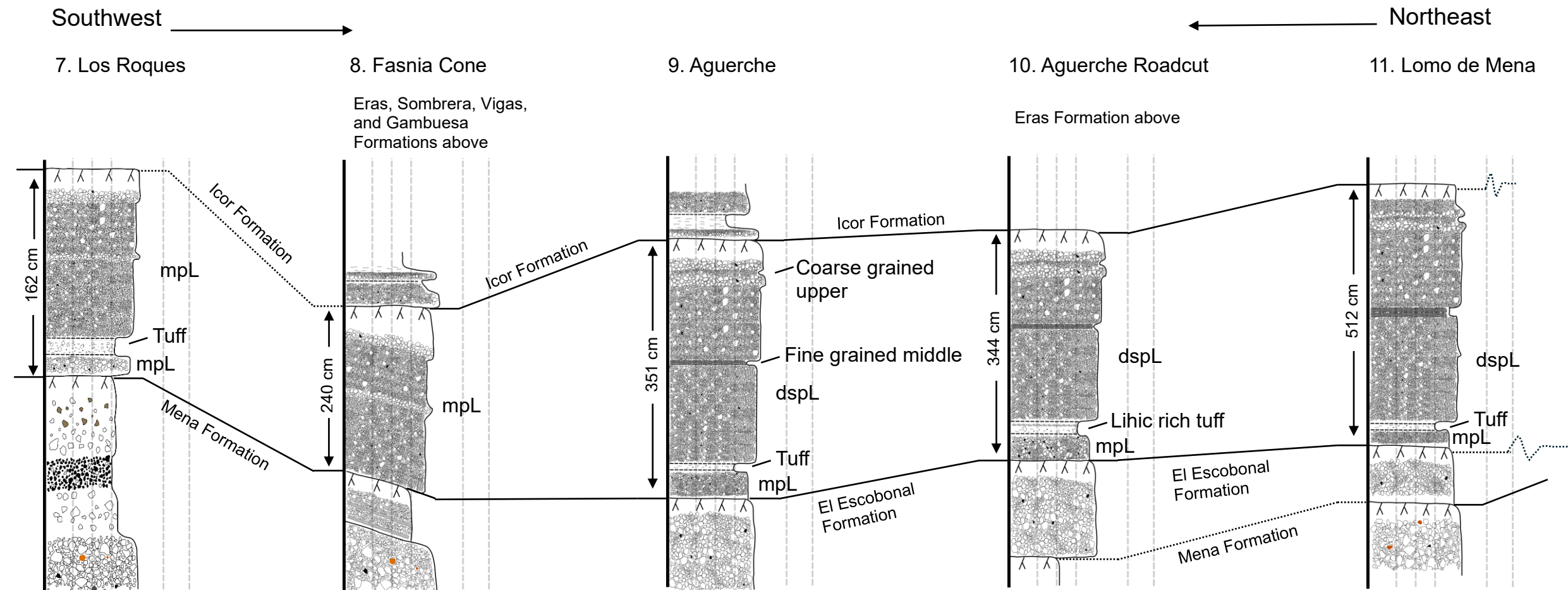
Zarza Formation



Log	East	North
1	359565	3118639
2	355807	3120280
3	358057	3120514
4	356527	3121207
5	359953	3120397
6	357810	3121611



Zarza Formation



Log	East	North
7	360930	3122294
8	359340	3123727
9	359584	3125862
10	358896	3125488
11	361482	3128672

Scoria

Blocky Lava

Banded Pumice

Weathered Fall Deposit

Paleosol

Lithic clast

Hydrothermally altered lithic clasts

Undifferentiated Lavas

Pumice Lapilli Fall Deposit

Certain Correlation

Uncertain Correlation

No Correlation or Exposure

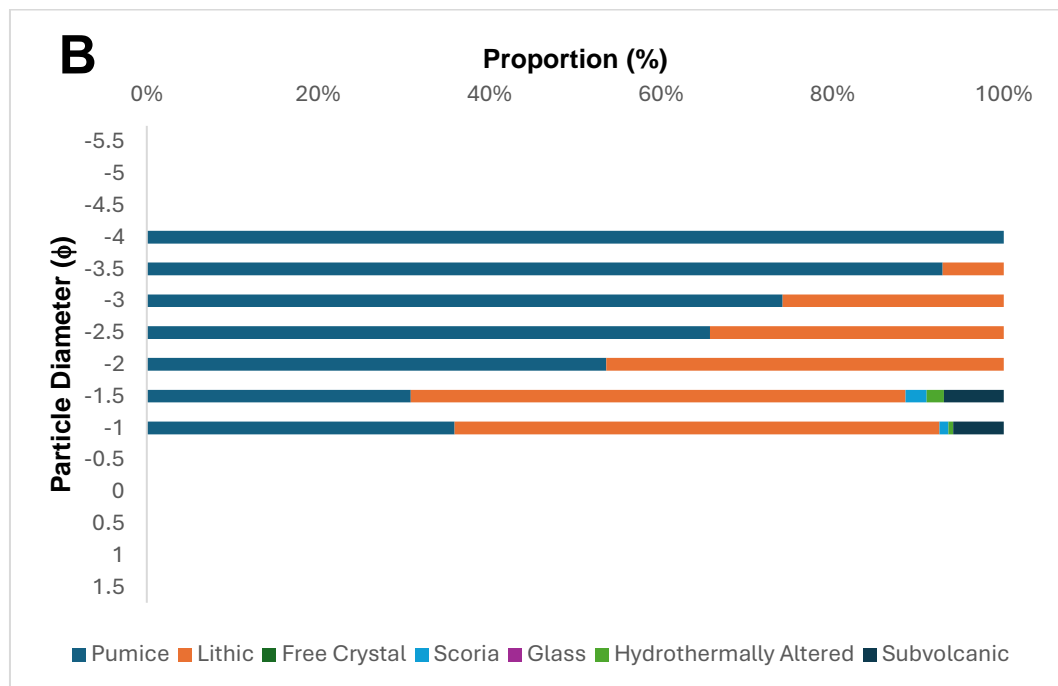
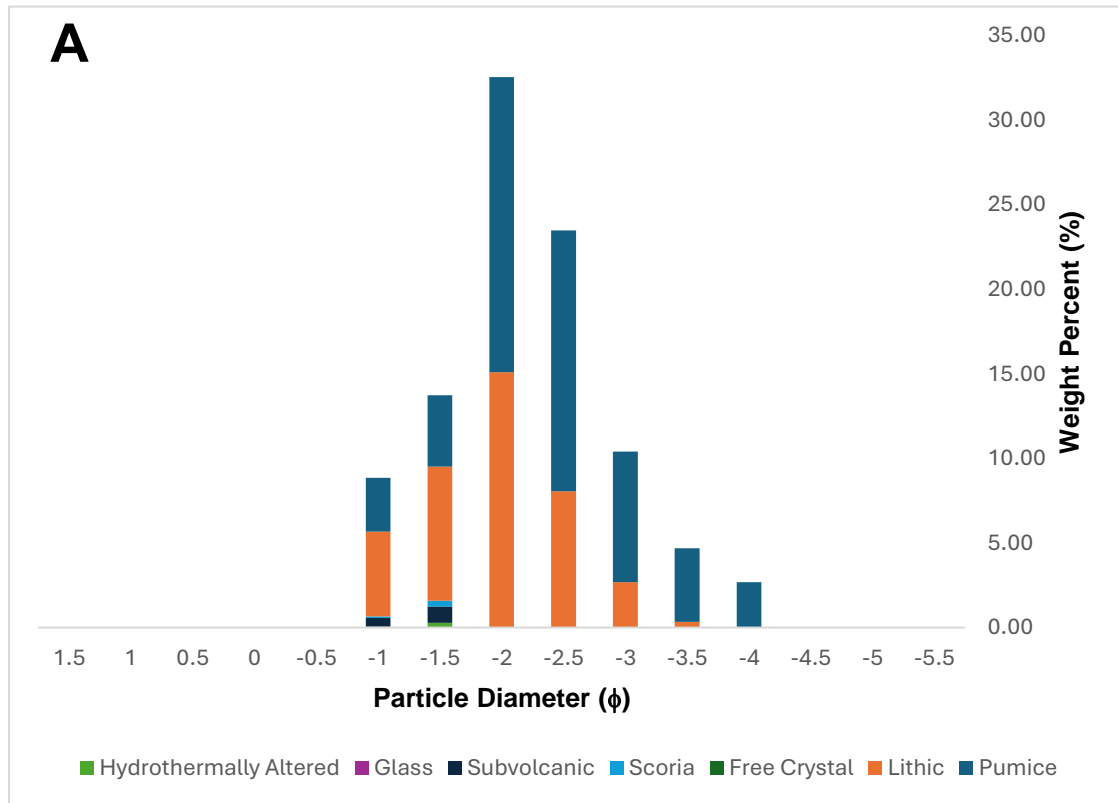
Figure 3.20 - Stratigraphic logs of the Zarza Formation across the Fasnía Region. UTM coordinates and inset map of locations are provided. The logs represent stratigraphic relationships with under- and overlying units.

3.1.7.3 Zarza Member A

Zarza Member A is a lithic-rich phonolite pumice fall deposit at the base of the Zarza Formation. At the type section it is 22 cm thick, massive, clast-supported, cream, well-sorted, coarse-grained, sub-angular pumice lapilli deposit. The pumice is ≤ 6 cm in diameter, generally aphyric with sparse biotite, pyroxene and k-feldspar phenocrysts. The pumice is microvesiculated, with sparse rounded vesicles < 3 mm in diameter. The member has 30-40 vol% lithic clasts of grey and black lavas and sparse red, vesiculated scoria. At the type section, the member has a sharp contact to member B above and the paleosol below.

Grain-Size and Componentry:

Zarza Member A was sieved at the type locality in 0.5ϕ intervals from -5.5ϕ to -2ϕ and in the laboratory from -1.5ϕ to 1.5ϕ . The deposit is unimodal, well-sorted ($\sigma\phi = 0.86$) and medium-grained lapilli ($Md\phi = -2.32$). Componentry was performed on fractions coarser than -1ϕ , where 96% of material is analysed. The formation contains components of pumice, lithic clasts, scoria, subvolcanic rocks, and hydrothermally altered rock. Proportionally, pumice clasts dominate fractions -3.5ϕ to -4ϕ and lithic clasts dominate fractions finer than -3ϕ . As a weight percentage, the deposit is composed of mostly pumice (57%) and lithic clasts (40.6%), with minor components of subvolcanic rock (1.5%), scoria (0.44%) and hydrothermally altered rock (0.33%) (figure 3.22).



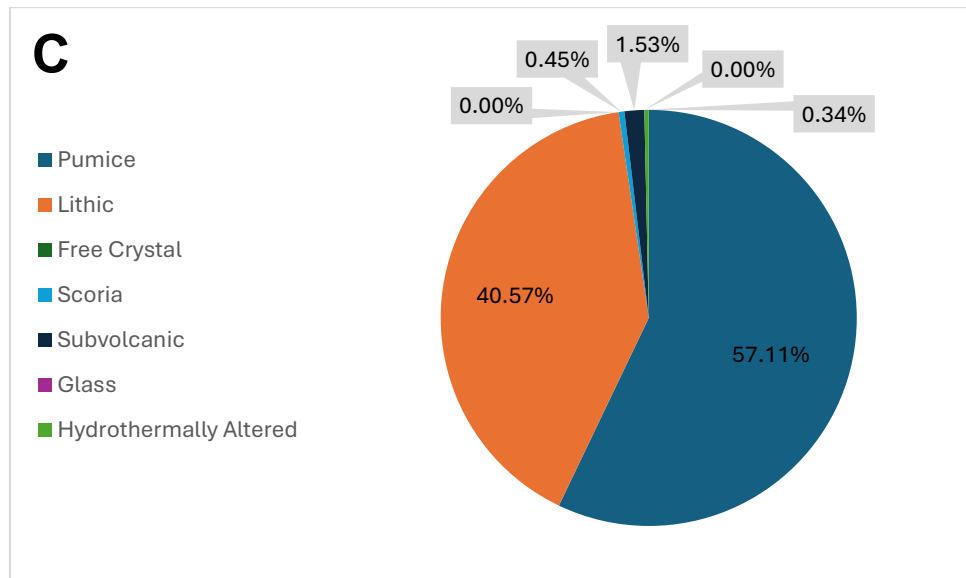


Figure 3.21 – Zarza Formation Member A. A) Proportion of components as a weight percentage of the total sample weight B) Proportion of components within each grain size C) Total weight percentage of components

3.1.7.2 Zarza Member B

Zarza Member B is a lithic-rich phonolite ash layer. At the type section, it is 2 cm thick, pink to orange, matrix supported, poorly sorted, ash deposit with sparse coarse grained pumice lapilli. At the top of the member is a <1 cm layer with >60 vol% fine grained lithic clasts. The member has a sharp contact to Zarza Member A above and Member C below.

Grain-Size and Componentry:

Due to the extremely fine grained, thin, and often cemented nature of this deposit, grain size analysis was not performed.

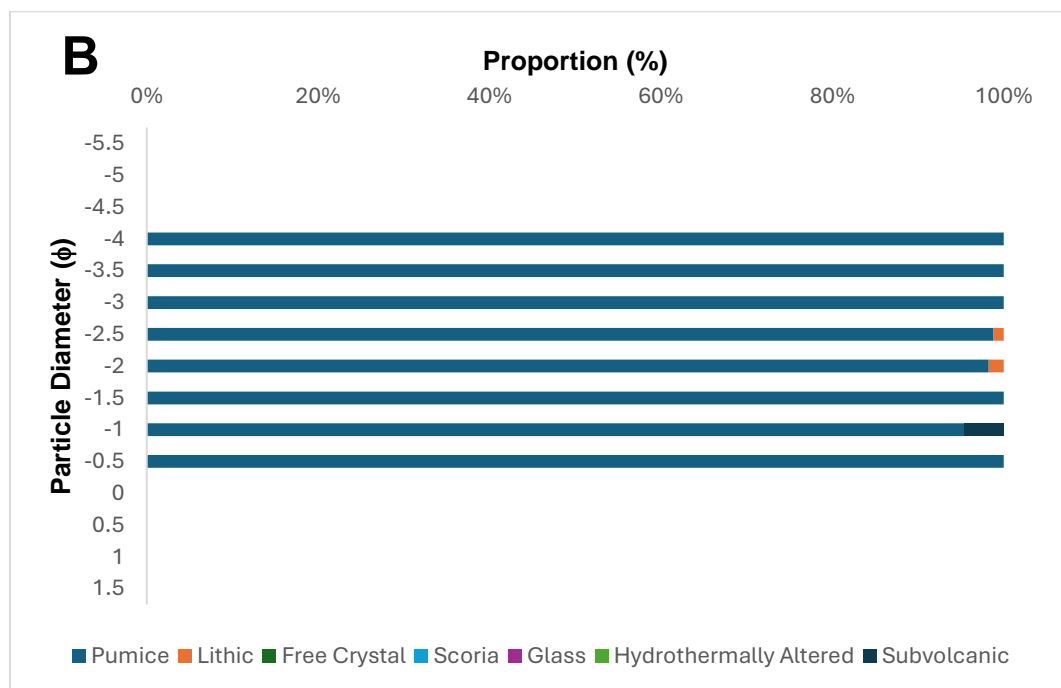
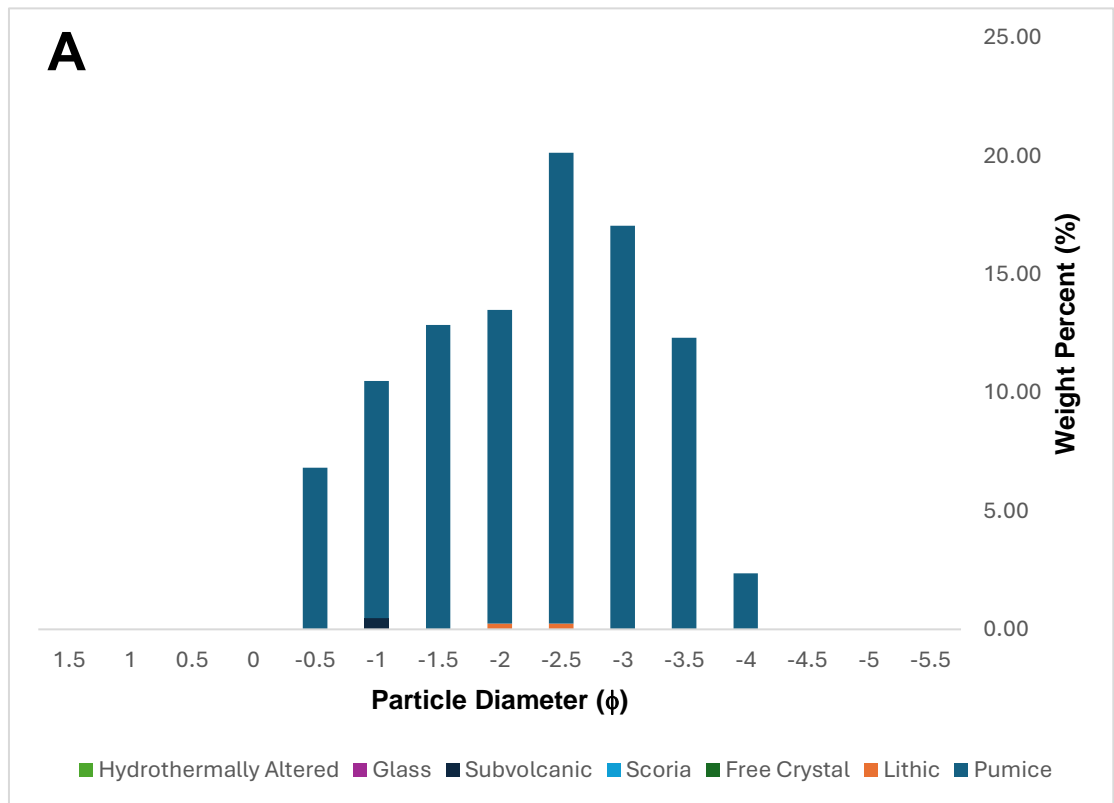
3.1.7.1 Zarza Member C

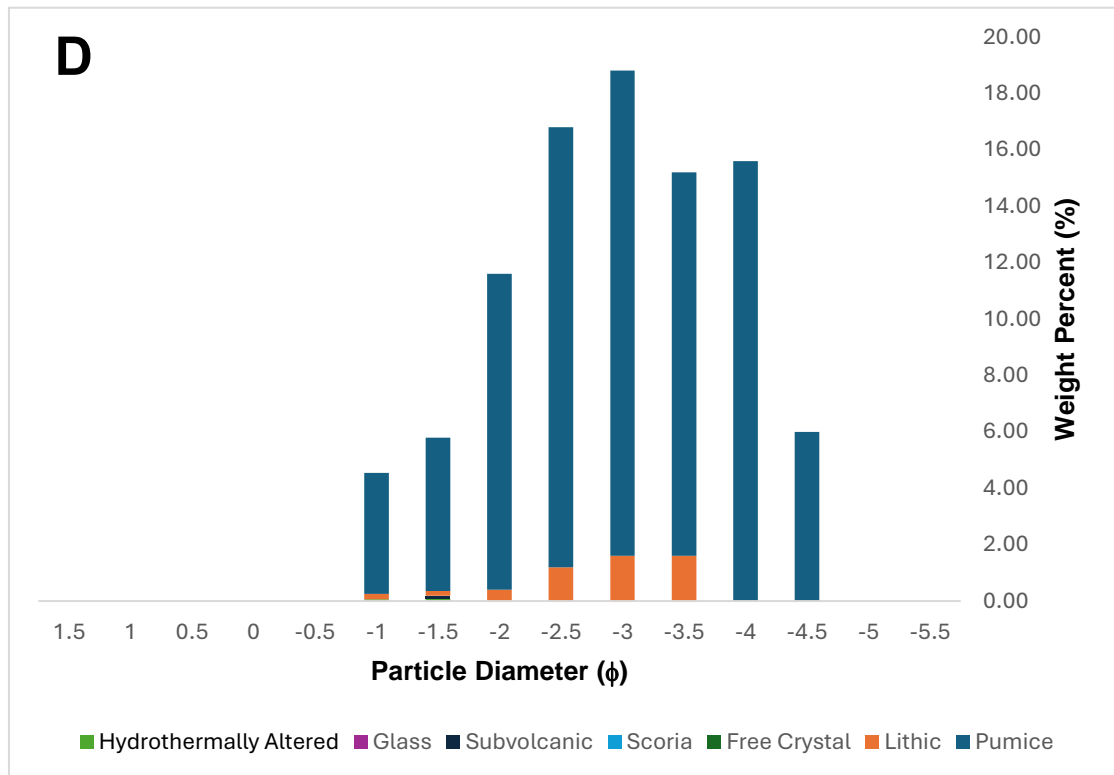
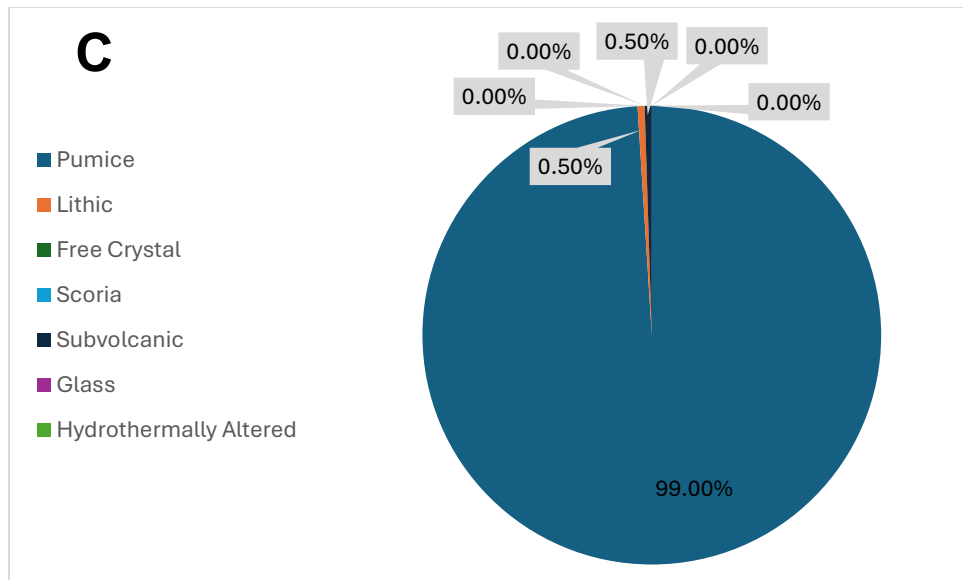
Zarza Member C is a phonolite pumice fall deposit at the top of the Zarza Formation. At the type section, it is 176 cm thick, moderately sorted, diffuse stratified, medium to fine-grained, sub-angular pumice lapilli. At ~90 cm from the base of the member, there is a ~5 cm band of coarse grained, angular pumice lapilli. Towards the northeast, this coarse-grained layer is fine-grained, sub-rounded pumice lapilli. The upper 15 cm of the member grades into well-sorted, coarse grained, angular pumice lapilli. The pumice is

commonly ≤ 4 cm in diameter, however, can be up to 7 cm at the top of the deposit, generally aphyric with sparse biotite, pyroxene and k-feldspar phenocrysts, and has rounded vesicles < 2 cm in diameter. Zarza Member A has < 5 vol% grey and black lithic clasts that grade in size from ≤ 2 cm at the base to ≤ 4 cm at the top. At the type section, the member grades into a 30 cm, orange to beige, fine-grained paleosol above, which in turn rests below the Icor Formation. The member has a sharp contact to Zarza Member B below (figure 3.19).

Grain-Size and Componentry:

Zarza Member C was sieved at the type locality in 0.5ϕ intervals from -5.5ϕ to -2ϕ and in the laboratory from -1.5ϕ to 1.5ϕ . Due to the thickness of the deposit being > 1 m the deposit was sieved at two intervals, 50 cm and 120 cm from the base. At 50 cm, the deposit is unimodal, well-sorted ($\sigma\phi = 1.1$) and medium-grained lapilli ($Md\phi = -2.52$). Componentry was performed on fractions coarser than -0.5ϕ , where 96% of material is analysed. The formation contains components of pumice, lithic clasts, and subvolcanic rocks. Proportionally, pumice clasts dominate each fraction from -0.5ϕ to -4ϕ . As a weight percentage, the deposit is composed of almost entirely pumice (99%), with the remaining 1% equally split between lithic clasts and subvolcanic rock. At 120 cm, the deposit is unimodal, well-sorted ($\sigma\phi = 1.16$) and medium to coarse-grained lapilli ($Md\phi = -3.16$). Componentry was performed on fractions coarser than -1ϕ , where 96% of material is analysed. The formation contains components of pumice, lithic clasts, subvolcanic rocks, and hydrothermally altered rock. Proportionally, pumice clasts dominate each fraction from -1ϕ to -4ϕ . As a weight percentage, the deposit is composed of almost entirely pumice (94%) with minor lithic clasts (5.5%), and subvolcanic and hydrothermally altered rock each consisting of $< 1\%$ (figure 3.21).





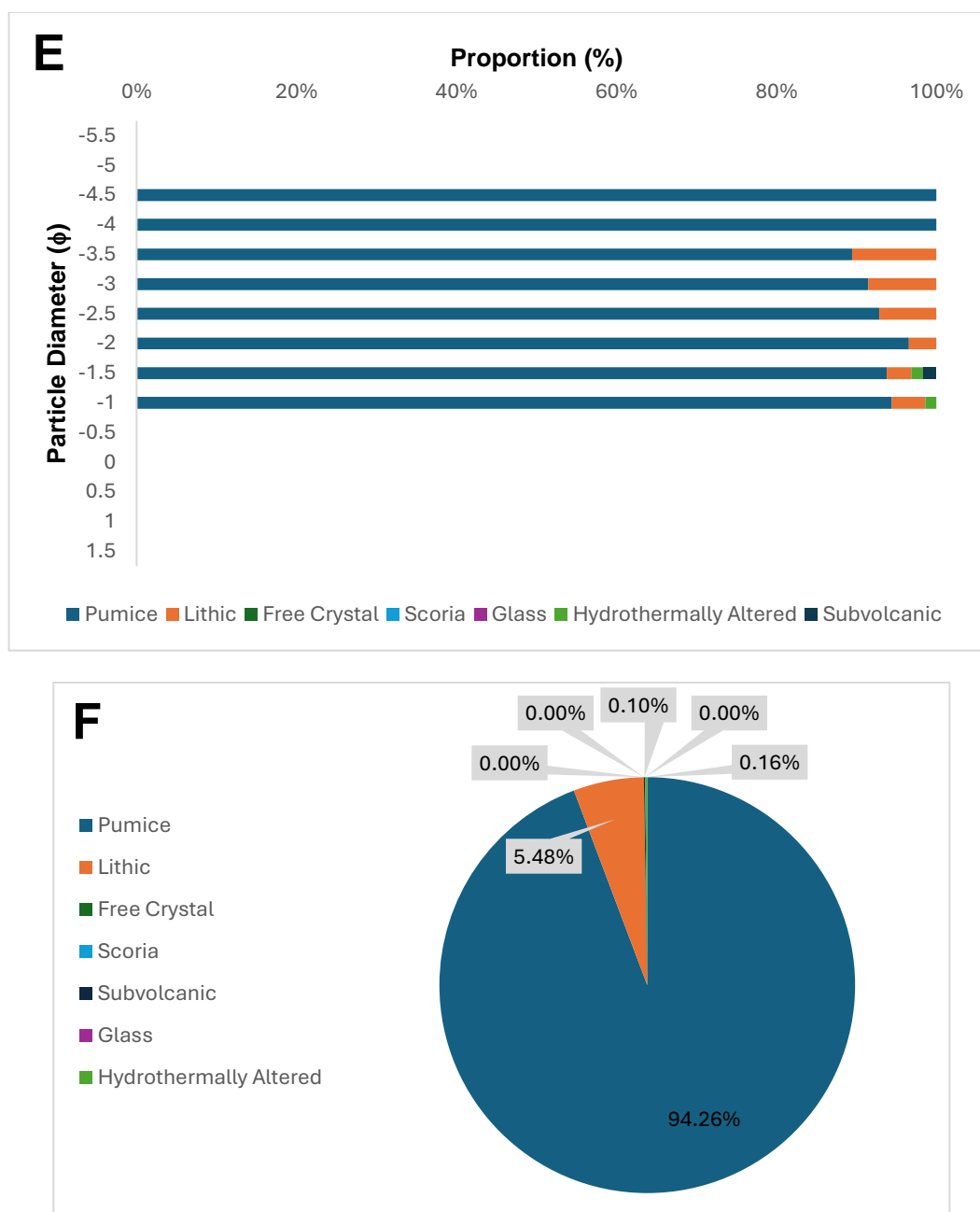


Figure 3.22 – Zarza Formation Member C. **A)** Proportion of components as a weight percentage of the total sample weight at 50cm. **B)** Proportion of components within each grain size at 50cm. **C)** Total weight percentage of components at 50cm. **D)** Proportion of components as a weight percentage of the total sample weight at 120cm. **E)** Proportion of components within each grain size at 120cm. **F)** Total weight percentage of components at 120cm

Dispersal, Volume, and Column Height:

The Zarza Formation is dispersed across SE Bandas Del Sur from Icor to Lomo de Mena. Zarza Member C has an easterly dispersal, thinning to the northeast, before Zarza

Member A shifted to a northeast dispersal, thinning to the southwest. The formation has a minimum dispersal of $\sim 346 \text{ km}^2$ with a minimum onshore volume of 0.894 km^3 .

Table 3.4 - Eruption parameters for the Zarza Formation

Volume (km^3)			VEI	Column Height		
<i>Exponential</i>	<i>Powerlaw</i>	<i>Weibull</i>		Carey and Spark (1986)	Pyle (1989)	Bonadonna and Costa (2013)
				Zarza C	Zarza B	Zarza A
1.356 – 1.671	2.037 – 3.3236	0.894 – 1.242	5	>15.5	-	>20.4
						>41
						45-55

Interpretation:

The Zarza Formation is a phonolite pumice fall deposit from a Plinian eruption with three main phases of activity. The eruption began with an easterly eruption column, with abundant lithics suggesting significant vent clearance. The eruption then briefly terminated, likely due to plugging as there is a thin lithic layer at the top of Zarza Member B. The eruption restarted with a shift in dispersal to the northeast, generating an eruption column with minor fluctuations in intensity given the diffusely stratified nature of the deposit. The coarse-grained layer in the southwest, that decreases in grainsize to the northeast, suggests a potential brief shift in dispersal to the south. The grainsize then increases towards the final stages over the eruption, with stratification seen at localities closest to the dispersal axis. This could suggest an increase in eruption intensity, vent widening, and then instability of the eruption column before termination. However, no pyroclastic density current deposit has been located for this formation.

3.1.8 Icor Formation

The Icor Formation, named after a town located 700m south of the type locality, comprises 6 phonolite pumice fall layers (Icor Member A-F) (figure 3.24). The formation has been measured across $\sim 18 \text{ km}^2$ from Las Eras to Fasnía, with a maximum thickness of 141 cm in La Zarza. The Icor Formation is found in Aguerche, however was inaccessible to measure (locality 1, figure 3.17). The type locality is found northwest of Icor at the top of Barranco de Icor O las Carretas.

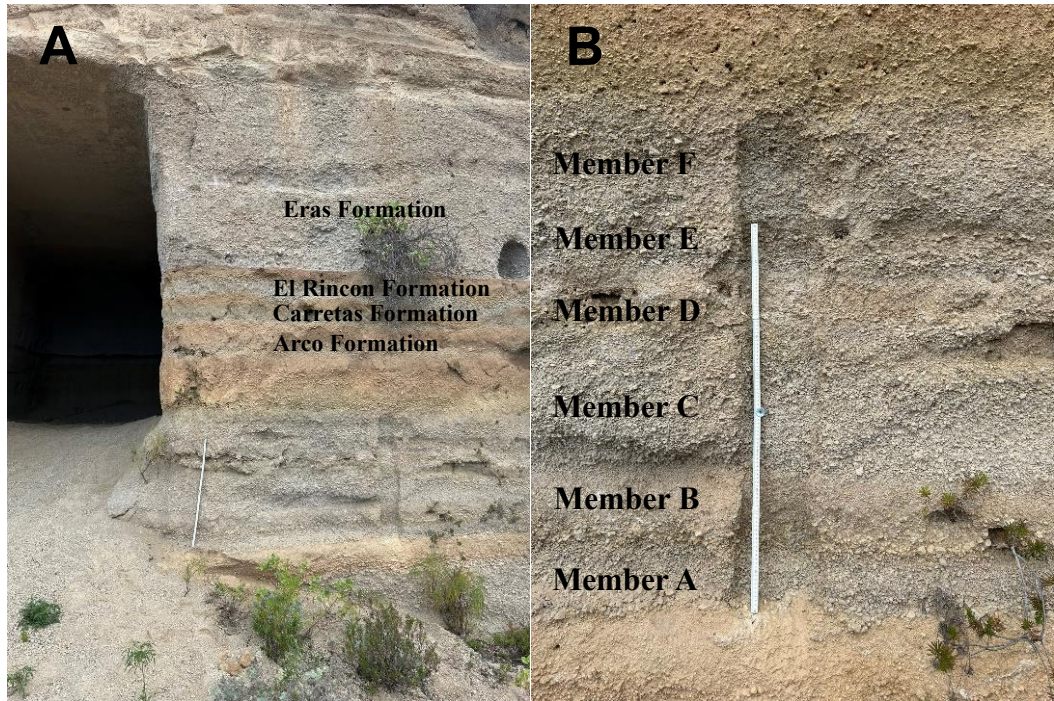


Figure 3.23 – **A)** The Icor Formation at North Icor, beneath the Arco, Carretas, El Rincon and Eras Formations. **B)** Each member of the Icor Formation at North Icor.

Icor Formation

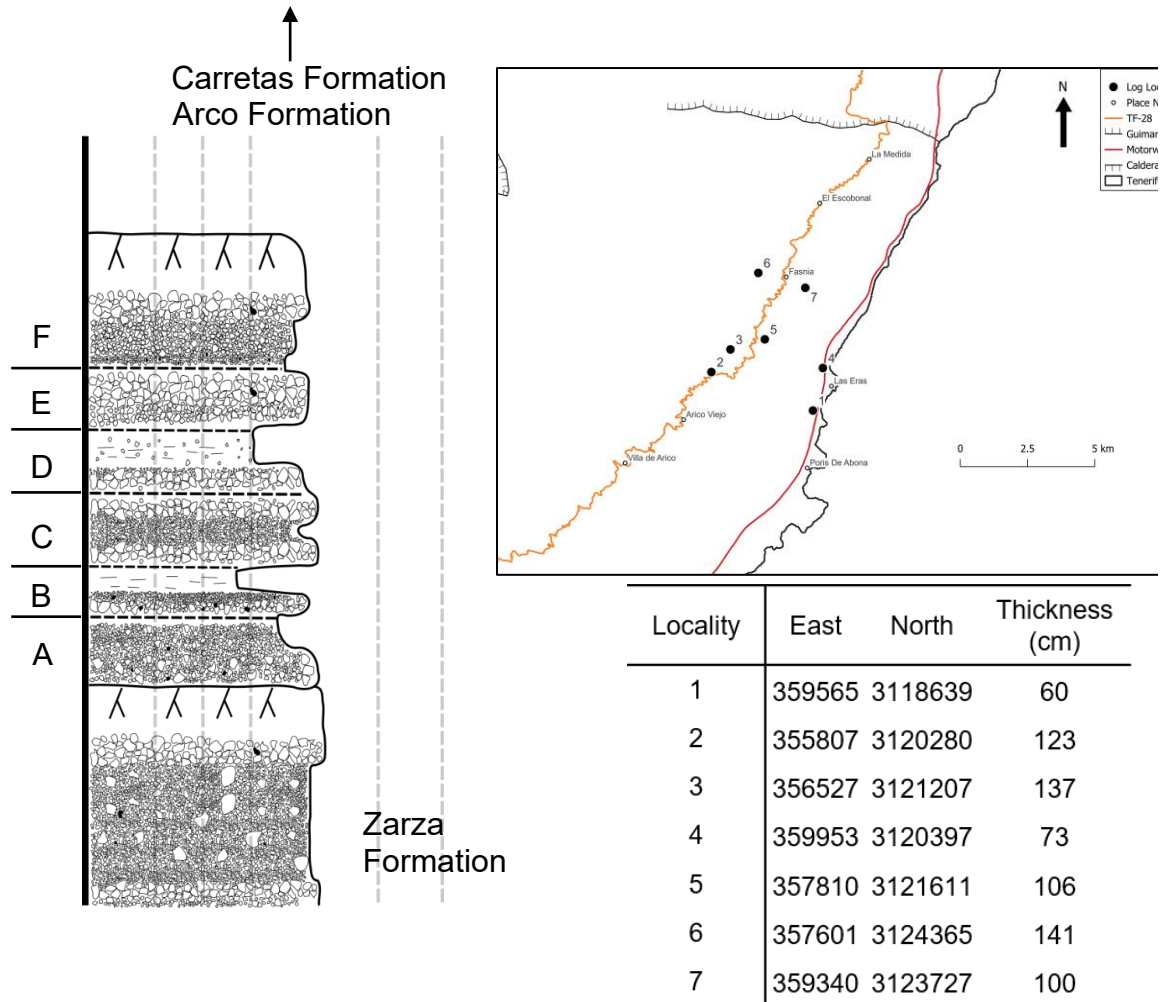


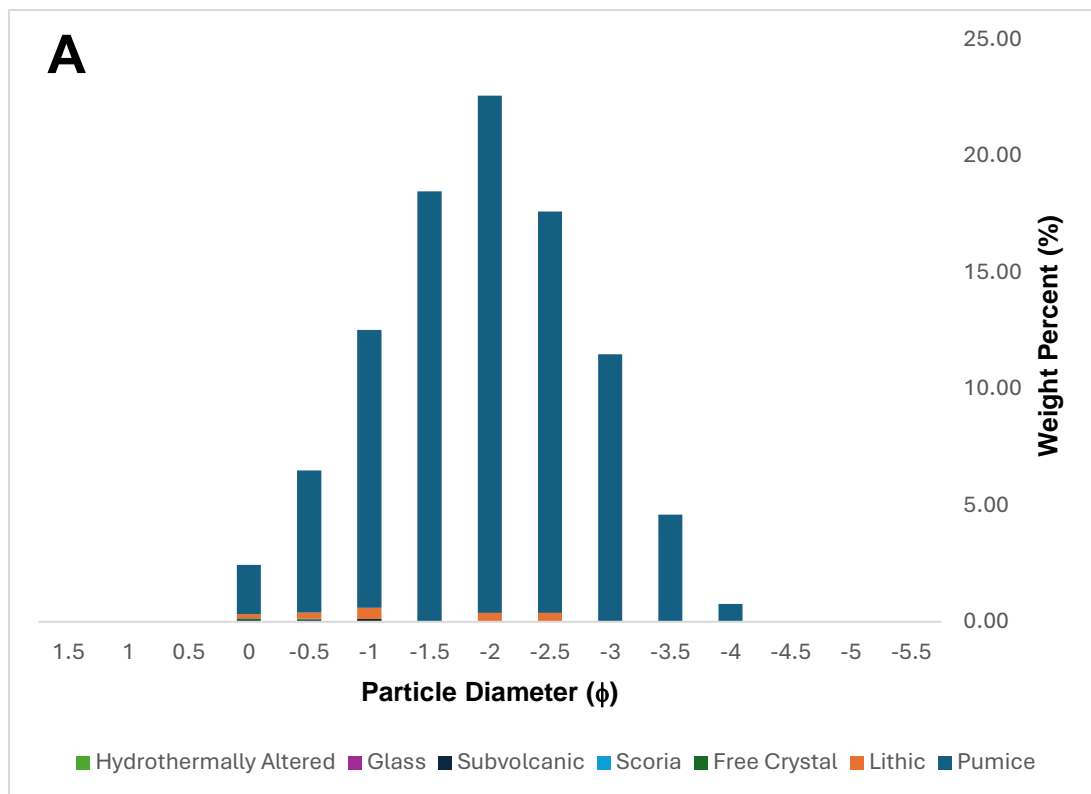
Figure 3.24 - Stratigraphic log of the Icor Formation across the Fasnía Region. UTM coordinates and inset map of locations are provided. The logs represent stratigraphic relationships with under- and overlying units.

3.1.8.6 Icor Member A

Icor Member A is a phonolite pumice fall deposit at the bottom of the Icor Formation. At the type locality, it is 19 cm thick, normally graded, clast supported, cream, well sorted, medium to fine-grained, sub-angular pumice lapilli deposit (figure 3.23). The pumice is ≤ 4 cm in diameter, generally aphyric with sparse k-feldspar, and is microvesicular. The member has ~5 vol% lithics of lava and obsidian that are < 1 cm in diameter, with frequent free crystals of Sanidine. The member has a sharp contact with the paleosol below, which is in turn above the Zarza Formation, and a sharp contact with Icor Member B above.

Grain-Size and Componentry:

Icor Member A was sieved at the type locality in 0.5ϕ intervals from -5.5ϕ to -2ϕ and in the laboratory from -1.5ϕ to 1.5ϕ . The deposit is unimodal, well sorted ($\sigma\phi = 0.94$) lapilli pumice ($Md\phi = -2.15$). Componentry was performed on fractions coarser than 0ϕ , where 97% of material is analysed. The formation contains components of pumice, lithic clasts, free crystals, subvolcanic rocks, and juvenile glass. Proportionally, pumice clasts dominate each fraction ($>85\%$), with minor lithic clasts in fractions finer than -1ϕ ($>4\%$). As a weight percentage, the deposit is composed of mostly pumice (97.8%) with minor lithic clasts (1.73%), with the remaining components each $<1\%$ of the total weight (figure 3.30).



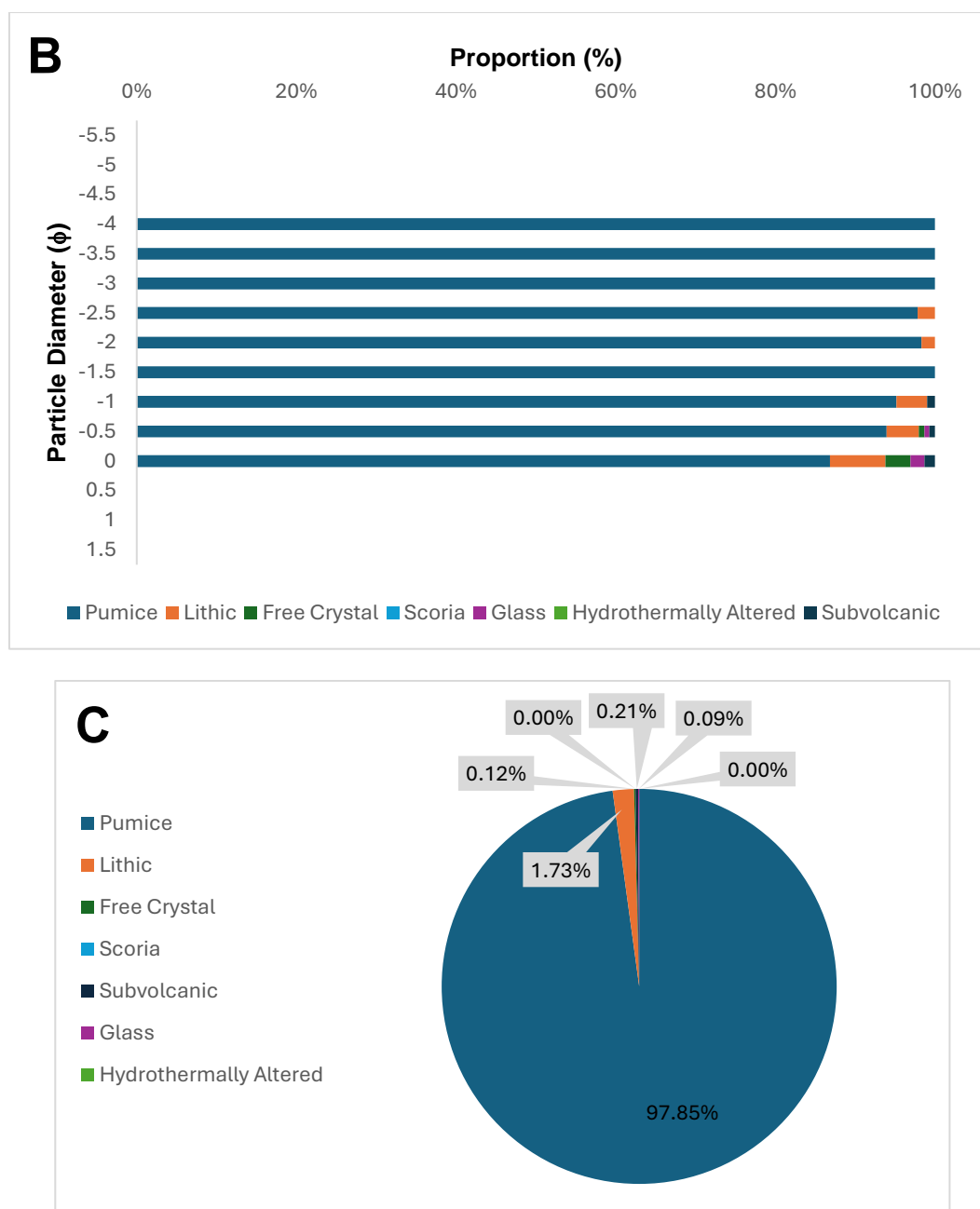


Figure 3.25 – Icor Formation Member A. A) Proportion of components as a weight percentage of the total sample weight B) Proportion of components within each grain size C) Total weight percentage of components

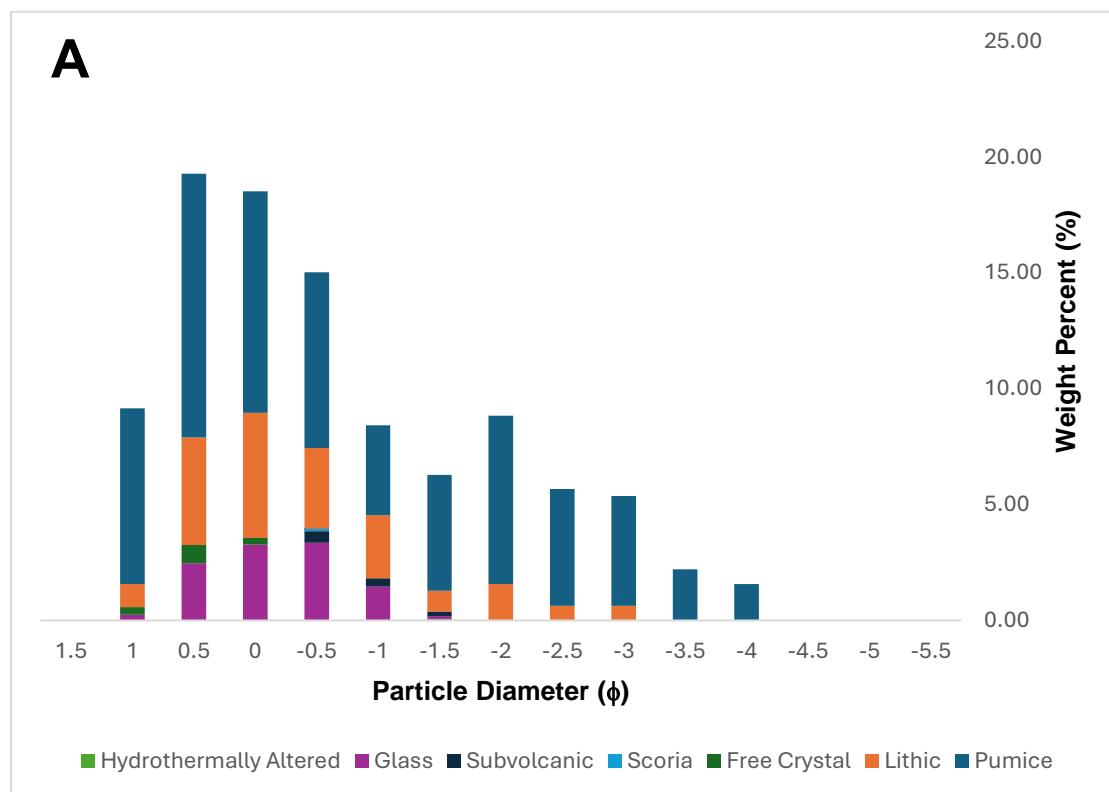
3.1.8.5 Icor Member B

Icor Member B is a phonolite pumice fall deposit. At the type locality, it is 22 cm thick, normally graded, clast supported, yellow to beige, well sorted, medium to fine-grained, sub-angular to sub-rounded pumice lapilli deposit (figure 3.23). The pumice is ≤ 4 cm in diameter, generally aphyric with sparse k-feldspar and biotite phenocrysts, highly vesiculated cream pumice and microvesiculated dark grey pumice. The member has ~5 vol% lithic clasts of grey lava and obsidian that are < 1 cm in diameter. and sparse free

crystals of Sanidine. The member has a sharp contact with Icor Member C above and Icor Member A below.

Grain-Size and Componentry:

Icor Member B was sieved at the type locality in 0.5ϕ intervals from -5.5ϕ to -2ϕ and in the laboratory from -1.5ϕ to 1.5ϕ . The deposit is bimodal, moderately sorted ($\sigma\phi = 1.33$) lapilli pumice and ash ($Md\phi = -0.56$). Componentry was performed on fractions coarser than 1ϕ , where 99% of material is analysed. The formation contains components of pumice, lithic clasts, free crystals, scoria, subvolcanic rocks, juvenile glass, and hydrothermally altered rock. Proportionally, pumice clasts dominate each fraction coarser than -1.5ϕ ($>80\%$), with abundant lithic clasts in fractions finer than -1ϕ ($>45\%$) and frequent juvenile glass in fractions -1ϕ to 0.5ϕ ($>10\%$). As a weight percentage, the deposit is composed of pumice (65.6%), lithic clasts (20.9%), juvenile glass (10.9%), and minor free crystals (1.41%) and subvolcanic rock (1.05%), with the remaining components each $<1\%$ of the total weight (figure 3.29).



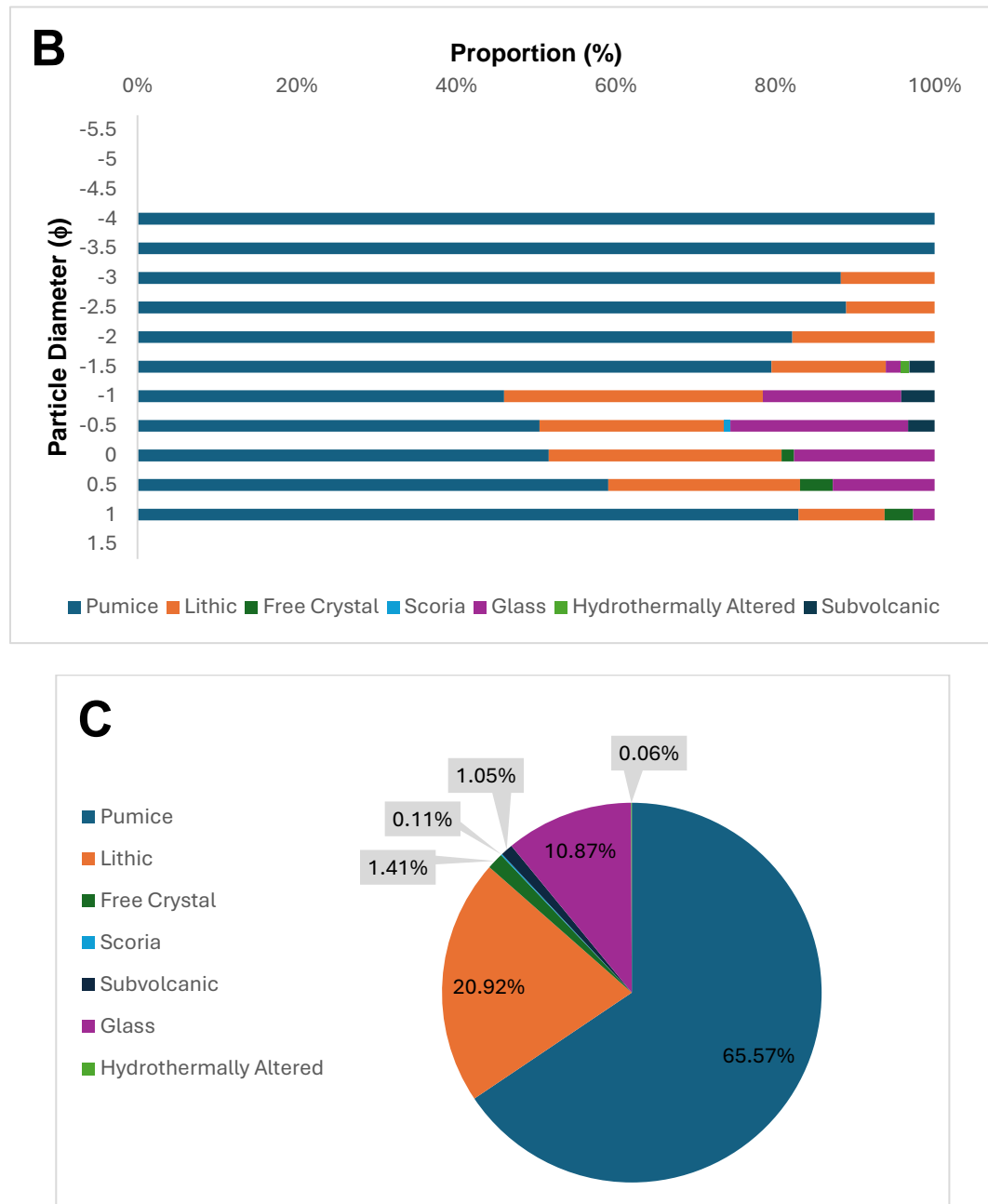


Figure 3.26 – Icor Formation Member B. A) Proportion of components as a weight percentage of the total sample weight B) Proportion of components within each grain size C) Total weight percentage of components

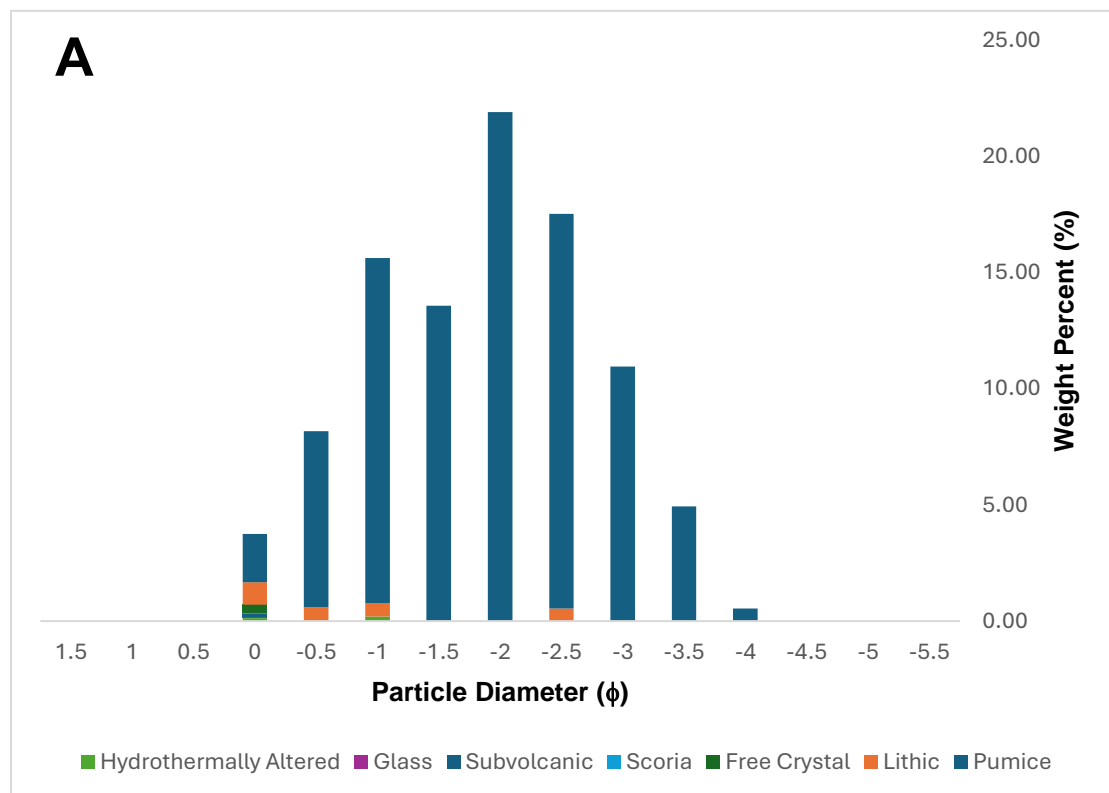
3.1.8.4 Icor Member C

Icor Member C is a phonolite pumice fall deposit. At the type locality, it is 30 cm thick, symmetrically graded, clast supported, cream, moderately sorted, coarse to medium to coarse-grained, sub-angular pumice lapilli deposit (figure 3.23). The pumice is ≤ 4 cm in diameter, aphyric, with elongated vesicles ≤ 2 cm in length, and frequent mingled

pumice. The member has <1 vol% lithic clasts. The member grades into Icor Member D above and a sharp contact to Icor Member B below.

Grain-Size and Componentry:

Icor Member C was sieved at the type locality in 0.5ϕ intervals from -5.5ϕ to -2ϕ and in the laboratory from -1.5ϕ to 1.5ϕ . The deposit is bimodal, well sorted ($\sigma\phi = 0.97$) lapilli pumice ($Md\phi = -2.14$). Componentry was performed on fractions coarser than 0ϕ , where 97% of material is analysed. The formation contains components of pumice, lithic clasts, free crystals, scoria, subvolcanic rocks, juvenile glass, and hydrothermally altered rock. Proportionally, pumice clasts dominate each fraction coarser than -0.5ϕ (>90%), with abundant lithic clasts in fractions finer than 0ϕ (>26%). As a weight percentage, the deposit is composed of mostly pumice (96.3%) with minor lithic clasts (2.77%), with the remaining components each <1% of the total weight (figure 3.28).



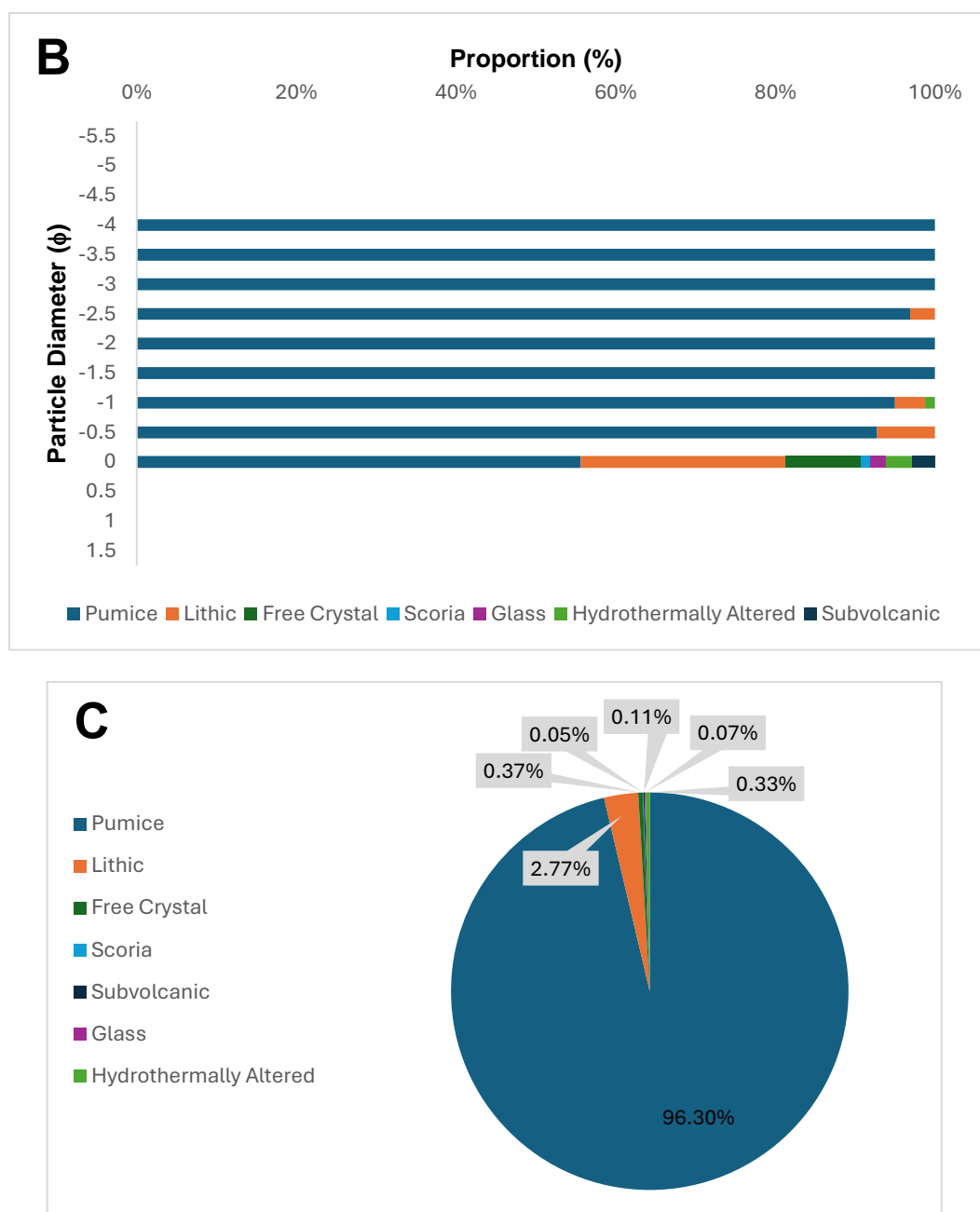


Figure 3.27 – Icor Formation Member C. **A)** Proportion of components as a weight percentage of the total sample weight **B)** Proportion of components within each grain size **C)** Total weight percentage of components

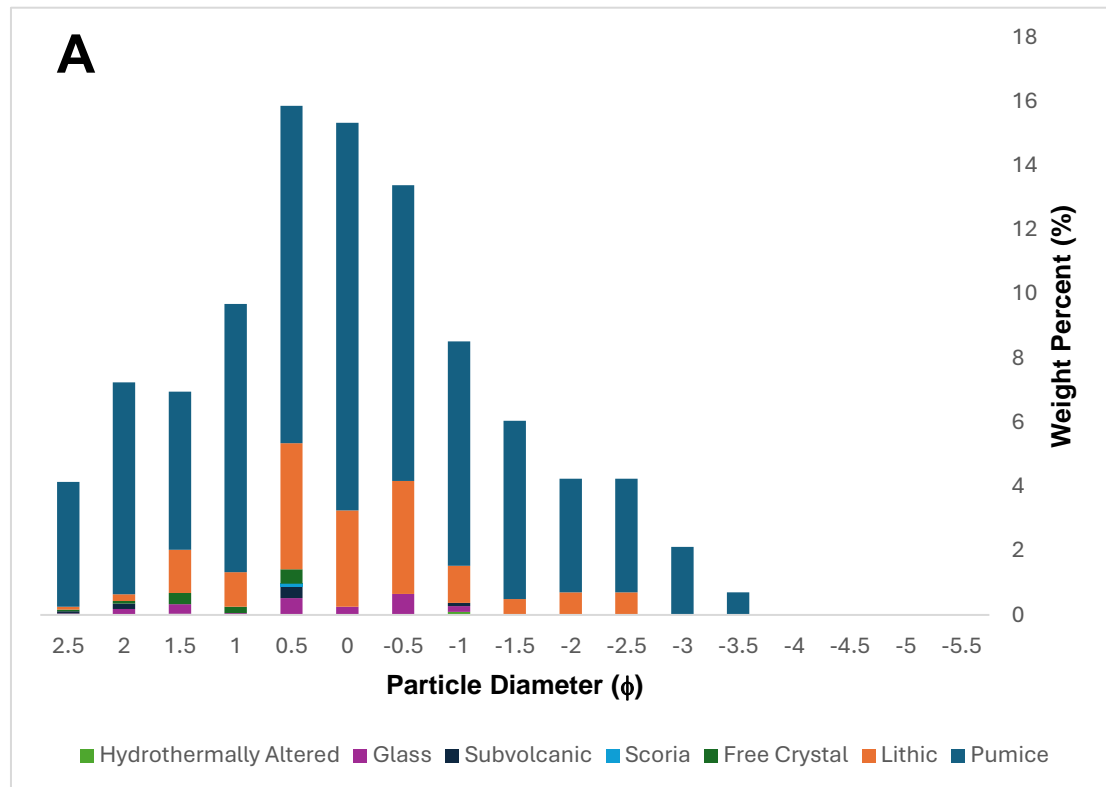
3.1.8.3 Icor Member D

Icor Member D is a phonolite pumice fall deposit. At the type locality, it is 26 cm thick, normally graded, clast supported, cream to orange, poorly sorted, moderately to fine-grained, sub-angular to sub-rounded pumice lapilli deposit (figure 3.23). The pumice is ≤ 2 cm in diameter, generally aphyric with sparse k-feldspar and pyroxene phenocrysts,

and elongated vesicles <0.5 cm in diameter. The member has <5 vol% lithic clasts of lava, orange hydrothermally altered clasts, and obsidian. The member has a sharp contact with Icor Member E above and grades into Icor Member C below.

Grain-Size and Componentry:

Icor Member D was sieved at the type locality in 0.5 ϕ intervals from -5.5 ϕ to -2 ϕ and in the laboratory from -1.5 ϕ to 2.5 ϕ . The deposit is unimodal, moderately sorted ($\sigma\phi = 1.41$) lapilli pumice and ash (Md $\phi = -0.17$). Componentry was performed on fractions coarser than 2.5 ϕ , where 98% of material is analysed. The formation contains components of pumice, lithic clasts, free crystals, scoria, juvenile glass, subvolcanic rocks, and hydrothermally altered rock. Proportionally, pumice clasts dominate each fraction, with fluctuations in lithic clasts from 10-30% in fractions 1.5 ϕ to -1 ϕ . As a weight percentage, the deposit is composed of mostly pumice (79.2%) and lithic clasts (16.5%) and minor free crystal (1.13%) and juvenile glass components (2.21%), with the remaining components each <1% of the total weight (figure 3.27).



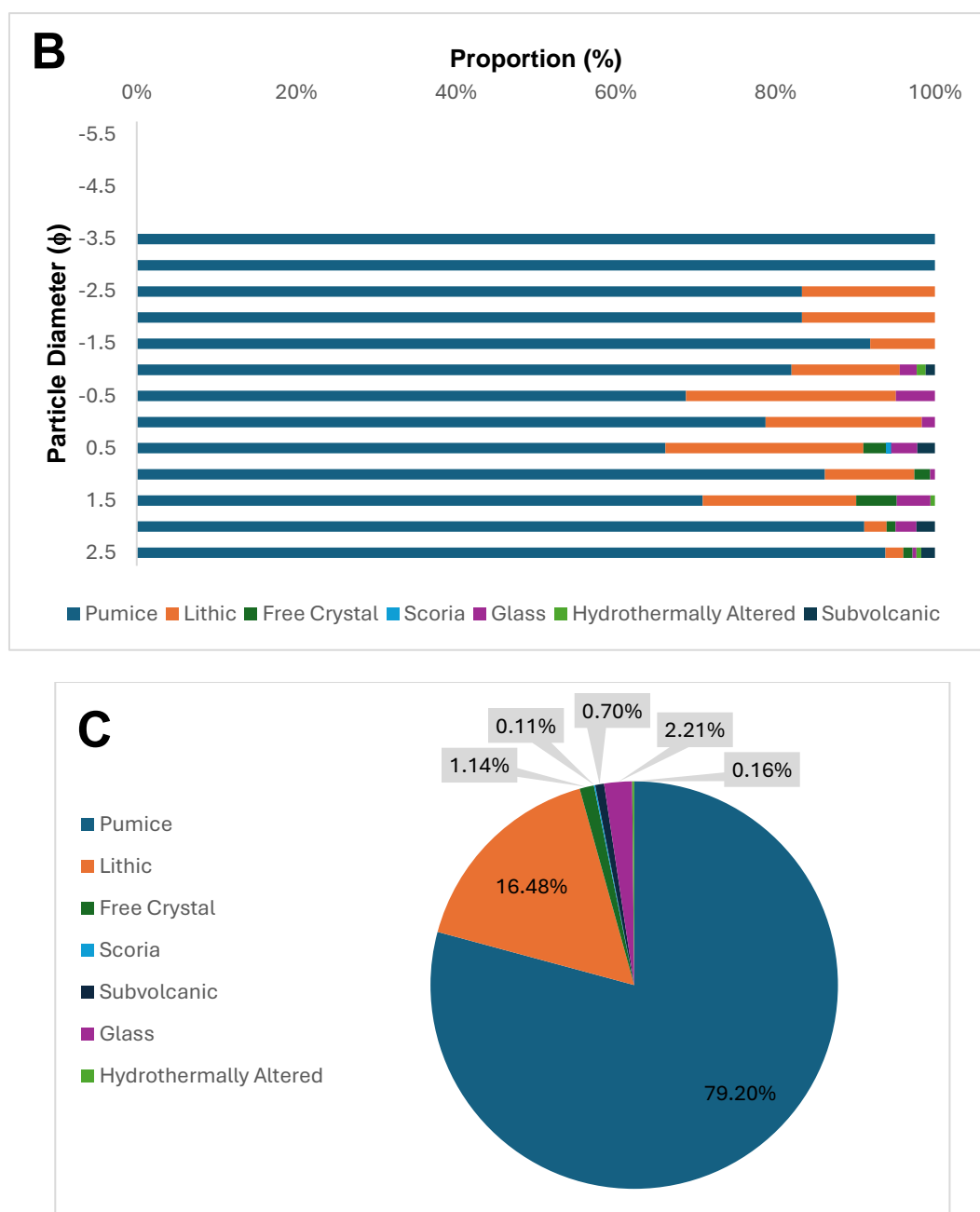


Figure 3.28 – Icor Formation Member D. **A)** Proportion of components as a weight percentage of the total sample weight **B)** Proportion of components within each grain size **C)** Total weight percentage of components

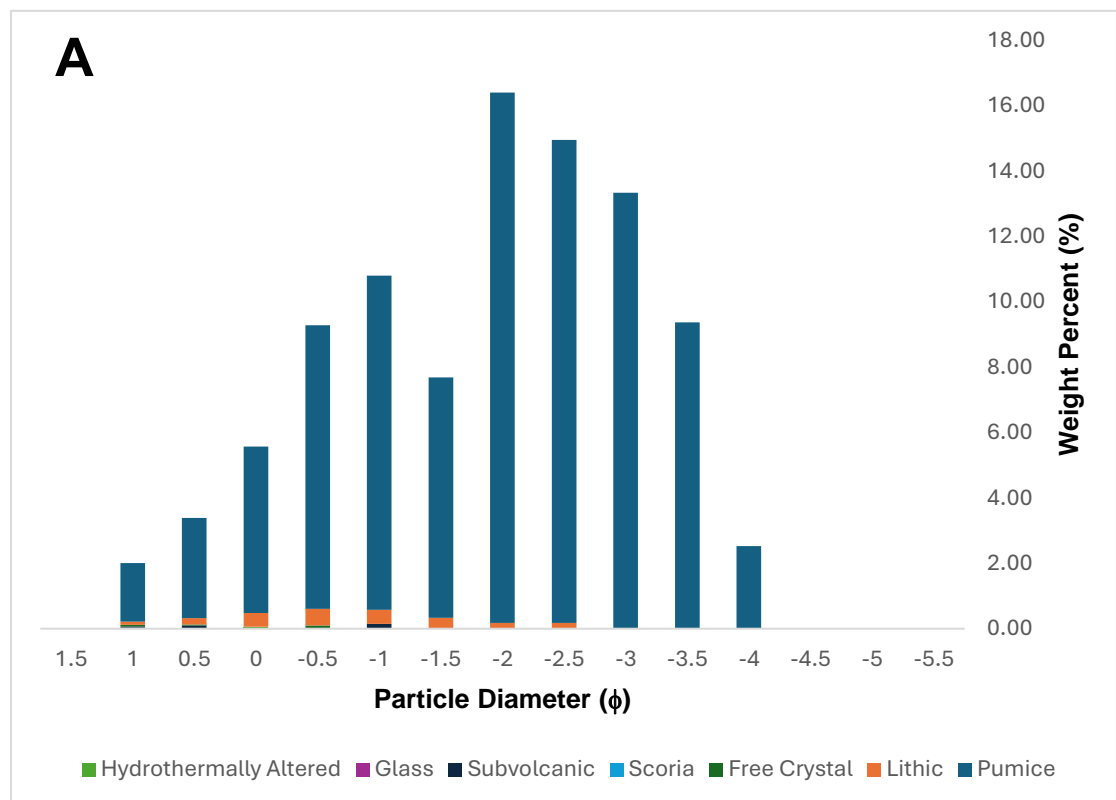
3.1.8.2 Icor Member E

Icor Member E is a phonolite pumice fall deposit. At the type locality, it is 13 cm thick, massive, clast-supported, cream to grey, moderately sorted, coarse-grained, sub-angular pumice lapilli deposit (figure 3.23). The pumice is ≤ 3 cm in diameter, generally aphyric with sparse k-feldspar and biotite phenocrysts, microvesicular, with sparse mingled pumices. The member has ~5 vol% of grey and black lithic clasts that are <1 cm in

diameter. The member has a sharp contact with Icor Member F above and Icor Member D below.

Grain-Size and Componentry:

Icor Member E was sieved at the type locality in 0.5ϕ intervals from -5.5ϕ to -2ϕ and in the laboratory from -1.5ϕ to 1.5ϕ . The deposit is bimodal, moderately sorted ($\sigma\phi = 1.33$) lapilli pumice ($Md\phi = -2.23$). Componentry was performed on fractions coarser than 1ϕ , where 95% of material is analysed. The formation contains components of pumice, lithic clasts, free crystals, subvolcanic rocks, juvenile glass, and hydrothermally altered rock. Proportionally, pumice clasts dominate each fraction, with minor lithic clasts in fractions finer than 0ϕ . As a weight percentage, the deposit is composed of mostly pumice (97.0%) with minor lithic clasts (2.5%), with the remaining components each $<1\%$ of the total weight (figure 3.26).



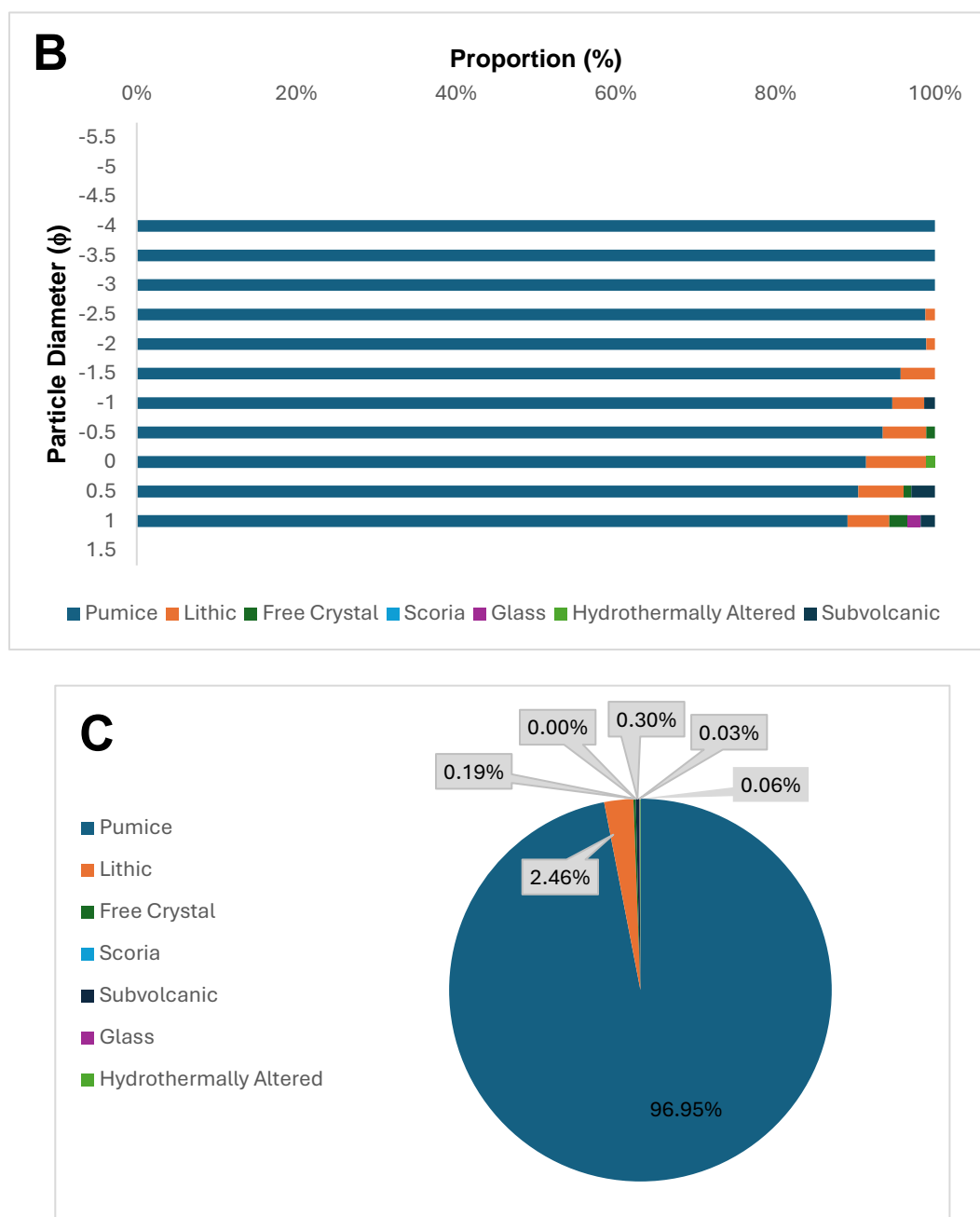


Figure 3.29 – Icor Formation Member E. A) Proportion of components as a weight percentage of the total sample weight B) Proportion of components within each grain size C) Total weight percentage of components

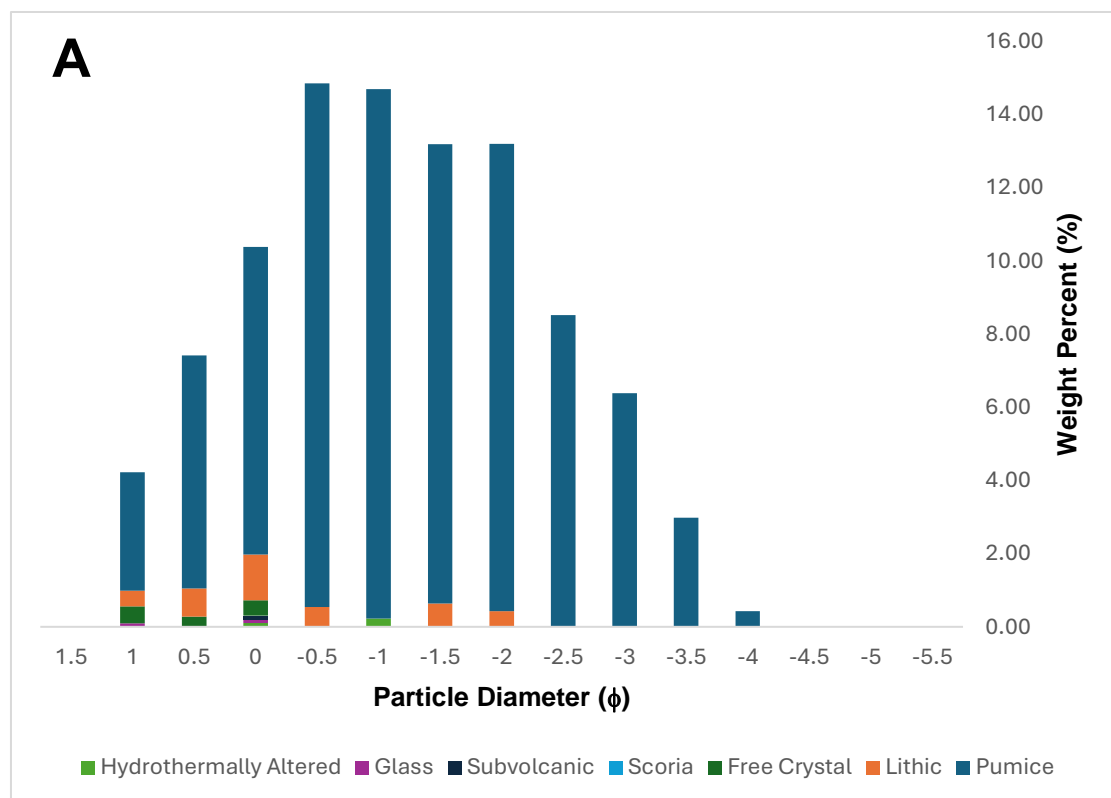
3.1.8.1 Icor Member F

Icor Member F is a phonolite pumice fall deposit at the top of the Icor Formation. At the type locality, it is 27 cm thick, inverse graded, clast supported, cream to grey, poorly to moderately sorted, fine to medium grained, sub-angular pumice lapilli deposit (figure 3.23). The pumice is ≤ 3 cm in diameter, generally aphyric with sparse biotite phenocrysts, generally microvesicular with sparse elongated vesicles, and sparse mingled

pumice. The member grades in lithic populations, with ~10 vol% lithic clasts at the base, reducing to ~5 vol% at the top. The member grades into the paleosol above, which is 59 cm thick, green to pink, matrix-supported with sparse coarse-grained pumice and obsidian fragments, and a 5 cm coarse pumice layer ~40 cm from the base. The paleosol is in turn overlain by the Arco Formation. Icor Member F has a sharp contact with Icor Member E below.

Grain-Size and Componentry:

Icor Member F was sieved at the type locality in 0.5ϕ intervals from -5.5ϕ to -2ϕ and in the laboratory from -1.5ϕ to 1.5ϕ . The deposit is unimodal, moderately sorted ($\sigma\phi = 1.26$) lapilli pumice ($Md\phi = -1.33$). Componentry was performed on fractions coarser than 1ϕ , where 96% of material is analysed. The formation contains components of pumice, lithic clasts, free crystals, subvolcanic rocks, juvenile glass, and hydrothermally altered rock. Proportionally, pumice clasts dominate each fraction, with minor lithic clasts in fractions finer than 0ϕ and minor free crystals at 1ϕ . As a weight percentage, the deposit is composed of mostly pumice (93.9%) with minor lithic clasts (4.2%) and free crystals (1.2%), with the remaining components each <1% of the total weight (figure 3.25).



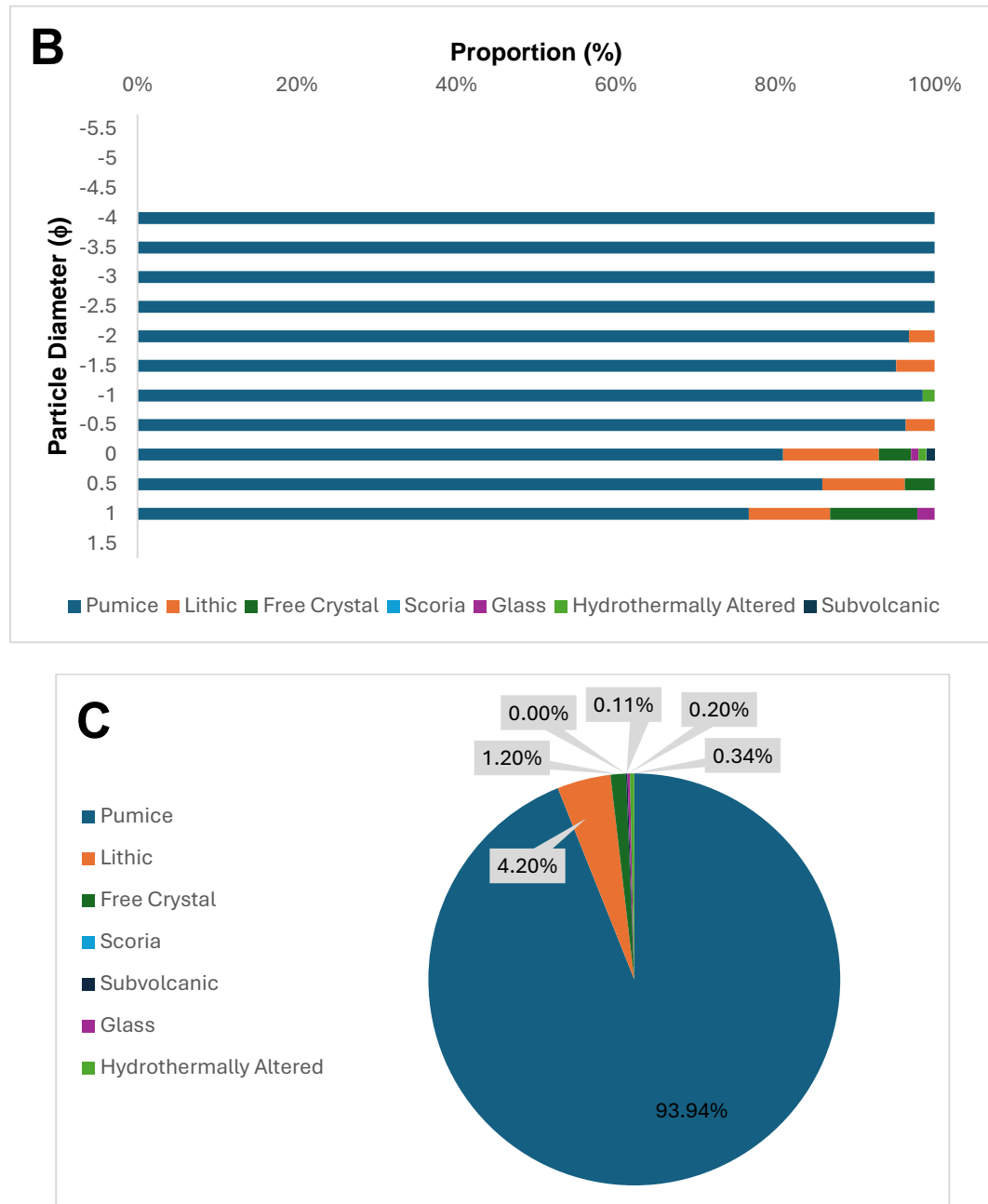


Figure 3.30 – Icor Formation Member F. A) Proportion of components as a weight percentage of the total sample weight B) Proportion of components within each grain size C) Total weight percentage of components

Dispersal, Volume, and Column Height:

The Icor Formation is dispersed across SE Bandas Del Sur from Icor to Fasnía Cone. Each Member of the Icor Formation has an easterly dispersal, with slight deviations to each other in the north and south. The formation has a minimum dispersal of $\sim 185\text{km}^2$ with a minimum onshore volume of 0.172km^3 .

Table 3.5 - Eruption parameters for the Icor Formation

Volume (km ³)			VEI
<i>Exponential</i>	<i>Powerlaw</i>	<i>Weibull</i>	
0.368 – 0.485	0.580 – 1.601	0.172 – 2.472	4

Interpretation:

The Icor Formation is a phonolite pumice fall deposit from a Plinian eruption that exhibits frequent stop-start behaviour and fluctuations in eruption intensity throughout its duration. The eruption began with an easterly dispersed eruption column, with limited vent clearance, that quickly waned in intensity (Icor Member A). A sudden increase in the abundance of lithic clasts may indicate a brief termination in the eruption due to vent blockage, before restarting, with a small shift in dispersal to the northeast, and quickly waning in intensity (Icor Member B). The intensity of the eruption increased and fluctuated (Icor Member C), with increased vent widening and potential partial vent collapse before waning to a potential termination (Icor Member D). The eruption increased in intensity again, with a stable eruption column (Icor Member E) before another potential termination or vent blockage, due to increased lithics at the base of the member above. The eruption then restarted, gradually increasing in column height, a lack of lithics suggests this is due to increase in eruption rate rather than vent widening, before the end of the eruption (Icor Member F).

3.1.9 Arco Formation

The Arco Formation, named after Barranco del Arco located south of the type locality northwest of Icor, is a phonolite pumice fall deposit (locality 1, figure 3.32). At the type locality, it is 19 cm thick, massive, non-graded, well-sorted, fine-grained, sub-rounded, pumice lapilli and ash (figure 3.31). The pumice is <2 cm in diameter, grey, aphyric, with rounded vesicles <1 mm in diameter. The formation has low lithic populations (<3 vol%) of dark grey lava that are <0.5 cm in diameter. At the type locality, the Arco Formation has a gradational contact to the paleosol below, above the Icor Formation, and the paleosol above. The overlying paleosol is 11 cm thick, light brown, fine-grained with scarce medium-grained pumice lapilli and <1 vol% lithic clasts of lava. The paleosol is in turn overlain by the Carretas Formation.

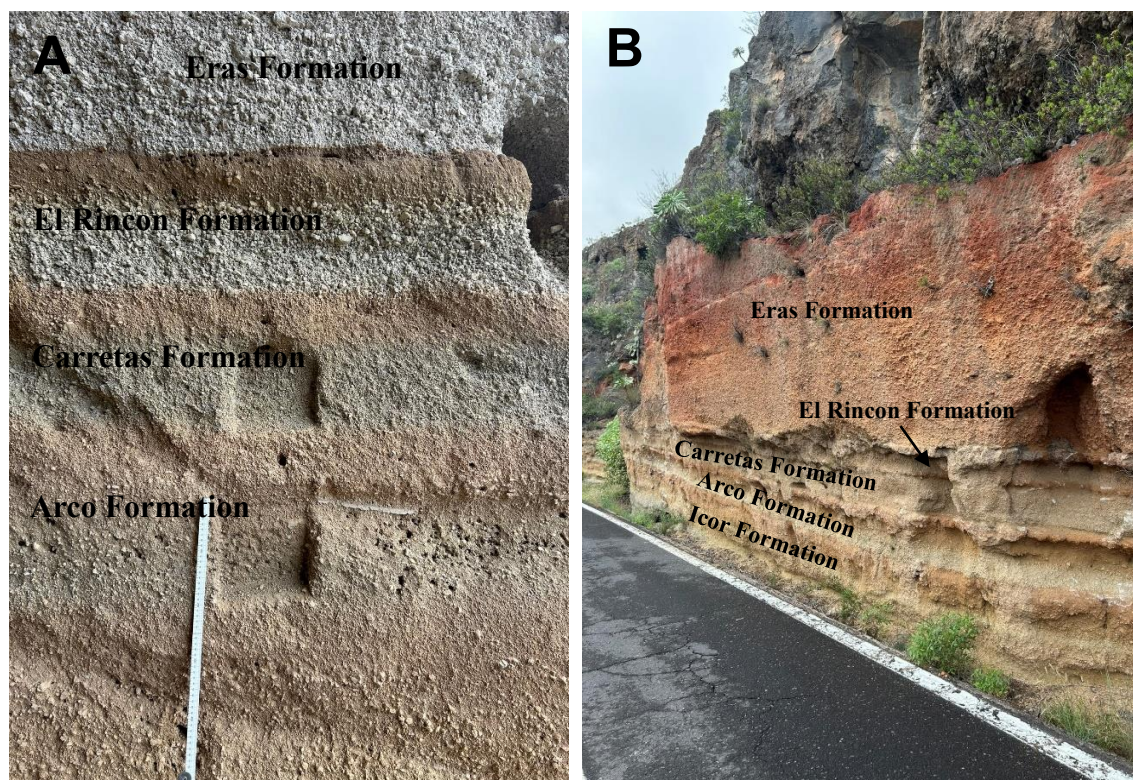


Figure 3.31 – A) The Arco, Carretas, and El Rincon Formations, below the Eras Formation in North Icor. Note the distinct dark brown paleosol between the Eras and El Rincon Formations. B) The Arco, Carretas, and El Rincon Formations beneath the Eras Formation and above the Icor Formation in La Zarza.

Arco

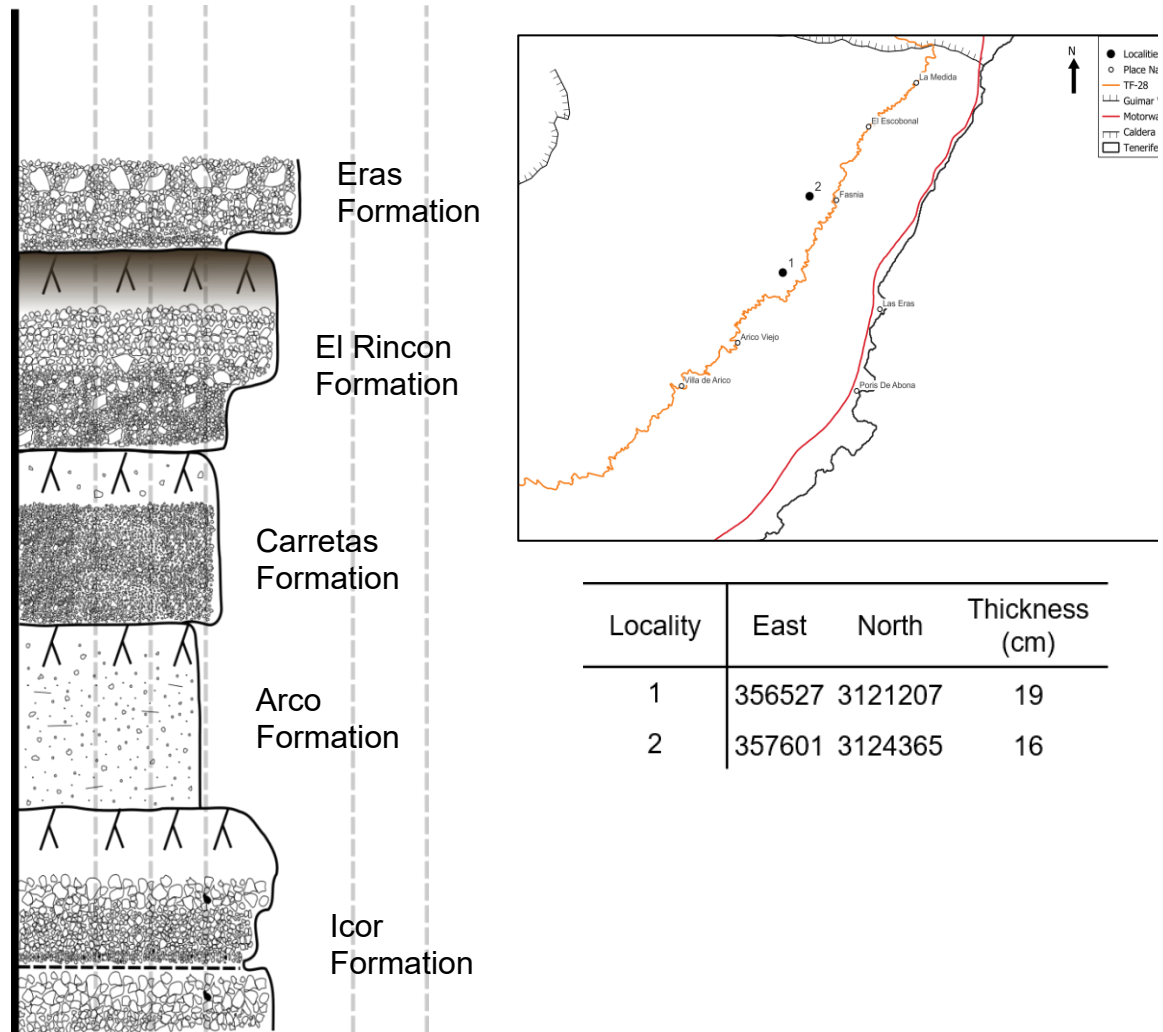


Figure 3.32 - Stratigraphic log of the Arco Formation across the Fasnia Region. UTM coordinates and inset map of locations are provided. The logs represent stratigraphic relationships with under- and overlying units.

Interpretation:

The Arco Formation is the product of a small scale Plinian or sub-Plinian eruption with an easterly dispersal across the Bandas Del Sur. It is uncertain whether the fine lapilli and ash is due to high fragmentation efficiency, or the deposit is on the edge of dispersal for a larger, unexposed eruption.

3.1.10 Carretas Formation

The Carretas Formation, named after Barranco de Icor O las Carretas located east of the type locality northwest of Icor, is a phonolite pumice fall deposit (locality 1, figure 3.33). At the type locality, it is 19 cm thick, massive, non-graded, moderately to well-sorted, fine-grained, sub-rounded pumice lapilli (figure 3.31). The pumice is <2 cm in diameter, grey to dark green, aphyric, with rounded vesicles <2 mm in diameter. The formation has low lithic populations (<3 vol%) of grey lava that are <0.5 cm in diameter. At the type locality the Carretas Formation has a gradational contact to the paleosol below, above the Arco Formation, and to the paleosol above, which is in turn below the El Rincon Formation. The overlying paleosol is 10 cm thick, light brown to pink, and fine-grained.

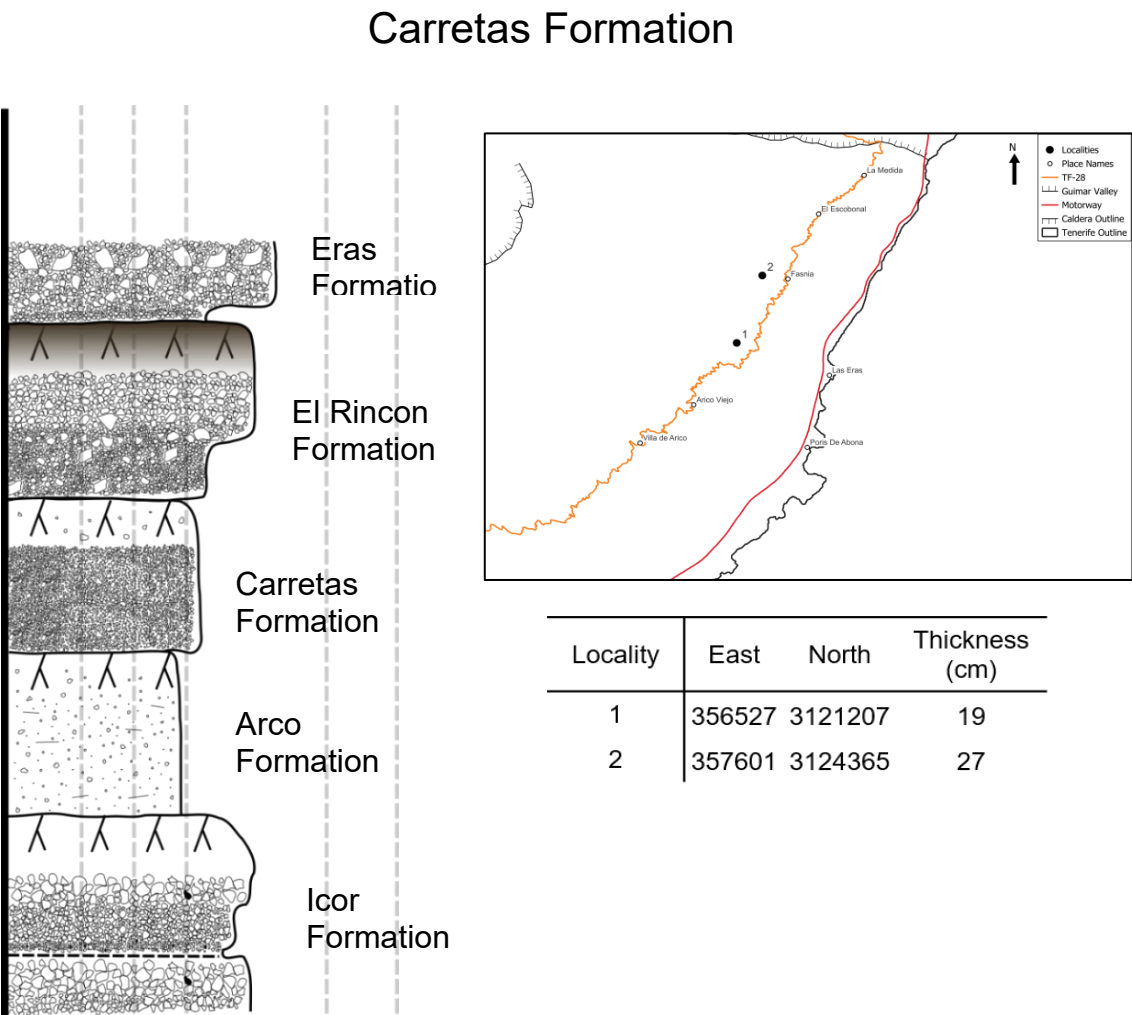


Figure 3.33 - Stratigraphic log of the Carretas Formation across the Fasnía Region. UTM coordinates and inset map of locations are provided. The logs represent stratigraphic relationships with under- and overlying units.

Interpretation:

The Carretas Formation is the product of a small scale Plinian or sub-Plinian eruption with an easterly dispersal across the Bandas Del Sur. It is uncertain whether the fine lapilli and ash is due to high fragmentation efficiency, or the deposit is on the edge of dispersal for a larger, unexposed eruption. Further information is required for more detailed conclusions.

3.1.11 El Rincon Formation

The El Rincon Formation, named after a coastal landmark west of Las Eras at the edge of its dispersal, comprises a phonolite pumice fall deposit. The type locality is found northwest of Icor at the top of Barranco de Icor O las Carretas (locality 3, figure 3.34). At the type locality, it is 20 cm thick, massive, reverse-graded, well-sorted, medium-grained, sub-angular pumice lapilli (figure 3.30). The pumice is <3 cm in diameter, dark cream to light grey, aphyric, with vesicles of varied morphologies that are <1 cm in diameter. The formation has low lithic populations (<2 vol%) of dark grey lava that are <1 cm in diameter. At the type locality, the formation has gradational contact with the paleosol below, above the Carretas Formation, and a sharp contact to the paleosol above, which is in turn overlain by the Eras Formation. The paleosol above is 11 cm thick, distinctly dark brown, and very fine-grained, resembling clay.

El Rincon Formation

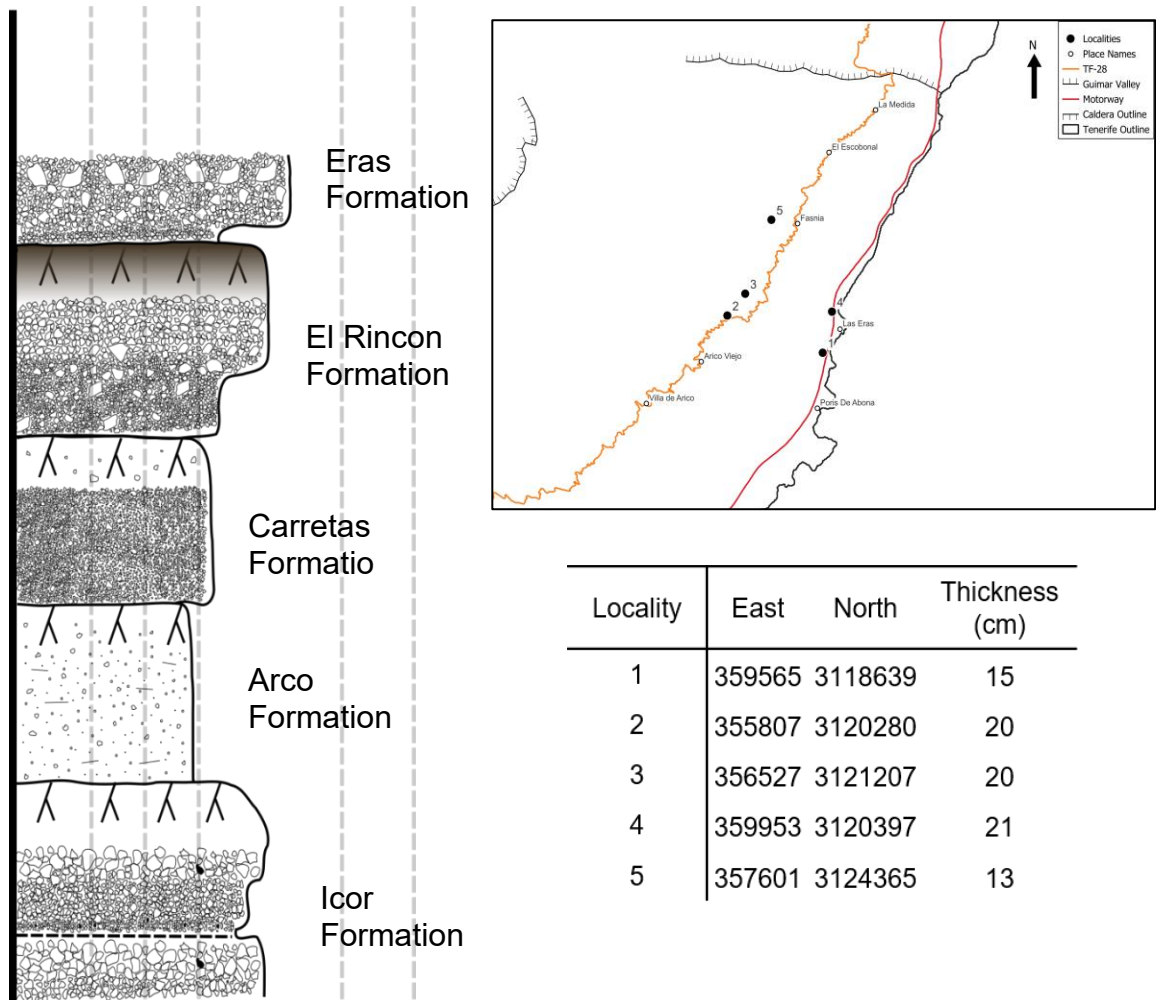


Figure 3.34 - Stratigraphic log of the El Rincon Formation across the Fasnía Region. UTM coordinates and inset map of locations are provided. The logs represent stratigraphic relationships with under- and overlying units.

Dispersal, Volume, and Column Height:

The El Rincon Formation has an easterly dispersal across SE Bandas Del Sur from Icor to La Zarza. The formation has a minimum dispersal of $\sim 122\text{km}^2$ with a minimum onshore volume of 0.036km^3 .

Table 3.6 - Eruption parameters for the El Rincon Formation

Volume (km^3)			VEI
Exponential	Powerlaw	Weibull	
0.036 – 0.061	0.098 – 0.499	0.047 – 0.121	3–4

Interpretation:

The El Rincon Formation is the product of a Plinian eruption with an easterly dispersal across the Bandas del Sur. The well-sorted deposit suggests a steady eruption column that increased in intensity over time, seen in reverse-grading. The low lithic populations suggest a lack of vent wall erosion throughout the eruption.

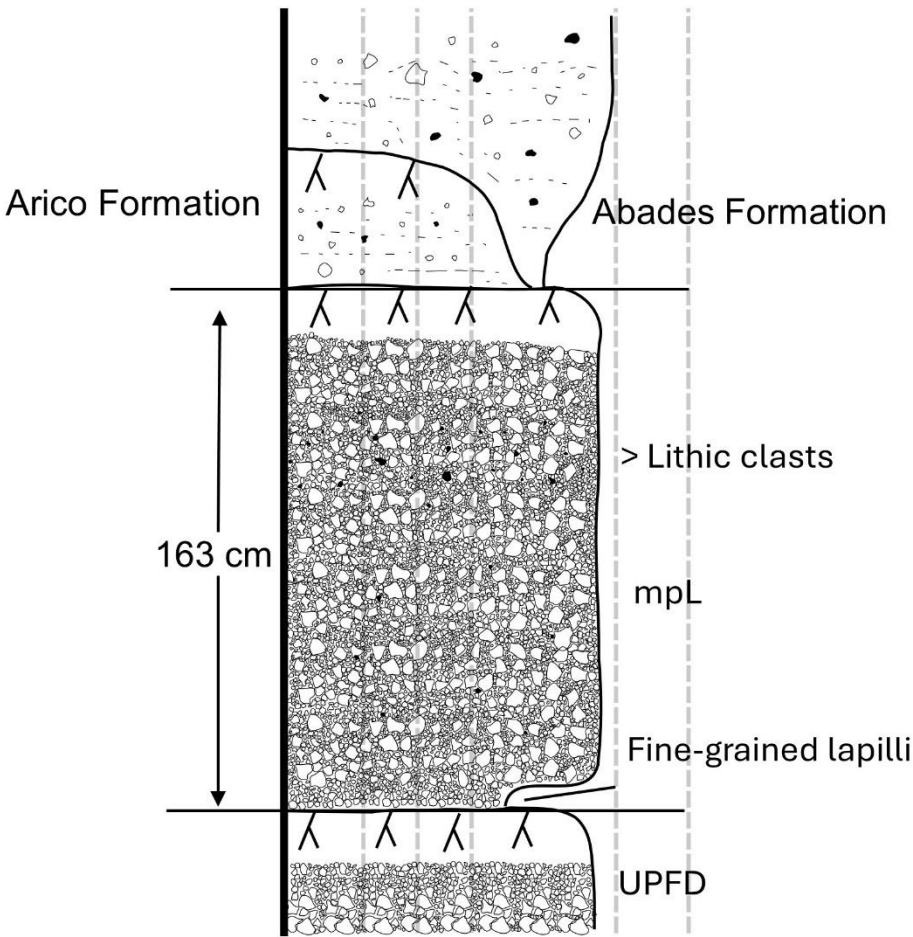
3.1.12 Eras Formation

The Eras formations was first characterised by Brown et al., (2003) and is the only known ignimbrite forming eruption in this study, therefore a crucial deposit in understanding the age boundaries and identifying new eruptive units. The Eras Formation, named after the coastal town of Las Eras, comprises of a phonolite pumice fall deposit overlain by a phonolite ignimbrite. Here we only describe the fall deposit. The type locality is found at a roadcut section west of Mirador de Las Eras (locality 13, figure 3.35). At the type locality, the pumice fall is 195 cm thick, massive to minor diffuse stratification, moderately to poorly sorted, angular pumice lapilli (figures 3.36 and 3.37). The base 5 cm thick fine-grained lapilli that grades into medium-grained lapilli with frequent coarse-grained lapilli scattered throughout the deposit. The pumice is <5 cm in diameter, dark cream and green in colour, grading into mingled green and black pumices at the top, and abundant sanidine and biotite phenocrysts. Highly vesicular, pale brown, transparent pumices can be found throughout the deposit. The pumice fall has low lithic populations, however, increase in abundance towards the top from <2 vol% to <5 vol%, of dark grey lavas that are <3 cm in diameter. An abundance of free sanidine crystals can be found throughout the deposit. At the type locality, the pumice fall has a gradational contact to the Eras Ignimbrite above, and a sharp contact to the dark brown paleosol below, which is above the El Rincon Formation.

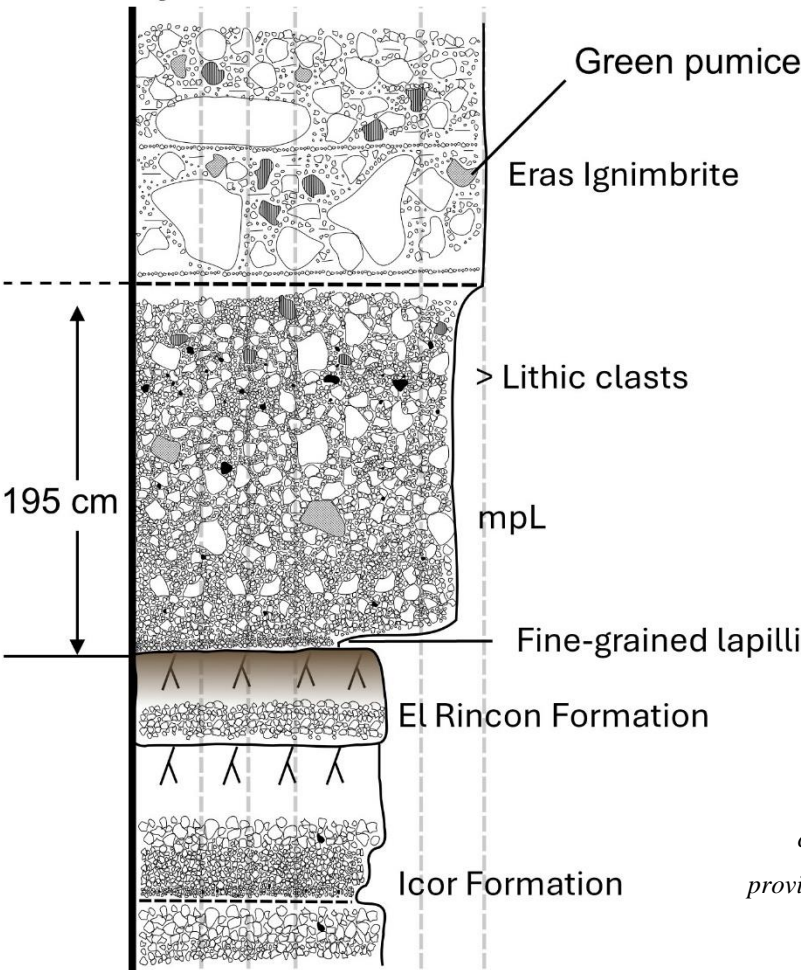
The Eras Formation is thought to be related to the Moradas Formation of Davila-Harris et al., (2023) due to the similarities in pumice characteristics, deposit structure, stratigraphic position, and ages. Locality 6 is the previous type locality of the Moradas Formation (figure 3.35) (Davila-Harris et al., 2009).

Eras Formation

Locality 6: Barranco de las Moradas



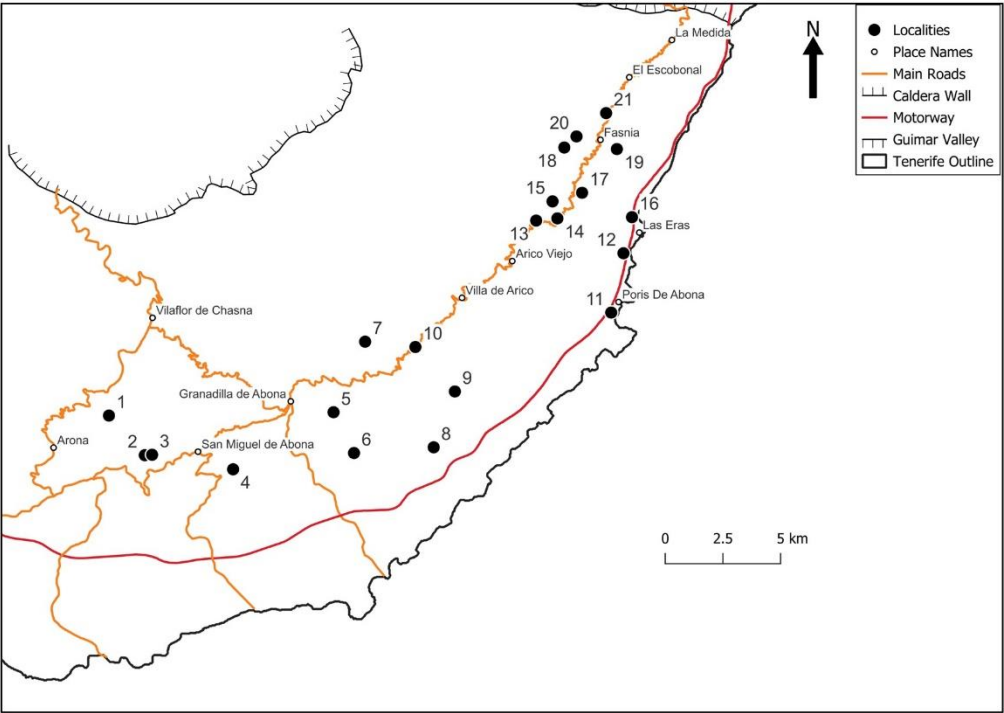
Locality 13: Mirador de las Eras



- Mingled Pumice
- Ignimbrite
- Paleosol
- Lithic Clasts
- Hydrothermally altered clasts
- Lava
- Pumice lapilli

Figure 3.35 - Stratigraphic logs of the Eras and Moradas Formations, showing the similarities between them. UTM coordinates and inset map of locations and thicknesses are provided. The logs represent stratigraphic relationships with under- and overlying units.

Locality	East	North	Thickness (cm)	Locality	East	North	Thickness (cm)
1	337201	3110999	277	12	359565	3118639	>72
2	338726	3109045	>179	13	355807	3120280	195
3	339043	3109061	274	14	356726	3120374	230
4	342540	3108304	214	15	356527	3121207	210
5	346923	3111033	240	16	359953	3120397	144
6	347785	3109031	163	17	357810	3121611	>300
7	348335	3114460	413.5	18	357066	3123830	>210
8	351237	3109267	200	19	359340	3123727	199
9	352189	3111980	191	20	357601	3124365	270
10	350507	3114173	261	21	358896	3125488	208
11	358999	3115750	116				



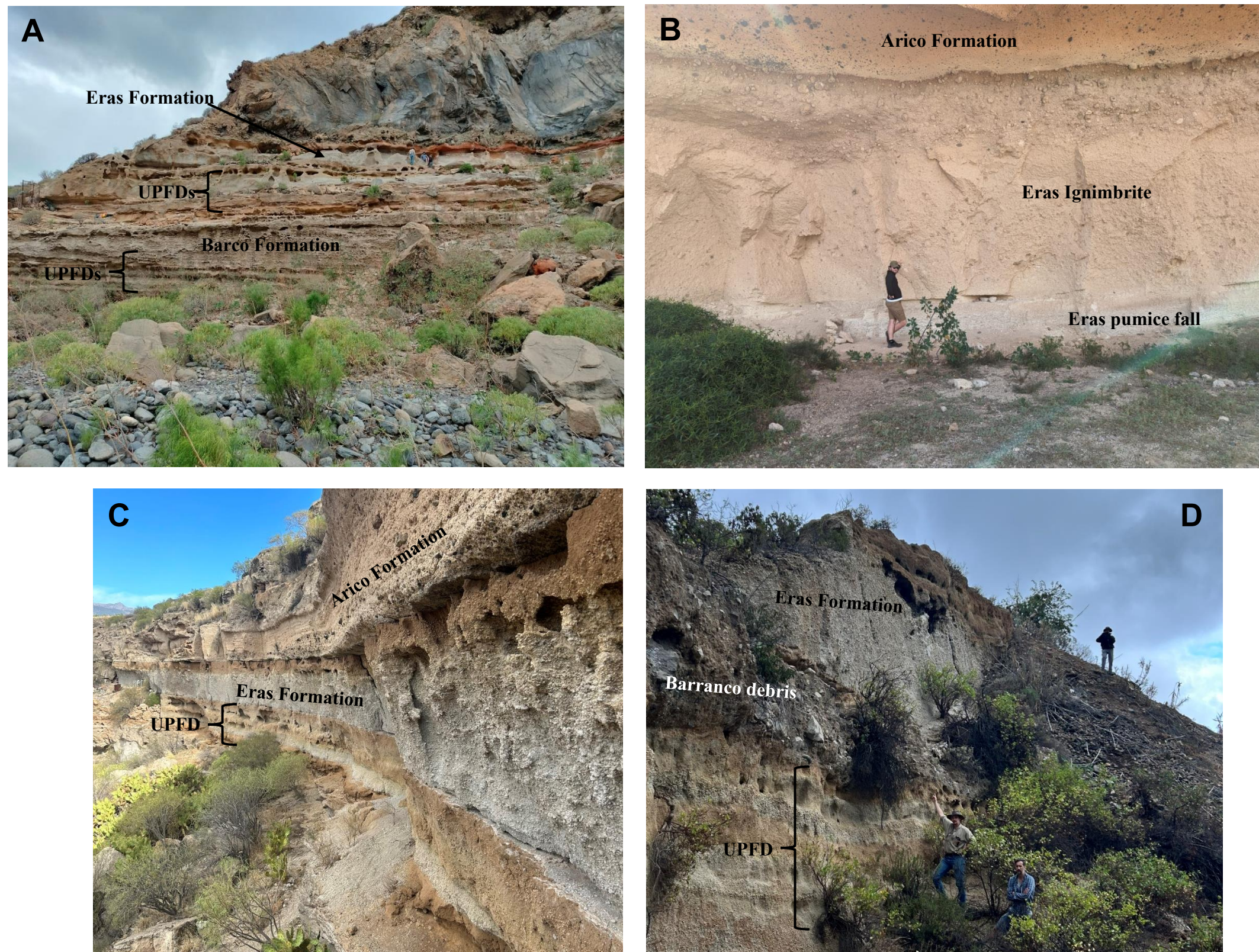


Figure 3.36 – **A)** The Eras Formation at Barranco del Rio (locality 9) beneath a phonolite lava and above at least three UPFDs, before an unconformity and the Barco Formation at the base. **B)** The Eras Formation, including the Eras Ignimbrite, beneath the Arico Formation at Poris de Abona (locality 11). **C)** The Eras Formation beneath the Arico Formation at the previous type locality of the Moradas Formation at Barranco de las Moradas (locality 6). **D)** The Eras Formation, above at least 4 UPFDs at the current thickest locality at Barranco de las Vegas (locality 7).

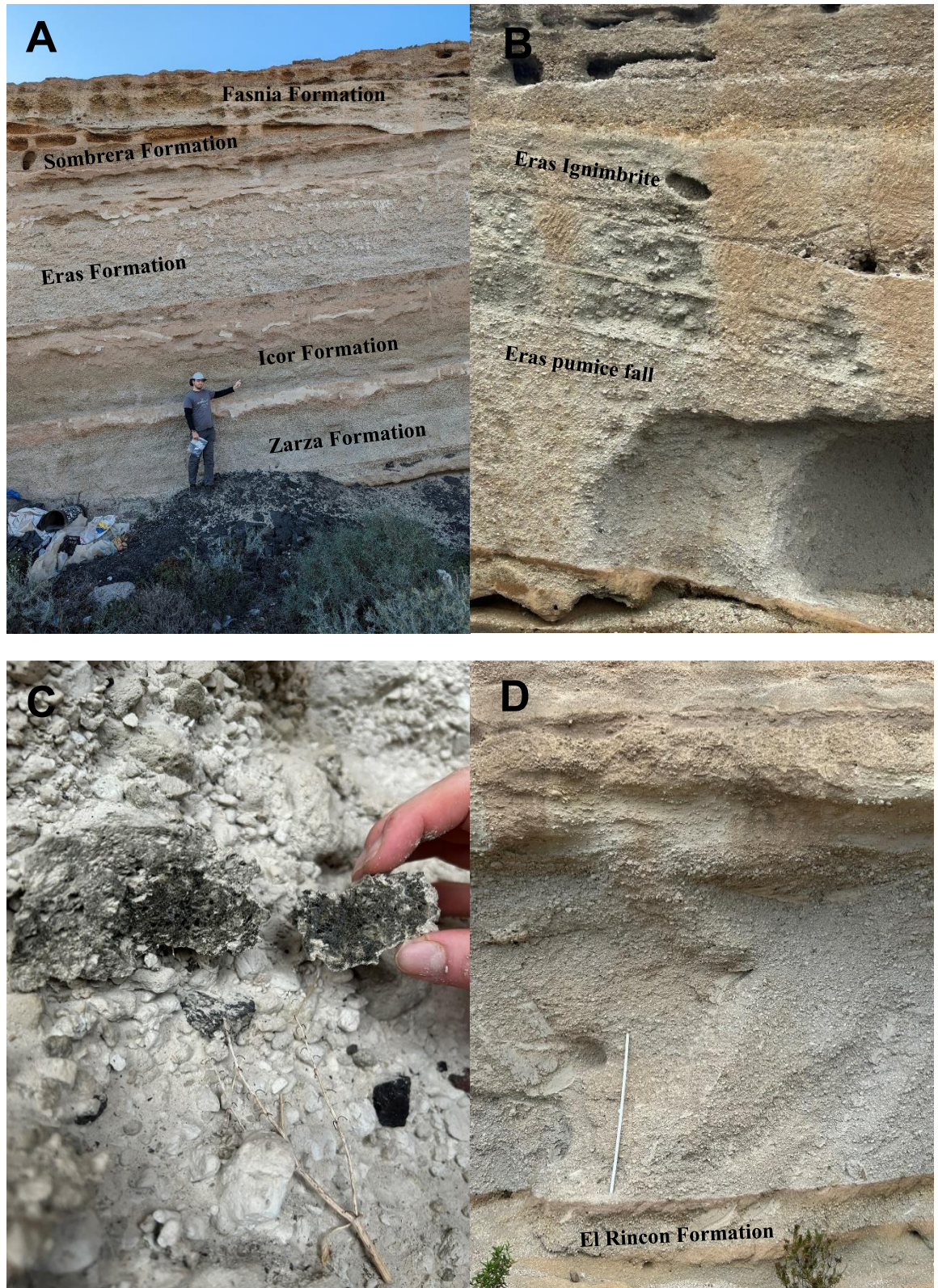
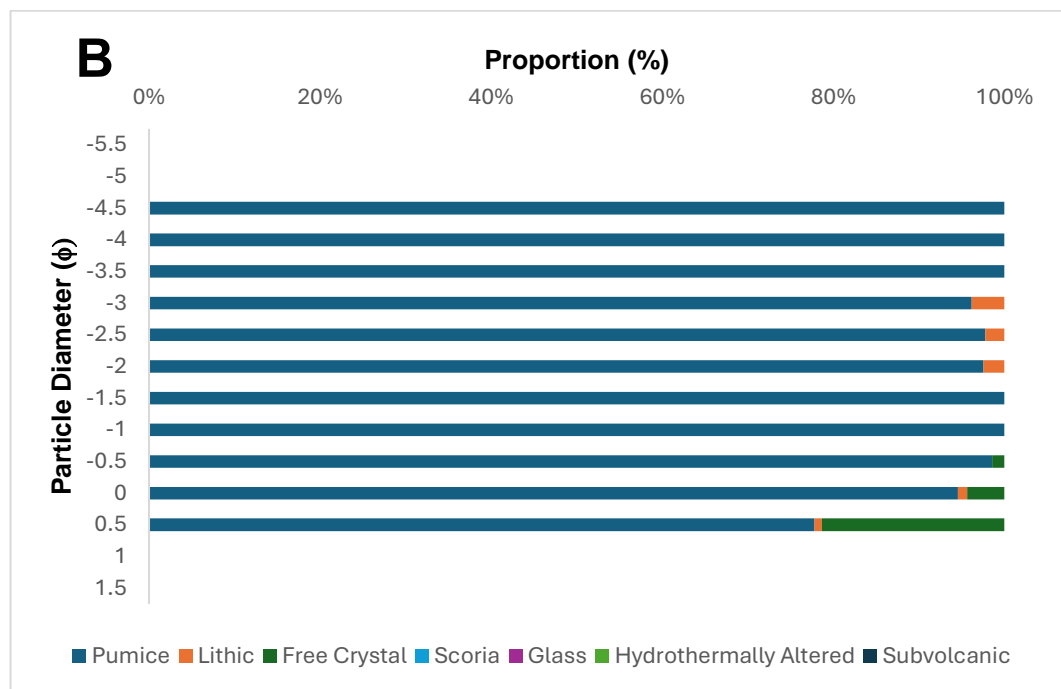
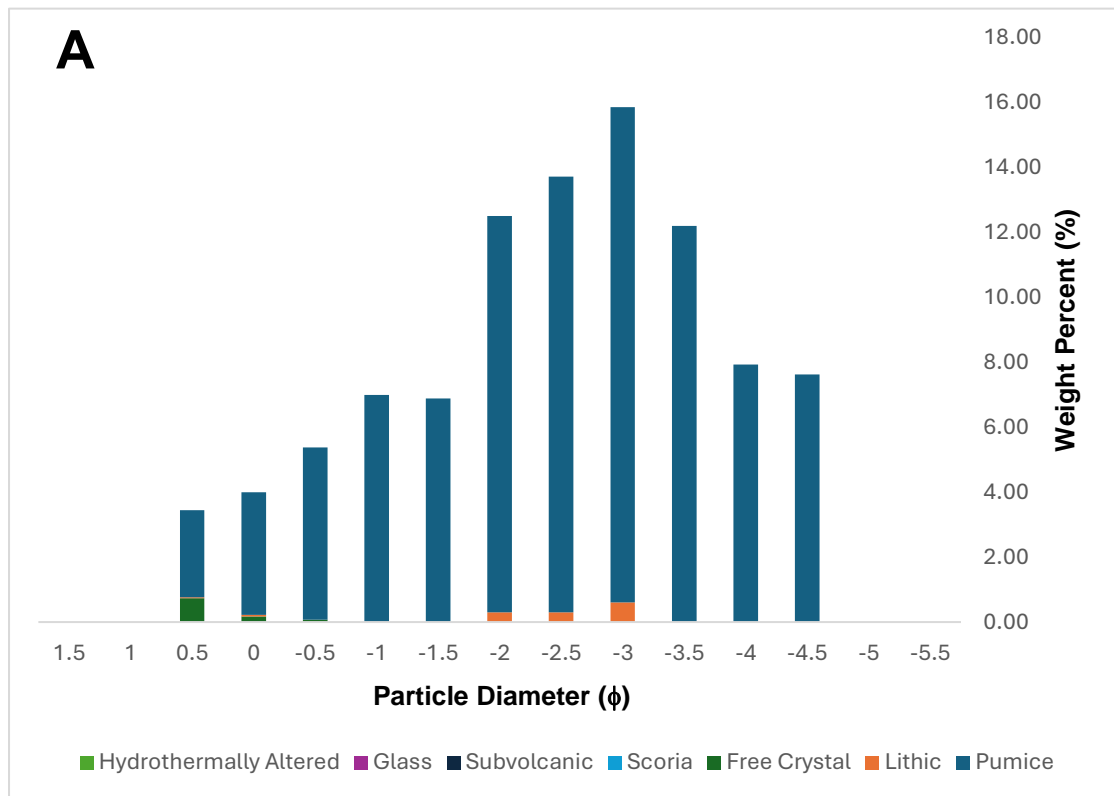
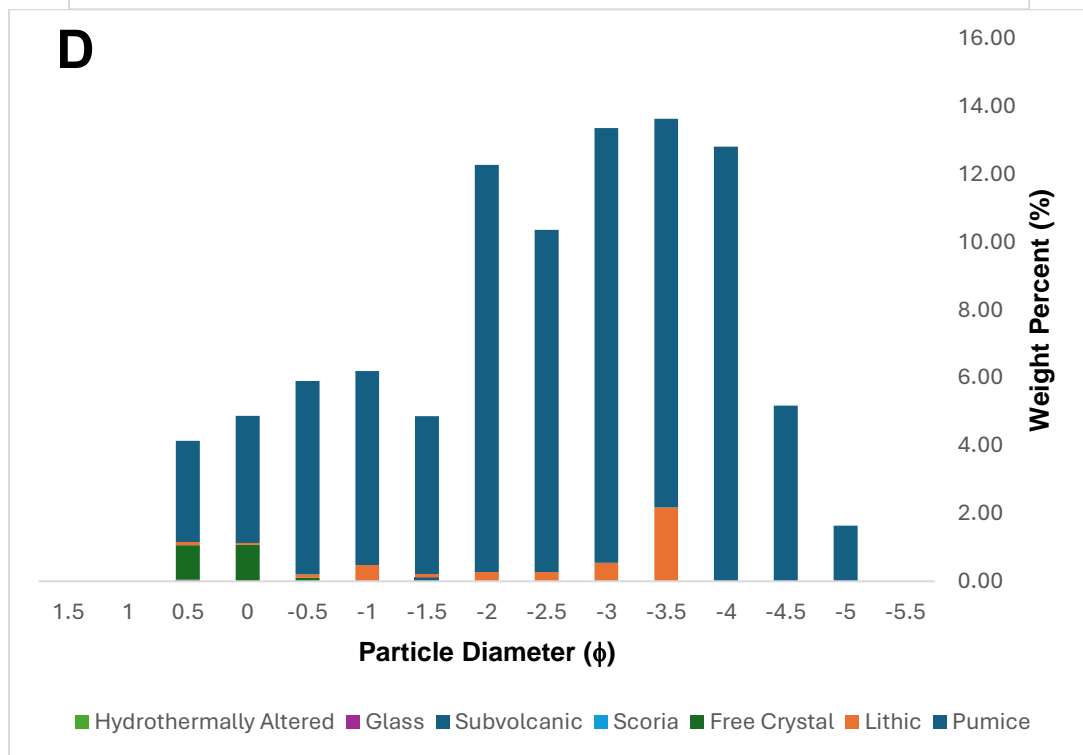
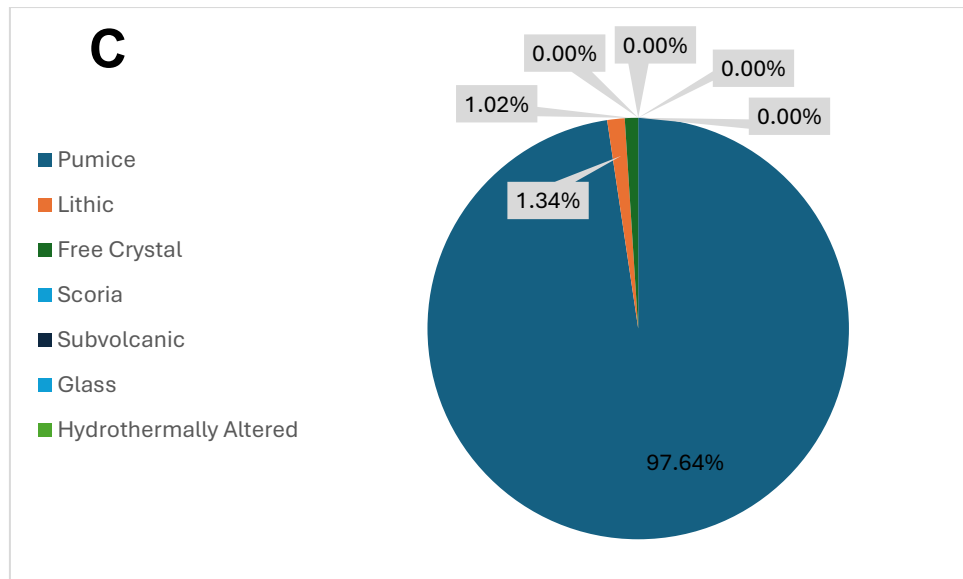


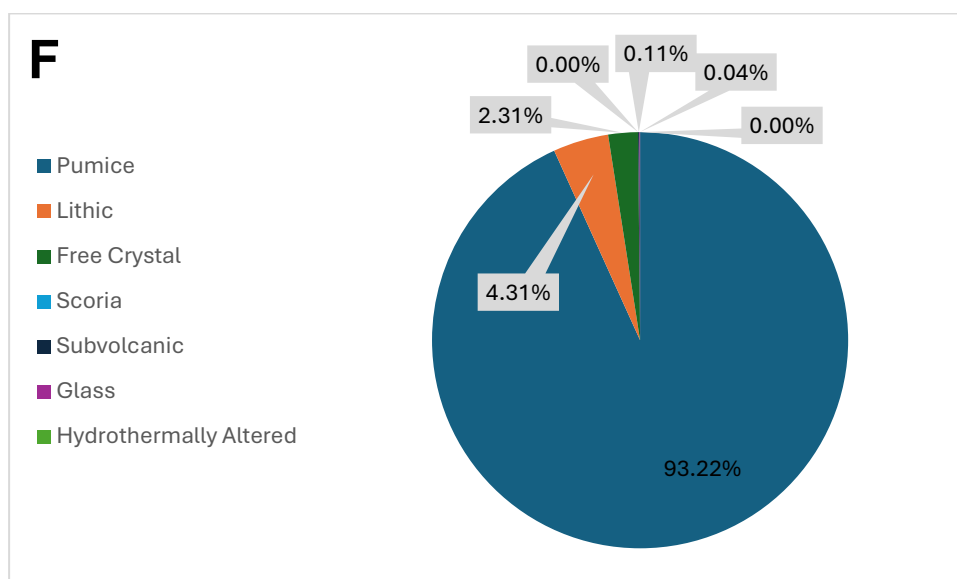
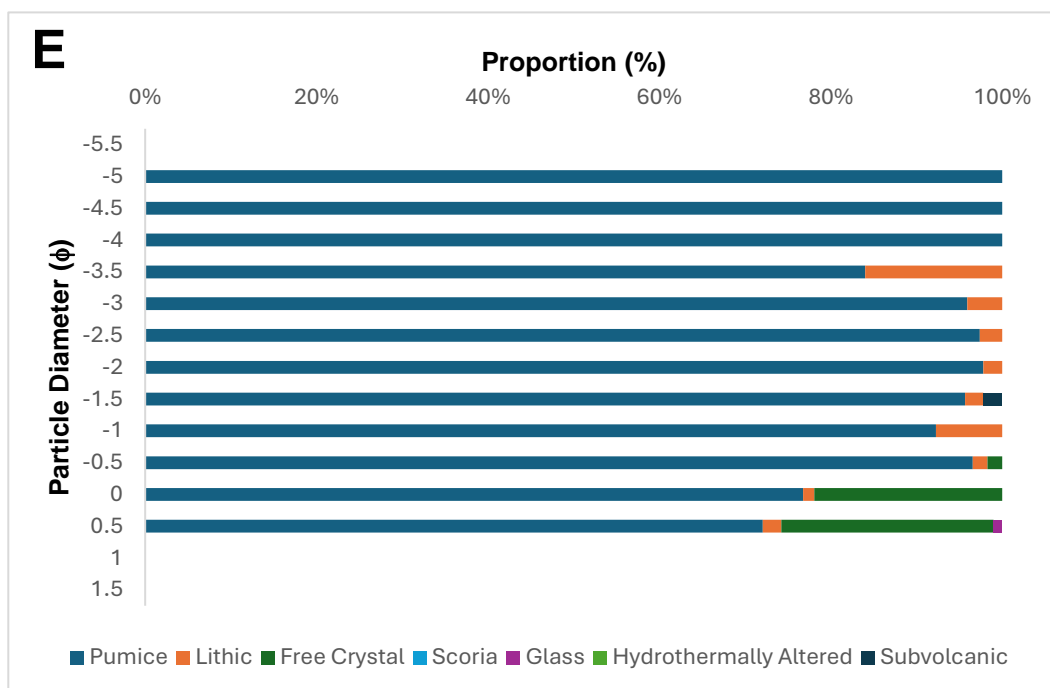
Figure 3.37 – **A)** The Eras Formation at Las Eras above the Icor and Zarza Formations (locality 16). **B)** The Eras Formation at Mirador de las Eras above the El Rincon Formation (locality 13). **C)** The black, mingled pumice that can be found in the Eras Formation. **D)** The Eras Formation above the El Rincon Formation at North Icor (locality 15).

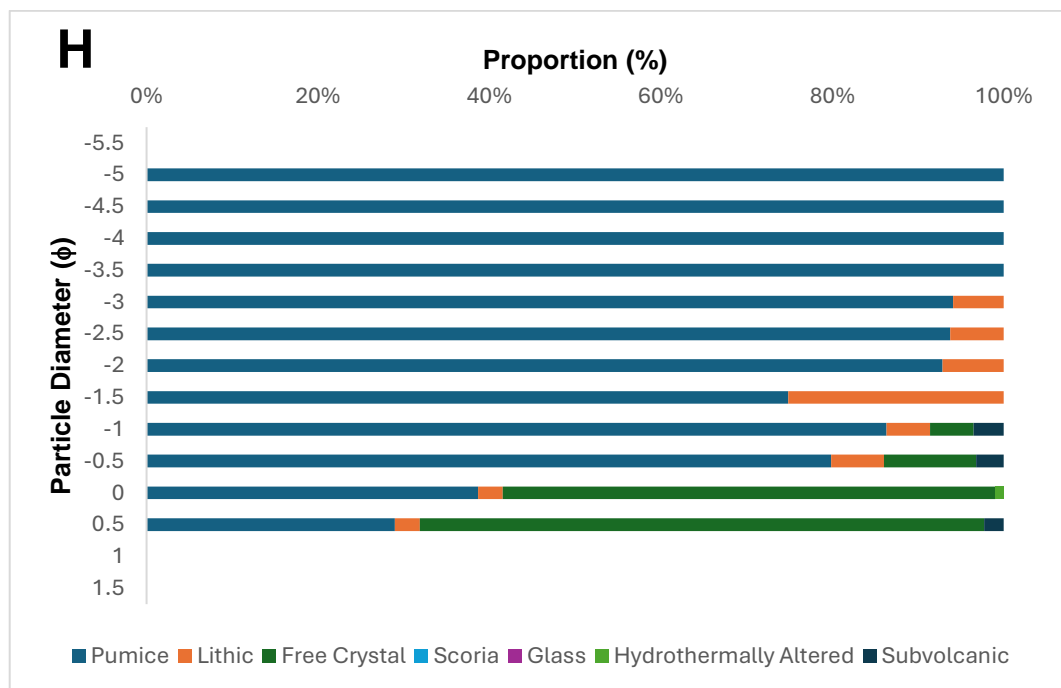
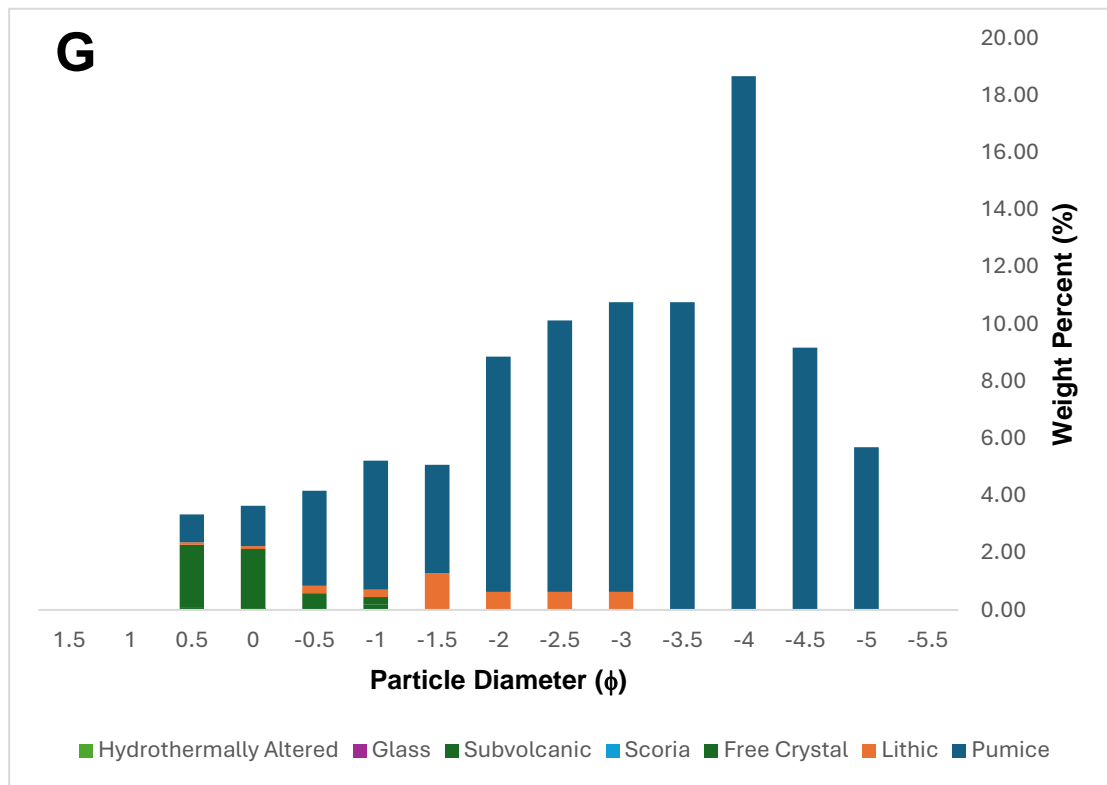
Grain-Size and Componentry:

The Eras pumice fall was sieved at the top of Icor Vineyard, ~2.5 km SW of the type locality, in 0.5 ϕ intervals from -5.5 ϕ to -2 ϕ and in the laboratory from -1.5 ϕ to 1.5 ϕ . Due to the thickness of the deposit being >2 m the deposit was sieved at three intervals, 50 cm, 100 cm, and 150cm from the base. At 50 cm, the deposit is unimodal, moderately sorted ($\sigma\phi = 1.49$) and medium-grained lapilli ($Md\phi = -2.77$). Componentry was performed on fractions coarser than 0.5 ϕ , where 96% of material is analysed. The formation contains components of pumice, lithic clasts, and free crystals. Proportionally, pumice clasts dominate each fraction, with abundant free crystals at 0.5 ϕ (21%). As a weight percentage, the deposit is composed of almost entirely pumice (97.6%), with minor lithic (1.34%) and free crystals (1.02%). At 100 cm, the deposit is trimodal, poorly sorted ($\sigma\phi = 1.68$) and medium grained lapilli ($Md\phi = -2.80$). Componentry was performed on fractions coarser than 0.5 ϕ , where 95% of material is analysed. The formation contains components of pumice, lithic clasts, free crystals, subvolcanic rocks, and juvenile glass. Proportionally, pumice clasts dominate each fraction, with abundant free crystals in fractions finer than 0 ϕ (>20%). As a weight percentage, the deposit is composed of almost entirely pumice (93.2%) with minor lithic clasts (4.3%) and free crystals (2.3%), with the remaining components each <1% of the total weight. At 150 cm the deposit is unimodal, poorly sorted ($\sigma\phi = 1.67$), medium to coarse-grained lapilli ($Md\phi = -3.27$). Componentry was performed on fractions coarser than 0.5 ϕ , where 97% of material is analysed. The formation contains components of pumice, lithic clasts, free crystals, subvolcanic rocks, and hydrothermally altered rock. Proportionally, pumice clasts dominate each fraction from -5 ϕ to -0.5 ϕ (>75%), with free crystals dominating fractions 0 ϕ to 0.5 ϕ (>50%). As a weight percentage, the deposit is composed of almost entirely pumice (90.2%), with minor free crystals (5.24%) and lithic clasts (4.08%) and with the remaining components each <1% of the total weight (figure 3.38).









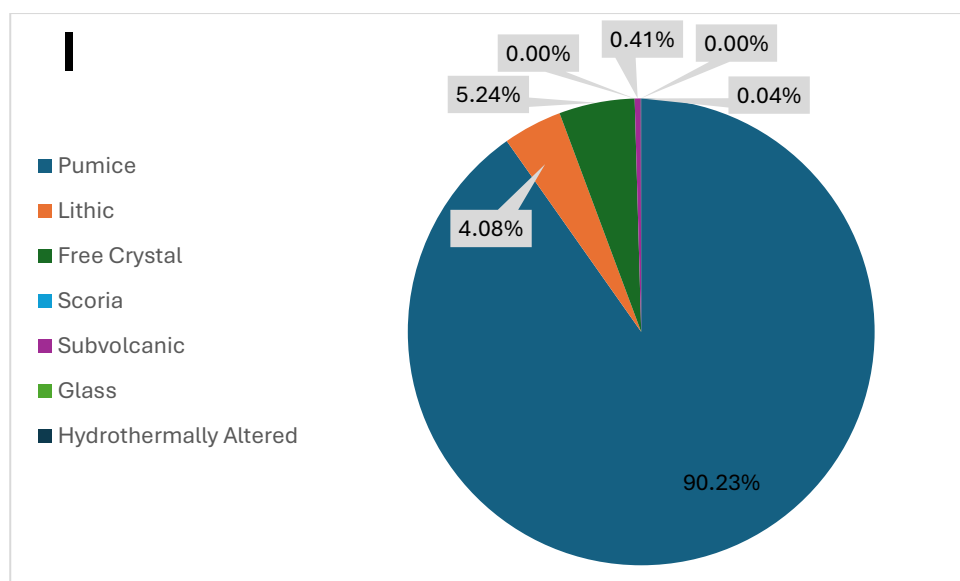


Figure 3.38 – Eras Formation A) Proportion of components as a weight percentage of the total sample weight at 50cm. **B)** Proportion of components within each grain size at 50cm. **C)** Total weight percentage of components at 50cm. **D)** Proportion of components as a weight percentage of the total sample weight at 100cm. **E)** Proportion of components within each grain size at 100cm. **F)** Total weight percentage of components at 100cm. **G)** Proportion of components as a weight percentage of the total sample weight at 150cm. **H)** Proportion of components within each grain size at 150cm. **I)** Total weight percentage of components at 150cm.

Dispersal, Volume, and Column Height:

The Eras Formation pumice fall has a southeasterly dispersal located across the Bandas Del Sur from Arona to El Escobonal, an area of 473km². The pumice fall, not including the Eras Ignimbrite, has a minimum onshore volume of 2.984km³ (table 3.7).

Table 3.7 - Eruption parameters for the Eras Formation pumice fall

Volume (km ³)			VEI
<i>Exponential</i>	<i>Powerlaw</i>	<i>Weibull</i>	
3.015 – 6.341	12.313 – 34.51	2.984 – 4.130	5-6

Interpretation:

The Eras Formation is the product of a large-scale, ignimbrite forming Plinian eruption with a southeasterly dispersal. The eruption would have begun gradually, seen in the fine-grained lapilli pumice at the base of the fall deposit, before becoming a sustained Plinian eruption. The slight diffuse-bedded structure suggest minor pulsating or fluctuations in column height throughout the eruption, however the eruption is largely stable and sustained until climax. Towards the top of the fall deposit is a layer of

increased lithic clasts, which may suggest vent widening towards to end of the eruption, coinciding with an increase in mafic content of pumice clasts. The eruption column then collapsed, producing PDCs that deposited a widespread ignimbrite. The true scale of the eruption has yet to be constrained, with further investigation required for a greater detailed interpretation of this eruption.

3.1.13 Sombrera Formation

The Sombrera Formation, named after a small village ~1.8km northwest of the type locality, is a phonolite pumice fall deposit with four members (Sombrera A to D) (figure 3.39). The type locality is located at a vineyard northeast of Icor (locality 2, figure 3.40). The formation is exposed across a ~15 km² area from Icor to Fasnía and on the coast at Las Eras, and has a maximum thickness of 147 cm. However, no measurements were taken at Las Eras due to inaccessibility.

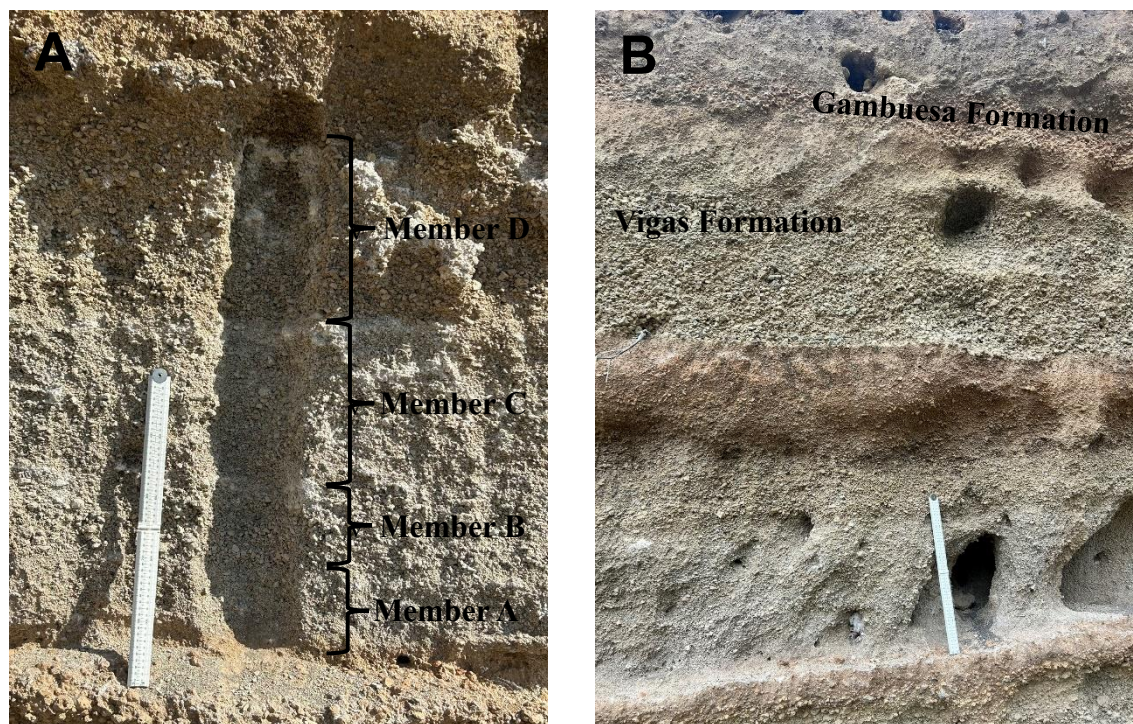
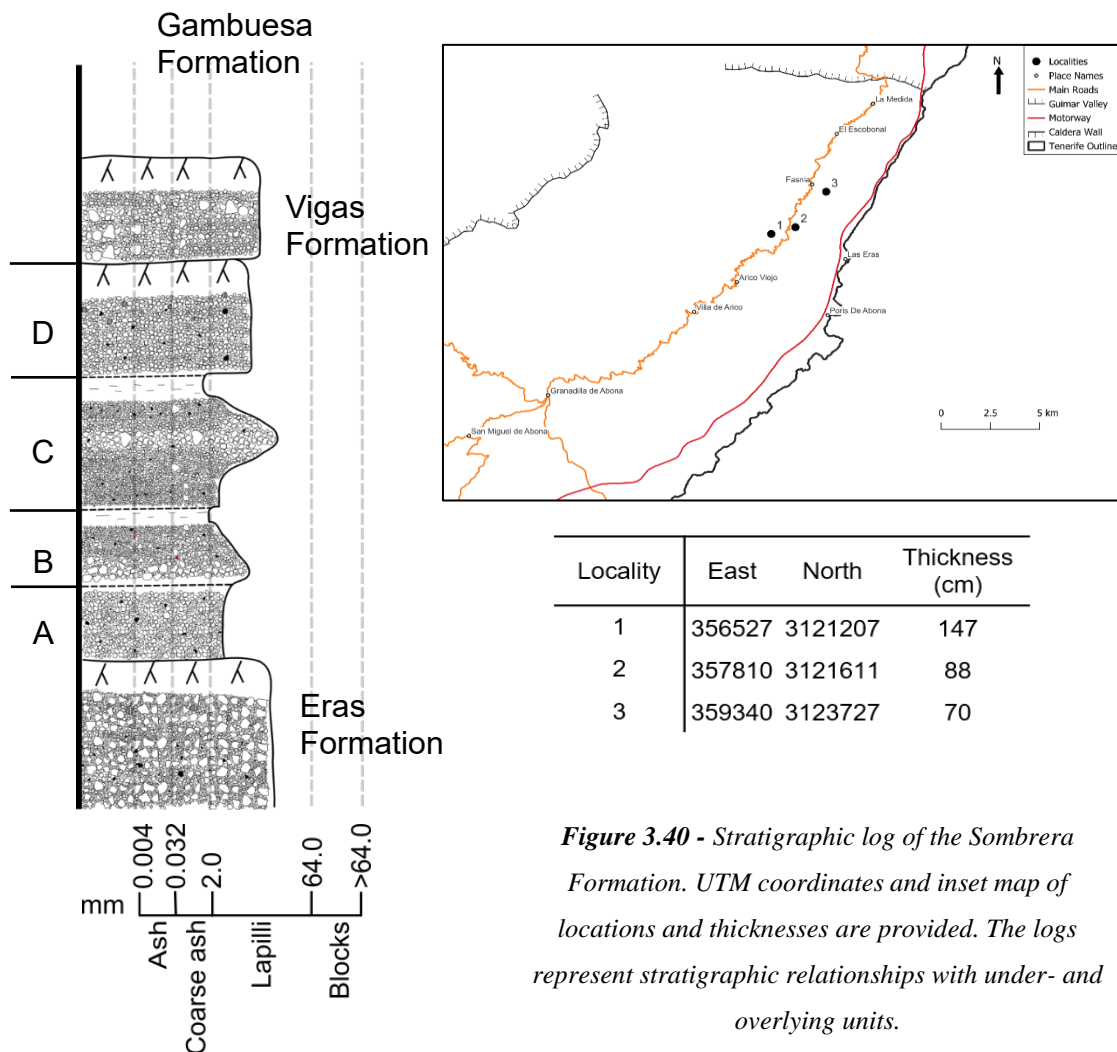


Figure 3.39 – **A)** The Sombrera Formation at Icor Vineyard (locality 2). **B)** The Sombrera Formation beneath the Vigas and Gambuesa Formations at Fasnía Cone (locality 3).

Sombrera Formation

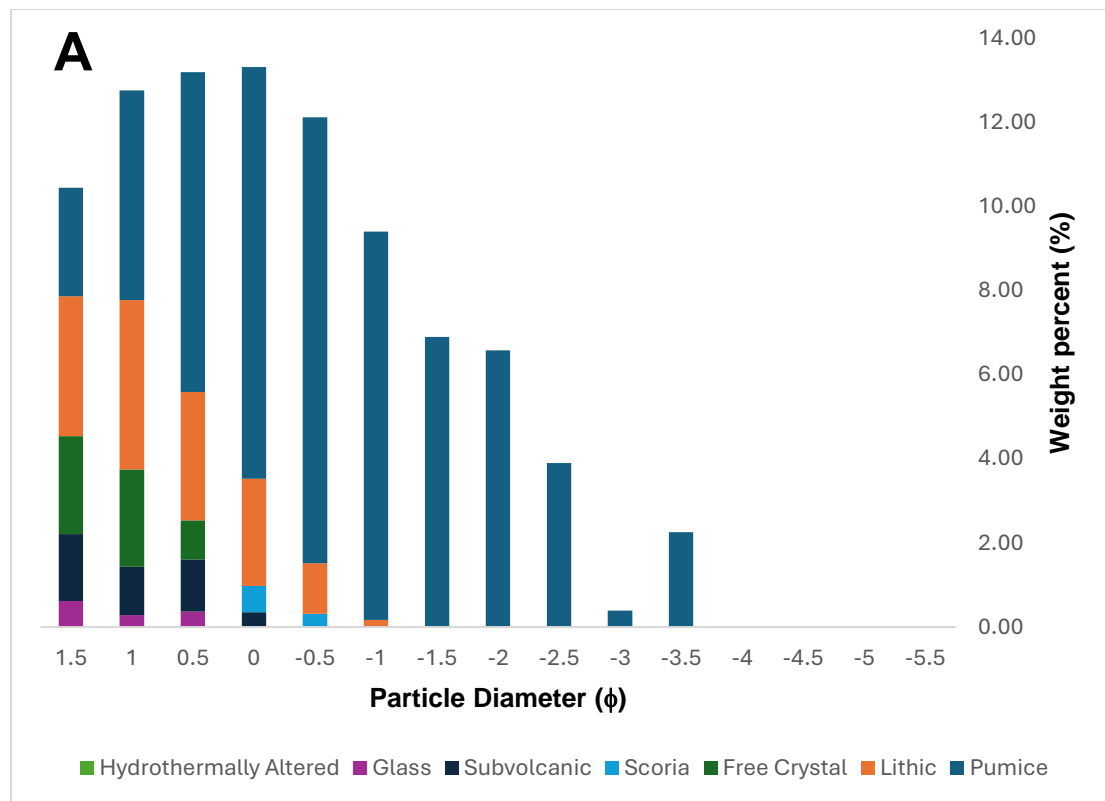


3.1.13.4 Sombrera Member A

Sombrera Member A is a phonolite pumice fall at the base of the Sombrera Formation. At the type locality it is 10 cm thick, massive, non-graded, moderately sorted, fine-grained, sub-rounded pumice lapilli (figure 3.39). The pumice is <2 cm in diameter, grey to cream, vesicular with small, rounded vesicles, and has no mafic mingling. The pumice has biotite, pyroxene and k-feldspar phenocrysts. The member has 20-30 vol% lithic clasts of dark grey lava that are <0.5 cm in diameter. The member has a sharp contact with Sombrera Member B above and a sharp contact with the paleosol below, which is above the Eras Formation.

Grain-Size and Componentry:

Sombrera Member A was sieved at the type locality in 0.5ϕ intervals from -5.5ϕ to -3ϕ and in the laboratory from -2.5ϕ to 1.5ϕ . The deposit is unimodal, moderately sorted ($\sigma\phi = 1.29$) and fine lapilli to ash ($Md\phi = -0.3$). Componentry was performed on fractions coarser than 1.5ϕ , where 94% of material is analysed. The formation contains components of pumice, lithic clasts, free crystals, scoria, subvolcanic rock, and juvenile glass. Proportionally, pumice clasts dominate in fractions coarser than 0ϕ ($>74\%$) and lithic clasts are abundant in fractions finer than 0ϕ ($>19\%$). As a weight percentage, the deposit is mostly pumice (69.3%) and lithic clasts (15.3%) with minor free crystals (6%), subvolcanic rock (4.63%), scoria (3.44%) and juvenile glass (1.36%) (figure 3.44).



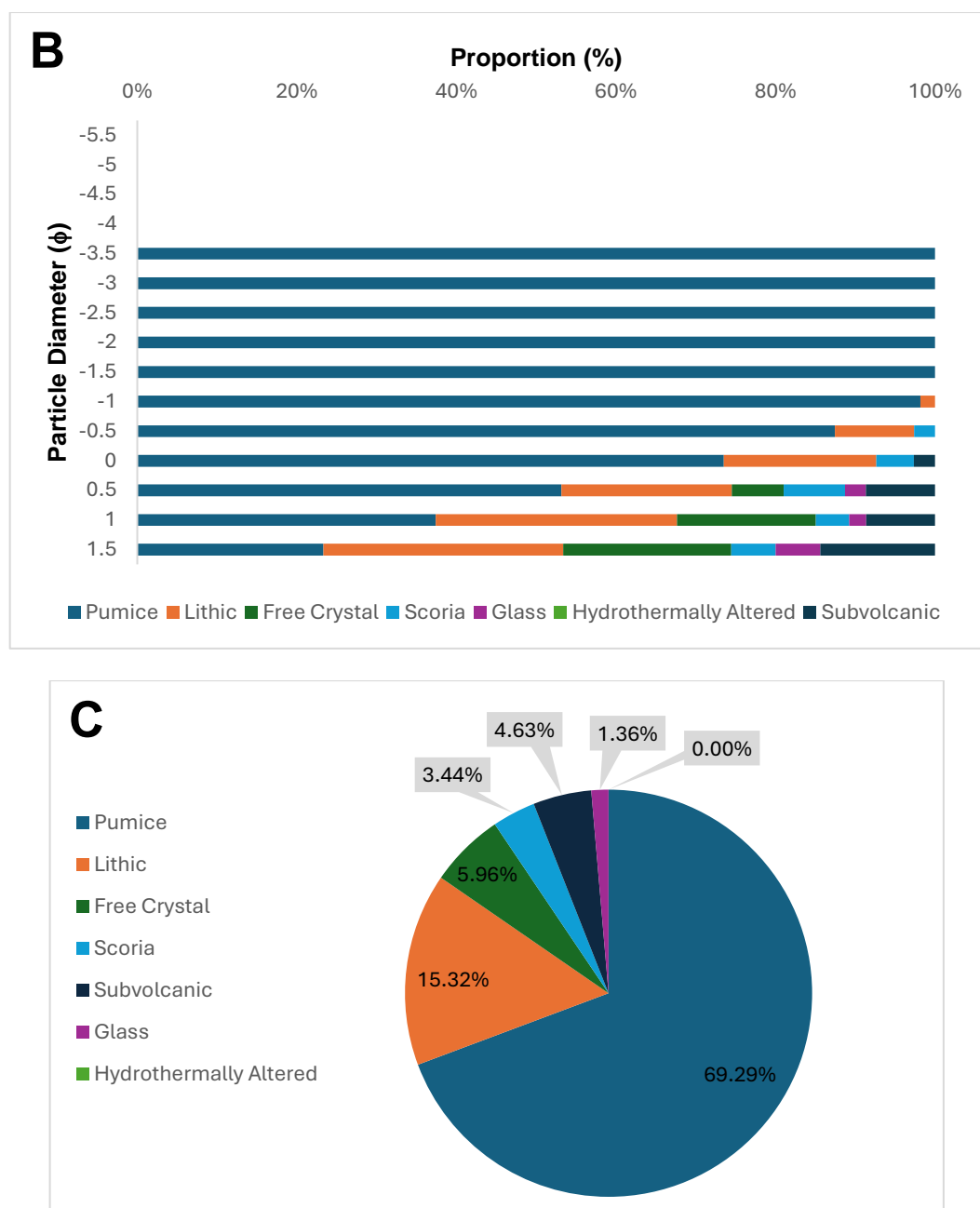


Figure 3.41 – Sombreira Formation Member A **A)** Proportion of components as a weight percentage of the total sample weight **B)** Proportion of components within each grain size **C)** Total weight percentage of components

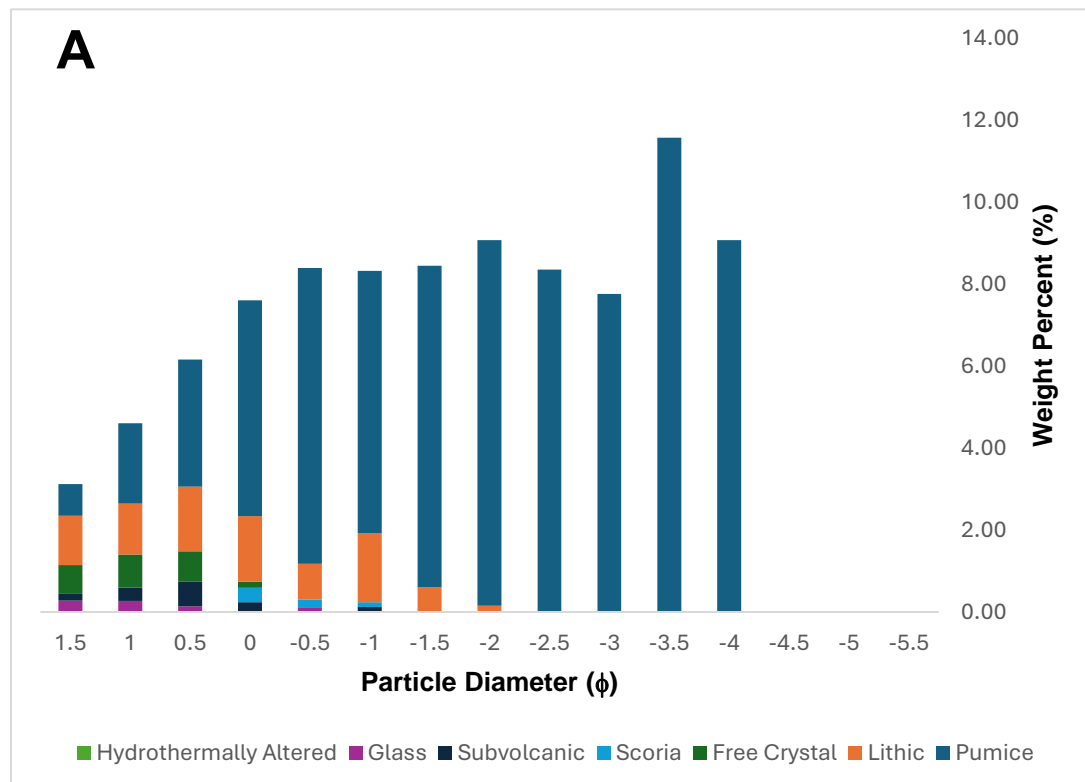
3.1.13.3 Sombreira Member B

Sombreira Member B is a phonolite pumice fall. At the type locality, it is 16 cm thick, massive, normally graded, moderately to well-sorted, medium to fine-grained, sub-angular to sub-rounded pumice lapilli (figure 3.39). The pumice is <2 cm in diameter, light cream, highly vesicular with rounded and elongated vesicles, and scarce mafic mingling. The pumice has biotite (?), pyroxene, k-feldspar and titanite phenocrysts. The

member has 25-30 vol% lithic clasts of red, vesiculated scoria and crystalline lavas, typically 2-3 mm in diameter. The member has a gradational contact with Sombrera Member A above and a sharp contact with Sombrera Member C below.

Grain-Size and Componentry:

Sombrera Member B was sieved at the type locality in 0.5ϕ intervals from -5.5ϕ to -3ϕ and in the laboratory from -2.5ϕ to 1.5ϕ . The deposit is bimodal, moderately sorted ($\sigma\phi = 1.46$) and fine lapilli ($Md\phi = -1.44$). Componentry was performed on fractions coarser than 1.5ϕ , where 93% of material is analysed. The formation contains components of pumice, lithic clasts, free crystals, scoria, subvolcanic rock, and juvenile glass. Proportionally, pumice clasts dominate in fractions coarser than 0ϕ ($>69\%$) and lithic clasts are abundant in fractions finer than 0ϕ ($>20\%$). As a weight percentage, the deposit is mostly pumice (84.2%), with minor lithic clasts (9.61%), free crystals (2.58%), subvolcanic rock (1.58%) and scoria (1.17%), with the remaining components each $<1\%$ of the total weight (figure 3.43).



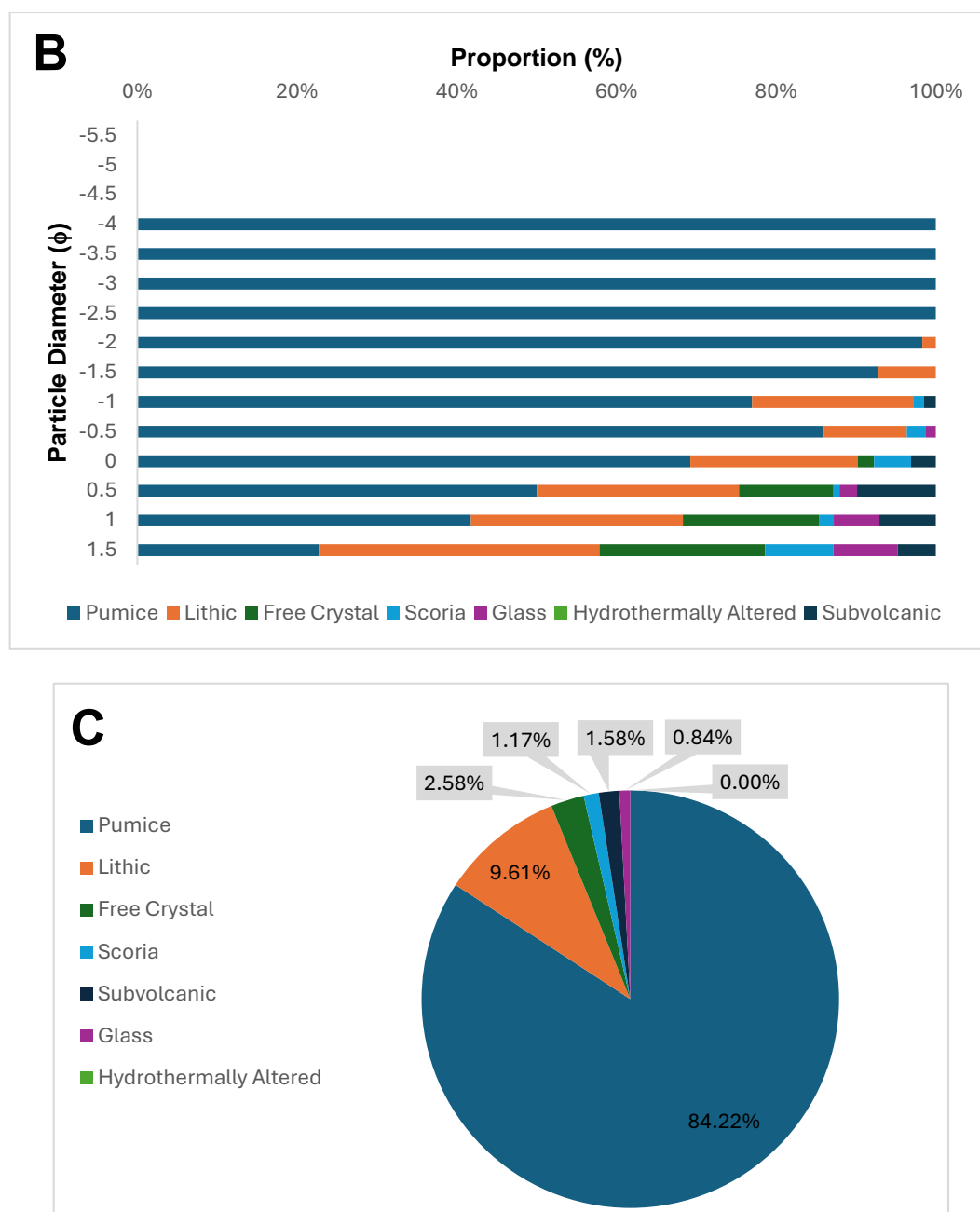


Figure 3.42 – Sombreira Formation Member B **A)** Proportion of components as a weight percentage of the total sample weight **B)** Proportion of components within each grain size **C)** Total weight percentage of components.

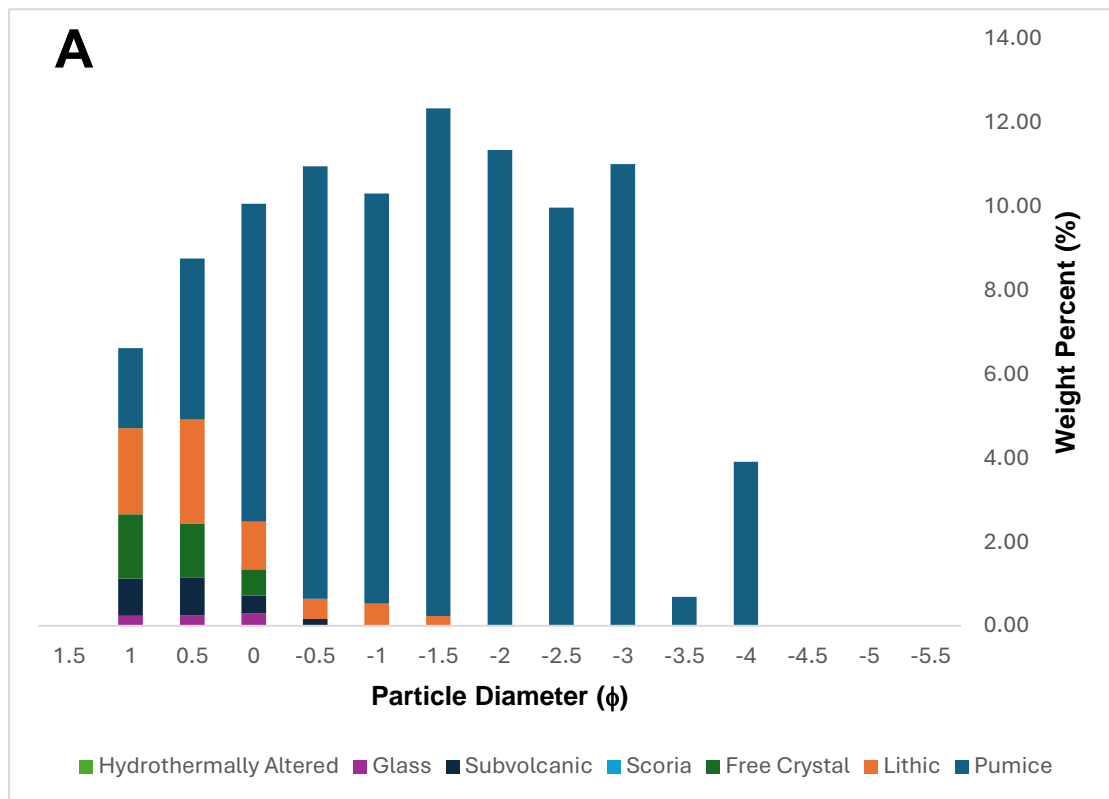
3.1.13.2 Sombreira Member C

Sombreira Member C is a phonolite pumice fall. At the type locality, it is 28 cm thick, massive, symmetrically graded, moderately sorted, fine to medium-grained, sub-angular pumice lapilli (figure 3.39). The pumice is <2 cm in diameter, light cream, highly vesicular with rounded and elongated vesicles, and scarce mafic mingling. The pumice has frequent pyroxene, biotite (?), k-feldspar and titanite phenocrysts. The member

grades in lithic populations from 10-15 vol% at the base to 5-10 vol% at the top of mafic and silicic lavas. The member has a sharp contact with Sombrera Member B above and a gradational contact with Sombrera Member D below.

Grain-Size and Componentry:

Sombrera Member C was sieved at the type locality in 0.5 ϕ intervals from -5.5 ϕ to -3 ϕ and in the laboratory from -2.5 ϕ to 1.5 ϕ . The deposit is bimodal, moderately sorted ($\sigma\phi = 1.46$) and fine lapilli ($Md\phi = -1.44$). Componentry was performed on fractions coarser than 1 ϕ , where 96% of material is analysed. The formation contains components of pumice, lithic clasts, free crystals, scoria, subvolcanic rock, and juvenile glass. Proportionally, pumice clasts dominate in fractions coarser than 0 ϕ (>75%) and lithic clasts are abundant in fractions finer than 0.5 ϕ (>25%) alongside high free crystal amounts (>10%). As a weight percentage, the deposit is mostly pumice (85.5%), with minor lithic clasts (7.17%), free crystals (3.56%) and subvolcanic rock (2.48%), with the remaining components each <1% of the total weight (figure 3.42).



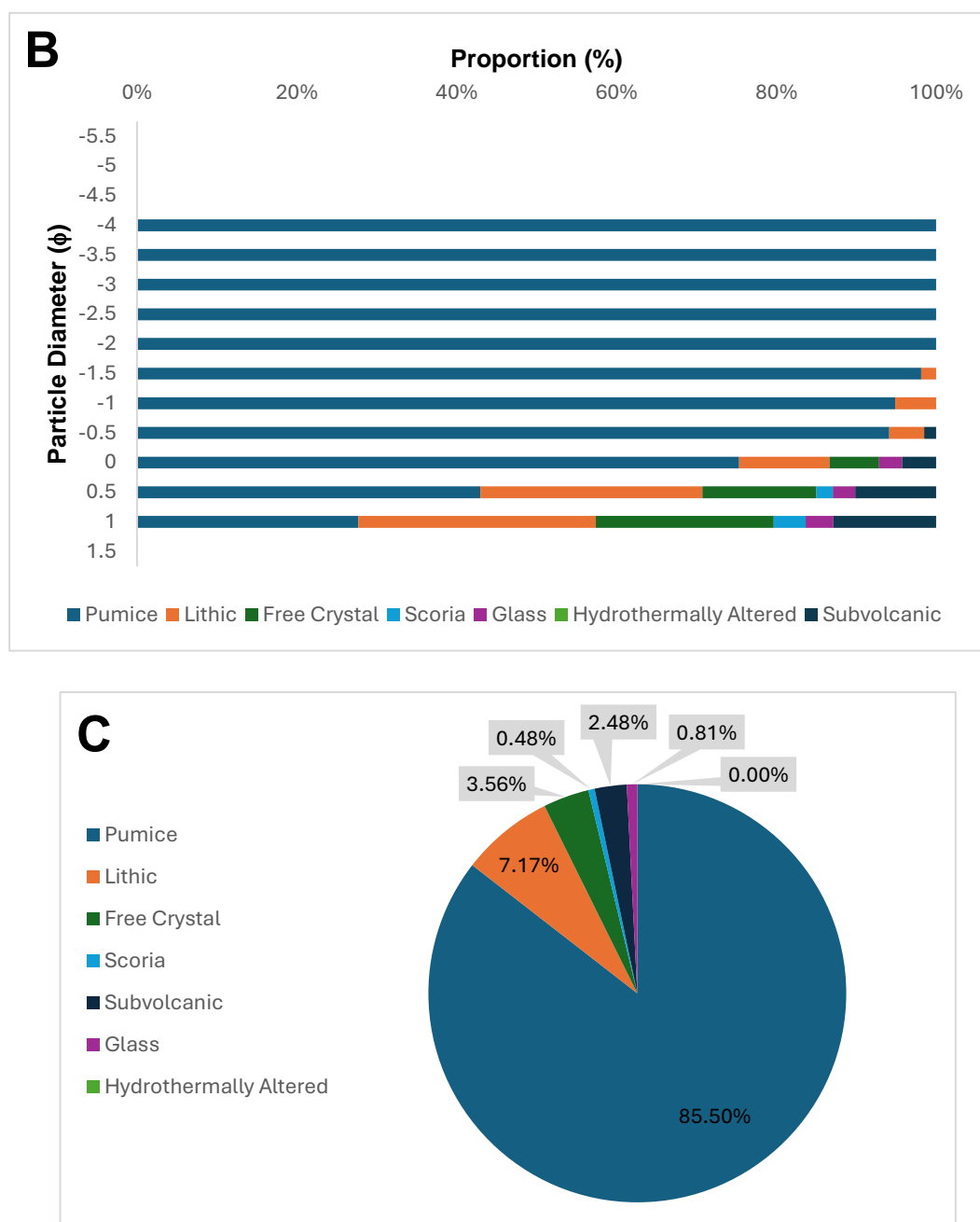


Figure 3.43 – Sombrera Formation Member C **A)** Proportion of components as a weight percentage of the total sample weight **B)** Proportion of components within each grain size **C)** Total weight percentage of components.

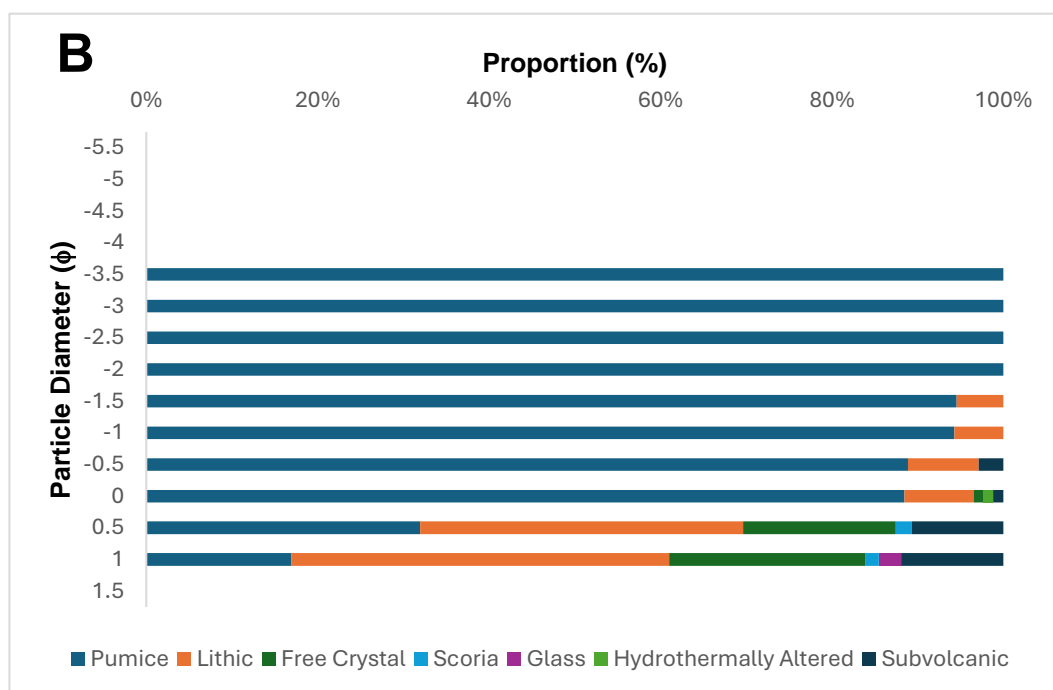
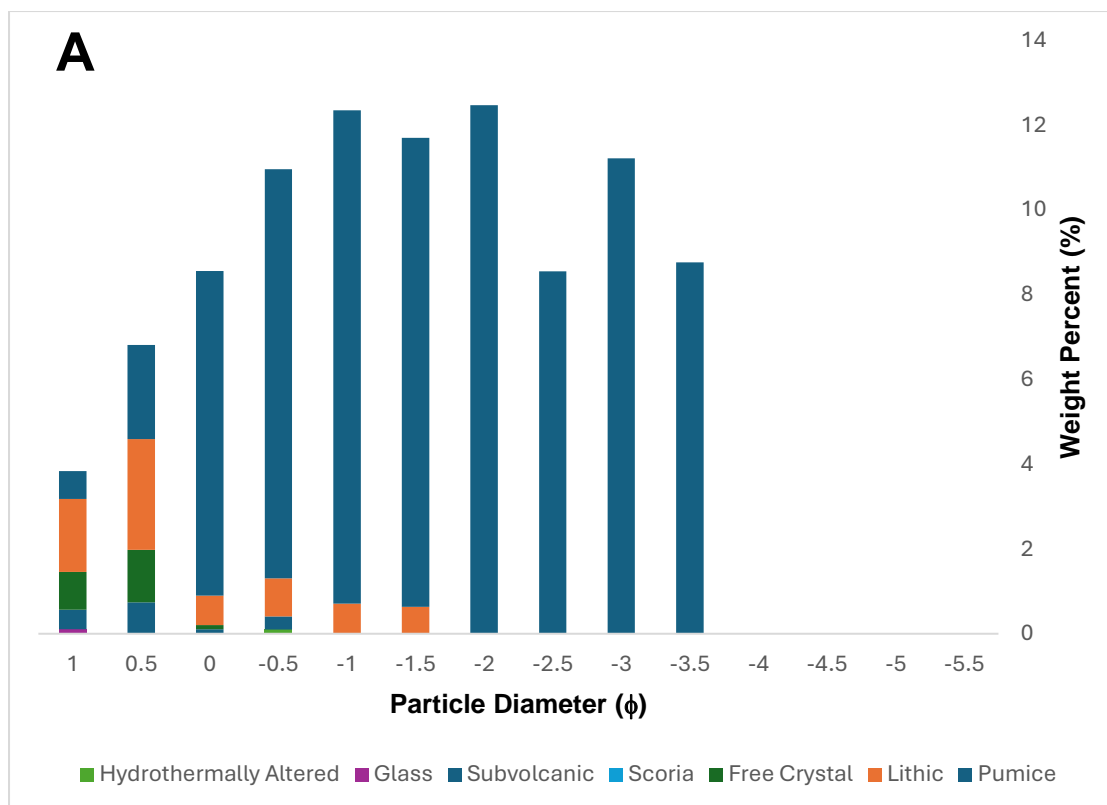
3.1.13.1 Sombrera Member D

Sombrera Member D is a phonolite pumice fall at the top of the Sombrera Formation. At the type locality, it is 34 cm thick, massive, non-graded, poorly to moderately sorted, medium to fine-grained, sub-angular pumice lapilli (figure 3.39). The pumice is <2 cm in diameter, dark cream to grey with a green, silky interior. Mingled pumices are common, with dark grey mafic streaks and rounded blebs. The pumice has frequent pyroxene,

biotite, k-feldspar phenocrysts, and elongated vesicles <1 cm long. The member has lithic populations of 10-15 vol%, with mafic and silicic lavas and infrequent dark red scoria, typically <3 mm in diameter. The member has a sharp contact with the paleosol above, which is overlain by the Vigas Formation, and a sharp contact with Sombrera Member C below. The paleosol above is 45 cm thick, poorly sorted with scattered lithic clasts and pumice clasts that are <3 cm in diameter, and grades from creamy brown to pink-brown.

Grain-Size and Componentry:

Sombrera Member D was sieved at the type locality in 0.5 ϕ intervals from -5.5 ϕ to -3 ϕ and in the laboratory from -2.5 ϕ to 1.5 ϕ . The deposit is bimodal, moderately sorted ($\sigma\phi = 1.40$) and fine lapilli ($Md\phi = -1.67$). Componentry was performed on fractions coarser than 1 ϕ , where 95% of material is analysed. The formation contains components of pumice, lithic clasts, free crystals, scoria, subvolcanic rock, juvenile glass, and hydrothermally altered rock in fractions coarser than 1 ϕ . Proportionally, pumice clasts dominate in fractions coarser than 0 ϕ (>85%) and lithic clasts are abundant in fractions finer than 0.5 ϕ (>35%) alongside high free crystal amounts (>18%). As a weight percentage, the deposit is mostly pumice (87.9%), with minor lithic clasts (7.62%), free crystals (2.34%) and subvolcanic rock (1.70%), with the remaining components each <1% of the total weight (figure 3.41).



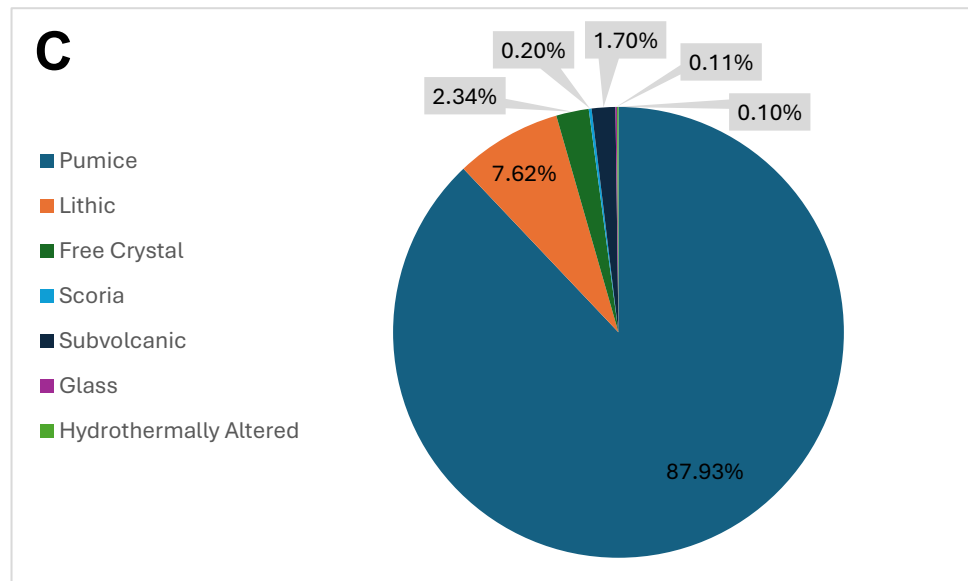


Figure 3.44 – Sombra Formation Member D **A)** Proportion of components as a weight percentage of the total sample weight **B)** Proportion of components within each grain size **C)** Total weight percentage of components.

Interpretation:

The Sombra Formation is a phonolite Plinian eruption that began with a steady eruption column, with high lithic clast populations suggesting significant initial vent clearance (Sombra Member A). The eruption increased in column height before waning to a potential termination, decrease in intensity, or column height (Sombra Member B). The eruption gradually increased in intensity or column height before decreasing to a potential termination (Sombra Member C). The eruption moved to a steady eruption column, with an upwards increase in mafic mingling of pumice, from the mechanical mingling of mafic and phonolitic magma, and continued vent wall erosion (Sombra Member D).

3.1.14 Vigas Formation

The Vigas Formation is a phonolite pumice fall deposit named after Barranco de las Vigas O de Cera, located ~3.3 km southwest of the type locality. The type locality is found at the top of Barranco del Morito, northwest of Mirador Virgen de la Montaña (locality 3, figure 3.46). At the type locality, it is 66 cm thick, massive, normally graded, moderately to well-sorted, medium to coarse-grained, sub-angular pumice lapilli (figure 3.45). The pumice is <3 cm, dark cream to grey, vesiculated with elongated vesicles and a silky texture. The pumice has pyroxene, biotite, k-feldspar, and sparse hauyine

phenocrysts. The member has <1 vol% lithic clasts throughout. At the type locality, the formation has a sharp contact to the paleosol below, above the Sombrera Formation, and a gradational contact to the paleosol above, below the Gambuesa Formation. The paleosol above is ~12 cm thick, grades from light cream to light brown, and is rich in fine-grained pumice lapilli and ash.

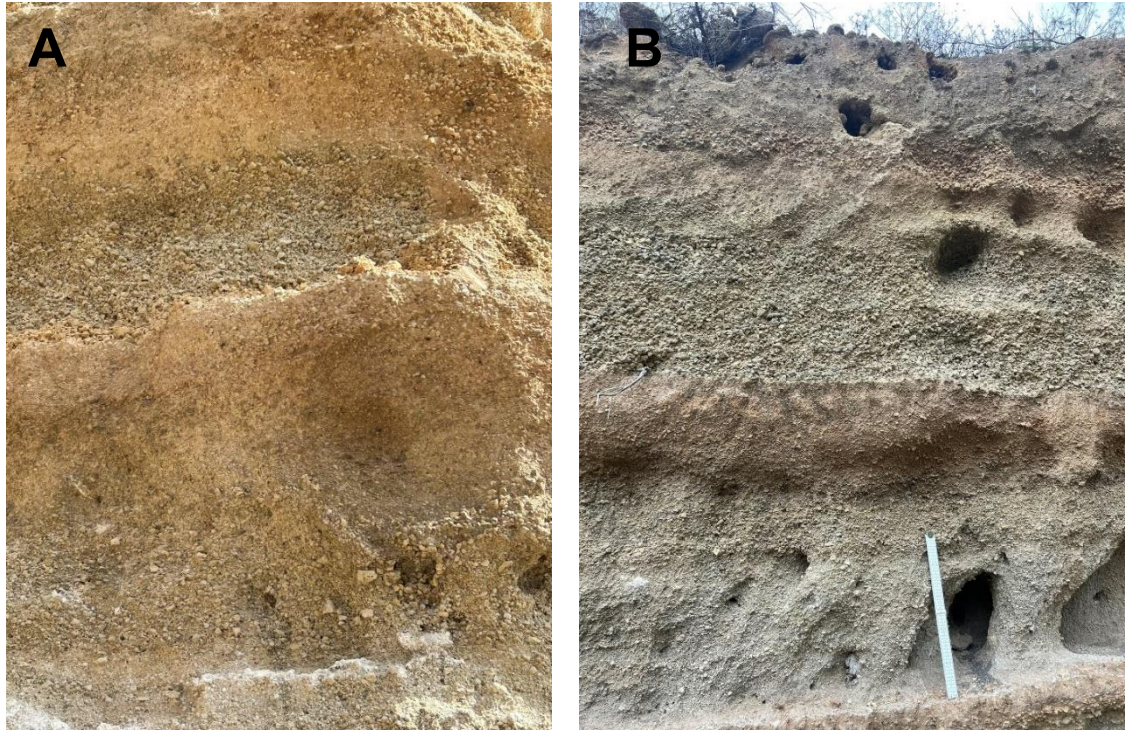


Figure 3.45 – **A)** *The Vigas Formation above the Sombrera Formation at Icor Vineyard (locality 1).* **B)** *The Vigas Formation above the Sombrera Formation and below the Gambuesa Formation at Fasnía Cone (locality 3).*

Vigas Formation

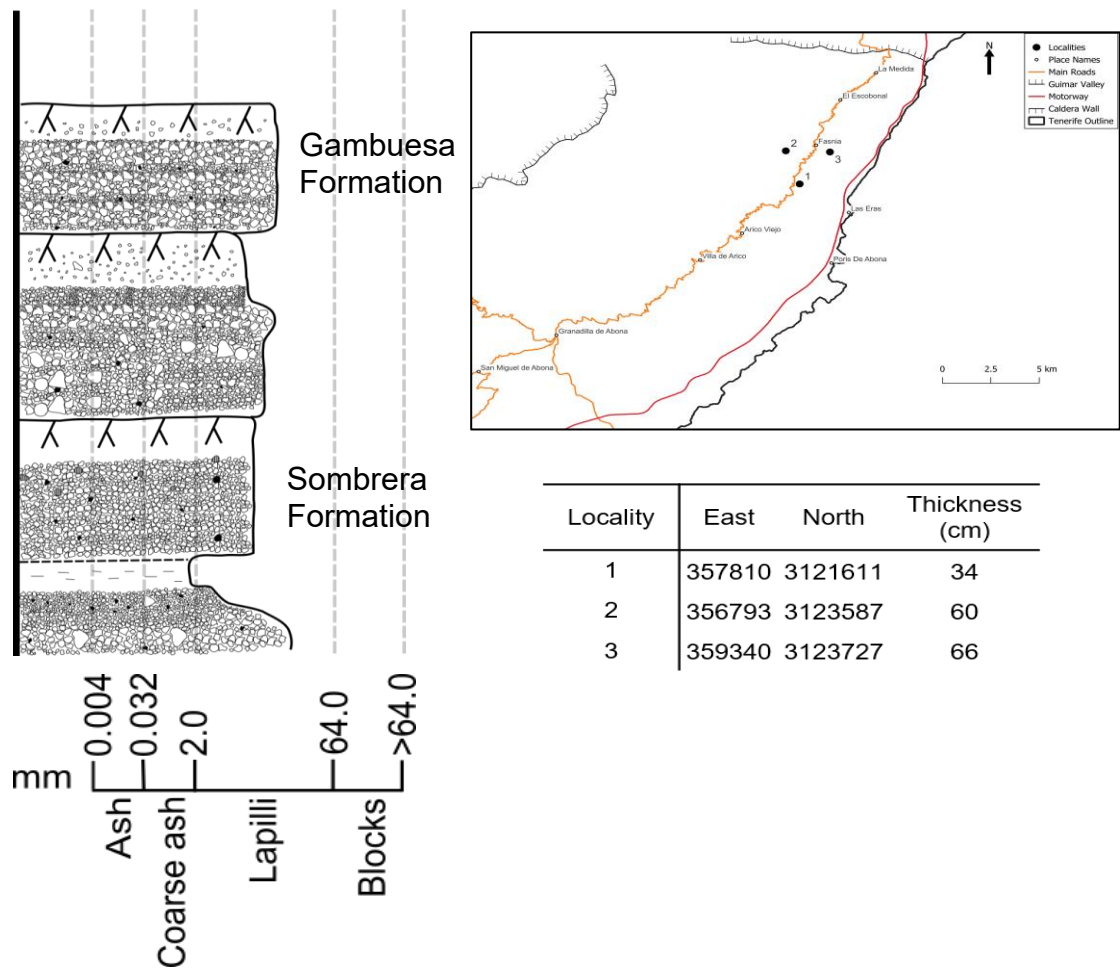
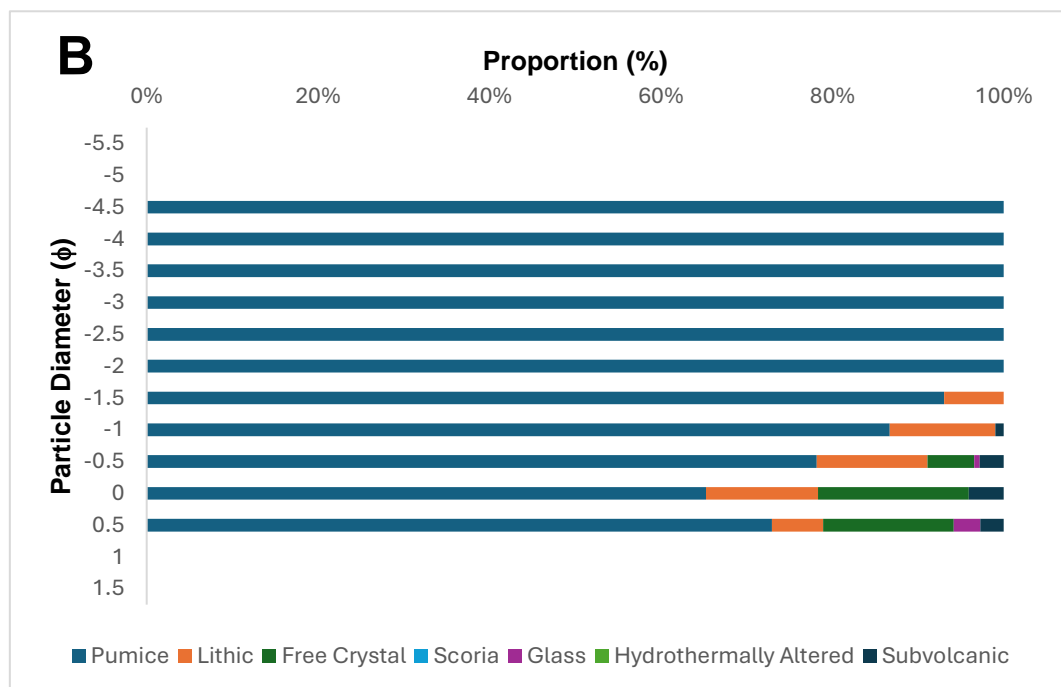
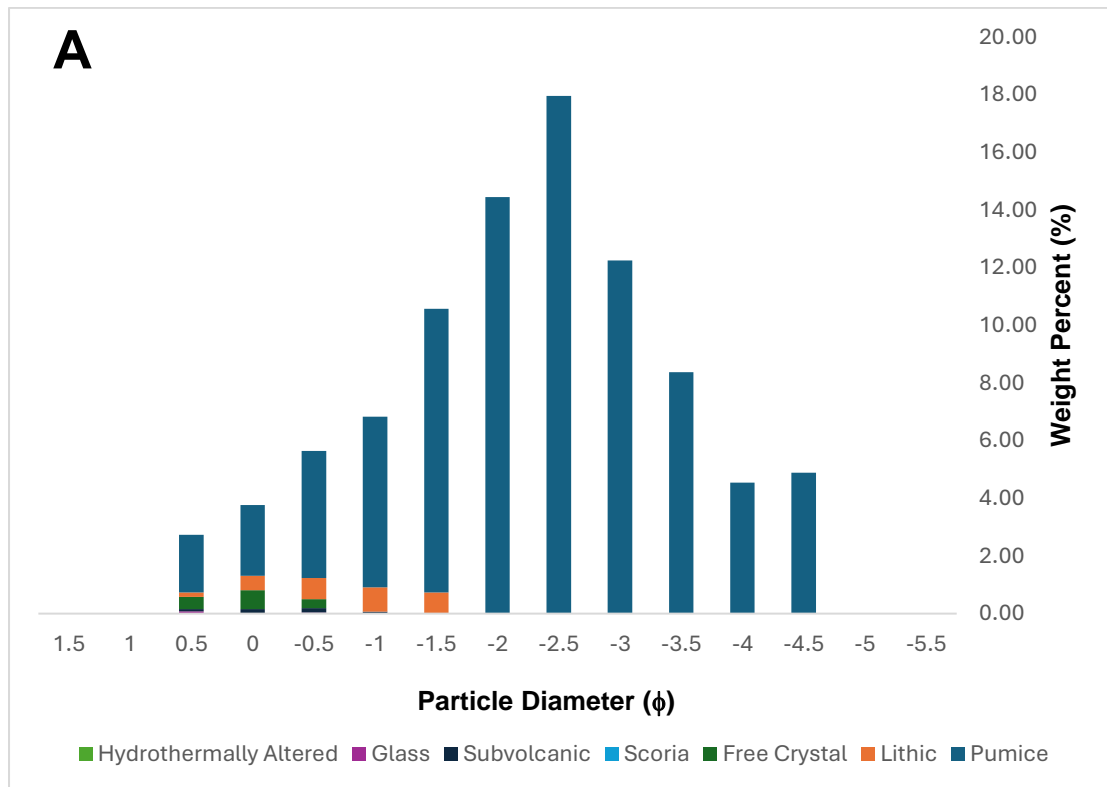


Figure 3.46 - Stratigraphic log of the Vigas Formation. UTM coordinates and inset map of locations and thicknesses are provided. The logs represent stratigraphic relationships with under- and overlying units.

Grain-Size and Componentry:

The Vigas Formation was sieved at Icor Vinyard, ~2.5 km SW of the type locality, in 0.5ϕ intervals from -5.5ϕ to -3ϕ and in the laboratory from -2.5ϕ to 1.5ϕ . The deposit is unimodal, moderately sorted ($\sigma\phi = 1.429$) and medium grained lapilli ($Md\phi = -2.48$). Componentry was performed on fractions coarser than 0.5ϕ , where 93% of material is analysed. The formation contains components of pumice, lithic clasts, free crystals, subvolcanic rock, and juvenile glass. Proportionally, pumice clasts dominate all fractions ($>65\%$), with $>15\%$ free crystals in fractions finer than 0ϕ . As a weight percentage, the deposit is mostly pumice (94.6%), with minor lithic clasts (3.22%) and free crystals (1.51%), with the remaining components each $<1\%$ of the total weight (figure 3.47).



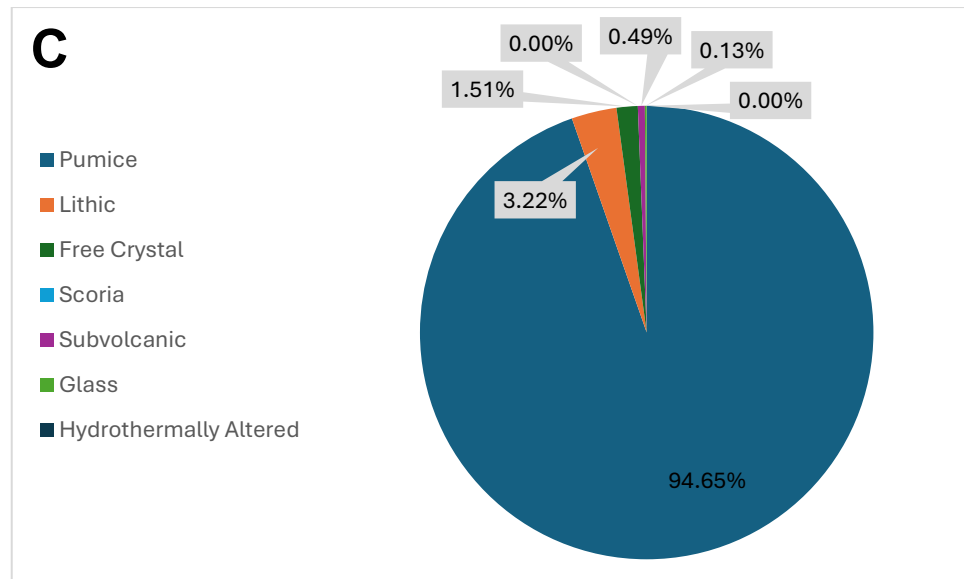


Figure 3.47 – Vigas Formation **A)** Proportion of components as a weight percentage of the total sample weight **B)** Proportion of components within each grain size **C)** Total weight percentage of components

Interpretation:

The Vigas Formation is a phonolite pumice fall deposit from a Plinian eruption that began with a steady eruption column with limit vent clearance. The eruption slightly increased in column height before waning to termination.

3.1.15 Gambuesa Formation

The Gambuesa Formation is a phonolite pumice fall named after Mirador del Barranco de la Gambuesa located ~2.5 km north of the type locality. The type locality is found at the top of Icor Vineyard, south of Barranco de la Linde (locality 1, figure 3.48). At the type locality, it is 45 cm thick, massive, non-graded, moderately to well sorted, medium to coarse-grained, sub-angular pumice lapilli. The pumice <3 cm in diameter, cream to white, microvesicular, and has sparse biotite (?) phenocrysts. The formation has sparse mingled and dark grey to black pumices found throughout. The formation has <5 vol% lithics of dark grey lava that are <0.5 cm in diameter. At the type locality, the formation has a sharp contact with the paleosol below, above the Vigas Formation, and a sharp contact with the paleosol above, which is at the top of the wall section.

Gambuesa Formation

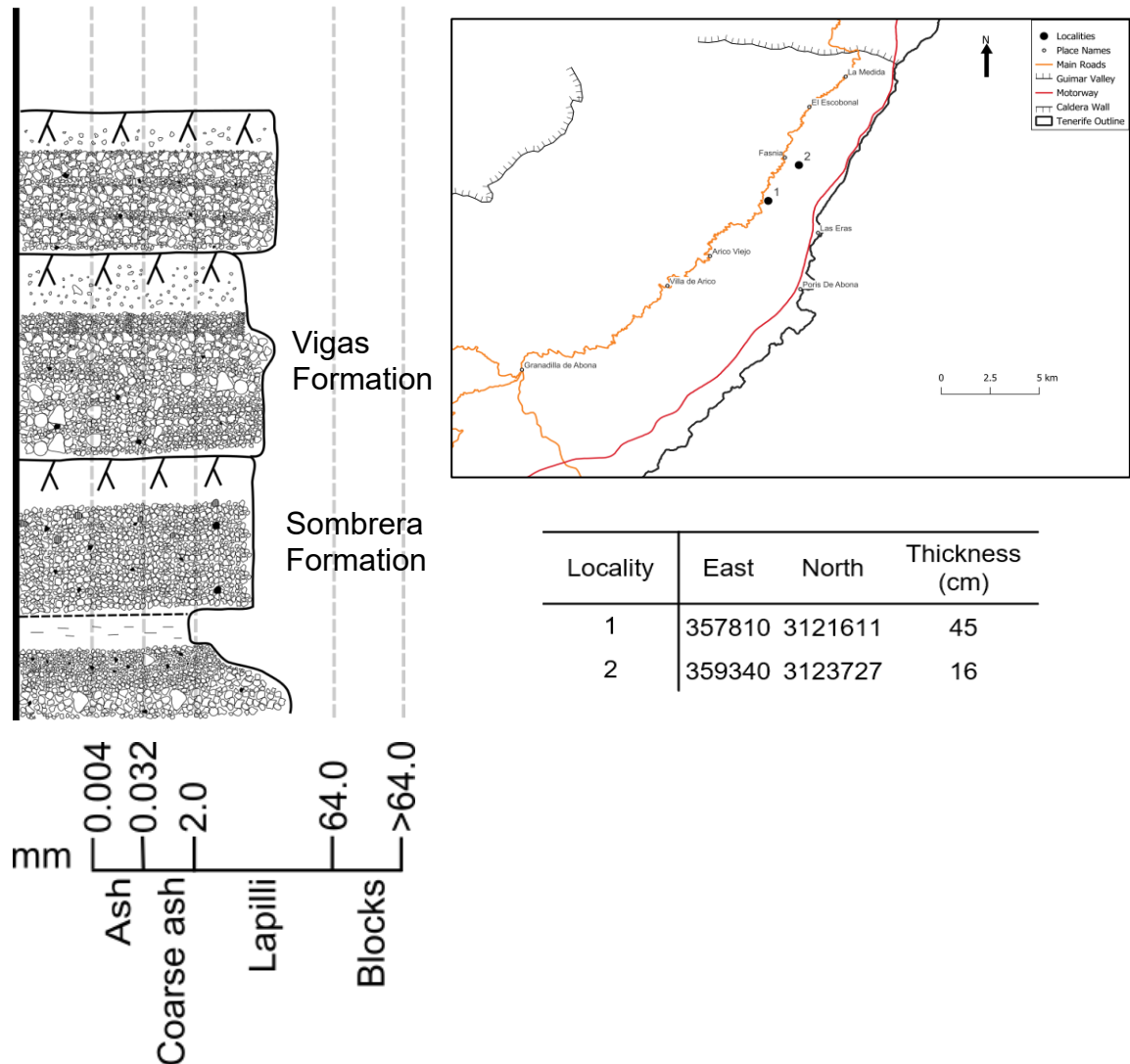
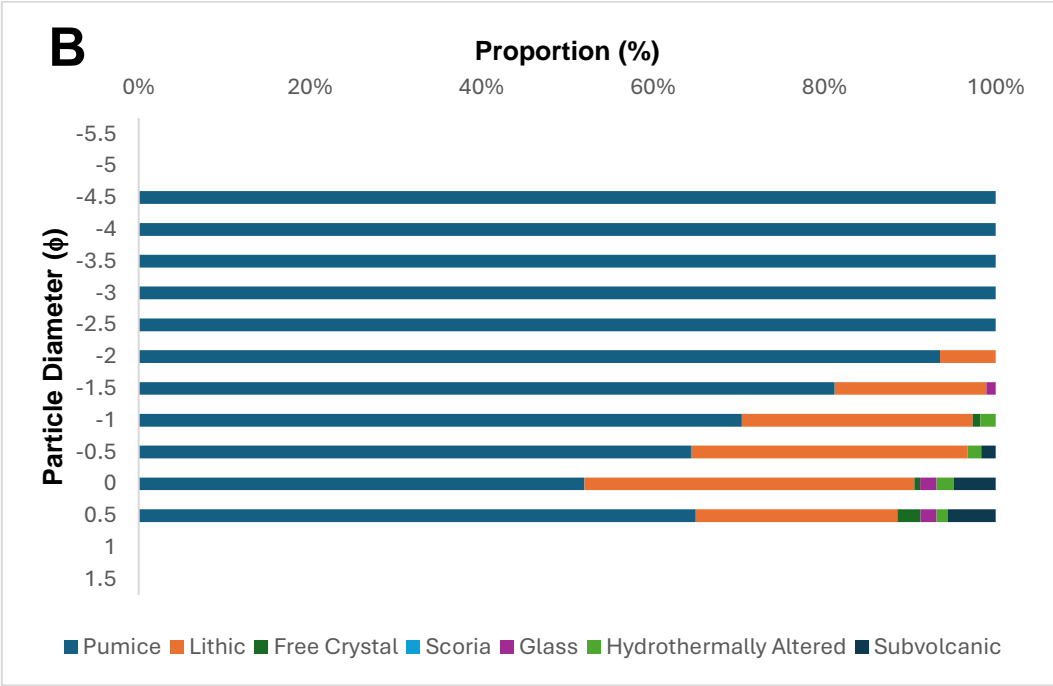
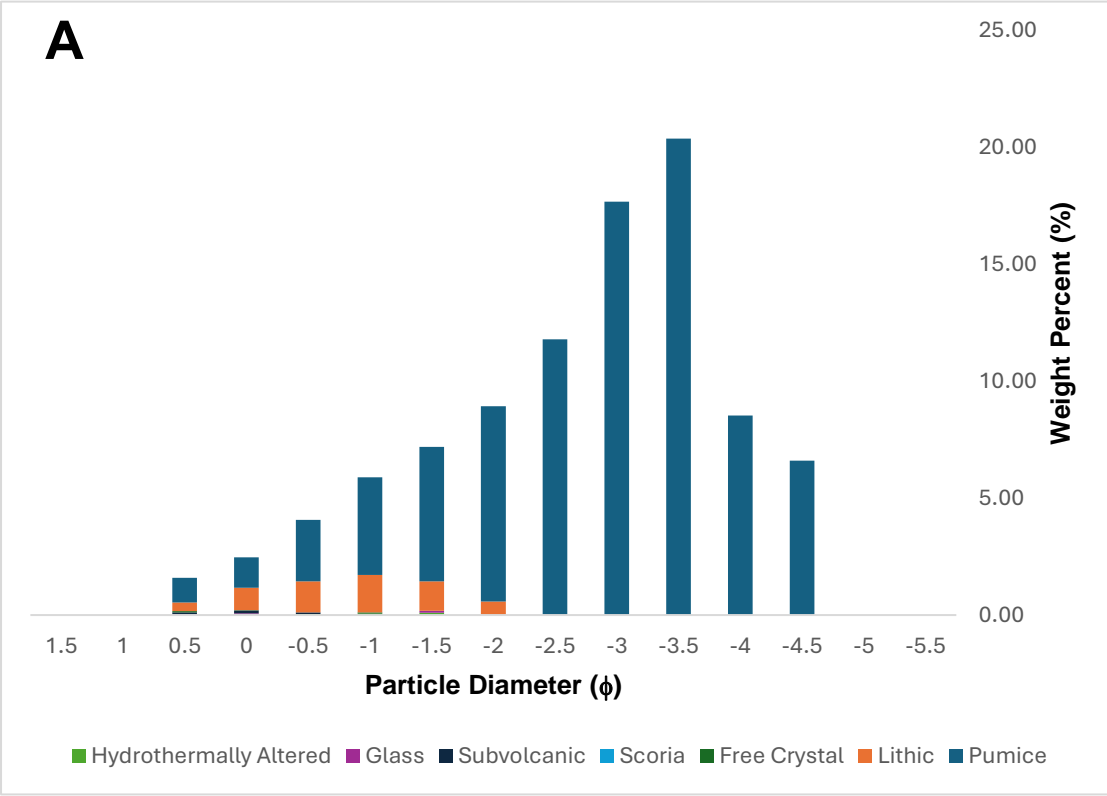


Figure 3.48 - Stratigraphic log of the Gambuesa Formation. UTM coordinates and inset map of locations and thicknesses are provided. The logs represent stratigraphic relationships with under- and overlying units

Grain-Size and Componentry:

The Gambuesa Formation was sieved at the type locality in 0.5ϕ intervals from -5.5ϕ to -3ϕ and in the laboratory from -2.5ϕ to 1.5ϕ . The deposit is unimodal, moderately sorted ($\sigma\phi = 1.28$) and medium to coarse grained lapilli ($Md\phi = -3.14$). Componentry was performed on fractions coarser than 0.5ϕ , where 95% of material is analysed. The formation contains components of pumice, lithic clasts, free crystals, subvolcanic rock, juvenile glass, and hydrothermally altered rock. Proportionally, pumice clasts dominate

all fractions (>52%), with high lithic clast proportions from -1.5 ϕ to 0.5 ϕ (>18%). As a weight percentage, the deposit is mostly pumice (92.8%), with minor lithic clasts (6.41%), with the remaining components each <1% of the total weight (figure 3.49).



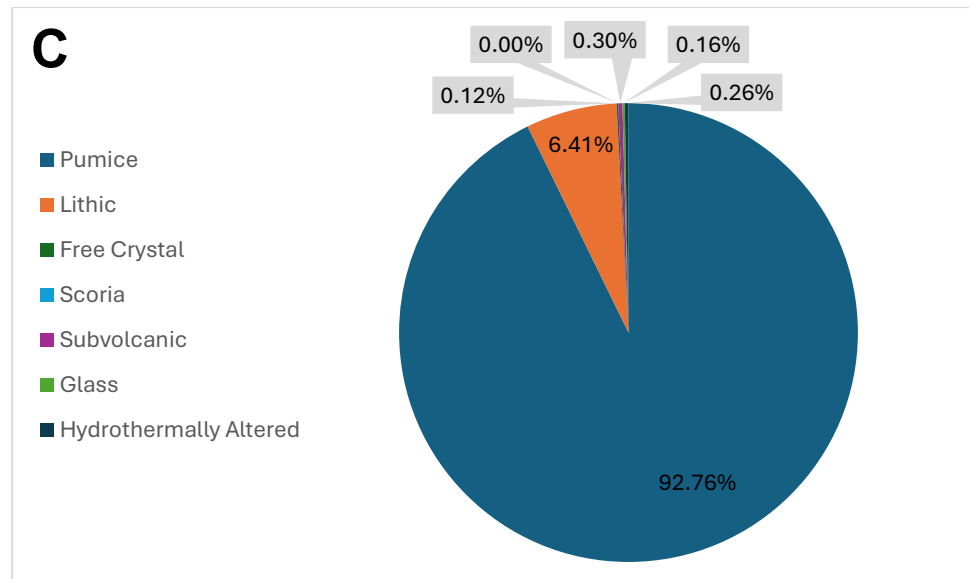


Figure 3.49 – Gambuesa Formation **A)** Proportion of components as a weight percentage of the total sample weight **B)** Proportion of components within each grain size **C)** Total weight percentage of components

Interpretation:

The Gambuesa Formation is a phonolite pumice fall deposit from a Plinian eruption with a steady eruption column throughout the duration of the eruption, with limited vent wall erosion. The formation has mingled pumices throughout, suggesting consistent mechanical mingling of mafic and silicic magma throughout the duration of the eruption. The lack of dispersal makes interpretation of the eruption challenging.

3.1.16 Other Volcanic Units

Across SE Tenerife there are at least 7 unknown pumice fall deposits (UPFDs), and 3 scoria fall deposits located within this stratigraphic succession.

3.1.16.1 Pre-Mena Pumice Fall Deposits

At a single locality by the town of La Medida, 5 unknown pumice fall deposits can be found separated by paleosols beneath the Mena Formation (figure 3.50).

UPFD 1:

Sitting at the bottom of the succession above a thick paleosol, UPFD 1 is 46 cm thick, normally graded, moderately sorted, clast supported, medium to fine-grained, sub-angular pumice lapilli. The pumice is <3 cm in diameter, vesiculated with a silky interior and rounded vesicles, aphyric, and often mingled with occasional black pumices. The

unit has 5-10 vol% lithic clasts of red, vesiculated scoria and dark black lava <2 cm in size. The unit has a sharp contact with the paleosol below and a sharp contact with the paleosol above. The paleosol above is 12 cm thick and contains black tephra and pumice (scoria fall 'a'), which is overlain by UPFD 2.

UPFD 2:

UPFD 2 is 19 cm thick, normally graded, moderately sorted, clast supported, medium to fine-grained, sub-rounded pumice lapilli. The pumice is <1 cm in diameter, and has large, rounded vesicles and aphyric. The unit has <2 vol% lithic clasts of both phonolite and basalt lava. The unit has a sharp contact with the paleosol below and a gradational contact with the paleosol above. The paleosol above is 32 cm thick when UPFD 3 is present, otherwise it is 77 cm thick, and light brown with dark brown patches.

UPFD 3:

UPFD 3 is 8 cm thick, massive, non-graded, poorly sorted, fine-grained, sub-rounded pumice lapilli. The pumice is generally <0.3 cm, however, clasts can be up to 2 cm in diameter, aphyric, and have large, rounded vesicles. The unit has <5 vol% lithic clasts of basalt and phonolite lava, typically <0.2 cm in diameter. The unit is not laterally consistent, with frequent lensing across the wall section. The unit has a sharp contact with the paleosol below and a sharp contact with the paleosol above. The paleosol above is 37 cm thick, light brown with dark brown patches, and overlain by UPFD 4.

UPFD 4:

UPFD 4 is 12 cm thick, massive, non-graded, well sorted, clast supported, fine-grained, sub-rounded pumice lapilli. The pumice is <1 cm in diameter, cream, aphyric, with a variety of macro- and microvesiculated pumices. The unit contains <2 vol% lithic clasts of lava <0.5 cm in diameter. The deposit has a sharp contact with the paleosol above and below. The paleosol above is 16 cm thick, light brown to dark orange, and overlain by UPFD 5.

UPFD 5:

UPFD 5 is 21 cm thick, massive, non-graded, well sorted, clast supported, coarse-grained, angular pumice lapilli. The pumice is <5 cm in diameter, and has large,

elongated and rounded vesicles, with a streaky interior. The pumice has biotite (?) and pyroxene (?) phenocrysts. The deposit has <1 vol% lithic clasts of basalt and phonolite lava, alongside dark red vesiculated scoria. The deposit has a sharp contact with the paleosol above and below. The paleosol above is 50 cm thick, light brown to orange, and has lenses of fine-grained, matrix-supported, pumice lapilli. The paleosol is overlain by the Mena Formation.

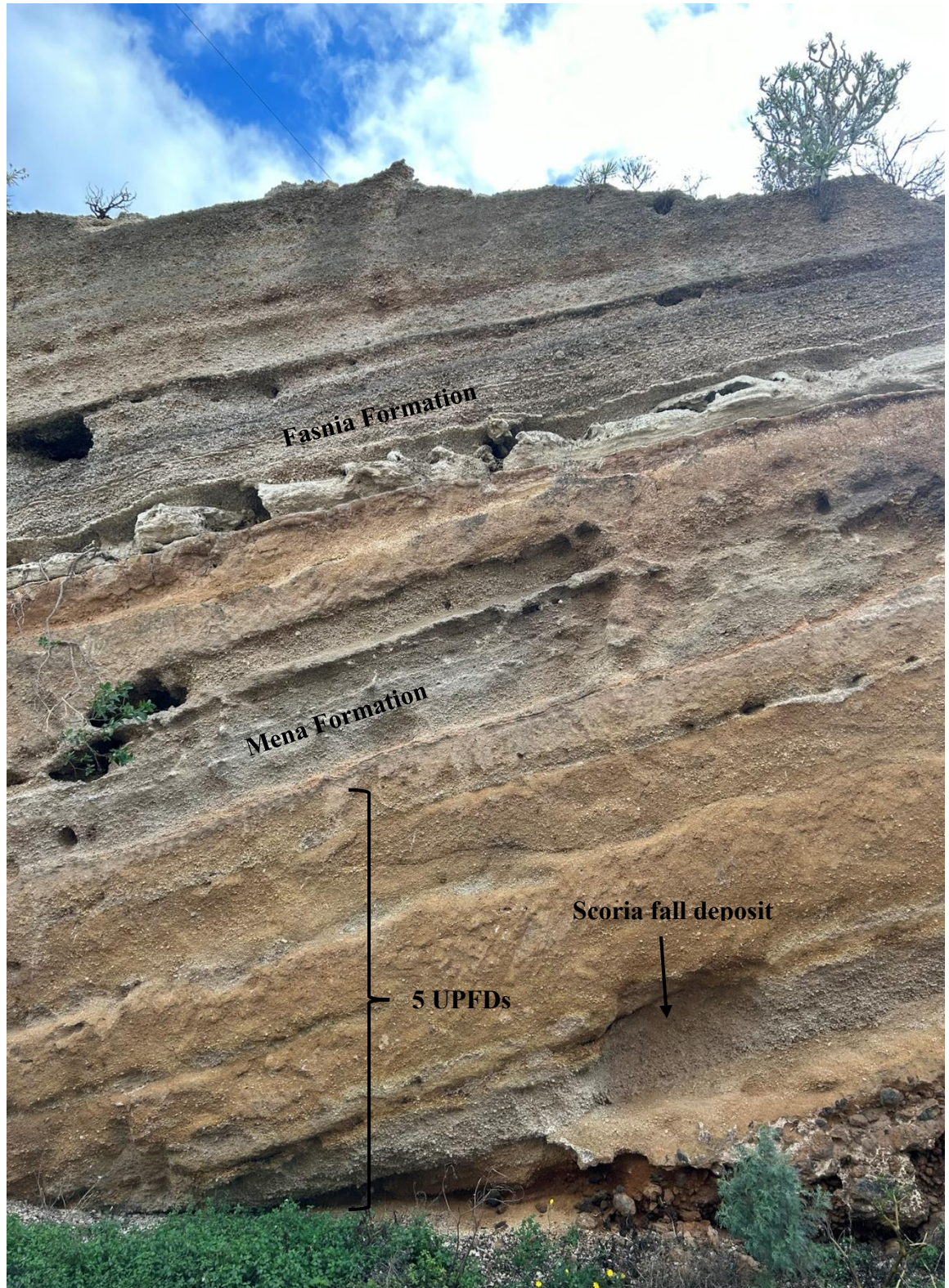


Figure 3.50 – The pre-Mena pumice fall deposits in La Medida (UTM: 361611; 3128810).

3.1.16.2 Pre-Eras Pumice Fall Deposits

The Pre-Eras pumice fall units are found at a single locality at Mirador de las Eras, where a stratigraphic succession can be found resting beneath the Fasnia Formation and

the Granadilla Regolith. The succession includes alternating paleosols and heavily weathered pumice falls, where only two pumice falls could be described. Both pumice falls (UPFD 6 and UPFD 7) rest beneath a thin massive lapilli tuff and thin massive lapilli pumice interpreted to be the Eras Formation (figure 3.51).

UPFD 6:

UPFD 6 is a phonolite pumice fall deposit that can be split into three units (6A, 6B, 6C) and has a maximum thickness of 52 cm. UPFD 6C is 20 cm thick, moderately sorted, clast supported, non-graded, massive, medium to fine-grained, sub-angular pumice lapilli. The pumice is <2 cm in diameter, microvesiculated with a silky interior, and includes sparse biotite phenocrysts. UPFD 6C has <2 vol% lithic clasts of black and grey lava and hydrothermally altered clasts. UPFD 6B is 2 cm thick, massive, non-graded, well sorted, matrix-supported, fine-grained pumice lapilli to ash. The pumice is <3 mm in diameter and cream with sparse orange staining. UPFD 6B has 25-30 vol% lithic clasts of black and grey lavas, orange to yellow hydrothermally altered clasts and obsidian fragments. UPFD 6A is 30 cm thick, moderately sorted, clast supported, non-graded, massive, medium grained, sub-angular pumice lapilli. The pumice is <2 cm in diameter, microvesiculated with a silky interior, and sparse biotite phenocrysts. UPFD 6A grades into the paleosol above, which is >3 m thick, pumice rich, and orange. Directly above UPFD 6A, within the paleosol, is a scoria fall deposit (scoria fall 'c').

UPFD 7:

UPFD 7 is a 54 cm thick, well to moderately sorted, massive, non-graded, clast supported, fine grained, sub-rounded pumice fall deposit. The pumice is <2 in diameter, aphyric, and variable vesicles sizes with sparse elongated vesicles. The deposit has <1 vol% lithic clasts. The bottom of the deposit is heavily weathered with a white mineralised surface. The deposit overlies a large paleosol, which is above UPFD 6, and has a sharp contact to the paleosol above, which rests beneath the Eras Formation.

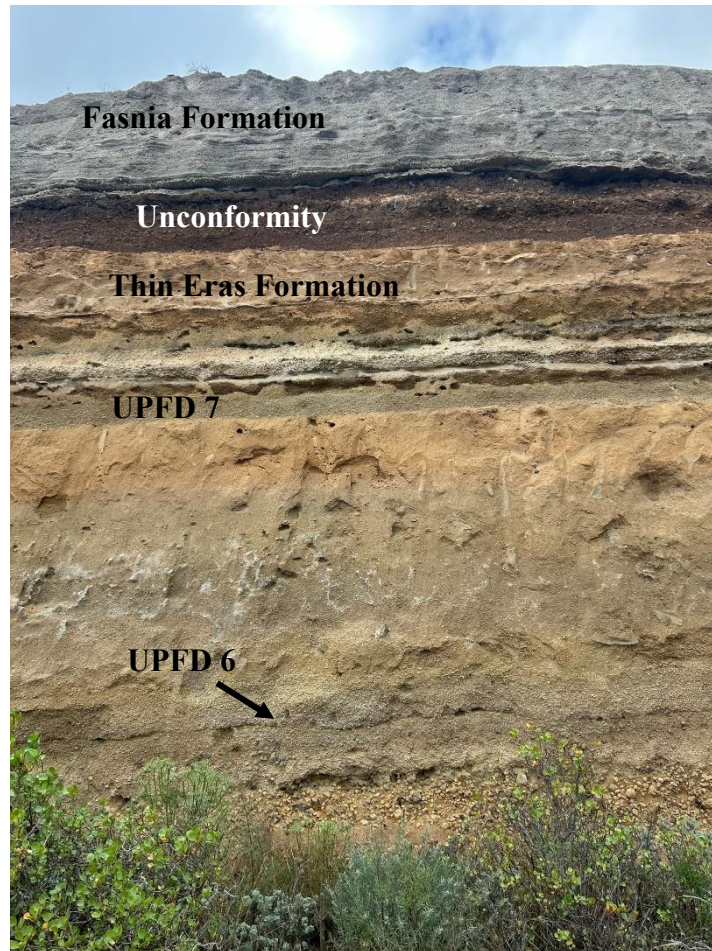


Figure 3.51 – Pre-Eras fall deposits nearby Mirador de las Eras (UTM: 356768; 3120066).

3.1.16.3 Scoria Fall Deposits

At least three scoria fall deposits can be found within the pyroclastic succession.

- a) Located directly above UPFD 1 in La Medida, a 12 cm thick scoria fall unit and dark grey to black pumice can be found within the paleosol.
- b) Located at a single locality west of Los Roques within Barranco de San Joaquin, an 8 cm thick, black scoria fall deposit is well pronounced above the Mena Formation and is laterally continuous. This scoria deposit is unrelated to the Mena Formation and is likely to be from a nearby scoria cone forming eruption that has since been buried or eroded.
- c) Found directly above UPFD 6 is an 8-10 cm matrix supported; laterally discontinuous scoria fall deposit.

It is possible these basaltic units are related to Dorsal Ridge basalts given the proximity and overlapping estimated ages of 0.9 Ma to 0.78 Ma where increased growth of the Dorsal Ridge occurred (Anchochea et al., 1990; Cas et al., 2022). Another possibility is that these basaltic deposits originated from basaltic volcanism occurring within the southern Bandas Del Sur region from 0.948 Ma to 0.779 Ma (Kröcher and Buchner 2009).

3.1.16.4 Effusive Lavas

Throughout the Bandas Del Sur, stratigraphic successions are either capped or begin with basalt or phonolite lavas >5 m in thickness. There is a noticeable trend between different regions as to whether the stratigraphic succession rests on top or beneath a lava flow. At each locality from La Medida to Icor, the stratigraphic succession is found resting above the rubbly top of a basaltic lava flow, typically capped by a large, younger, ignimbrite such as the Fasnía Formation, or the Arico Formation. However, southwest of Las Eras, the succession is found beneath a large, columnar jointed lava flow. An exception to the trend is in La Zarza, a town west of Fasnía closer to the caldera wall, where the succession rests beneath a large lava flow and is heavily baked. It is possible that, if dated or identified, these lava flows could be used to give improved age constraints on the stratigraphic succession, such as the 0.69 Ma Las Pílas Unit of trachybasalt lava flows within the Bandas Del Sur (Anchochea et al., 1999).

Chapter 4: Discussion

4.1 The Guajara Stratigraphic Succession

4.1.1 Stratigraphic Trends

In this study at least 19 new Plinian pumice fall deposits have been identified within the Guajara Eruption Cluster, with 14 correlated and characterised across southeast Tenerife's Fasnía region. These eruptions exhibit distinct trends in pyroclastic fall deposit deposition and relative stratigraphy.

Basal Stratigraphy

The La Linde and Honduras formations represent the base of this pyroclastic succession, however whether they represent the base of the Guajara Eruption Cluster is uncertain as they are never identified above a major unconformity. These formations typically overlie blocky basalt lava; however, the base is not exposed at all outcrops. At La Zarza and Mirador de las Eras, basalt lava flows intersect the base of the pyroclastic succession, flowing into nearby barrancos. Inaccessible pyroclastic deposits visible beneath these flows may belong to the older Ucanca Eruption Cluster or represent earlier Guajara deposits. The age of the bottom of the pyroclastic succession is therefore highly uncertain.

Middle Stratigraphy

The El Rincon formation consistently underlies the Eras formation, separated by a distinctive thin, dark brown paleosol. In the absence of El Rincon, a pale orange paleosol occurs beneath Eras. While the reason for this relationship is unclear, it serves as a key marker for correlating El Rincon across the Eras formation's dispersal area. The Arco and Carretas formations typically underlie El Rincon as a package of three, separated by thin paleosols. The El Rincon locality is the sole exception to this pattern.

Upper Stratigraphy

The Gambuesa formation caps the pyroclastic sequence, with the Arico formation overlying it at Las Eras. This suggests an age range of 0.738-0.668 Ma for the eruptions.

In many localities, particularly northeast of Fasnía Cone, the ~0.312 Ma Fasnía formation tops the pyroclastic succession.

4.1.2 Correlations from SE to NE

A complete stratigraphic succession of the Guajara Eruption Cluster remains uncertain due to the apparent separation of eruptive units between the El Río region (Davila-Harris et al., 2009; 2023) and the Fasnía region (this study). However, a correlation could be made between the Eras Formation (Brown et al., 2003) and the Moradas Formation (Davila-Harris et al., 2009; 2023).

Eras and Moradas Formations

Similarities between the Eras and Moradas Formations were found in the deposit and pumice characteristics. These formations share striking similarities:

- Fine-grained lapilli base
- Diffuse stratification
- Mingled pumices towards the top
- Large, highly vesiculated pumices throughout
- Increased lithic clasts towards the top
- High proportion of sanidine phenocrysts throughout

Further deposits of the Eras Formation likely exist across Tenerife, particularly in the Arona region (SW Tenerife) and the full extent of the Eras ignimbrite remains uncertain. No other units could be correlated across the two regions. New eruptive units in this study appear restricted to the Fasnía region, with uncertain stratigraphic positions relative to the Helecho and Río Formations (Davila-Harris et al., 2009; 2023). Therefore, it is challenging to provide a complete stratigraphy of the Guajara Eruption Cluster for the current known units.

Zarza and Mena Formations

Middleton (2006) suggested the Zarza and Mena Formations could be found in the El Río region. However, field investigations indicate no correlation between the pyroclastic deposits in the El Río region to the Zarza and Mena Formations in this study. The dispersal characteristics suggest thinning to the southwest, likely resulting in thin or absent deposits in the El Río region. Furthermore, the Blanquitos Formation cannot be

found in the NE and is not part of this pyroclastic succession. The new descriptions and dispersal of the Zarza and Mena Formations in this study should be used from here on.

Age Uncertainties

It remains uncertain whether eruptions older than the Eras eruption (0.738 Ma) predate the Rio eruption (0.747 Ma). Given the short time span between events (11 eruptions in ~10 kyrs), many eruptions in this study are likely older than the Rio eruption. A deposit at the bottom of the Guajara caldera wall dates to 0.85 Ma, suggesting eruptions older than Eras fall between 0.738-0.850 Ma (Marti et al., 1994). The Tosca eruption (0.88 Ma) disputes the 0.85 Ma start of the Guajara, adding uncertainty to the cluster's beginning and the ages of eruptions in this study (Davila-Harris et al., 2023).

4.1.3 Unknown deposits

La Medida Deposits

Five UPFDs lie beneath the Mena Formation in La Medida (figure 3.50):

- UPFD 1: Exhibits mingled pumices, black pumices, and red vesiculated scoria lithics. Possible correlations:
 - Honduras Formation: Similar lithic clasts and structure, but inconsistent with known thinning trends
 - Vegas Member (Middleton, 2006): Shares black pumice and scoria characteristics, but limited information hinders correlation
- UPFDs 2-5: Potentially distal deposits of known eruptions or new eruptions with NE dispersal into Guimar Valley

Mirador de las Eras Outcrop

A ~10m succession beneath the Fasnía Formation and Granadilla Regolith contains two UPFDs (figure 3.51):

- UPFD 6: Similarities to Mena Formation
 - Three-part structure: coarse base, fine centre, coarse top
 - Hydrothermally altered lithics
 - Sparse black basaltic tephra in upper paleosol, like at Los Roques
 - Caution in correlation due to erosion and lack of surrounding units

- UPFD 7: Relatively featureless, potentially correlates with pre-Eras Formation eruptions

Regional Context

Across the Abona and El Rio regions, many UPFDs were found alongside the Eras, Rio, Blanquitos, and Vegas Formations that may correlate with the deposits in this study, with samples taken on occasion. However, they were not characterised and further investigation of these deposits is required.

4.1.4 Eruption Frequency

Previous studies on eruptions in the Guajara Eruption Cluster have identified 1 major eruption every 35kyrs, from ~0.6 Ma (Granadilla Formation) to ~0.88 Ma (Tosca Formation) (Davila-Harris et al., 2023). However, this estimate focusses on eruptions that produce ignimbrite sheets, excluding eruptions that solely produce pumice fall deposits. Current data reveals at least 24 Plinian eruptions within the 280 kyr Guajara Eruption Cluster:

- Sixteen Plinian pumice fall deposits.
- Eight ignimbrite-forming eruptions.

This increases the eruption frequency to one eruption every 11,666 years. The frequency may increase further as several uncharacterised Guajara-age pumice fall deposits exist across the Bandas Del Sur. However, the precise beginning of the Guajara Eruption Cluster remains uncertain due to undated eruptions.

Table 4.1 – Eruptions within the Guajara Eruption Cluster and the region they are found, correlations across regions are highlighted in dark grey. Ages are from Davila-Harris et al., (2023)

Adeje Region (Age Ma)	Abona Region (Age Ma)	Fasnia Region (Age Ma)
	Granadilla (0.6)	
	Abades (0.56)	Abades (0.56)
	Incendio	Incendio
	Arico (0.668)	Arico (0.668)
		Gambuesa
		Vigas
	Helecho (0.733)	Sombrera
	Eras (Moradas) (0.738)	Eras (0.738)
	Rio (0.74)	El Rincon
	Blanquitos	Carretas
	Vegas	Arco
		Icor
		Zarza
		El Escobonal
		Mena
		Jurado
		Aguerche
		Honduras
		La Linde
Tosca (0.88)		

4.2 Eruption Volumes and Dispersal

4.1.5 Volume

Eruption volume estimates are a tool for assessing the scale of past volcanic activity and comparing eruptions on Tenerife with those elsewhere. However, the methods used to calculate these volumes face significant limitations and uncertainties, making interpretation challenging (Pyle, 1995; Bonadonna et al., 1998; 2002; Bonadonna and Costa, 2013; Bonadonna et al., 2015a). Due to the lack of distal and proximal thickness data for all Plinian fall deposits in the Guajara Eruption Cluster, volume estimates are likely to represent minimum values and should be interpreted with caution.

Data Limitations

One major limitation in estimating pyroclastic deposit volumes is the scarcity of data points. For this study, volumes were calculated using between one and five isopach contours, with data often limited to medial distances from the vent. Additionally, vent locations remain unknown for many deposits. As a result, different methods for volume

estimation—Exponential, Power-law, and Weibull—produce significantly varying results. Previous studies have shown that the power-law method yields larger volume estimates compared to the Weibull and exponential methods. The exponential method is known to underestimate true volumes (Pyle, 1995; Bonadonna et al., 1998; 2002; Bonadonna and Costa, 2013), while the Weibull method is considered the most accurate but struggles with limited data points, often producing a down-trending concave curve (figure 4.1). For consistency with prior studies (e.g., Bryan et al., 1998; Edgar et al., 2007), this study uses average volumes derived from the exponential method for comparison with other pyroclastic deposits on Tenerife. Volume estimates for all Guajara formations and major formations from other studies are presented in Table 4.2.

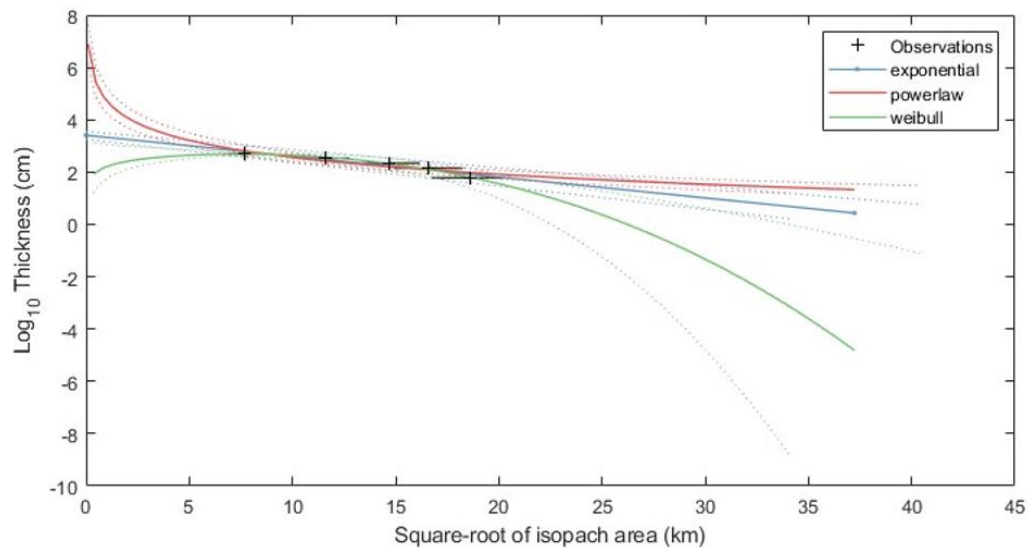


Figure 4.1 - An example of a concave curve produced by the Weibull method when calculating the estimated volume of the Zarza Formation.

Comparisons

Among the deposits studied, the Eras Formation has the largest volume estimate; however, this calculation only includes its fall deposit. A ~10 m thick ignimbrite associated with the Eras Formation has yet to be fully constrained and is therefore excluded from current volume estimates. The Zarza Formation represents one of the largest calculated volumes for a fall deposit on Tenerife without an associated ignimbrite. Its volume is comparable to those of the La Caleta, Abades, and Poris fall deposits,

which all have associated ignimbrites. Notably, more than half of Zarza's dispersal lies across the Guimar Valley, a region formed by a major landslide between ~ 0.54 Ma and ~ 0.84 Ma, which likely removed evidence of older deposits. This raises the possibility that an ignimbrite associated with Zarza may have formed but is no longer exposed on the present-day surface. There is a potential trend in eruption volumes and time, with average volumes increasing from 0.2 km^3 (Ucanca Eruption Cluster) to 1.85 km^3 (Guajara Eruption Cluster) to 3.87 km^3 (Diego Hernandez Eruption Cluster). However, it should be noted that not all volumes from Plinian eruptions have been calculated and interpretations that the size of Plinian eruptions are increasing towards the present day should be taken with caution. There is limited evidence of a series of smaller volume Plinian eruptions ($<2 \text{ km}^3$) before a larger Plinian eruption ($>4 \text{ km}^3$), with the trend only evident leading up to the 0.738 Ma Eras eruption. Further investigations into smaller volume Plinian eruptions, particularly within the Diego Hernandez and Ucanca Eruption Clusters is required.

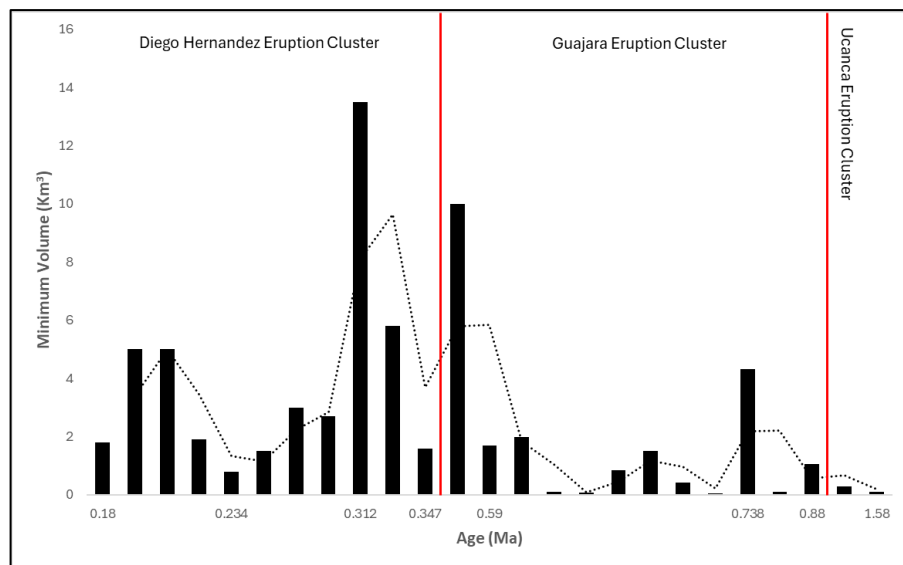


Figure 4.2 – Minimum volume of all pyroclastic deposits where calculated, separated into the three eruption clusters. The dashed line is a moving average.

Dispersal Constraints

The dispersal characteristics of each deposit pose a significant limitation in understanding the full scale of these eruptions. Accurate volume estimations require proximal, medial, and distal thickness data to avoid extrapolating thinning rates from incomplete datasets. On islands like Tenerife, obtaining distal data is particularly challenging without access to drilled cores, while proximal thicknesses are often

constrained to either large ignimbrite-forming eruptions or more recent events. Many deposits in this study are small-scale Plinian fall deposits older than 700 kya and are therefore likely to have been buried or removed by subsequent larger eruptions, lava flows, or landslides. This reduces their likelihood of being exposed on the present-day surface. While eruption volume estimates provide valuable insights into past volcanic activity, their limitations must be acknowledged. Future studies should prioritize identifying additional deposits across Tenerife's Bandas Del Sur region and beyond, incorporating proximal exposures as well as potential offshore correlations to refine these estimates further.

Table 4.2 – Minimum volumes for all pyroclastic deposits on Tenerife where calculated from: ^aBryan et al., (2000), ^bEdgar et al., (2003;2007), ^cMiddleton (2006), ^d Davila-Harris et al., (2009;2023). Ages from: ^eBryan et al., (1998), ^fBrown et al., (2003), ^gBrown and Branney, (2013)

Eruption Cluster	Formation	Minimum Volume km ³	Age (Ma)
Diego Hernandez	Abrigo ^b	1.8	0.18 ^e
	Benijos ^b	<5.0	
	Hidalga ^b	<5.0	
	Socorro ^b	1.9	
	Batista ^b	0.8	0.234 ^b
	Caleta ^b	1.5	0.221 ^f
	<i>Ignimbrite</i>	0.13	
	<i>Fall</i>	1.4	
	Arafo ^b	3.0	
	Poris ^b	2.7	0.273 ^g
	<i>Ignimbrite</i>	0.85	
	<i>Surge</i>	0.15	
	<i>Fall</i>	1.7	
	Fasnia ^b	13.5	0.312 ^{bd}
	<i>Ignimbrite</i>	1.2	
	<i>Surge</i>	0.15	
	<i>Fall</i>	12.2	
	Aldea ^b	5.8	0.319 ^b
	<i>Ignimbrite</i>	<1	
	<i>Fall</i>	4.8	
	Roque ^b	1.6	0.347 ^b
Guajara	Granadilla ^a	10.0	0.600 ^e
	<i>Flow</i>	5.0	
	<i>Fall</i>	5.0	
	Abades ^c	1.7	0.59 ^c
	Arico ^c	2.0	0.668 ^{ef}
	Honduras	0.20	
	Aguerche	0.08	
	Mena	0.84	
	Zarza	1.51	
	Icor	0.41	
	El Rincon	0.05	
	Eras	4.32	0.738 ^d
	<i>Fall</i>	4.32	
	<i>Flow</i>	-	
	Vigas	0.097	
	Tosca ^d	1.06	0.88 ^d
Ucanca	Adeje ^d	0.3	1.57 ^d
	<i>Fall</i>	0.3	
	<i>Flow</i>	-	
	Fanabe ^d	0.095	1.58 ^d
	<i>Fall</i>	0.095	
	<i>Flow</i>	-	

4.1.6 Dispersal

Excluding the Eras Formation, deposits in this study outcrop between Icor and La Medida, bounded by two geographical constraints, with each dispersal axis trending easterly. The Guimar Valley in the northeast limits exposure of deposits older than ~540ka, while the southwest area from Poris de Abona to Villa de Arico is dominated by the ~273ka Poris, ~600ka Granadilla, and ~660ka Arico Formations, with older deposits less prevalent. These boundaries have complicated volume estimations and hindered confident correlations with pumice fall deposits from Davila-Harris et al. (2023) in the El Rio region. The Mena and Zarza formations, exposed at their thickest near the Guimar Valley, including five UPFDs in La Medida, suggest potential Guajara age eruptions in the Guimar Valley, warranting further exploration. Several pumice deposits dated between 0.68Ma and 1.31Ma have been identified in drill cores 953A and 954A, located 156km and 114km offshore respectively, along the dispersal axis of many formations in this study. Correlating these offshore units with onshore deposits could significantly improve our understanding of eruption dispersal patterns and improve volume estimates.

4.2 Eruption Dynamics

Each of the deposits in this study appear to have the dispersal of Plinian pumice fall deposits, with thinning trends similar to that of known Plinian eruptions (figure 4.3). Many of the pumice fall deposits described in this study are similar, with the La Linde, Aguerche, Jurado, El Escobonal, Arco, Carretas, Vigas, and Gambuesa Formations all representing well-sorted, massive, pumice-rich (<90%) fall deposits. It is possible this is a trend in eruption styles, with frequent, stable, short-lived eruption columns travelling downwind with limited vent clearance and wind variability before abruptly terminating. However, it is possible these deposits show limited variability due to erosion given their ages (>700kya) or may be a more distal locality of a larger, more complex eruption. The absence of associated ignimbrites suggests stable eruptions that waned before termination. However, pyroclastic density currents may have occurred but remained limited to upper flanks or are no longer exposed. The Honduras, Mena, Zarza, Icor, El Rincon, Eras, and Sombrera Formations exhibit unique characteristics in deposit architecture, grain size, and componentry.

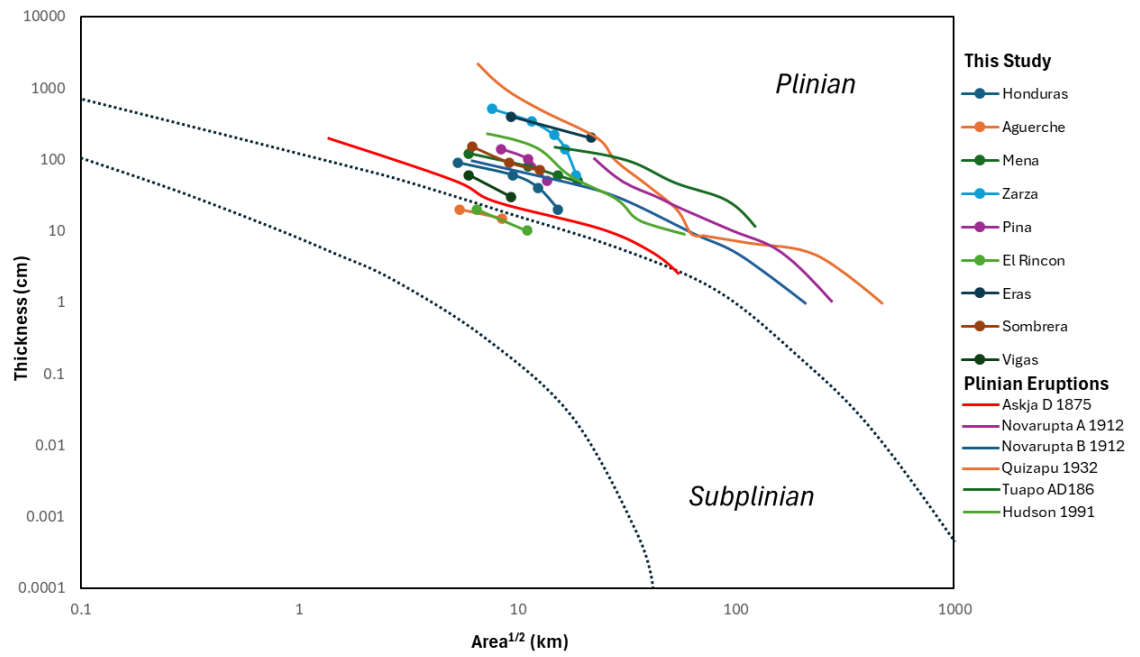


Figure 4.3 – Thickness vs $\text{Area}^{1/2}$ plot comparing eruptions in this study with known Plinian eruptions: Askja D 1875 (Sparks et al., 1981); Novarupta 1912 (Fierstein and Hildreth, 1992); Quizapu 1932 (Hildreth and Drake, 1992); Tuapo AD186 (Walker, 1980); Hudson 1991 (Scasso et al., 1994). Data extrapolated from similar pots produced by Alfano et al., (2011) and Miyabuchi et al., (2013).

4.2.1 Grain Size

The grain size plot shows that each eruption in this study are mostly well-sorted ($\sigma\phi$ 0.86 to 1.68) and fit within the Plinian fall field of Walker (1971; 1983) for a ‘dry’ magmatic eruption (figure 4.4). Comparison of grain size is challenging as the vent location for each eruption is uncertain and grain size varies with distance to the vent (Sparks et al., 1992). Grain size as a function of weight percentage has shown bimodality (Mena Member B, Icor Member B/C/E, Sombrera Member B/C/D). For Icor Member C/E the apparent bimodality occurs between -2ϕ and 1.5ϕ , where the transition between field and lab sieving occurs and may be due to material being crushed during transportation. The bimodality in the remaining deposits indicate the finer nature (-0.56ϕ to -1.99ϕ) and poorer sorting ($\sigma\phi$, 1.33 to 1.7).

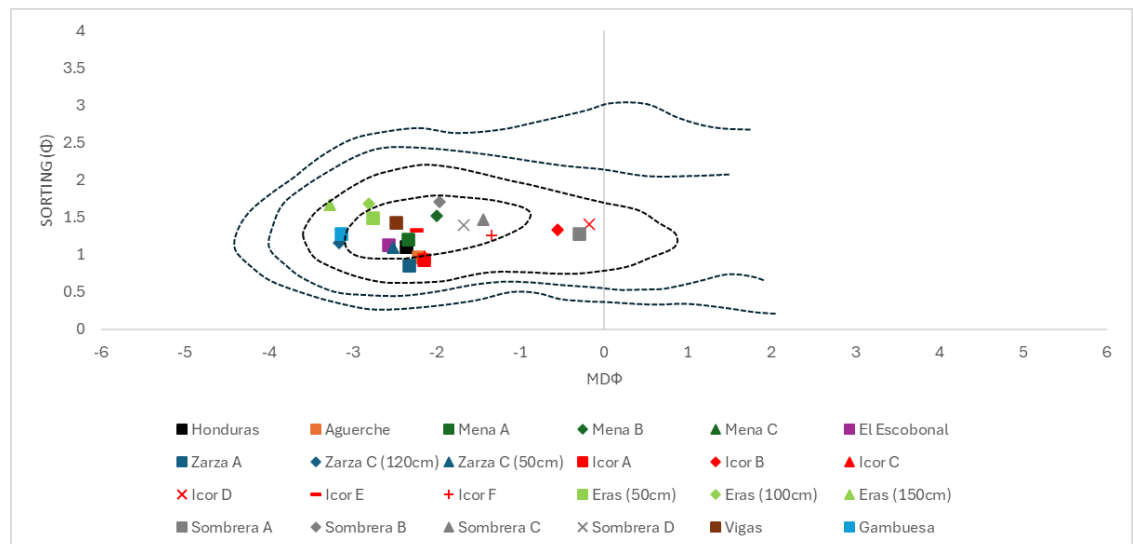


Figure 4.4 – Median diameter ($Md\phi$) versus sorting coefficient ($\sigma\phi$) for single locality grain-size data for each eruption. The dashed lines represent 8%, 4%, 2%, 1% contours of Plinian fall deposits from Walker (1971; 1983).

4.2.2 Grading

Grading patterns in pumice fall deposits provide valuable insights into eruption dynamics and intensity variations. These patterns manifest as normal grading (decreasing grain size) or inverse grading (increasing grain size), each reflecting distinct eruptive processes.

Normal Grading

Normal grading, seen in the Honduras and El Rincon Formations, indicates a gradual decline in eruption intensity and plume height (Jurado-Chichay and Walker, 2001; Pyle, 2016). This pattern is most evident at maximum thickness localities, possibly due to eruption column narrowing. Consequently, normal grading is primarily visible along the dispersal axis, with grain size decreases from waning less apparent at peripheral localities.

Inverse Grading

Inverse grading represents periods of increased eruption intensity, column height, and vent widening, where grain size increases either gradually or abruptly (Duffield et al., 1979; Jurado-Chichay and Walker, 2001; Houghton and Carey, 2015). The Zarza and Icor Formations uniquely exhibit inverse grading before termination, suggesting a gradual increase in plume height followed by abrupt termination. This structure often precedes ignimbrite formation, potentially indicating increased discharge rates and eruption intensities reaching unstable levels (Sparks et al., 1973). Similar patterns are observed in the Fasnía and Aldea Blanca Formations on Tenerife (Edgar et al., 2007), supporting the possibility that the Zarza and Icor Formations may have produced as-yet-undiscovered ignimbrites from column collapse.

Complex Grading Patterns

The Mena, Zarza, Icor, and Sombrera Formations display complex grain size and grading patterns, reflecting frequent fluctuations in eruption intensity and column height. The cause of decreasing column height may be due to clogging of the vent, where the subsequent layer includes higher lithic clast proportions and abrupt changes in grain size as the eruption restarts, such examples include Icor Member B and Sombrera Member C. Sharp boundaries in grain size can be seen in Mena Member B, Mena Member C, Zarza Member B, the Icor Member B/C boundary and Icor Member E/F boundary. These sharp boundaries represent abrupt changes in the eruption intensity, either to a complete shutdown or an abrupt waxing pulse.

External Influences

Wind conditions can impact grain size distribution, as shown by Zarza Member C. This member shows a brief decrease in grain size in the east, coinciding with an increase in the west, likely due to a brief shift in wind direction and change in the dispersal axis.

Mena Member B presents a complex eruptive unit with frequent grain size stratifications, interpreted as fluctuations in eruptive intensity. The observed bimodality and interbedding of fine and coarse pumice might suggest water-related processes. However, there is an absence of accretionary lapilli or fine-grained ash ($>3\phi$).

4.2.3 Lithic Clasts

Plinian fall deposits typically contain varying proportions of lithic clasts, originating from magma chamber and conduit erosion, vent opening, or vent wall collapses. In this study, pumice fall deposits exhibit lithic clast contents ranging from 0-10wt%, with some formations containing up to 50wt%. Several formations (Honduras, Aguerche, El Escobonal, Eras, Vigas, and Gambuesa) contain $>90\text{wt}\%$ pumice with minor, uniformly distributed lithic clasts. This suggests relatively easy vent opening at eruption onset and limited conduit erosion throughout the eruption. The Eras Formation shows a distinct upward increase in lithic clasts (1.3wt% at 50cm from base to 4wt% at 100cm and 150cm from base). This trend likely indicates vent widening as the eruption progresses, with a distinct horizon at 150cm potentially indicating vent wall collapse or a clearing episode.

Vent Opening and Widening

Different formations exhibit various vent opening characteristics. Mena Member A has a thin fine-grained lithic layer at the base represents initial vent opening. Zarza Member A and Sombrera Member A are examples of significant vent opening and widening during initial eruption phases. Icor Members B/D, and Sombrera Member B show ongoing vent wall erosion leading to widening during eruption and vent clearing episodes.

Lithic Clast Types

The studied deposits contain three notable types of lithic clasts: hydrothermally altered lithics, accessory lithic clasts, and juvenile lithic clasts. Hydrothermally altered lithics, characterised by their orange colour and tendency to stain surrounding pumice clasts, are

unique to the Mena Formation. This suggests that the Mena eruption may have a different vent location than other eruptions in this study, potentially indicating the presence of a hydrothermal reservoir. Juvenile (cognate) lithic clasts, primarily consisting of glassy obsidian, are present in almost all deposits. However, a significant proportion (11wt%) is observed only in Icor Member B, a fine-grained pumice lapilli member. The obsidian clasts may be from sintering of ash fragments within the conduit during significant in-fill, further evidenced from waning and waxing episodes seen in the Icor Formation and fine-grained nature of Icor Member B (Gardner et al., 2017; Wadsworth et al., 2022). It is uncertain why this process is only seen in the Icor Formation, particularly given that ash sintering can happen over various time and magmatic conditions (Gardner et al., 2017). Accessory lithic clasts are typically basaltic or phonolitic lava, however the origin is unknown. Further analysis into the composition of lithic clasts could improve understanding on the depth of fragmentation, source of lithics, and depth of the magma chamber.

4.2.4 Magma Heterogeneity

Scoria

Scoria can occur as either accessory lithic clasts or juvenile material, potentially indicating mafic content in eruptions. For most deposits in this study scoria is a minor component, with two exceptions: Sombrera Member C and D, with >1wt% scoria, coinciding with increased mafic mingled pumice clasts, potentially suggesting juvenile origin.

Magma Mixing

Mafic mingled pumice clasts are observed in the Honduras, Eras, and Sombrera Formations, predominantly towards the top of deposits. This could be sourced from two possible scenarios: the interaction and mixing of compositionally distinct magma, or the evolution of a single magma in a closed system. Both scenarios could result in more evolved magma erupting first, followed by less evolved magma as the eruption continues. The exact mechanisms contributing towards mingled pumices remain uncertain. To fully understand these processes, further chemical and petrological studies

could reveal: the origin and composition of scoria clasts, the extent and nature of magma mixing, and the evolution of magma composition during eruptions.

4.3 Volcanic Hazards

Although the last major Plinian eruption occurred on Tenerife ~160,000 years ago, it does not indicate the end of large-scale eruptions, particularly with two previous hiatuses of activity between each eruption cluster (González-García et al., 2022; Dávila-Harris et al., 2023). This study provides insights into the smaller-scale Plinian eruptions that have occurred between major caldera-forming eruptions, significantly increasing the number of known explosive eruptions on Tenerife. It is likely that similar eruptions discussed here have occurred within the Ucanca and the Diego Hernandez Eruption Clusters and have yet to be reported, and therefore the amount of Plinian eruptions that have occurred in the last 1.5 Ma has been underestimated.

4.4 Limitations

Correlation Difficulties

An issue that arises in any field investigation on Tenerife is the difficulty correlating pyroclastic deposits across disconnected outcrops, particularly when units are not bound by easily recognisable formations and marker features. Many of the formations in this study do not have uniquely identifiable characteristics, therefore identification outside the bounds of a common stratigraphic sequence (same formation above and below) is challenging. Furthermore, many pyroclastic deposits have highly eroded surface, making for ambiguous identification and small-scale textural features unidentifiable. This underscores the need for careful documentation of pyroclastic deposits, and the usefulness of a multifaceted approach, combining stratigraphic, geochemical, and petrological data to improve correlation of pyroclastic deposits.

4.5 Future Studies

This study has provided initial stratigraphic characteristics, lithofacies descriptions, and emplacement processes for 12 previously unstudied eruptive units, with renewed analysis of the Zarza, Mena, and Eras Formations. However, several areas for future research have been identified.

Chemical and Petrological Analysis

Further work would attempt to provide whole-rock and glass chemistry for each eruptive unit to support correlation to unknown units and information regarding the overall magmatic system generating phonolitic Plinian eruptions on Tenerife.

Expanded Field Investigation

Although a detailed field investigation was carried out, covering a significant accessible portion of the Bandas Del Sur, there is still the possibility of further exposures yet to be found. Focus should be put on the Arico region to possibly identify exposures correlating the NE and SE stratigraphy's. Emphasis can be put onto the caldera wall, to allow correlation to proximal deposits, and offshore cores, to correlate distal sites. Edgar et al., (2003) referenced Guajara age pyroclastic deposits in the La Orotava, Icod, and Santa Cruz regions that could yield important findings

Potential for Future Correlations

Pyroclastic deposits in this study may correlate with those in the El Rio and Abona regions, particularly as the Honduras and Sombrera formations show potential thickening trends to the southwest. To aid SE to NE correlations, the following areas should be explored:

1. Barranco Tamadaya Cuerna
2. Barranco Lere O de los Caballos
3. Barranco de Piedra Bermeja
4. La Cisnera region (Barranco Guasigre, Barranco de Magdalena, Barranco Luchon)

These localities, between Fasnía and El Río, are dominated by the 0.6 Ma Granadilla Formation at the surface. Deeper barranco exposures may reveal older pyroclastic

deposits. Identifying the Rio Formation alongside deposits from this study will be crucial in unravelling a more comprehensive Guajara pyroclastic succession.

Systematic Dating

Without correlation of eruptive units across the Bandas Del Sur, it puts emphasis on obtaining systematic Ar/Ar dating from the base of the Guajara and up. This would allow a more confident assessment for the stratigraphy of the Guajara Eruption Cluster.

Comprehensive Study of the Las Cañadas Caldera

Future work should attempt to identify similar smaller-scale Plinian pumice fall deposits across the Ucanca and Diego Hernandez Eruption Clusters, as currently work has focused on the major, ignimbrite forming eruptions. This could improve understanding of the eruptions that occur between major caldera forming eruptions, whether there is a buildup in eruption scale, or providing further information towards to question of eruption cyclicity.

Chapter 5: Conclusion

- a) A new pyroclastic stratigraphy of the Guajara Eruption Cluster can be made containing 14 newly defined pyroclastic formations (La Linde, Honduras, Aguerche, Jurado, Mena, El Escobonal, Zarza, Icor, Arco, Carretas, El Rincon, Sombrera, Vigas, Gambuesa Formations) and an updated Eras Formation.
- b) Each formation has been described and the eruptive and transportive processes interpreted in relation to the pyroclastic lithofacies and grain size analysis of the deposit. Each of the deposits fit within the Plinian pyroclastic fall deposit zone in $Md\phi$ vs $\sigma\phi$ graphs, with many of the deposits consisting of largely pumice lapilli and minor lithic clasts.
- c) Volumes were calculated for 7 formations, with the Eras Formation having the largest volume, similar to the Aldea Blanca pumice fall. The Zarza Formation has one of the largest volumes of any pumice fall without an associated ignimbrite on Tenerife. Average volumes in the Guajara Eruption Cluster are smaller than that of the Diego Hernandez Formation. The dispersal and thickness of eruptions in this study similarly compare to widely studied Plinian eruptions elsewhere.
- d) Correlations between pumice fall deposits in the Fasnía region and El Río region could not be made except for the Eras and Moradas Formations. The Zarza and Mena Formations from Middleton (2006) have been redefined.
- e) Eruption frequencies for the Guajara Eruption Cluster have been redefined to total one Plinian eruption every 11,666 years, with further eruptions yet to be defined likely increasing the eruption frequency further.
- f) Future studies should attempt to provide Ar/Ar dating, as well as geochemical and petrological investigations on these deposits. Studies should attempt to describe and identify the unknown deposits mentioned here and search for further fall deposits across the Bandas Del Sur.

Chapter 6: Bibliography

Ablay, G.J., Ernst, G.G.J., Marti, J., Sparks, R.S.J., 1995. The - 2 ka subplinian eruption of Montafia Blanca, Tenerife. *Bulletin of Volcanology*.

Ablay, G.J., Kearey, P., 2000. Gravity constraints on the structure and volcanic evolution of Tenerife, Canary Islands. *Journal of Geophysical Research: Solid Earth* 105, 5783–5796. <https://doi.org/10.1029/1999JB900404>

Ablay, G.J., Martí, J., 2000. Stratigraphy, structure, and volcanic evolution of the Pico Teide–Pico Viejo formation, Tenerife, Canary Islands. *Journal of Volcanology and Geothermal Research* 103, 175–208. [https://doi.org/10.1016/S0377-0273\(00\)00224-9](https://doi.org/10.1016/S0377-0273(00)00224-9)

Alfano, F., Bonadonna, C., Volentik, A.C.M., Connor, C.B., Watt, S.F.L., Pyle, D.M., Connor, L.J., 2011. Tephra stratigraphy and eruptive volume of the May, 2008, Chaitén eruption, Chile. *Bulletin of Volcanology* 73, 613–630. <https://doi.org/10.1007/s00445-010-0428-x>

Ancochea, E., Fuster, J., Ibarrola, E., Cendrero, A., Coello, J., Hernan, F., Cantagrel, J.M., Jamond, C., 1990. Volcanic evolution of the island of Tenerife (Canary Islands) in the light of new K-Ar data. *Journal of Volcanology and Geothermal Research* 44, 231–249. [https://doi.org/10.1016/0377-0273\(90\)90019-C](https://doi.org/10.1016/0377-0273(90)90019-C)

Ancochea, E., Huertas, M.J., Cantagrel, J.M., Coello, J., Arnaud, N., Ibarrola, E., 1999. Evolution of the Cañadas edifice and its implications for the origin of the Cañadas Caldera (Tenerife, Canary Islands). *Journal of Volcanology and Geothermal Research* 88, 177–199.

Aubry, T.J., Engwell, S.L., Bonadonna, C., Mastin, L.G., Carazzo, G., Van Eaton, A.R., Jessop, D.E., Grainger, R.G., Scollo, S., Taylor, I.A., Jellinek, A.M., Schmidt, A., Biass, S., Gouhier, M., 2023. New Insights Into the Relationship Between Mass Eruption Rate and Volcanic Column Height Based On the IVESPA Data Set. *Geophysical Research Letters* 50, e2022GL102633. <https://doi.org/10.1029/2022GL102633>

Bechtel, B., 2016. The Climate of the Canary Islands by Annual Cycle Parameters. *Int. Arch. Photogramm. Remote Sens. Spatial Inf. Sci.* XLI-B8, 243–250. <https://doi.org/10.5194/isprsarchives-XLI-B8-243-2016>

Bernard, O., Li, W., Costa, F., Saunders, S., Itikarai, I., Sindang, M., Bouvet De Maisonneuve, C., 2022. Explosive-effusive-explosive: The role of magma ascent rates and paths in modulating caldera eruptions. *Geology* 50, 1013–1017. <https://doi.org/10.1130/G50023.1>

Biass, S., Bagheri, G., Aeberhard, W.H., Bonadonna, C., 2014. TError: towards a better quantification of the uncertainty propagated during the characterization of tephra deposits. *Statistics in Volcanology* 1, 1–27. <https://doi.org/10.5038/2163-338x.1.2>

Biass, S., Bagheri, G., Bonadonna, C., 2015. A Matlab implementation of the Carey and Sparks (1986) model to estimate plume height and wind speed from isopleth maps.

- Biass, S., Bonadonna, C., 2011. A quantitative uncertainty assessment of eruptive parameters derived from tephra deposits: the example of two large eruptions of Cotopaxi volcano, Ecuador. *Bull Volcanol* 73, 73–90. <https://doi.org/10.1007/s00445-010-0404-5>
- Biass, S., Bonadonna, C., Houghton, B.F., 2019. A step-by-step evaluation of empirical methods to quantify eruption source parameters from tephra-fall deposits. *J Appl. Volcanol.* 8, 1. <https://doi.org/10.1186/s13617-018-0081-1>
- Blake, S., 1981. Eruptions from zoned magma chambers. *JGS* 138, 281–287. <https://doi.org/10.1144/gsjgs.138.3.0281>
- Blott, S.J., Pye, K., 2001. GRADISTAT: a grain size distribution and statistics package for the analysis of unconsolidated sediments. *Earth Surf Processes Landf* 26, 1237–1248. <https://doi.org/10.1002/esp.261>
- Bogaard, P. van den, 1998. ⁴⁰Ar/³⁹Ar Ages of Pliocene-Pleistocene Fallout Tephra Layers and Volcaniclastic Deposits in the Sedimentary Aprons of Gran Canaria and Tenerife (Sites 953, 954, and 956). *Proceedings of the Ocean Drilling Program* 157. <https://doi.org/10.2973/odp.proc.sr.157.1998>
- Bonadonna, C., Biass, S., Costa, A., 2015a. Physical characterization of explosive volcanic eruptions based on tephra deposits: Propagation of uncertainties and sensitivity analysis. *Journal of Volcanology and Geothermal Research* 296, 80–100. <https://doi.org/10.1016/j.jvolgeores.2015.03.009>
- Bonadonna, C., Cioni, R., Pistolesi, M., Connor, C., Scollo, S., Pioli, L., Rosi, M., 2013. Determination of the largest clast sizes of tephra deposits for the characterization of explosive eruptions: a study of the IAVCEI commission on tephra hazard modelling. *Bull Volcanol* 75, 680. <https://doi.org/10.1007/s00445-012-0680-3>
- Bonadonna, C., Costa, A., 2013. Plume height, volume, and classification of explosive volcanic eruptions based on the Weibull function. *Bull Volcanol* 75, 742. <https://doi.org/10.1007/s00445-013-0742-1>
- Bonadonna, C., Costa, A., 2012. Estimating the volume of tephra deposits: A new simple strategy. *Geology* 40, 415–418. <https://doi.org/10.1130/G32769.1>
- Bonadonna, C., Costa, A., Folch, A., Koyaguchi, T., 2015b. Tephra Dispersal and Sedimentation, in: *The Encyclopedia of Volcanoes*. Elsevier, pp. 587–597. <https://doi.org/10.1016/B978-0-12-385938-9.00033-X>
- Bonadonna, C., Houghton, B.F., 2005. Total grain-size distribution and volume of tephra-fall deposits. *Bull Volcanol* 67, 441–456. <https://doi.org/10.1007/s00445-004-0386-2>
- Booth, B., 1973. The Granadilla pumice deposit of Southern Tenerife, Canary Islands. *Proceedings of the Geologists' Association* 84, 353-IN5. [https://doi.org/10.1016/S0016-7878\(73\)80039-2](https://doi.org/10.1016/S0016-7878(73)80039-2)
- Branney, M.J., Kokelaar, B.P., 2002. *Pyroclastic Density Currents and Sedimentation of Ignimbrites*, Geological Society Memoir. The Geological Society, Bath, UK.

- Brown, R., Barry, T., Branney, M., Pringle, M., Bryan, S., 2003. The Quaternary pyroclastic succession of southeast Tenerife, Canary Islands: Explosive eruptions, related caldera subsidence, and sector collapse. *Geological Magazine* 140, 265.
<https://doi.org/10.1017/S0016756802007252>
- Brown, R.J., Branney, M.J., 2013. Internal flow variations and diachronous sedimentation within extensive, sustained, density-stratified pyroclastic density currents flowing down gentle slopes, as revealed by the internal architectures of ignimbrites on Tenerife. *Bull Volcanol* 75, 727. <https://doi.org/10.1007/s00445-013-0727-0>
- Brown, R.J., Branney, M.J., 2004. Event-stratigraphy of a caldera-forming ignimbrite eruption on Tenerife: the 273 ka Poris Formation. *Bull Volcanol* 66, 392–416.
<https://doi.org/10.1007/s00445-003-0321-y>
- Bryan, S.E., Cas, R.A.F., Martí, J., 2000. The 0.57 Ma plinian eruption of the Granadilla Member, Tenerife (Canary Islands): an example of complexity in eruption dynamics and evolution. *Journal of Volcanology and Geothermal Research* 103, 209–238.
[https://doi.org/10.1016/S0377-0273\(00\)00225-0](https://doi.org/10.1016/S0377-0273(00)00225-0)
- Bryan, S.E., Martí, J., Cas, R.A.F., 1998. Stratigraphy of the Bandas del Sur Formation: an extracaldera record of Quaternary phonolitic explosive eruptions from the Las Cañadas edifice, Tenerife (Canary Islands). *Geol. Mag.* 135, 605–636.
<https://doi.org/10.1017/S0016756897001258>
- Bryan, S.E., Martí, J., Leosson, M., 2002. Petrology and Geochemistry of the Bandas del Sur Formation, Las Cañadas Edifice, Tenerife (Canary Islands). *Journal of Petrology* 43, 1815–1856. <https://doi.org/10.1093/petrology/43.10.1815>
- Burden, R.E., Phillips, J.C., Hincks, T.K., 2011. Estimating volcanic plume heights from depositional clast size: ESTIMATING VOLCANIC PLUME HEIGHTS. *J. Geophys. Res.* 116, n/a-n/a. <https://doi.org/10.1029/2011JB008548>
- Bursik, M., 1993. Subplinian eruption mechanisms inferred from volatile and clast dispersal data. *Journal of Volcanology and Geothermal Research* 57, 57–70.
[https://doi.org/10.1016/0377-0273\(93\)90031-L](https://doi.org/10.1016/0377-0273(93)90031-L)
- Bursik, M., Sparks, R.S.J., Gilbert, J.S., Carey, S., 1992. Sedimentation of tephra by volcanic plumes : I. Theory and its comparison with a study of the Fogo A plinian deposit, Sao Miguel (Azores). *Bulletin of Volcanology* 54, 329–344.
<https://doi.org/10.1007/bf00301486>
- Carey, S., Bursik, M., 2015. Volcanic Plumes, in: *The Encyclopedia of Volcanoes*. Elsevier, pp. 571–585. <https://doi.org/10.1016/B978-0-12-385938-9.00032-8>
- Carey, S., Sigurdsson, H., 1989. The intensity of plinian eruptions. *Bull Volcanol* 51, 28–40. <https://doi.org/10.1007/BF01086759>

- Carey, S., Sparks, R.S.J., 1986. Quantitative models of the fallout and dispersal of tephra from volcanic eruption columns. *Bull Volcanol* 48, 109–125. <https://doi.org/10.1007/BF01046546>
- Carracedo, J.C., 1999. Growth, structure, instability and collapse of Canarian volcanoes and comparisons with Hawaiian volcanoes. *Journal of Volcanology and Geothermal Research* 94, 1–19. [https://doi.org/10.1016/S0377-0273\(99\)00095-5](https://doi.org/10.1016/S0377-0273(99)00095-5)
- Carracedo, J.C., Badiola, E.R., Guillou, H., Paterne, M., Scaillet, S., Torrado, F.J.P., Paris, R., Fra-Paleo, U., Hansen, A., 2007. Eruptive and structural history of Teide Volcano and rift zones of Tenerife, Canary Islands. *Geological Society of America Bulletin* 119, 1027–1051. <https://doi.org/10.1130/B26087.1>
- Carracedo, J.C., Guillou, H., Nomade, S., Rodriguez-Badiola, E., Perez-Torrado, F.J., Rodriguez-Gonzalez, A., Paris, R., Troll, V.R., Wiesmaier, S., Delcamp, A., Fernandez-Turiel, J.L., 2011. Evolution of ocean-island rifts: The northeast rift zone of Tenerife, Canary Islands. *Geological Society of America Bulletin* 123, 562–584. <https://doi.org/10.1130/B30119.1>
- Cas, R., Giordano, G., Wright, J.V., 2024. *Volcanology: Processes, Deposits, Geology and Resources*. Springer Textbooks in Earth Sciences, Geography and Environment.
- Cas, R.A.F., Wolff, J.A., Marti, J., Olin, P.H., Edgar, C.J., Pittari, A., Simmons, J.M., 2022. Tenerife, a complex end member of basaltic oceanic island volcanoes, with explosive polygenetic phonolitic calderas, and phonolitic-basaltic stratovolcanoes.
- Cas, R.A.F., Wright, J.V., 1987. *Volcanic Successions Modern and Ancient*. Springer Netherlands, Dordrecht. <https://doi.org/10.1007/978-94-009-3167-1>
- Cashman, K.V., Scheu, B., 2015. Magmatic Fragmentation, in: *The Encyclopedia of Volcanoes*. Elsevier, pp. 459–471. <https://doi.org/10.1016/B978-0-12-385938-9.00025-0>
- Chamberlain, K.J., Barclay, J., Preece, K., Brown, R.J., Davidson, J.P., 2016. Origin and evolution of silicic magmas at ocean islands: Perspectives from a zoned fall deposit on Ascension Island, South Atlantic. *Journal of Volcanology and Geothermal Research* 327, 349–360. <https://doi.org/10.1016/j.jvolgeores.2016.08.014>
- Cioni, R., Bertagnini, A., Andronico, D., Cole, P.D., Mundula, F., 2011. The 512 AD eruption of Vesuvius: complex dynamics of a small scale subplinian event. *Bulletin of Volcanology* 73, 789–810. <https://doi.org/10.1007/s00445-011-0454-3>
- Cioni, R., Pistolesi, M., Rosi, M., 2015. Plinian and Subplinian Eruptions, in: *The Encyclopedia of Volcanoes*. Elsevier, pp. 519–535. <https://doi.org/10.1016/B978-0-12-385938-9.00029-8>
- Cioni, R., Sulpizio, R., Garruccio, N., 2003. Variability of the eruption dynamics during a Subplinian event: the Greenish Pumice eruption of Somma–Vesuvius (Italy). *Journal of Volcanology and Geothermal Research* 124, 89–114. [https://doi.org/10.1016/S0377-0273\(03\)00070-2](https://doi.org/10.1016/S0377-0273(03)00070-2)

- Civetta, L., Galati, R., Santacroce, R., 1991. Magma mixing and convective compositional layering within the Vesuvius magma chamber. *Bulletin of Volcanology* 53, 287–300. <https://doi.org/10.1007/BF00414525>
- Daggitt, M.L., Mather, T.A., Pyle, D.M., Page, S., 2014. AshCalc—a new tool for the comparison of the exponential, power-law and Weibull models of tephra deposition. *Journal of Applied Volcanology* 3, 7. <https://doi.org/10.1186/2191-5040-3-7>
- Dávila-Harris, P., 2009. Explosive ocean-island volcanism: the 1.8–0.7 Ma explosive eruption history of Cañadas volcano recorded by the pyroclastic successions around Adeje and Abona, southern Tenerife, Canary Islands (Ph.D. Thesis). University of Leicester.
- Dávila-Harris, P., Branney, M.J., Storey, M., Taylor, R.N., Sliwinski, J.T., 2023. The upper Pleistocene (1.8–0.7 Ma) explosive eruptive history of Las Cañadas, ocean-island volcano, Tenerife. *Journal of Volcanology and Geothermal Research* 436, 107777. <https://doi.org/10.1016/j.jvolgeores.2023.107777>
- Dávila-Harris, P., Branney, M.J., Storey, M., 2011. Large eruption-triggered ocean-island landslide at Tenerife: Onshore record and long-term effects on hazardous pyroclastic dispersal. *Geology* 39, 951–954. <https://doi.org/10.1130/G31994.1>
- Dávila-Harris, P., Ellis, B.S., Branney, M.J., Carrasco-Núñez, G., 2013. Lithostratigraphic analysis and geochemistry of a vitric spatter-bearing ignimbrite: the Quaternary Adeje Formation, Cañadas volcano, Tenerife. *Bulletin of Volcanology* 75, 722. <https://doi.org/10.1007/s00445-013-0722-5>
- De Vivo, B., Lima, A., Webster, J.D., 2005. Volatiles in Magmatic-Volcanic Systems. *Elements* 1, 19–24. <https://doi.org/10.2113/gselements.1.1.19>
- Dóniz-Páez, J., Romero-Ruiz, C., Sánchez, N., 2012. Quantitative Size Classification of Scoria Cones: The Case of Tenerife (Canary Islands, Spain). *Physical Geography* 33, 514–535. <https://doi.org/10.2747/0272-3646.33.6.514>
- Duffield, W.A., Bacon, C.R., Roquemore, G.R., 1979. Origin of reverse-graded bedding in air-fall pumice, Coso Range, California. *Journal of Volcanology and Geothermal Research* 5, 35–48. [https://doi.org/10.1016/0377-0273\(79\)90031-3](https://doi.org/10.1016/0377-0273(79)90031-3)
- Edgar, C.J., 2003. The Stratigraphy & Eruption Dynamics of a Quaternary Phonolitic Plinian Eruption Sequence (Ph.D. Thesis). Monash University, Australia.
- Edgar, C.J., Cas, R.A.F., Olin, P.H., Wolff, J.A., Martí, J., Simmons, J.M., 2017. Causes of complexity in a fallout dominated plinian eruption sequence: 312 ka Fasnía Member, Diego Hernández Formation, Tenerife, Spain. *Journal of Volcanology and Geothermal Research* 345, 21–45. <https://doi.org/10.1016/j.jvolgeores.2017.07.008>
- Edgar, C.J., Wolff, J.A., Olin, P.H., Nichols, H.J., Pittari, A., Cas, R.A.F., Reiners, P.W., Spell, T.L., Martí, J., 2007. The late Quaternary Diego Hernández Formation, Tenerife: Volcanology of a complex cycle of voluminous explosive phonolitic eruptions. *Journal of*

Volcanology and Geothermal Research 160, 59–85.

<https://doi.org/10.1016/j.jvolgeores.2006.06.001>

Engwell, S., Sparks, R., Aspinall, W., 2013. Quantifying uncertainties in the measurement of tephra fall thickness. *J Appl. Volcanol.* 2, 5.

<https://doi.org/10.1186/2191-5040-2-5>

Engwell, S.L., Aspinall, W.P., Sparks, R.S.J., 2015. An objective method for the production of isopach maps and implications for the estimation of tephra deposit volumes and their uncertainties. *Bulletin of Volcanology* 77, 61.

<https://doi.org/10.1007/s00445-015-0942-y>

Eychenne, J., Engwell, S.L., 2022. The grainsize of volcanic fall deposits: Spatial trends and physical controls. *GSA Bulletin*. <https://doi.org/10.1130/B36275.1>

Fierstein, J., Hildreth, W., 1992. The plinian eruptions of 1912 at Novarupta, Katmai National Park, Alaska. *Bulletin of Volcanology* 54, 646–684.

<https://doi.org/10.1007/BF00430778>

Fierstein, J., Nathenson, M., 1992. Another look at the calculation of fallout tephra volumes. *Bulletin of Volcanology* 54, 156–167. <https://doi.org/10.1007/BF00278005>

García, O., Bonadonna, C., Martí, J., Pioli, L., 2012. The 5,660 yBP Boquerón explosive eruption, Teide–Pico Viejo complex, Tenerife. *Bulletin of Volcanology* 74, 2037–2050.

<https://doi.org/10.1007/s00445-012-0646-5>

García, O., Guzmán, S., Martí, J., 2014. Stratigraphic correlation of Holocene phonolitic explosive episodes of the Teide–Pico Viejo Volcanic Complex, Tenerife. *JGS* 171, 375–387. <https://doi.org/10.1144/jgs2013-086>

García, O., Martí, J., Aguirre, G., Geyer, A., Iribarren, I., 2011. Pyroclastic density currents from Teide–Pico Viejo (Tenerife, Canary Islands): implications for hazard assessment. *Terra Nova* 23, 220–224. <https://doi.org/10.1111/j.1365-3121.2011.01002.x>

Gardner, J.E., Llewellyn, E.W., Watkins, J.M., Befus, K.S., 2017. Formation of obsidian pyroclasts by sintering of ash particles in the volcanic conduit. *Earth and Planetary Science Letters* 459, 252–263. <https://doi.org/10.1016/j.epsl.2016.11.037>

Gardner, J.E., Thomas, R.M.E., Jaupart, C., Tait, S., 1996. Fragmentation of magma during Plinian volcanic eruptions. *Bulletin of Volcanology* 58, 144–162.

<https://doi.org/10.1007/s004450050132>

Geyer, A., Martí, J., 2010. The distribution of basaltic volcanism on Tenerife, Canary Islands: Implications on the origin and dynamics of the rift systems. *Tectonophysics* 483, 310–326. <https://doi.org/10.1016/j.tecto.2009.11.002>

González-García, D., Petrelli, M., Perugini, D., Giordano, D., Vasseur, J., Paredes-Mariño, J., Martí, J., Dingwell, D.B., 2022. Pre-Eruptive Conditions and Dynamics Recorded in Banded Pumices from the El Abrigo Caldera-Forming Eruption (Tenerife,

Canary Islands). *Journal of Petrology* 63, 1-24.

<https://doi.org/10.1093/petrology/egac009>

Gottsmann, J., Camacho, A.G., Martí, J., Wooller, L., Fernández, J., García, A., Rymer, H., 2008. Shallow structure beneath the Central Volcanic Complex of Tenerife from new gravity data: Implications for its evolution and recent reactivation. *Physics of the Earth and Planetary Interiors* 168, 212–230. <https://doi.org/10.1016/j.pepi.2008.06.020>

Guillou, H., Carracedo, J.C., Paris, R., Pérez Torrado, F.J., 2004. Implications for the early shield-stage evolution of Tenerife from K/Ar ages and magnetic stratigraphy. *Earth and Planetary Science Letters* 222, 599–614. <https://doi.org/10.1016/j.epsl.2004.03.012>

Hildreth, W., Drake, R., 1992. Volcan Quizapu, Chilean Andes. *Bulletin of Volcanology* 54, 93-125.

Horn, E.L., Taylor, R.N., Gernon, T.M., Stock, M.J., Farley, E.M.R., 2022. Composition and Petrology of a Mush-Bearing Magma Reservoir beneath Tenerife. *Journal of Petrology* 63, 1-26. <https://doi.org/10.1093/petrology/egac095>

Houghton, B., Carey, R.J., 2015. Pyroclastic Fall Deposits, in: *The Encyclopedia of Volcanoes*. Elsevier, pp. 599–616. <https://doi.org/10.1016/B978-0-12-385938-9.00034-1>

Huertas, M.J., Arnaud, N.O., Ancochea, E., Cantagrel, J.M., Fu, J.M., 2002. ⁴⁰Ar/³⁹Ar stratigraphy of pyroclastic units from the Cañadas Volcanic Edifice (Tenerife, Canary Islands) and their bearing on the structural evolution. *Journal of Volcanology and Geothermal Research* 115, 351-365.

Jurado-Chichay, Z., Walker, G.P.L., 2001. Variability of plinian fall deposits: examples from Okataina Volcanic Centre, New Zealand. *Journal of Volcanology and Geothermal Research* 111, 239–263. [https://doi.org/10.1016/S0377-0273\(01\)00229-3](https://doi.org/10.1016/S0377-0273(01)00229-3)

Jurado-Chichay, Z., Walker, G.P.L., 2000. Stratigraphy and dispersal of the Mangaone Subgroup pyroclastic deposits, Okataina Volcanic Centre, New Zealand. *Journal of Volcanology and Geothermal Research* 104, 319–380. [https://doi.org/10.1016/S0377-0273\(00\)00210-9](https://doi.org/10.1016/S0377-0273(00)00210-9)

Keating, G.N., Valentine, G.A., 1998. Proximal stratigraphy and syn-eruptive faulting in rhyolitic Grants Ridge Tuff, New Mexico, USA. *Journal of Volcanology and Geothermal Research* 81, 37–49. [https://doi.org/10.1016/S0377-0273\(97\)00075-9](https://doi.org/10.1016/S0377-0273(97)00075-9)

Klawonn, M., Houghton, B.F., Swanson, D.A., Fagents, S.A., Wessel, P., Wolfe, C.J., 2014a. From field data to volumes: constraining uncertainties in pyroclastic eruption parameters. *Bulletin of Volcanology* 76, 839. <https://doi.org/10.1007/s00445-014-0839-1>

Klawonn, M., Houghton, B.F., Swanson, D.A., Fagents, S.A., Wessel, P., Wolfe, C.J., 2014b. Constraining explosive volcanism: subjective choices during estimates of eruption magnitude. *Bulletin of Volcanology* 76, 793. <https://doi.org/10.1007/s00445-013-0793-3>

- Le Pennec, J.-L., Ruiz, G.A., Ramón, P., Palacios, E., Mothes, P., Yepes, H., 2012. Impact of tephra falls on Andean communities: The influences of eruption size and weather conditions during the 1999–2001 activity of Tungurahua volcano, Ecuador. *Journal of Volcanology and Geothermal Research* 217–218, 91–103. <https://doi.org/10.1016/j.jvolgeores.2011.06.011>
- Legros, F., 2000. Minimum volume of a tephra fallout deposit estimated from a single isopach. *Journal of Volcanology and Geothermal Research* 96, 25–32. [https://doi.org/10.1016/S0377-0273\(99\)00135-3](https://doi.org/10.1016/S0377-0273(99)00135-3)
- Martí, J., Hurlimann, M., Ablay, G.J., Gudmundsson, A., 1997. Vertical and lateral collapses on Tenerife (Canary Islands) and other volcanic ocean islands. *Geology* 25, 879–882. [https://doi.org/10.1130/0091-7613\(1997\)025<0879:VALCOT>2.3.CO;2](https://doi.org/10.1130/0091-7613(1997)025<0879:VALCOT>2.3.CO;2)
- Martí, J., Mitjavila, J., Araña, V., 1994. Stratigraphy, structure and geochronology of the Las Cañadas caldera (Tenerife, Canary Islands). *Geol. Mag.* 131, 715–727. <https://doi.org/10.1017/S0016756800012838>
- Melluso, L., Scarpati, C., Zanetti, A., Sparice, D., De' Gennaro, R., 2022. The petrogenesis of chemically zoned, phonolitic, Plinian and sub-Plinian eruptions of Somma-Vesuvius, Italy: Role of accessory phase removal, independently filled magma reservoirs with time, and transition from slightly to highly silica undersaturated magmatic series in an ultrapotassic stratovolcano. *Lithos* 430–431, 106854. <https://doi.org/10.1016/j.lithos.2022.106854>
- Middleton, J., Cas, R.A.F., Wolff, J.A., Marti, J., Olin, P.H., 2006. The Guajara Formation: the stratigraphy and eruption dynamics of a -280,000 year long explosive plinian eruption cycle associated with incremental caldera collapse from the Las Canadas caldera, Tenerife, Canary Islands (Ph.D. Thesis). Monash University.
- Miyabuchi, Y., Hanada, D., Niimi, H., Kobayashi, T., 2013. Stratigraphy, grain-size and component characteristics of the 2011 Shinmoedake eruption deposits, Kirishima Volcano, Japan. *Journal of Volcanology and Geothermal Research* 258, 31–46. <https://doi.org/10.1016/j.jvolgeores.2013.03.027>
- Nelson, B.K., Carracedo, J.C., Badiola, E.R., Hamilton, A., Guetschow, H., 2005. Spatial and Temporal Isotopic Gradients in the Western Canary Islands 2005, V41C-1471.
- Paulick, H., Franz, G., 1997. The color of pumice: case study on a trachytic fall deposit, Meidob volcanic field, Sudan. *Bulletin of Volcanology* 59, 171–185. <https://doi.org/10.1007/s004450050184>
- Pittari, A., Cas, R.A.F., Wolff, J.A., Nichols, H.J., Larson, P.B., Marti, J., 2008. The Use of Lithic Clast Distributions in Pyroclastic Deposits to Understand Pre- and Syn-Caldera Collapse Processes: A Case Study of the Abrigo Ignimbrite, Tenerife, Canary Islands. *Developments in Volcanology* 10, 98–143.
- Pyle, D.M., 2016. Field Observations of Tephra Fallout Deposits, in: *Volcanic Ash*. Elsevier, pp. 25–37. <https://doi.org/10.1016/B978-0-08-100405-0.00004-5>

- Pyle, D.M., 1998. Forecasting sizes and repose times of future extreme volcanic events. *Geol* 26, 367. [https://doi.org/10.1130/0091-7613\(1998\)026<0367:FSARTO>2.3.CO;2](https://doi.org/10.1130/0091-7613(1998)026<0367:FSARTO>2.3.CO;2)
- Pyle, D.M., 1995. Assessment of the minimum volume of tephra fall deposits. *Journal of Volcanology and Geothermal Research* 69, 379–382. [https://doi.org/10.1016/0377-0273\(95\)00038-0](https://doi.org/10.1016/0377-0273(95)00038-0)
- Pyle, D.M., 1989. The thickness, volume and grainsize of tephra fall deposits. *Bulletin of Volcanology* 51, 1–15. <https://doi.org/10.1007/BF01086757>
- Rodehorst, U., Schmincke, H.-U., Sumita, M., 1998. Geochemistry and Petrology of Pleistocene Ash Layers Erupted at Las Cañadas Edifice (Tenerife). *Proceedings of the Ocean Drilling Program* 157. <https://doi.org/10.2973/odp.proc.sr.157.1998>
- Ruzié, L., Moreira, M., 2010. Magma degassing process during Plinian eruptions. *Journal of Volcanology and Geothermal Research* 192, 142–150. <https://doi.org/10.1016/j.jvolgeores.2010.02.018>
- Scasso, R., Corbella, H., Tiberi, P., 1994. Sedimentology analysis of the tephra from the 12-15 August 1991 eruption of Hudson volcano. *Bulletin of Volcanology* 121–132.
- Seifert, R., Malfait, W.J., Petitgirard, S., Sanchez-Valle, C., 2013. Density of phonolitic magmas and time scales of crystal fractionation in magma chambers. *Earth and Planetary Science Letters* 381, 12–20. <https://doi.org/10.1016/j.epsl.2013.08.039>
- Smith, N.J., Kokelaar, B.P., 2013. Proximal record of the 273 ka Poris caldera-forming eruption, Las Cañadas, Tenerife. *Bulletin of Volcanology* 75, 768. <https://doi.org/10.1007/s00445-013-0768-4>
- Soriano, C., Galindo, I., Martí, J., Wolff, J., 2006. Conduit-vent structures and related proximal deposits in the Las Cañadas caldera, Tenerife, Canary Islands. *Bulletin of Volcanology* 69, 217–231. <https://doi.org/10.1007/s00445-006-0069-2>
- Soriano, C., Zafrilla, S., Martí, J., Bryan, S., Cas, R., Ablay, G., 2002. Welding and rheomorphism of phonolitic fallout deposits from the Las Cañadas caldera, Tenerife, Canary Islands. *Geological Society of America Bulletin* 114, 883–895. [https://doi.org/10.1130/0016-7606\(2002\)114<0883:WAROPF>2.0.CO;2](https://doi.org/10.1130/0016-7606(2002)114<0883:WAROPF>2.0.CO;2)
- Sparks, R., Bursik, M.I., Carey, S.N., Gilbert, J.S., Glaze, L.S., Sigurdsson, H., Woods, A.W., 1997. *Volcanic Plumes*. John Wiley, Chichester, UK.
- Sparks, R.S.J., 1986. The dimensions and dynamics of volcanic eruption columns. *Bulletin of Volcanology* 48, 3–15. <https://doi.org/10.1007/BF01073509>
- Sparks, R.S.J., Bursik, M.I., Ablay, G.J., Thomas, R.M.E., Carey, S.N., 1992. Sedimentation of tephra by volcanic plumes. Part 2: controls on thickness and grain-size variations of tephra fall deposits. *Bulletin of Volcanology* 54, 685–695. <https://doi.org/10.1007/BF00430779>

Sparks, R.S.J., J., B., Jaupart, C., Mader, H.M., Phillips, J.C., 1994. Physical aspects of magma degassing I. Experimental and theoretical constraints on vesiculation. *Volatiles in Magmas*, 414–445.

Sparks, R.S.J., Wilson, L., 1976. A model for the formation of ignimbrite by gravitational column collapse. *JGS* 132, 441–451. <https://doi.org/10.1144/gsjgs.132.4.0441>

Sparks, R.S.J., Wilson, L., Sigurdsson, H., 1981. The pyroclastic deposits of the 1875 eruption of Askja, Iceland. *Philosophical transactions of the Royal Society of London, A, Mathematical and Physical Sciences* 299, 241–273.

Sparks, S.R.J., Sigurdsson, H., Wilson, L., 1977. Magma mixing: a mechanism for triggering acid explosive eruptions. *Nature* 267, 315–318.
<https://doi.org/10.1038/267315a0>

Suhendro, I., Toramaru, A., Miyamoto, T., Miyabuchi, Y., Yamamoto, T., 2021. Magma chamber stratification of the 1815 Tambora caldera-forming eruption. *Bulletin of Volcanology* 83, 63. <https://doi.org/10.1007/s00445-021-01484-x>

Sulpizio, R., Costa, A., Massaro, S., Selva, J., Billotta, E., 2024. Assessing volumes of tephra fallout deposits: a simplified method for data scarcity cases. *Bulletin of Volcanology* 86, 62. <https://doi.org/10.1007/s00445-024-01753-5>

Thirlwall, M.F., Singer, B.S., Marriner, G.F., 2000. 39 Ar– 40 Ar ages and geochemistry of the basaltic shield stage of Tenerife, Canary Islands, Spain. *Journal of Volcanology and Geothermal Research* 103, 247–297. [https://doi.org/10.1016/S0377-0273\(00\)00227-4](https://doi.org/10.1016/S0377-0273(00)00227-4)

Troll, V.R., Carracedo, J.C., 2016. The Geology of Tenerife, in: *The Geology of the Canary Islands*. Elsevier, pp. 227–355. <https://doi.org/10.1016/B978-0-12-809663-5.00005-0>

Valentine, G.A., Wohletz, K.H., 1989. Numerical models of Plinian eruption columns and pyroclastic flows. *J. Geophys. Res.* 94, 1867–1887.
<https://doi.org/10.1029/JB094iB02p01867>

Wadsworth, F.B., Llewellyn, E.W., Castro, J.M., Tuffen, H., Schipper, C.I., Gardner, J.E., Vasseur, J., Foster, A., Damby, D.E., McIntosh, I.M., Boettcher, S., Unwin, H.E., Heap, M.J., Farquharson, J.I., Dingwell, D.B., Iacovino, K., Paisley, R., Jones, C., Whattam, J., 2022. A reappraisal of explosive–effusive silicic eruption dynamics: syn-eruptive assembly of lava from the products of cryptic fragmentation. *Journal of Volcanology and Geothermal Research* 432, 107672. <https://doi.org/10.1016/j.jvolgeores.2022.107672>

Walker, G.P.L., 1983. Ignimbrite types and ignimbrite problems. *Journal of Volcanology and Geothermal Research* 17, 65–88.

Walker, G.P.L., 1981. Plinian eruptions and their products. *Bulletin of Volcanology* 44, 223–240. <https://doi.org/10.1007/BF02600561>

- Walker, G.P.L., 1980. The Taupo pumice: Product of the most powerful known (ultraplinian) eruption? *Journal of Volcanology and Geothermal Research* 8, 69–94. [https://doi.org/10.1016/0377-0273\(80\)90008-6](https://doi.org/10.1016/0377-0273(80)90008-6)
- Walker, G.P.L., 1971. Grain-Size Characteristics of Pyroclastic Deposits. *The Journal of Geology* 79, 696–714. <https://doi.org/10.1086/627699>
- Whitham, A.G., Sparks, R.S.J., 1986. Pumice. *Bulletin of Volcanology* 48, 209–223. <https://doi.org/10.1007/BF01087675>
- Wilson, L., 1976. Explosive Volcanic Eruptions—III. Plinian Eruption Columns. *Geophysical Journal of the Royal Astronomical Society* 1, 543–556. <https://doi.org/10.1111/j.1365-246X.1958.tb05342.x>
- Wilson, L., 1972. Explosive Volcanic Eruptions-II The Atmospheric Trajectories of Pyroclasts. *Geophys J Int* 30, 381–392. <https://doi.org/10.1111/j.1365-246X.1972.tb05822.x>
- Wilson, L., Sparks, R.S.J., Walker, G.P.L., 1980. Explosive volcanic eruptions — IV. The control of magma properties and conduit geometry on eruption column behaviour. *Geophysical Journal of the Royal Astronomical Society* 63, 117–148. <https://doi.org/10.1111/j.1365-246X.1980.tb02613.x>
- Wilson, L., Walker, G.P.L., 1987. Explosive volcanic eruptions - VI. Ejecta dispersal in plinian eruptions: the control of eruption conditions and atmospheric properties. *Geophysical Journal International* 89, 657–679. <https://doi.org/10.1111/j.1365-246X.1987.tb05186.x>
- Wolff, J.A., 1985. Zonation, mixing and eruption of silica-undersaturated alkaline magma: a case study from Tenerife, Canary Islands. *Geol. Mag.* 122, 623–640. <https://doi.org/10.1017/S0016756800032039>
- Woods, A.W., 1995. The dynamics of explosive volcanic eruptions. *Reviews of Geophysics* 33, 495–530. <https://doi.org/10.1029/95RG02096>

Chapter 7: Appendices

Appendix I: Sample names, locations, and descriptions from southeast Tenerife. *The sample number represents an older naming system, e.g. ZZ/A used to represent Zarza Member A as the top of the Zarza Formation, however the naming system changed and represents Zarza Member C in this study.

Sample Number	Site	UTM E	UTM N	Source	Eruption	Description
TF.6.LV-1.LV1	Las Vegas	348125	3114570	Guajara	Vegas - 1	0.12 m minimum thickness. Las Vegas Package 5: bmpL(nl): clast supported, phonolitic pumice with lithic-rich base. Upper Boundary: Las Vegas Package 2; Lower Boundary: Fluvial sediments, palaeosols and Vallito Formation
TF.6.LV-1.LV3	Las Vegas	348125	3114570	Guajara	Vegas - 3	0.10 m minimum thickness. Las Vegas Package 3: mpL(nl, ip) and pLT (n): clast supported, massive pumice below a bed of pumice lapilli ash. Upper Boundary: Las Vegas Package 4; Lower Boundary: Las Vegas Package 20
TF.6.LV-1.LV4	Las Vegas	348125	3114570	Guajara	Vegas - 4	0.29 m minimum thickness. Las Vegas Package 4: dspL/mpL(nl, ip): clast supported, cream, crystal poor phonolite pumice minor mingled pumice, black and grey clasts. Upper Boundary: Las Vegas Package 5; Lower Boundary: Las Vegas Package 3.
TF.6.LV-1.LV5	Las Vegas	348125	3114570	Guajara	Vegas - 5	0.21 m minimum thickness. Las Vegas Package 5: scplL(nl, ip): clast supported, black pumice and scoria, crystal rich, poorly vesiculated, partially absorbed into soil. Upper Boundary: Soil and Draguito M; Lower Boundary: Las Vegas Package 4.
TF.20.EL-1.MN/A	El Rincon, Las Eras	359715	3118737	Guajara	Mena C	Upper Member of Mena Formation, massive pumice fall, 36cm thick, pumice <2cm in size
TF.6.LV-1.MN	Las Vegas	348180	3114539	Guajara	Mena (Middleton)	0.39 m minimum thickness. bpL: <5 layers of poorly sorted, clast supported, angular pumice, partially soil. Has brown to orange soil above. Upper Boundary: Pumice rich soil and Chavez M; Lower Boundary: Salto M.
TF.20.LR-1.ZZ/A	Los Roques	360930	3122294	Guajara	Zarza C	Upper Member of Zarza Formation, 150cm massive pumice lapilli with slight diffuse stratifications in places, distinct coarse layer runs through the middle of the Member
TF.6.LV-1.ZZ	Las Vegas	348180	3114539	Guajara	Zarza (Middleton)	0.36 m minimum thickness. mpL: poorly sorted, normally graded, aphanitic pumice, <2% lithics of lava and scoria. Upper Boundary: Usasa M; Lower Boundary Blanquitos M.
TF.11.IC-1.EL	Icor	356554	3121207	Guajara	El Rincon	A 20cm thick massive fine grained <1cm pumice lapilli fall deposit in a package of three (Arco, Carretas, El Rincon) below the Eras Formation
TF.6.LV-1.US	Las Vegas	348180	3114539	Guajara	Usasa	0.38 m minimum thickness. mpL: moderately to well sorted, symmetrically graded, phaneritic (2% biotite maybe), angular pumice. Upper Boundary: regolith or Helecho, Abona Member; Lower Boundary: Zarza M.

Sample Number	Site	UTM E	UTM N	Source	Eruption	Description
TF.6.IQ-1.GB	Icor Vineyard	357813	3121561	Guajara	Gambuesa	A 45cm thick massive fall deposit above the Vigas formation. This caps the eastern stratigraphy with limited exposure
TF.2.BRV-1.UPFD/3	Barranco de las Vegas	348342	3114444	Guajara	Unknown	UPFD/3 (mpL (n)) sits directly above UPFD/2 - Callao
TF.11.IC-1.HD	Icor	356554	3121207	Guajara	Honduras	Lowest formation of eastern section below Aguerche, 52cm thick massive to inverse graded fall deposit, distinct red scoria lithics, and banded pumice in top 10cm
TF.6.LV-1.CV	Las Vegas	348180	3114539	Guajara	Chavez	0.2 m minimum thickness. mpL: heavily pedogenised "ghost fall", angular pumice, reverse graded, some lithics of red scoria, lava and hydrothermally altered material. Upper Boundary: palaeosols and laterites; Lower Boundary: Mena M.
TF.6.LV-1.CH	Las Vegas	348180	3114539	Guajara	Chimiche	0.16 m minimum thickness. mpL: Pink, ash/loess rich, poorly to moderately sorted, aphanitic, microvesicular. Upper Boundary: Blanquitos M; Lower Boundary: Las Rosas M.
TF.11.IC-1.AG	Icor	356554	3121207	Guajara	Aguerche	A 23cm thick massive well sorted pumice fall deposit above Honduras formation, pumice <1cm, lithics <3%
TF.11.IC-1.IC/A	Icor	356554	3121207	Guajara	Icor F	Member F of Icor Formation, a 27cm thick normal graded coarse pumice lapilli below the Arco formation
TF.3.BR-4 .BQ	Barranco del Rio	352213	3111933	Guajara	Blanquitos	1.6 m minimum thickness. mpL: moderately sorted pumice fall, obsidian lithic population ~15% in upper horizon. Upper boundary: Usasa M; Lower Boundary: Fluvial sediments and Las Vegas M.
TF.11.IC-1.AR	Icor, Icor	356554	3121207	Guajara	Arco	A 19cm thick massive fine grained (<0.5cm) pumice lapilli fall deposit in a package of three (Arco, Carretas, El Rincon) below the Eras Formation
TF.11.BTC-1.UPFD/15/A	Barranco Tamadaya Cuerna	356859	3118650	Guajara	Unknown	Black Pumice at top of fall deposit UPFD/15. The base of a new package of stratigraphy under a phonolite lava flow.
TF.11.BTC-1.UPFD/15/B	Barranco Tamadaya Cuerna	356859	3118650	Guajara	Unknown	White pumice of UPFD/15, a ~2m thick fall deposit with a clear finer basal section and coarser upper section before the stratified black pumice at the top
TF.6.LV-1.LR	Las Vegas	348180	3114539	Guajara	Unknown	0.21 m minimum thickness. mpL(n-ip): symmetrically graded, angular to subangular, partially indurated, phaneritic (<2%). Upper Boundary: Chimiche M; Lower Boundary Desierto M.
TF.5.BDLMJ-5.MN	Barranco de las Monjas	350467	3109800	Guajara	Mena (Middleton) (?)	0.62 m minimum thickness. bpL: 2 layers of well to poorly sorted, normally graded pumice. 10% lithics (lavas). Upper Boundary: Blanquitos M; Lower Boundary Las Vegas M.
TF.PRE.LV-1.LV	Las Vegas	348180	3114539	Guajara	Vegas	Unknown thickness. White phonolitic pumice fall, dspL-mpL, angular-subangular pumice. Upper Boundary: Las Vegas Package 5; Lower Boundary: Palaeosols and fluvial sediments.
TF.2.EL-2.ES	El Rincon, Las Eras	359499	3118894	Guajara	Eras Ignimbrite	Eras ignimbrite, black and banded pumices

Sample Number	Site	UTM E	UTM N	Source	Eruption	Description
TF.2.EL-2.ES	El Rincon, Las Eras	359499	3118894	Guajara	Eras Ignimbrite	Eras ignimbrite matrix
TF.2.EL-2.ES	El Rincon, Las Eras	359499	3118894	Guajara	Eras Ignimbrite	Eras ignimbrite white coloured pumice
TF.2.EL-2.ES	El Rincon, Las Eras	359499	3118894	Guajara	Eras Ignimbrite	Eras ignimbrite dark green coloured pumice
TF.4.BDM-1.MD	Barranco de las Moradas	347809	3109033	Guajara	Moradas	Frothy pumice reticulite-like. From lower 50-90 cm of deposit. Mostly aphanitic, some phenocrysts of sanidine may be present.
TF.2.BRV-1.MD	Las Vegas, Barranco de las Vegas	348342	3114444	Guajara	Moradas	4.13 m minimum thickness. mpL: moderatley sorted, no apparent grading, lithic layer 2 m above base, lithics of hydrothermally altered lavas, angular to subangular pumice, phaneritic. Upper Boundary: UPFD/1 - Callao M.
TF.4.BDLV-1.MD	Las Vegas	348342	3114444	Guajara	Moradas	Black Pumice at top of moradas fall, laterally discontinuous seemingly restricted to 'pockets'.
TF.15.ER-1.ES	Eras Roadcut	359953	3120397	Guajara	Eras	Eras formation, 144cm thick diffusely stratified fall deposit with large (<10cm) pumices and banded pumices in places.
TF.5.BG-1.AU	Barranco Ganige	351869	3110645	Guajara	Aulagas Member	Aulagas Member at the top of the Helecho Formation, a locality from Davila-Harris et al (2009)
TF.9.AG-2.EE	Aguerche	359557	3125874	Guajara	El Escobonal	A 52cm thick massive fall deposit that sits between Mena and Zarza formations
TF.2.BRV-1.UPFD/1	Barranco de las Vegas	348342	3114444	Guajara	Unknown	UPFD/1 sits directly above Moradas - Yaco
TF.2.BRV-1.UPFD/2	Barranco de las Vegas	348342	3114444	Guajara	Unknown	UPFD/2 sits directly above UPFD/1 - Isidro
TF.3.BRR-1.UPFD/4	Barranco del Rio	353152	3110629	Guajara	Unknown	Fall deposit below Rio ignimbrite within a sequence of 3 fall deposits.
TF.3.BRR-1.UPFD/5	Barranco del Rio	353152	3110629	Guajara	Unknown	Fall deposit below UPFD/4 within a sequence of 3 fall deposits.
TF.3.BRR-1.UPFD/6	Barranco del Rio	353152	3110629	Guajara	Unknown	Fall deposit below UPFD/5 within a sequence of 3 fall deposits.
TF.4.VG-1.UPFD/7	Vista Gorda	342594	3108916	Guajara (?)	Unknown ignimbrite	Ignimbrite unknown origin
TF.6.LE-1.UPFD/8	La Escalona	337217	3110989	Guajara	Unknown	Unknown deposit below Moradas
TF.9.LM-3.UPFD/9	Lomo de Mena	361583	3128793	Guajara	Unknown	A 46cm thick normally graded fall deposit above lava, <3cm pumice, grades into soil with black pumice
TF.9.LM-3.UPFD/10	Lomo de Mena	361583	3128793	Guajara	Unknown	A 12cm soilified deposit of black pumice
TF.9.LM-3.UPFD/11	Lomo de Mena	361583	3128793	Guajara	Unknown	A 19cm thick normally graded, moderatley sorted fall deposit with <2% lithics, pumice <1cm
TF.9.LM-3.UPFD/12	Lomo de Mena	361583	3128793	Guajara	Unknown	A 8cm thick poorly sorted fall deposit, clasts as big as 2cm but generally <0.5cm
TF.9.LM-3.UPFD/13	Lomo de Mena	361583	3128793	Guajara	Unknown	A 12cm thick well sorted fall deposit with slight symmetrical grading, pumice <1cm.
TF.9.LM-3.UPFD/14	Lomo de Mena	361583	3128793	Guajara	Unknown	A 21cm thick wekk sorted fall deposit of coarse pumice up to 5cm, crystalline, lithics <2%.
TF.11.BTC-1.UPFD/16	Barranco Tamadaya Cuerna	356859	3118650	Guajara	Unknown ignimbrite	Suspected juveniles from Ignimbrite. Has similar characteristics to Eras with large white/green pumice blocks in cream ash matrix
TF.11.IC-1.CT	Icor, Icor	356554	3121207	Guajara	Carretas	A 19cm thick massive fine grained (<0.5cm) pumice lapilli fall deposit in

Sample Number	Site	UTM E	UTM N	Source	Eruption	Description
						a package of three (Arco, Carretas, El Rincon) below the Eras Formation
TF.11.IC-1.IC/F	Icor, Icor	356554	3121207	Guajara	Icor A	Member A of the Icor Formation, a 19cm medium grained inverse graded pumice lapilli. Above the Zarza formation
TF.6.IQ-2.JR	Icor Vineyard	357813	3121561	Guajara	Jurado	A 14cm thick, massive, fine grained, moderately sorted fall deposit. Lithics 1-3% and <5mm. Between the Aguerche and Mena formations
TF.6.IQ-2.LL	Icor Vineyard	357813	3121561	Guajara	La Linde	A 10cm thick, well sorted fall deposit with lateral inconsistencies, weaving in and out of the soil and lava below
TF.2.IQ-1.SM/A	Icor Vineyard	357813	3121561	Guajara	Sombrera D	Member D of Sombrera formation. A 88cm thick normally graded poorly sorted pumice lapilli. Banded pumice, 10-15% lithics
TF.2.IQ-1.VG	Icor Vineyard	357813	3121561	Guajara	Vigas	A 34cm thick normally graded moderately sorted fall deposit. Lithics <1%
TF.6.LV-1.AN	Las Vegas	348125	3114570	Guajara	Unknown	0.47 m minimum thickness. mpL: vitric pumice with chatoyant lustre, poorly sorted, mostly aphanitic, angular to subangular, lithic populous of <5%. Upper Boundary: Desierto M; Lower Boundary: palaeosols and laterites and Chavez M.
TF.6.LV-1.DS	Las Vegas	348125	3114570	Guajara	Unknown	0.17 m minimum thickness. mpL(n): grey and streaky pumice, an 'inconspicuous' deposit. Upper Boundary: Las Rosas M; Lower Boundary: Animas M.
TF.6.LV-1.DG	Las Vegas	348125	3114570	Guajara	Unknown	0.085 m minimum thickness. mpL(n): poorly sorted, pale grey, subangular and aphanitic pumice. Upper Boundary: well developed pumiceous soils; Lower Boundary: Las Vegas M.
TF.6.LV-1.SL	Las Vegas	348125	3114570	Guajara	Unknown	0.07 m minimum thickness. //bpT: normally graded, angular, grey pumice-rich ash. Upper Boundary: Mena Member; Lower Boundary: Vicacaro M.
TF.6.LV-1.VC	Las Vegas	348125	3114570	Guajara	Unknown	0.21 m minimum thickness. mpL(ip,nl): symmetrically graded, subangular to subrounded, salmon-pink and white, aphanitic pumice. Upper Boundary: Salto M; Lower Boundary: well developed soils.
TF.2.LV-1.BC	Las Vegas	348125	3114570	Ucanca	Unknown	0.78 m minimum thickness. mpL - bpL - bLT - CompL: 11 individual layers/5 units of green, banded and black pumice, lithics of lava, hydrothermal material and sub-volcanics (25%). Upper Boundary: palaeosols and fluvial sediments; Lower Boundary: Unknown
TF.5.BDLMJ-5.CV	Barranco de las Monjas	348830	3109851	Guajara	Unknown	0.25 m minimum thickness. mpL(ip): reverse graded lithic rich >10%, angular to subangular pumice. Upper Boundary: Rio Fm; Lower Boundary: Mena M.
TF.1.GQ-1.IC?	GeoT Quarry	356780	3120048	Guajara	Unknown	Potentially Icor formation but largely unknown. 3 units, lower and upper are mpL and lithic rich (40%). Fine middle layer, lithic rich, hydrothermally altered material
TF.6.LE-1.MD	La Escalona	337217	3110989	Guajara	Moradas	Moradas fall deposit "basal section". Deposit thickness: 2.77 m, fine base <5 cm.
TF.6.LE-1.MD	La Escalona	337217	3110989	Guajara	Moradas	Moradas fall deposit "Top Horizon" Deposit thickness: 2.77 m, mpL with frothy pumice.

Sample Number	Site	UTM E	UTM N	Source	Eruption	Description
TF.6.LZ-1.VG	La Zarza	357076	3123817	Guajara	Vigas	A 60cm thick normally graded fall deposit with lithics <2%.
TF.3.BR-4.US	Barranco del Rio	352213	3111964	Guajara	Unknown	0.4 m minimum thickness. mpL: angular-subangular, microvesicular pumice. Upper Boundary: Moradas M; Lower Boundary: Blanquitos
TF.1.GQ-1.72	GeoT Quarry	356780	3120048	Guajara	Unknown	Massive fall deposit below the Eras Formation. Potentially one of Arco, Carretas, or El Rincon.
TF.15.ER-1.AG	Eras Roadcut, Las Eras	359953	3120397	Guajara	Aguerche	Massive pumice fall deposit above Honduras formation
TF.1.GQ-2.ES	GeoT Quarry	356780	3120048	Guajara	Eras	A thin Eras formation with potential ignimbrite above. All evidence suggests Eras
TF.15.ER-1.HD	Eras Roadcut	359953	3120397	Guajara	Honduras	Lowest formation of eastern section below Aguerche
TF.1.GQ-2.IC?	GeoT Quarry	356780	3120048	Guajara	Unknown	Potentially Icor formation but largely unknown. 3 units, lower and upper are mpL and lithic rich (40%). Fine middle layer, lithic rich, hydrothermally altered material
TF.11.IC-1.IC/B	Icor	356554	3121207	Guajara	Icor E	Member E of Icor Formation, fine massive pumice lapilli
TF.11.IC-1.IC/C	Icor	356554	3121207	Guajara	Icor D	Member D of Icor Formation, inverse graded fine pumice lapilli
TF.11.IC-1.IC/D	Icor	356554	3121207	Guajara	Icor C	Member C of Icor Formation, symmetrically graded from coarse to fine to coarse
TF.15.ER-1.IC/F	Eras Roadcut	359953	3120397	Guajara	Icor A	Member A of the Icor Formation, a fine grained inversegraded pumice lapilli
TF.11.IC-1.IC/E	Icor	356554	3121207	Guajara	Icor B	Member B of the Icor Formation, a fine grained inverse graded pumice lapilli
TF.15.ER-1.IC/F	Eras Roadcut	359953	3120397	Guajara	Icor A	Member A of the Icor Formation, a medium grained inverse graded pumice lapilli
TF.20.FC-1.MN/A	Fasnía Cone	359338	3123698	Guajara	Mena C	Upper Member of Mena Formation, massive pumice fall
TF.20.EL-1.MN/B	El Rincon, Las Eras	359499	3118894	Guajara	Mena B	Middle Member of Mena Formation, ash
TF.20.FC-1.MN/B	Fasnía Cone	359338	3123698	Guajara	Mena B	Middle Member of Mena Formation, Stratified pumice lapilli/ash
TF.20.EL-1.MN/C	El Rincon, Las Eras	359499	3118894	Guajara	Mena A	Lower Member of Mena Formation, massive pumice fall
TF.20.FC-1.MN/C	Fasnía Cone	359338	3123698	Guajara	Mena A	Lower Member of Mena Formation, massive pumice fall
TF.3.BR-4.MD	Barranco del Rio	352213	3111964	Guajara	Moradas	Moradas Fall deposit, 2-3m, white phonolite, abundant highly vesiculated pumice
TF.6.BLV-1.MD	Barranco de las Vegas	348342	3114444	Guajara	Moradas	4.13 m minimum thickness. mpL - dbpL. Taken roughly 1 metre above the deposit base.
TF.6.BLV-2.MD	Barranco de las Vegas	348342	3114444	Guajara	Moradas	4.13 m minimum thickness. mpL - dbpL. Taken roughly 1 metre above the deposit base.
TF.4.VG-1.MD(?)	Vista Gorda	342594	3108916	Guajara	Moradas (?)	Pumice fall that looks like moradas fall deposit
TF.2.IQ-1.SM/B	Icor Vineyard	357813	3121561	Guajara	Sombrera C	Member C of Sombrera formation. Symmetrically graded slightly. Lithic % increase from 5-10% at bottom to 15-20% at top.
TF.2.IQ-1.SM/C	Icor Vineyard	357813	3121561	Guajara	Sombrera B	Member B of Sombrera formation. Normally graded with 25-30% lithics. High crystallinity
TF.3.BR-1.LV	Barranco del Rio	353232	3110504	Guajara	Vegas	Vegas deposit, scoria from the upper section

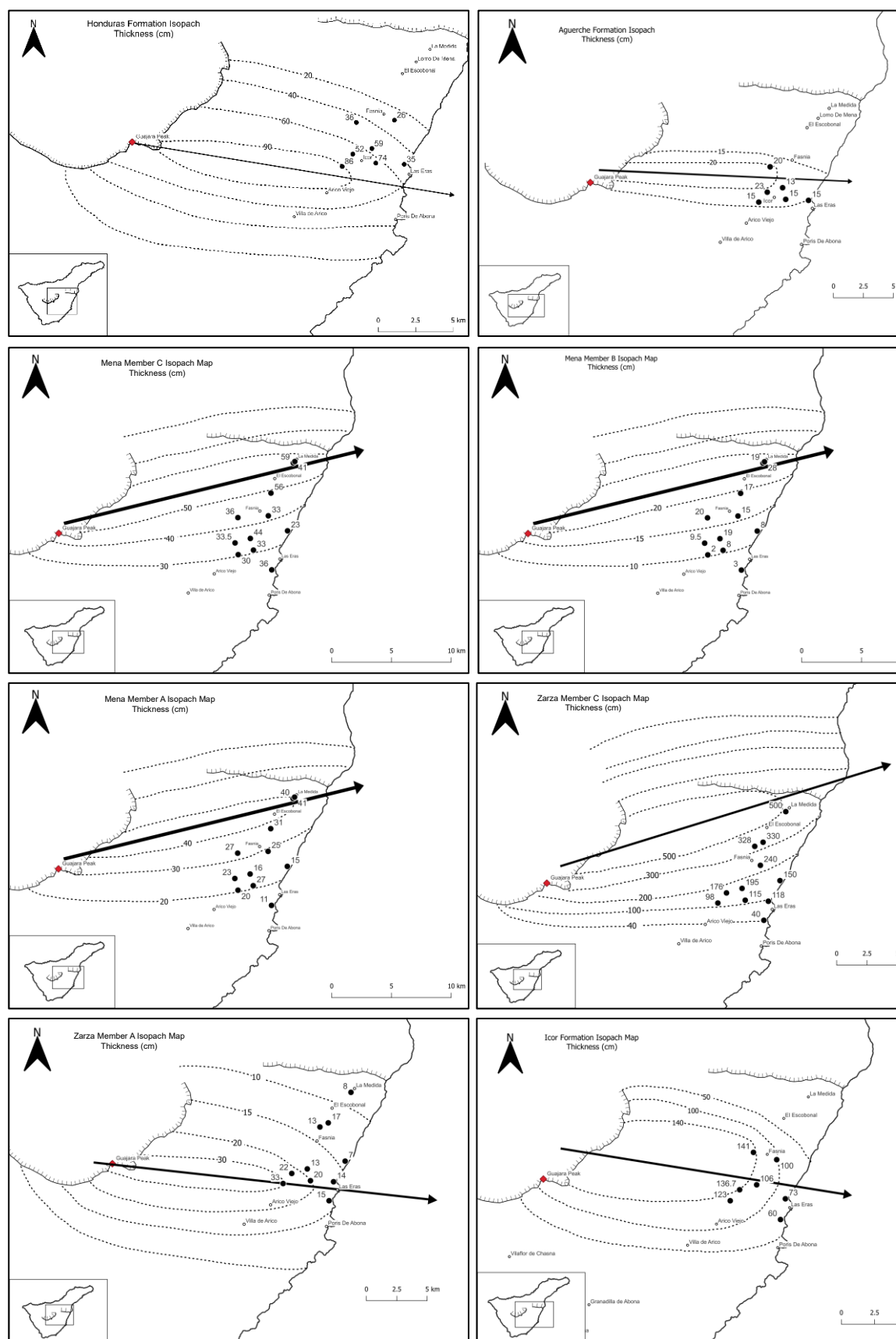
Sample Number	Site	UTM E	UTM N	Source	Eruption	Description
TF.3.BR-1.LV	Barranco del Rio	353232	3110504	Guajara	Vegas	Vegas deposit, white pumice
TF.23.AG-2.ZZ/A	Barranco de Fasnía y Guimar	359116	3143955	Guajara	Zarza C	Upper Member of Zarza Formation, Massive pumice lapilli with slight diffuse stratifications in places.
TF.20.EL-1.ZZ/A	El Rincon, Las Eras	359499	3118894	Guajara	Zarza C	Upper Member of Zarza Formation, Massive pumice lapilli with slight diffuse stratifications in places.
TF.20.LR-1.ZZ/C	Los Roques	360930	3122294	Guajara	Zarza A	Lower Member of Zarza Formation, Massive pumice lapilli
TF.20.EL-1.ZZ/C	El Rincon, Las Eras	359499	3118894	Guajara	Zarza A	Lower Member of Zarza Formation, Massive pumice lapilli
TF.15.ER-1.ZZ/C	Eras Roadcut	359953	3120397	Guajara	Zarza A	Lower Member of Zarza Formation, Massive pumice lapilli

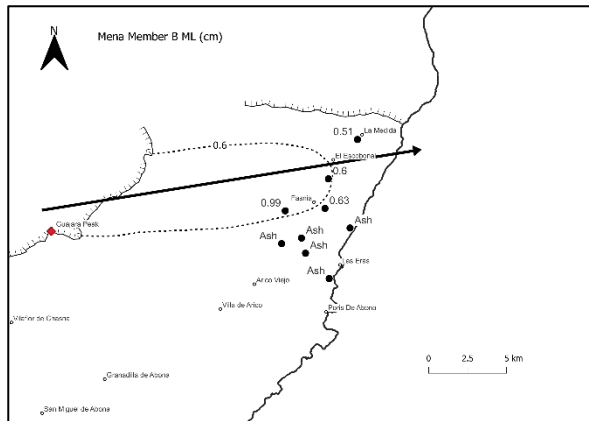
Appendix II: Localities visited in this study and the deposits found there. The localities and the surrounding deposits of the southwest Eras Formation locations are not provided here.

Location	UTM E	UTM N	Eruption deposits
El Rincon	359715	3118737	<i>Lava</i> <i>Eras</i> <i>El Rincon</i> <i>Icor</i> <i>Zarza</i> <i>Mena</i> <i>Lava</i> <i>At least 3 UPFUs</i>
Mirador de las Eras	355834	3120261	<i>Eras</i> <i>El Rincon</i> <i>Icor</i> <i>Zarza</i> <i>Mena (?)</i> <i>Aguerche</i> <i>Honduras</i> <i>Lava</i> <i>UPFD</i>
Icor	356554	3121207	<i>Diego Hernandez</i> <i>Sombrera</i> <i>Eras</i> <i>El Rincon</i> <i>Carretas</i> <i>Arco</i> <i>Icor</i> <i>Zarza</i> <i>Mena</i> <i>Aguerche</i> <i>Honduras</i> <i>Lava</i>
Icor Vineyard	357813	3121561	<i>Diego Hernandez</i> <i>Gambuesa</i> <i>Vigas</i> <i>Sombrera</i> <i>Eras</i> <i>El Rincon (?)</i> <i>Carretas (?)</i> <i>Arco (?)</i> <i>Icor</i> <i>Zarza</i> <i>Mena</i> <i>Jurado</i> <i>Aguerche</i> <i>Honduras</i> <i>La Linde</i> <i>Lava</i>
Windfarm	358057	3120514	<i>Eras</i> <i>Zarza</i> <i>Mena</i> <i>Aguerche</i> <i>Honduras</i>

Location	UTM E	UTM N	Eruption deposits
Eras Roadcut	359953	3120397	<i>Diego Hernandez</i> <i>Gambuesa (?)</i> <i>Vigas (?)</i> <i>Sombrera (?)</i> <i>Eras</i> <i>El Rincon</i> <i>Icor</i> <i>Zarza</i> <i>Mena</i> <i>Aguerche</i> <i>Honduras</i> <i>Lava</i>
Los Roques	360930	3122294	<i>Lava</i> <i>Icor (?)</i> <i>Zarza</i> <i>Mena</i>
Sabina Alta	356793	3123587	<i>Lava</i> <i>Vigas (?)</i> <i>Mena</i> <i>Jurado</i> <i>Aguerche</i> <i>Honduras</i> <i>Lava</i>
La Zarza	357655	3124364	<i>Lava</i> <i>Eras</i> <i>El Rincon</i> <i>Carretas</i> <i>Arco</i> <i>Icor</i> <i>Zarza</i> <i>Lava</i> <i>UPFD (?)</i>
Fasnia Cone	359338	3123698	<i>Diego Hernandez</i> <i>Gambuesa</i> <i>Vigas</i> <i>Sombrera</i> <i>Eras</i> <i>Icor</i> <i>Zarza</i> <i>Mena</i> <i>Honduras</i> <i>Lava</i> <i>At least 2 UPFUs</i>
Aguerche Roadcut	358896	3125488	<i>Lava</i> <i>Eras</i> <i>Zarza</i> <i>El Escobonal</i> <i>Lava</i>
Aguerche	359581	3125850	<i>Diego Hernandez</i> <i>Icor</i> <i>Zarza</i> <i>El Escobonal</i> <i>Mena</i>
Lomo de Mena	361482	3128672	<i>Diego Hernandez</i> <i>Zarza</i> <i>El Escobonal</i> <i>Mena</i>
La Medida	361611	3128810	<i>Diego Hernandez</i> <i>Mena</i> <i>At least 5 UPFDs</i> <i>Lava</i>

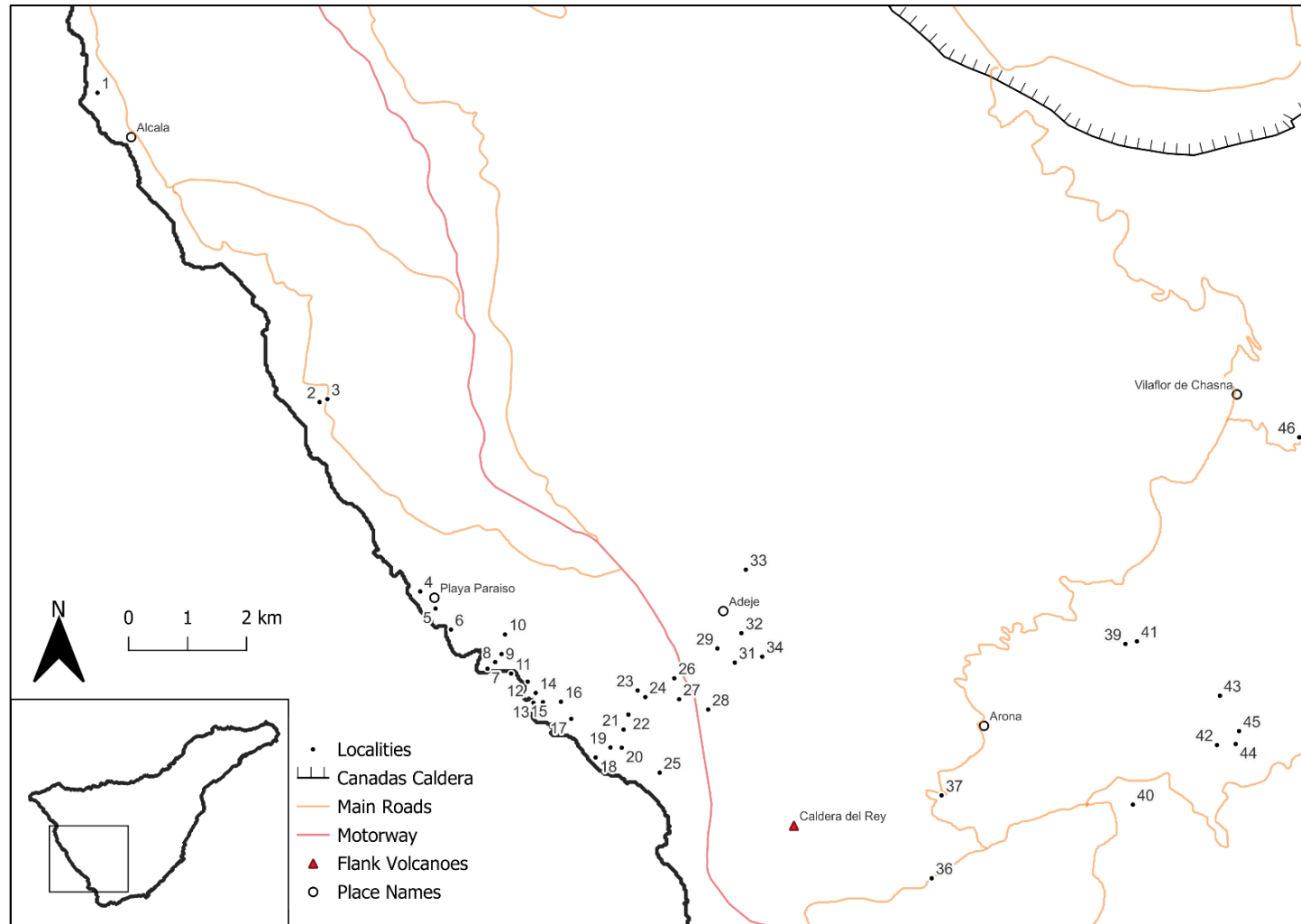
Appendix III: Isopach and Isopleth Maps

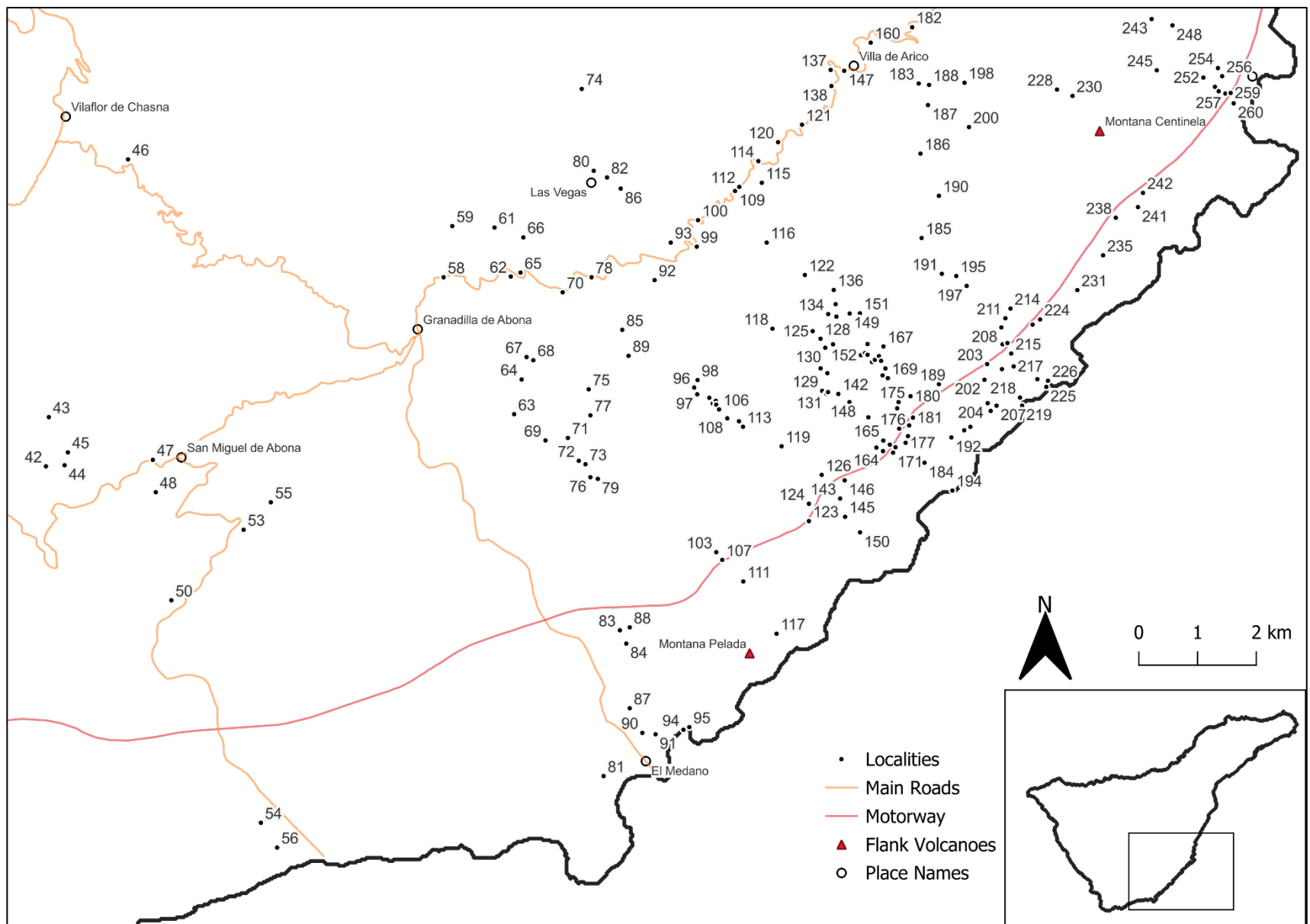


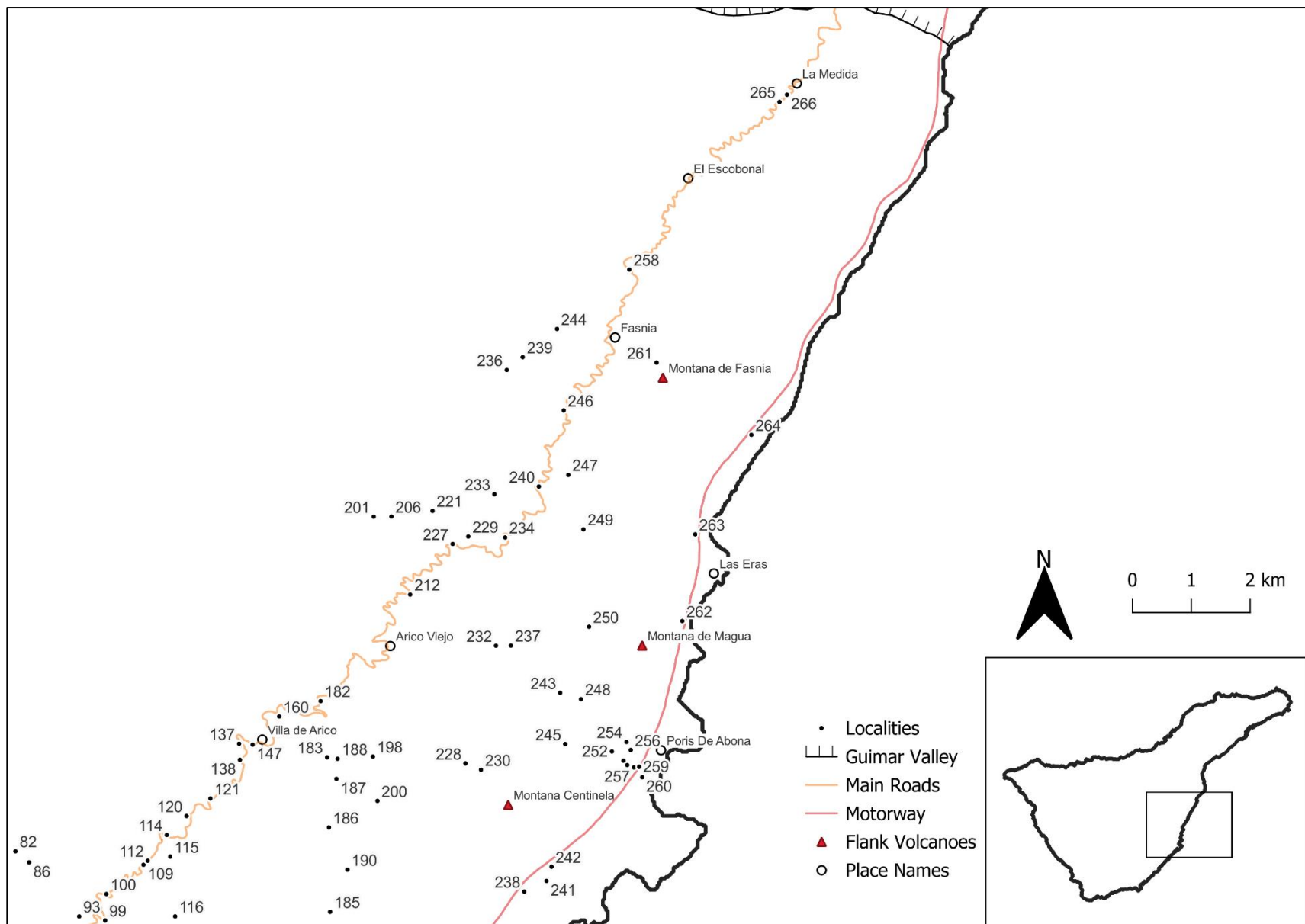


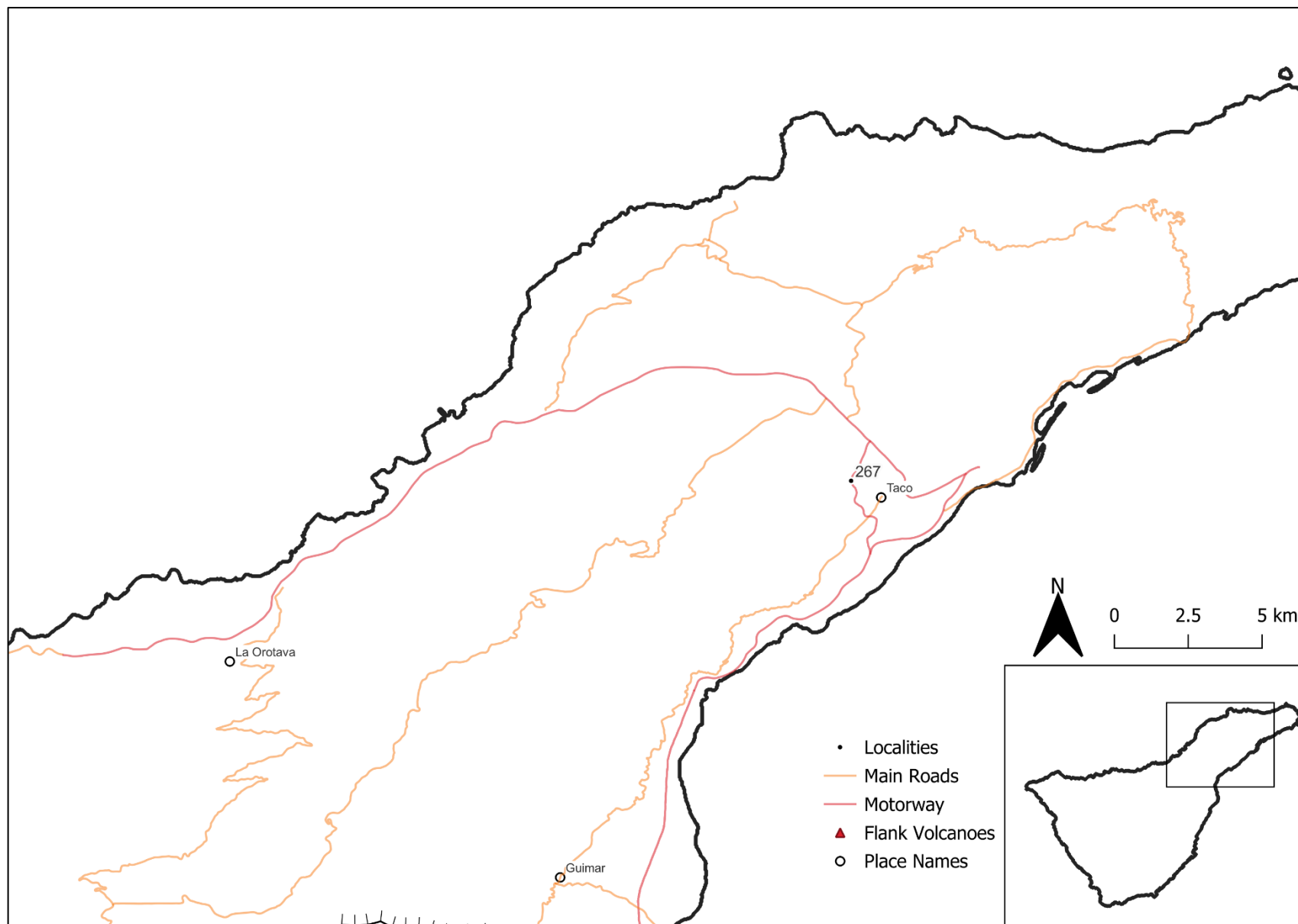
Appendix IV: Localities Map

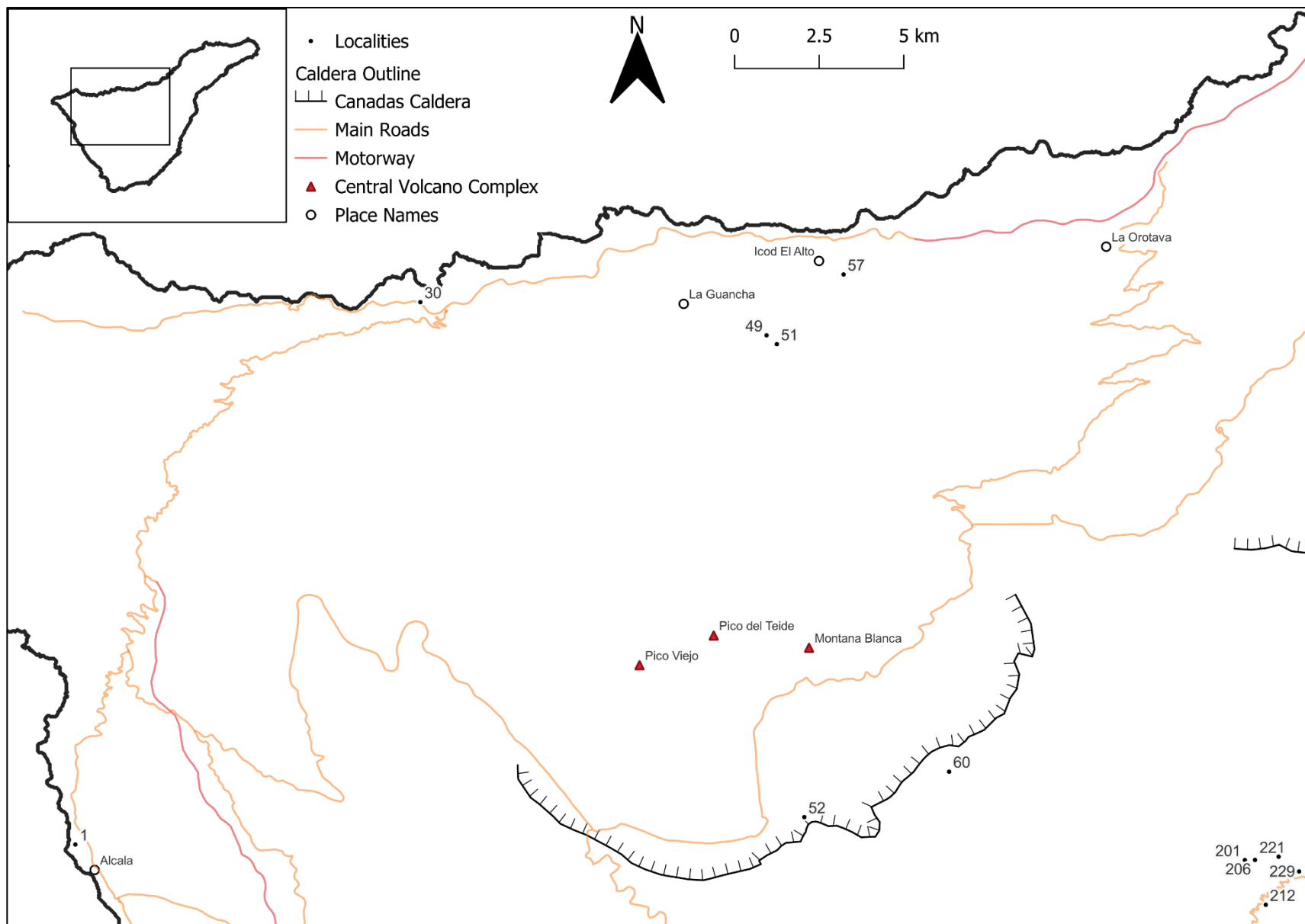
The localities represented are for Guajara age and older deposits derived from Bryan et al., (1998), Edgar et al., (2003), Middleton (2006), Davila-Harris et al., (2009), and this study. Overlapping localities or localities <100m apart, from multiple authors, were combined into a single locality, as it is likely error in coordinates.











Locality	Formation	East	North	Cluster	Source
1	Tosca Formation	319944	3121793	Guajara	Davila-Harris (2009)
2	Adeje Formation	323616	3115819	Ucanca	Davila-Harris (2009)
3	Adeje Formation	323749	3115875	Ucanca	Davila-Harris (2009)
	Tosca Formation	323828	3115888	Guajara	
	San Juan Formation	323839	3115900	Ucanca	
4	San Juan Formation	325268	3112172	Ucanca	Davila-Harris (2009)
5	Adeje Formation	325522	3111842	Ucanca	Davila-Harris (2009)
6	San Juan Formation	325778	3111436	Ucanca	Davila-Harris (2009)
	Adeje Formation	325801	3111443		
7	Adeje Formation	326385	3110678	Ucanca	Davila-Harris (2009)
8	Adeje Formation	326518	3110802	Ucanca	Davila-Harris (2009)
9	Adeje Formation	326628	3110954	Ucanca	Davila-Harris (2009)
10	Adeje Formation	326693	3111329	Ucanca	Davila-Harris (2009)
	Fanabe Formation				
11	Adeje Formation	326784	3110579	Ucanca	Davila-Harris (2009)
	Morteros Formation				
12	Gaviotas Formation	327063	3110422	Ucanca	Davila-Harris (2009)
	Morteros Formation				
13	Morteros Formation	327155	3110014	Ucanca	Davila-Harris (2009)
14	Gaviotas Formation	327196	3110203	Ucanca	Davila-Harris (2009)
	Morteros Formation	327227	3110250		
15	Fanabe Formation	327317	3110025	Ucanca	Davila-Harris (2009)
	Morteros Formation	327340	3110076		
16	Fanabe Formation	327621	3110028	Ucanca	Davila-Harris (2009)
17	Tosca Formation	327790	3109698	Guajara	Davila-Harris (2009)
18	Tosca Formation	328194	3108954	Guajara	Davila-Harris (2009)
	Agua Formation	328268	3108929	Ucanca	Davila-Harris (2009)
	Morteros Formation				
19	Tosca Formation	328448	3109142	Guajara	Davila-Harris (2009)
20	Fanabe Formation	328638	3109134	Ucanca	Davila-Harris (2009)
21	Agua Formation	328675	3109480	Ucanca	Davila-Harris (2009)
	Morteros Formation				
	Agua Formation	328721	3109519	Ucanca	Davila-Harris (2009)
22	Agua Formation	328761	3109766	Ucanca	Davila-Harris (2009)
23	Morteros Formation	328924	3110226	Ucanca	Davila-Harris (2009)
	Enramada Formation	328943	3110229		
24	Adeje Formation	329052	3110097	Ucanca	Davila-Harris (2009)
25	Fanabe Formation	329275	3108648	Ucanca	Davila-Harris (2009)
26	Adeje Formation	329548	3110450	Ucanca	Davila-Harris (2009)
27	Adeje Formation	329624	3110047	Ucanca	Davila-Harris (2009)
	Fanabe Formation				
28	Tosca Formation	330113	3109845	Guajara	Davila-Harris (2009)
29	Tosca Formation	330286	3111010	Guajara	Davila-Harris (2009)
30	Unknown Guajara	330400	3139750	Guajara	Edgar et al (2003)

Locality	Formation	East	North	Cluster	Source
31	Agua Formation Fanabe Formation Morro Formation Nicolas Formation	330577	3110736	Ucanca	Davila-Harris (2009)
32	Tosca Formation	330697	3111297	Guajara	Davila-Harris (2009)
33	Arico Formation Agua Formation Morro Formation	330790 330816	3112510 3112528	Guajara Ucanca	Middleton (2006) Davila-Harris (2009)
34	Fanabe Formation	331044	3110841	Ucanca	Davila-Harris (2009)
35	Tosca Formation	331840	3104515	Guajara	Davila-Harris (2009)
36	Granadilla Formation	333856	3106564	Guajara	Bryan et al (2000)
37	Granadilla Formation	334045	3108146	Guajara	Bryan et al (2000)
38	Tosca Formation	334070	3104659	Guajara	Davila-Harris (2009); Edgar et al (2003)
39	Eras (Moradas) Formation	337201	3110999	Guajara	This Study
40	Granadilla Formation	337286	3107925	Guajara	Bryan et al (2000)
41	Granadilla Formation	337397	3111048	Guajara	Bryan et al (2000)
42	Eras (Moradas) Formation	338726	3109045	Guajara	This Study
43	Granadilla Formation	338788	3109988	Guajara	Bryan et al (2000)
44	Eras (Moradas) Formation	339043	3109061	Guajara	This Study
45	Granadilla Formation	339103	3109307	Guajara	Bryan et al (2000)
46	Granadilla Formation Helecho Formation	340200 340202	3114912 3114588	Guajara	Bryan et al (2000) Davila-Harris (2009)
47	Granadilla Formation	340545	3109144	Guajara	Bryan et al (2000)
48	Granadilla Formation	340586	3108523	Guajara	Bryan et al (2000)
49	Unknown Guajara	340600	3138500	Guajara	Edgar et al (2003)
50	Granadilla Formation	340824	3106447	Guajara	Bryan et al (2000)
51	Unknown Guajara	340900	3138200	Guajara	Edgar et al (2003)
52	Arico Formation	341500	3122400	Guajara	Middleton (2006)
53	Granadilla Formation	342071	3107783	Guajara	Bryan et al (2000)
54	Incendio Formation Abades Formation	342290	3102160	Guajara	Middleton (2006) Middleton (2006); Edgar et al (2003)
55	Eras (Moradas) Formation	342540	3108304	Guajara	This Study
56	Abades Formation	342560	3101680	Guajara	Middleton (2006)
57	Unknown Guajara	342900	3140500	Guajara	Edgar et al (2003)
58	Granadilla Formation	345533	3112581	Guajara	Bryan et al (2000)
59	Eras (Moradas) Formation	345692	3113560	Guajara	Davila-Harris (2009)
60	Arico Formation Granadilla Formation	345800	3123860	Guajara	Middleton (2006)
61	Granadilla Formation Helecho Formation Eras (Moradas) Formation	346410 346489	3113523 3113661	Guajara Guajara	Bryan et al (2000) Davila-Harris (2009)
62	Helecho Formation	346675	3112580	Guajara	Davila-Harris (2009)
63	Granadilla Formation	346698	3109939	Guajara	Bryan et al (2000)
64	Granadilla Formation	346834	3110603	Guajara	Bryan et al (2000)

Locality	Formation	East	North	Cluster	Source
65	Granadilla Formation	346841	3112653	Guajara	Bryan et al (2000)
66	Helecho Formation	346898	3113328	Guajara	Davila-Harris (2009)
67	Eras (Moradas) Formation	346923	3111033	Guajara	This Study
68	Helecho Formation	347037	3110970	Guajara	Davila-Harris (2009)
	Eras (Moradas) Formation	347040	3110969		
69	Helecho Formation	347224	3109430	Guajara	Davila-Harris (2009)
	Helecho Formation	347337	3109308		
	Eras (Moradas) Formation	347338	3109310		
70	Granadilla Formation	347553	3112267	Guajara	Bryan et al (2000)
71	Granadilla Formation	347606	3109473	Guajara	Bryan et al (2000)
72	Eras (Moradas) Formation	347785	3109031	Guajara	This Study
73	Barco Formation	347898	3108964	Ucanca	Davila-Harris (2009)
	Eras (Moradas) Formation			Guajara	
74	Helecho Formation	347927	3116163	Guajara	Davila-Harris (2009)
75	Granadilla Formation	347971	3110400	Guajara	Bryan et al (2000)
76	Granadilla Formation	347979	3108715	Guajara	Bryan et al (2000)
77	Granadilla Formation	347994	3109901	Guajara	Bryan et al (2000)
78	Granadilla Formation	348048	3112549	Guajara	Bryan et al (2000)
79	Eras (Moradas) Formation	348105	3108681	Guajara	Davila-Harris (2009)
80	Vegas Formation	348110	3114590	Guajara	Middleton (2006)
	Blanquitos Formation				
81	Arico Formation	348130	3102980	Guajara	Middleton (2006)
82	Eras (Moradas) Formation	348335	3114460	Guajara	This Study
83	Granadilla Formation	348443	3105773	Guajara	Bryan et al (2000); Edgar et al (2003)
84	Granadilla Formation	348548	3105516	Guajara	Bryan et al (2000)
85	Granadilla Formation	348556	3111534	Guajara	Bryan et al (2000)
86	Helecho Formation	348564	3114243	Guajara	Davila-Harris (2009)
87	Granadilla Formation	348591	3104275	Guajara	Bryan et al (2000)
	Abades Formation				Edgar et al (2003)
88	Granadilla Formation	348611	3105826	Guajara	Bryan et al (2000)
89	Granadilla Formation	348657	3111034	Guajara	Bryan et al (2000)
90	Incendio Formation	348800	3103800	Guajara	Middleton (2006)
91	Abades Formation	349025	3103770	Guajara	Middleton (2006)
	Granadilla Formation	349097	3103814		Bryan et al (2000)
92	Granadilla Formation	349118	3112480	Guajara	Bryan et al (2000)
93	Granadilla Formation	349402	3113196	Guajara	Bryan et al (2000)
94	Abades Formation	349500	3103850	Guajara	Edgar et al (2003)
95	Abades Formation	349600	3103900	Guajara	Edgar et al (2003)
96	Mocán Formation	349765	3110411	Ucanca	Davila-Harris (2009)
97	Helecho Formation	349815	3110281	Guajara	Davila-Harris (2009)
	Mocán Formation	349817	3110329	Ucanca	
	Monjas Formation	349843	3110329		
98	Mocán Formation	349824	3110554	Ucanca	Davila-Harris (2009)
99	Granadilla Formation	349843	3113113	Guajara	Bryan et al (2000)

Locality	Formation	East	North	Cluster	Source
100	Granadilla Formation	349870	3113620	Guajara	Middleton (2006)
101	Helecho Formation	350019	3110212	Guajara	Davila-Harris (2009)
102	Helecho Formation	350076	3110102	Guajara	Davila-Harris (2009)
103	Granadilla Formation Abades Formation Arico Formation	350100	3107250	Guajara	Edgar et al (2003)
104	Barco Formation	350130	3110152	Ucanca	Davila-Harris (2009)
105	Derriscaderos Formation Helecho Formation Barco Formation	350135 350138	3110078 3110076	Ucanca Guajara Ucanca	Davila-Harris (2009) Davila-Harris (2009)
106	Derriscaderos Formation	350183	3109987	Ucanca	Davila-Harris (2009)
107	Granadilla Formation Abades Formation Arico Formation	350200	3107100	Guajara	Edgar et al (2003)
108	Helecho Formation Puegueros Formation Vallito Formation	350320	3109814	Guajara Ucanca	Davila-Harris (2009)
109	Eras (Moradas) Formation	350507	3114173	Guajara	This Study
110	Derriscaderos Formation Puegueros Formation	350518 350519	3109756 3109755	Ucanca	Davila-Harris (2009)
111	Barco Formation	350553	3106682	Ucanca	Davila-Harris (2009)
112	Granadilla Formation	350580	3114250	Guajara	Middleton (2006)
113	Monjas Formation Helecho Formation Puegueros Formation Barco Formation	350585 350585	3109648 3109655	Ucanca Guajara Ucanca	Davila-Harris (2009) Davila-Harris (2009)
114	Arico Formation	350910	3114740	Guajara	Middleton (2006)
115	Eras (Moradas) Formation	350964	3114324	Guajara	Davila-Harris (2009)
116	Granadilla Formation	351032	3113176	Guajara	Bryan et al (2000)
117	Granadilla Formation	351106	3105673	Guajara	Bryan et al (2000)
118	Granadilla Formation	351110	3111524	Guajara	Bryan et al (2000)
119	Eras (Moradas) Formation	351237	3109267	Guajara	This Study
120	Unknown Guajara	351250	3115100	Guajara	Edgar et al (2003)
121	Arico Formation	351660	3115430	Guajara	Middleton (2006)
122	Granadilla Formation	351673	3112547	Guajara	Bryan et al (2000)
123	Granadilla Formation	351683	3107826	Guajara	Bryan et al (2000)
124	Granadilla Formation	351687	3108159	Guajara	Bryan et al (2000)
125	Helecho Formation	351792	3111468	Guajara	Davila-Harris (2009)
126	Helecho Formation	351912	3108710	Guajara	Davila-Harris (2009)
127	Helecho Formation	351918	3110753	Guajara	Davila-Harris (2009)
128	Helecho Formation	351924	3111321	Guajara	Davila-Harris (2009)
129	Helecho Formation	351939	3110320	Guajara	Davila-Harris (2009)
130	Barco Formation Helecho Formation	352002	3111147	Ucanca Guajara	Davila-Harris (2009)

Locality	Formation	East	North	Cluster	Source
131	Helecho Formation	352008	3110268	Guajara	Davila-Harris (2009)
132	Granadilla Formation	352032	3110659	Guajara	Bryan et al (2000); Edgar et al (2003)
133	Helecho Formation	352039	3110297	Guajara	Davila-Harris (2009)
134	Helecho Formation	352061	3111792	Guajara	Davila-Harris (2009)
135	Helecho Formation	352135	3111211	Guajara	Davila-Harris (2009)
136	Granadilla Formation	352160	3112253	Guajara	Bryan et al (2000)
137	Arico Formation	352160	3116475	Guajara	Middleton (2006)
138	Incendio Formation	352170	3116165	Guajara	Middleton (2006)
139	Eras (Moradas) Formation	352189	3111980	Guajara	This Study
140	Puegueros Formation	352199	3111741	Ucanca	Davila-Harris (2009)
141	Helecho Formation	352206	3110997	Guajara	Davila-Harris (2009)
142	Granadilla Formation	352214	3110258	Guajara	Bryan et al (2000)
143	Granadilla Formation	352219	3108252	Guajara	Bryan et al (2000)
144	Granadilla Formation	352293	3111032	Guajara	Bryan et al (2000)
145	Unknown Guajara Abades Formation Granadilla Formation	352300	3107900	Guajara	Edgar et al (2003)
146	Granadilla Formation	352300	3108600	Guajara	Edgar et al (2003)
147	Arico Formation	352390	3116455	Guajara	Middleton (2006)
148	Unknown Guajara	352400	3110100	Guajara	Edgar et al (2003)
149	Eras (Moradas) Formation Barco Formation Vallito Formation	352425	3111798	Guajara Ucanca	Davila-Harris (2009)
150	Abades Formation	352550	3107600	Guajara	Edgar et al (2003)
151	Granadilla Formation	352600	3111800	Guajara	Edgar et al (2003)
152	Puegueros Formation Helecho Formation Rio Formation	352606 352613 352615	3110997 3111031 3110970	Ucanca Guajara	Davila-Harris (2009) Middleton (2006)
153	Puegueros Formation Barco Formation	352677 352681	3111037 3111027	Ucanca	Davila-Harris (2009)
154	Helecho Formation	352719	3109804	Guajara	Davila-Harris (2009)
155	Helecho Formation	352720	3111004	Guajara	Davila-Harris (2009)
156	Puegueros Formation	352722	3111210	Ucanca	Davila-Harris (2009)
157	Helecho Formation Barco Formation Puegueros Formation	352793	3110865	Guajara Ucanca	Davila-Harris (2009)
158	Incendio Formation Helecho Formation	352803 352808	3109480 3109447	Guajara	Middleton (2006) Davila-Harris (2009)
159	Helecho Formation	352843	3110905	Guajara	Davila-Harris (2009)
160	Granadilla Formation	352847	3116988	Guajara	Bryan et al (2000)
161	Barco Formation Helecho Formation	352848	3109221	Ucanca Guajara	Davila-Harris (2009)

Locality	Formation	East	North	Cluster	Source	
162	Puegueros Formation	352913	3110976	Ucanca	Davila-Harris (2009)	
	Barco Formation	352913	3110995	Ucanca		
	Helecho Formation	352913	3110995	Guajara		
163	Helecho Formation	352948	3110884	Guajara	Davila-Harris (2009)	
164	Helecho Formation	352959	3109153	Guajara	Davila-Harris (2009)	
165	Helecho Formation	352967	3109355	Guajara	Davila-Harris (2009)	
166	Rio Formation	352970	3110605	Guajara	Middleton (2006)	
167	Helecho Formation	352992	3111160	Guajara	Davila-Harris (2009)	
	Granadilla Formation				Edgar et al (2003)	
168	Barco Formation	353019	3110737	Ucanca	Davila-Harris (2009)	
	Helecho Formation			Guajara		
	Rio Formation					
169	Helecho Formation	353059	3110551	Guajara	Davila-Harris (2009)	
	Rio Formation	353091	3110577			
170	Helecho Formation	353077	3109275	Guajara	Davila-Harris (2009)	
171	Helecho Formation	353130	3109120	Guajara	Middleton (2006)	
	Arico Formation					
172	Helecho Formation	353152	3110375	Guajara	Davila-Harris (2009)	
173	Helecho Formation	353172	3109225	Guajara	Davila-Harris (2009)	
174	Incendio Formation	353210	3109970	Guajara	Middleton (2006)	
175	Abades Formation	353235	3110090	Guajara	Middleton (2006)	
176	Helecho Formation	353240	3109580	Guajara	Middleton (2006)	
177	Helecho Formation	353346	3109307	Guajara	Davila-Harris (2009)	
178	Helecho Formation	353387	3109435	Guajara	Davila-Harris (2009)	
179	Incendio Formation	353410	3109640	Guajara	Middleton (2006)	
180	Abades Formation	353440	3110200	Guajara	Middleton (2006)	
181	Granadilla Formation	353476	3109788	Guajara	Bryan et al (2000)	
182	Incendio Formation	353555	3117275	Guajara	Middleton (2006)	
	Abades Formation	353560	3117275			
183	Incendio Formation	353652	3116195	Guajara	Middleton (2006)	
184	Granadilla Formation	353662	3108921	Guajara	Bryan et al (2000)	
185	Granadilla Formation	353666	3113232	Guajara	Bryan et al (2000); Edgar et al (2003)	
186	Granadilla Formation	353666	3114850	Guajara	Bryan et al (2000)	
187	Granadilla Formation	353805	3115779	Guajara	Bryan et al (2000)	
188	Granadilla Formation	353829	3116166	Guajara	Bryan et al (2000)	
	Incendio Formation	353865	3116230		Middleton (2006)	
	Arico Formation				Edgar et al (2003)	
189	Granadilla Formation	353926	3110425	Guajara	Bryan et al (2000)	
190	Granadilla Formation	353970	3114037	Guajara	Bryan et al (2000)	
191	Granadilla Formation	354001	3112541	Guajara	Bryan et al (2000)	
192	Incendio Formation	354125	3109400	Guajara	Middleton (2006)	
193	Abades Formation	354125	3109400	Guajara	Middleton (2006)	
194	Helecho Formation	354130	3108382	Guajara	Davila-Harris (2009)	

Locality	Formation	East	North	Cluster	Source
195	Incendio Formation Abades Formation	354245	3112495	Guajara	Middleton (2006)
196	Arico Formation	354345	3109535	Guajara	Middleton (2006)
197	Granadilla Formation Abades Formation	354420	3112303	Guajara	Bryan et al (2000) Edgar et al (2003)
198	Arico Formation	354430	3116200	Guajara	Middleton (2006)
199	Arico Formation	354450	3109600	Guajara	Edgar et al (2003)
200	Granadilla Formation	354497	3115349	Guajara	Bryan et al (2000)
201	Unknown Guajara Arico Formation Abades Formation Granadilla Formation	354500 354600	3120800 3110750	Guajara	Edgar et al (2003)
202	Arico Formation Granadilla Formation	354700	3110500	Guajara	Edgar et al (2003)
203	Granadilla Formation	354750	3110800	Guajara	Edgar et al (2003)
204	Granadilla Formation	354750	3110050	Guajara	Edgar et al (2003)
205	Arico Formation	354800	3109900	Guajara	Edgar et al (2003)
206	Unknown Guajara	354800	3120800	Guajara	Edgar et al (2003)
207	Granadilla Formation	354900	3110000	Guajara	Edgar et al (2003)
208	Arico Formation Abades Formation	355000	3111500	Guajara	Edgar et al (2003)
209	Granadilla Formation	355000	3110700	Guajara	Edgar et al (2003)
210	Granadilla Formation	355016	3111176	Guajara	Bryan et al (2000)
211	Arico Formation	355070	3111675	Guajara	Middleton (2006)
212	Unknown Guajara	355100	3119300	Guajara	Edgar et al (2003)
213	Arico Formation Abades Formation Granadilla Formation	355100	3111200	Guajara	Edgar et al (2003)
214	Granadilla Formation	355160	3111860	Guajara	Middleton (2006)
215	Granadilla Formation	355161	3110997	Guajara	Bryan et al (2000)
216	Abades Formation Granadilla Formation	355200	3110300	Guajara	Edgar et al (2003)
217	Abades Formation	355200	3110750	Guajara	Edgar et al (2003)
218	Abades Formation	355300	3110150	Guajara	Edgar et al (2003)
219	Incendio Formation Abades Formation	355335	3109995	Guajara	Middleton (2006)
220	Arico Formation Abades Formation	355500	3111150	Guajara	Edgar et al (2003)
221	Unknown Guajara	355500	3120900	Guajara	Edgar et al (2003)
222	Granadilla Formation	355531	3111547	Guajara	Bryan et al (2000)
223	Abades Formation	355600	3110500	Guajara	Edgar et al (2003)
224	Granadilla Formation	355660	3111645	Guajara	Bryan et al (2000)
225	Arico Formation	355750	3110350	Guajara	Edgar et al (2003)
226	Incendio Formation	355780	3110468	Guajara	Middleton (2006)

Locality	Formation	East	North	Cluster	Source
227	Eras (Moradas) Formation El Rincon Formation Icor Formation Zarza Formation Mena Formation Aguerche Formation Honduras Formation	355834	3120261	Guajara	This Study
228	Granadilla Formation Abades Formation	356000	3116050	Guajara	Edgar et al (2003)
229	Arico Formation Abades Formation	356100	3120400	Guajara	Edgar et al (2003)
230	Arico Formation Granadilla Formation	356263 356360	3115925 3115947	Guajara	Middleton (2006) Bryan et al (2000)
231	Granadilla Formation	356300	3112200	Guajara	Edgar et al (2003)
232	Granadilla Formation Arico Formation	356545 356600	3118300 3118300	Guajara	Middleton (2006) Edgar et al (2003)
233	Sombrera Formation Eras (Moradas) Formation El Rincon Formation Carretas Formation Arco Formation Icor Formation Zarza Formation Mena Formation Aguerche Formation Honduras Formation	356554	3121207	Guajara	This Study
234	Eras (Moradas) Formation	356726	3120374	Guajara	This Study
235	Granadilla Formation	356746	3112862	Guajara	Bryan et al (2000)
236	Vigas Formation Mena Formation Jurado Formation Aguerche Formation Honduras Formation	356793	3123587	Guajara	This Study
237	Unknown Guajara	356800	3118300	Guajara	Edgar et al (2003)
238	Granadilla Formation	356970	3113580	Guajara	Bryan et al (2000)
239	Eras (Moradas) Formation	357066	3123830	Guajara	This Study
240	Incendio Formation	357310	3121345	Guajara	Middleton (2006)
241	Arico Formation Abades Formation	357350 357400	3113780 3113770	Guajara	Middleton (2006)
242	Granadilla Formation	357438	3114051	Guajara	Bryan et al (2000)
243	Granadilla Formation	357625	3117384	Guajara	Bryan et al (2000)

Locality	Formation	East	North	Cluster	Source
244	Eras (Moradas) Formation El Rincon Formation Carretas Formation Arco Formation Icor Formation Zarza Formation	357655	3124364	Guajara	This Study
245	Arico Formation	357700	3116400	Guajara	Edgar et al (2003)
246	Unknown Guajara	357750	3122800	Guajara	Edgar et al (2003)
247	Gambuesa Formation Vigas Formation Sombreira Formation Eras (Moradas) Formation El Rincon Formation Carretas Formation Arco Formation Icor Formation Zarza Formation Mena Formation Jurado Formation Aguerche Formation Honduras Formation La Linde Formation	357813	3121561	Guajara	This Study
248	Granadilla Formation	357977	3117258	Guajara	Bryan et al (2000)
249	Eras (Moradas) Formation Zarza Formation Mena Formation Aguerche Formation Honduras Formation	358057	3120514	Guajara	This Study
250	Arico Formation	358130	3118645	Guajara	Middleton (2006)
251	Arico Formation Granadilla Formation	358450	311620	Guajara	Edgar et al (2003)
252	Abades Formation	358490	3116250	Guajara	Middleton (2006)
253	Arico Formation	358685	3116070	Guajara	Middleton (2006); Edgar et al (2003)
254	Granadilla Formation	358740	3116430	Guajara	Middleton (2006); Edgar et al (2003)
255	Granadilla Formation	358747	3115985	Guajara	Bryan et al (2000); Edgar et al (2003)
256	Granadilla Formation	358810	3116273	Guajara	Bryan et al (2000); Edgar et al (2003)
257	Incendio Formation Abades Formation	358860	3115940	Guajara	Middleton (2006)
258	Eras (Moradas) Formation Zarza Formation El Escobonal Formation Mena Formation	358896	3125488	Guajara	This Study
259	Arico Formation	358950	3115950	Guajara	Edgar et al (2003)

Locality	Formation	East	North	Cluster	Source
260	Eras (Moradas) Formation	358999	3115750	Guajara	This Study
	Abades Formation	359040	3115630		Middleton (2006)
	Arico Formation	359050	3115740		
261	Granadilla Formation	359338	3123698	Guajara	Edgar et al (2003)
	Gambuesa Formation				
	Vigas Formation				
	Sombrera Formation				
	Eras (Moradas) Formation				This Study
	Icor Formation				
	Zarza Formation				
	Mena Formation				
	Honduras Formation				
262	Eras (Moradas) Formation	359715	3118737	Guajara	This Study
	El Rincon Formation				
	Icor Formation				
	Zarza Formation				
	Mena Formation				
263	Gambuesa Formation	359953	3120397	Guajara	This Study
	Vigas Formation				
	Sombrera Formation				
	Eras (Moradas) Formation				
	El Rincon Formation				
	Icor Formation				
	Zarza Formation				
	Mena Formation				
	Aguerche Formation				
	Honduras Formation				
	Incendio Formation	359965	3120340		Middleton (2006)
	Abades Formation	359970	3120345		
	Arico Formation	359980	3120285		
264	Icor Formation	360930	3122294	Guajara	This Study
	Zarza Formation				
	Mena Formation				
265	Zarza Formation	361482	3128672	Guajara	This Study
	El Escobonal Formation				
	Mena Formation				
266	Mena Formation	361611	3128810	Guajara	This Study
	Unknown Guajara				
	Unknown Guajara				
	Unknown Guajara				
	Unknown Guajara				
267	Unknown Guajara	371750	3148000	Guajara	Edgar et al (2003)

